Effects of human papillomavirus 16 (HPV16) E6 oncoprotein on cell polarity regulators in head and neck cancers

Lulić, Lucija

University of Zagreb

FACULTY OF SCIENCE
DEPARTMENT OF BIOLOGY

Lucija Lulić

EFFECTS OF HUMAN PAPILLOMAVIRUS 16 (HPV16) E6 ONCOPROTEIN ON CELL POLARITY REGULATORS IN HEAD AND NECK CANCERS

DOCTORAL DISSERTATION

Zagreb, 2022

Sveučilište u Zagrebu

PRIRODOSLOVNO-MATEMATIČKI FAKULTET
BIOLOŠKI ODSJEK

Lucija Lulić

UTJECAJ ONKOPROTEINA E6 PAPILOMAVIRUSA ČOVJEKA TIPA 16 (HPV16) NA REGULATORE STANIČNE POLARNOSTI U TUMORIMA GLAVE I VRATA

DOKTORSKI RAD

Zagreb, 2022

Hvala

... mojem mentoru, Vjekoslavu, na pruženoj prilici, ukazanom povjerenju, svakoj kritici, savjetu i podršci tijekom i nakon izrade ovog rada te svakom „Još malo i gotovo! :)“. Bile su ovo turbulentne godine, ali iz njih smo izvukli ono najbolje!

... mojim sadašnjim i bivšim „odraslim“ LMVB-ovcima, Magdaleni, Ivanu, Nini, Jasminki i Nathanielu, na savjetima i glasu zdravog razuma kada mi je zatrebao. Kseniji, na svakoj riječi podrške, kavi, Pacman tortama i smijehu iz petnih žila koji je prožimao svaki kutak LMVB-a.

... mojoj lab partnerici i prije svega prijateljici, najboljoj postdokici Josipi, za sve ranojutarnje kave, sve poslovne i privatne razgovore, sve diskusije, za svo znanje koje si podijelila sa mnom. Jo, prava si inspiracija! Ali najviše, hvala ti što si bila ono što mi je najviše trebalo u bilo kojem trenutku!

... mojim „curama s kata za ručak“, Tini, bike&hike buddyu i za ono malo odlazaka na Sljeme što nam je davalo snagu za nove lab pothvate. Ivani, Eni, Anamariji, Ani, za sve dijeljene trenutke, utješne riječi i riječi ohrabrenja. Hvala i Maji, Bastienu i Ani R., kolegama koji su tijekom ovog putovanja postali dragi prijatelji.

... mojim „vanjskim suradnicima“ Dragomiri Majhen, Filipu Rokiću i Maji Sabol na svim sugestijama, protokolima i mozganjima u pojedinim fazama ovog doktorskog istraživanja te mojim LAMBDAma dodatno na svim jutarnjim kavama i (ne)sportskim razgovorima!

... doc.dr.sc. Emilu Dediolu, dr.med., dr.sc. Antoniji Jakovčević, dr.med., Luki Manojloviću dr.med. i dr.sc. Spomenki Manojlović dr.med. na prikupljenim uzorcima i suradnji tijekom objave mojeg prvog znanstvenog rada.

... to the members of Parish/Roberts Empire, especially to Dr Jo Parish, for giving me the last chance to enjoy all the charms of student exchanges and for your selfless help. To Dr Sally Roberts, for every discussion and smile that the word 'DLG' would bring to your face! To Jack, for devoting your time to teach me new things and not freaking out for using your bench! To Megan, Kamini and Molly for your dedicated ring search and all the talks. To all other members, great scientists and even better laser-tag partners, for accepting me as your own and made this time unforgettable!

... najdražim prijateljima, na neograničenoj potpori i vjeri u životu! Hvala na svakom saslušanom jadikovanju o neuspjelim pokusima i što ste tolerirali moju pasivnu društvenost, posebno tijekom ove godine, i pritom niste odustali od mene!

Najposebnije hvala

... mojim roditeljima, Tanji i Jurici, mojim čvrstim osloncima u svakodnevnom životu i životnoj snazi. Hvala vam što ste me naučili da budem ono što jesam, da je važnije ono "tko si" od onoga "što si". Hvala mojim sestrama Petri i Marti te braći Stipi i Luki, na beskrajnoj ljubavi, razumijevanju, podršci i vjeri u mene! Svima vam hvala što ste bili moja stijena i što mi niste dopustili da odustanem kada bi postalo teško. Bez vas sada ne bih bila tu gdje jesam! Bolju obitelj nisam mogla niti sanjati! ♡

... Luki, što si bio uz mene na dijelu ovog putovanja kada je odustajanje često bila prihvatljiva misao. Tvoje strpljenje, ljubav i ohrabrenje su ga malkec olakšalili. Veselim se idućim zajedničkim koracima! ♡

Znanost može postavljati granice znanju, ali ne bi trebala postavljati granice mašti.

— Bertrand Russel

Science may set limits to knowledge but should not set limits to imagination.

— Bertrand Russel

This doctoral thesis was prepared at the Ruđer Bošković Institute, under the guidance of Vjekoslav Tomaić, PhD, senior research associate, as part of the postgraduate doctoral study of Biology at the Biology Department of the Faculty of Science, University of Zagreb.

The dissertation was prepared with the support of The Croatian Science Foundation within the program "Young Researchers' Career Development" and within the project "Elucidating the HPV E6/E7 Oncogenic Functions at Different Anatomical Sites" (supervisor: Vjekoslav Tomaić, PhD).

Supervisor

Vjekoslav Tomaić was born in Zagreb, Croatia. In 2001, he graduated in experimental biochemistry from Washington College in the State of Maryland, USA. After that, as a graduate student, he began studying human papillomaviruses (HPVs) in Richard Schlegel's laboratory at Georgetown University, Washington D.C., USA. In 2009 he received his PhD in Natural and Biomolecular Sciences researching HPVs at the International Center for Genetic Engineering and Biotechnology (ICGEB) in Trieste, Italy in collaboration with the Open University in Milton Keynes, UK, under the mentorship of Lawrence Banks and co-mentorship of John Doorbar, University of Cambridge. After obtaining his PhD, he continued his postdoctoral training at ICGEB in the field of viral oncology, researching HPV infection, productive viral cycle and HPV-induced malignant transformation. In 2015, he acquired the title of adjunct assistant professor. In 2016 he joined the Department of Molecular Medicine of the Ruđer Bošković Institute. He started a group within the Laboratory of Molecular Virology and Bacteriology with the aim to investigate the mechanisms of HPV-mediated malignancies, which better understanding could contribute to the development of new therapies. Furthermore, a part of his research is focused on discovery of new biomarkers that could predict the development of the disease at early stages. He is a principal investigator of international projects, editor and reviewer in scientific journals, organizer of several international scientific conferences and has received numerous awards for his scientific work.

University of Zagreb
Faculty of Science
Department of Biology

Doctoral thesis

Effects of human papillomavirus 16 (HPV16) E6 oncoprotein on cell polarity regulators in head and neck cancers

Lucija Lulić

Ruđer Bošković Institute

Human papillomaviruses (HPVs) are significant contributors to the global cancer burden by causing cancers at various anatomical sites, particularly in anogenital and head and neck (HN) area. A unique E6 feature of all oncogenic HPVs is the ability to target DLG1 and SCRIB proteins which play roles in the regulation of cell growth and polarity. Their contribution to the onset of HPV-induced HN malignancy is still unknown. Therefore, the potential impact of 16E6 on DLG1 and SCRIB protein localization and expression were investigated in keratinocytes derived from HN and genital areas, organotypic 3D raft cultures and oropharyngeal squamous cell carcinomas (OPSCCs). Obtained results suggest that 16E6 contributes to DLG1 delocalization but not exclusively, thus implying that any deregulation of DLG1 can contribute to malignancy. Additionally, 16E6 caused SCRIB upregulation in the cell lines and 3D raft cultures, suggesting its requirement for E6 protein stability. Interestingly, significant SCRIB downregulation was observed with the progression of OPSCCs, and was more evident in HPV16 OPSCCs, indicating that its loss could serve as a potential late-stage marker in oropharyngeal carcinogenesis.

(142 pages, 40 figures, 14 tables, 322 references, original in English)

Key words: HPV, OPSCC, E6, DLG1, SCRIB, cell polarity

Supervisor: Vjekoslav Tomaić, PhD

Reviewers: Ivana Ivančić Baće, PhD

Joanna Parish, PhD

Dijana Škorić, PhD

Sveučilište u Zagrebu
Prirodoslovno-matematički fakultet
Biološki odsjek

Doktorski rad

Utjecaj onkoproteina E6 papilomavirusa čovjeka tipa 16 (HPV16) na regulatore stanične polarnosti u tumorima glave i vrata

Uvod:

Virusne infekcije prepoznate su kao jedan od čimbenika rizika za razvoj karcinoma te se povezuju s 12-20% tumora diljem svijeta. Jedni od njih su i papilomavirusi čovjeka (eng. human papillomavirus, HPV) koji uzrokuju više od 600 000 karcinoma godišnje. HPV infekcije povezane su s gotovo 100% slučajeva raka vrata maternice koji je još uvijek na visokom četvrtom mjestu po učestalosti i smrtnosti. Osim toga, infekcije visokorizičnim mukoznim HPV tipovima povezane su i s oko 70% anogenitalnih karcinoma, a sve je više studija koje ih povezuju i s karcinomima pločastog epitela glave i vrata (engl. head and neck squamous cell carcinoma, HNSCC), šestom najčešćom zloćudnom bolesti diljem svijeta. HNSCC čine rak usana i usne šupljine, nazofarinksa, orofarinksa, grkljana i hipofarinksa, ali HPV se povezuje s 40-60% karcinoma pločastih stanica orofarinksa (eng. oropharyngeal squamous cell carcinoma, OPSCC) te samo s oko 5% karcinoma glave i vrata izvan područja orofarinksa. Iako su HPV infekcije najčešće spolno prenosive infekcije, u većini slučajeva imunosni sustav prepoznaje zaražene stanice te neutralizira infekciju unutar nekoliko mjeseci do dvije godine od početne infekcije. U suprotnom, kada infekcija HPV-om opstane kroz dulje vrijeme i postane kronična, zaražene osobe su pod povećanim rizikom za razvojem malignih promjena. Ovaj je proces od primarne infekcije do razvoja raka dobro definiran u vratu maternice. Dva glavna virusna onkoproteina, E6 i E7, izravno su odgovorna za razvoj zloćudnih bolesti uzrokovanih HPV-om. Oni kooperativno ciljaju različite stanične puteve uključene u regulaciju staničnog ciklusa i apoptoze. Poznato je da vežu i usmjeravaju za razgradnju tumorske supresore, p53 i pRb. Osim što potiče razgradnju p53, brojne studije su pokazale da E6 ima mnoge druge stanične mete uključujući i proteine koji sadrže PDZ (PSD95-Dlg1-zo-1) domene, module proteinskih interakcija uključene u održavanje stanične homeostaze. Neki od najbolje okarakteriziranih E6 interaktora su proteini koji sadrže PDZ domene iz kompleksa Scribble: Scribble (SCRIB) i Discs Large 1 (DLG1). Posljedično, E6 potiče njihovu razgradnju proteasomom. Obzirom da DLG1 i SCRIB imaju ključnu ulogu u uspostavljanju i održavanju

polariteta stanica, stanice koje eksprimiraju E6 formiraju slabije stanične kontakte i rastu na neorganiziraniji način. Samim time, posljedice ovih interakcija doprinose razvoju kasnijih stadija E6-uzrokovanih bolesti. Proteini DLG1 i SCRIB također su okarakterizirani i kao tumorski supresori, a do sada je njihovo ponašanje istraženo u karcinomima debelog crijeva. Osim toga, promjene proteina DLG1 primijećene su i u razvoju raka vrata maternice. Neke studije upućuju na to da ekspresija i lokalizacija DLG1 variraju u lezijama povezanim s HPV-om, što sugerira na njegovu ulogu u progresiji cervikalnih intraepitelnih lezija niskog stupnja. Zanimljivo je da je isti proces od početne infekcije do razvoja raka u području glave i vrata još uvijek neistražen, ali čini se da je znatno kraći nego u vratu maternice. Isto tako, gotovo 70% slučajeva raka vrata maternice i prekanceroznih lezija uzrokovano je dvama tipovima, HPV16 i HPV18, dok se ostatak pripisuje drugim visokorizičnim tipovima HPV-a. Interesantno, 90-95% tumora orofarinksa uzrokovano je isključivo HPV-om tipa 16. Ove varijacije u tipovima HPV-a i njihovog uzrokovanja zloćudnih promjena potencijalno mogu biti posljedica različitog intenziteta interakcija E6 s proteinima DLG1 i SCRIB, ovisno o anatomskom području. Prema tome bi razjašnjavanje funkcije onkoproteina E6 kao i potencijalnih odstupanja njegova učinka na navedene proteine dodatno pridonijelo boljem razumijevanju uloga ova dva tumorska supresora u procesu HPV-posredovane i neposredovane tumorigeneze u području glave i vrata. Također bi moglo dodatno razjasniti njihov potencijalni značaj kao biljega za predviđanje razvoja bolesti u ranim fazama.

Ciljevi istraživanja:

Proteini DLG1 i SCRIB prethodno su okarakterizirani kao stanične mete onkoproteina E6. Međutim, dosadašnja istraživanja pokazala su da onkoproteini E6 različitih tipova HPV-a imaju različite afinitete vezanja proteina DLG1 i SCRIB, odnosno, HPV16 E6 preferencijalno veže protein SCRIB dok je DLG1 učinkovitije vezan od strane HPV18 E6. Također, njihove su promjene u staničnoj lokalizaciji i ekspresiji pokazane u različitim karcinomima neovisno o prisustvu HPV-a što ukazuje na njihovu važnost u procesu onkogeneze općenito. Obzirom da je HPV16 prevladavajući tip u HPV-pozitivnim tumorima glave i vrata, primarni je cilj ovog istraživanja bio ispitati razlike u utjecaju onkoproteina 16E6 na DLG1 i SCRIB u stanicama izoliranim iz područja glave i vrata te anogenitalne regije, a zatim i u produktivnom ciklusu virusa proučavanog u modelu orofarinksa. Nadalje, cilj je bio i istražiti potencijalne promjene u ponašanju proteina DLG1 i SCRIB u arhivskim uzorcima tumora orofarinksa ovisno o prisustvu HPV16.

Da bi se do toga došlo, potrebno je:

- Uspostaviti prethodno imortalizirane stanične linije keratinocita izoliranih s različitih anatomskih mjesta; keratinocite zubnog mesa (eng. immortalized normal oral keratinocytes, iNOK), keratinocite tonzila čovjeka (eng. immortalized human tonsilar keratinocytes, iHTK) i keratinocite prepucija čovjeka (eng. immortalized human foreskin keratinocytes, iHFK) u kojima su stabilno eksprimirani onkoproteini E6/E7.
- Istražiti utjecaj onkoproteina E6 na intenzitet vezivanja te razinu proteina DLG1 i SCRIB u uspostavljenim staničnim linijama keratinocita.
- Istražiti promjene u staničnoj lokalizaciji i distribuciji DLG1 i SCRIB uzrokovane onkoproteinom 16E6 u uspostavljenim staničnim linijama keratinocita.
- Usporediti utjecaj razine transkripcije 16E6 na razinu transkripcije DLG1 i SCRIB u primarnim staničnim linijama keratinocita tonzila i prepucija (HTK i HFK) kao i u staničnim linijama izoliranim iz HPV-negativnih i HPV16-pozitivnih tumora orofarinksa.
- Povezati promjene na razinama transkripcije s promjenama u lokalizaciji proteina DLG1 i SCRIB tijekom produktivnog ciklusa HPV16 u organotipskim 3D *raft* kulturama HTK stanica.
- Razjasniti biološki utjecaj 16E6 na distribuciju proteina DLG1 i SCRIB u prikupljenim parafinskim uzorcima HPV-negativnih i HPV16-pozitivnih tumora orofarinksa.

Materijali i metode:

Istraživanje je započelo uspostavom staničnih linija imortaliziranih keratinocita izoliranih s različitih anatomskih područja (iNOK, iHTK te iHFK) u kojima se željelo uspostaviti stabilnu ekspresiju onkoproteina E6/E7 HPV tipa 16. Korišteni su različiti pristupi; „ubacivanje“ gena koristeći CRISPR-Cas9 Knock-in sustav, konstruiranje lentivirusa koji eksprimiraju onkoprotein E6 HPV tipa 16 te transfekciju cjelokupnim genomima HPV16. Uspješnost kreiranja *Knock-in* i lentivirusnog vektora provjerena je umnažanjem lančanom reakcijom polimerazom (eng. polymerase chain reaction, PCR) gena HPV16 E6 te sekvenciranjem dok je uspješnost uspostave linija dokazana umnažanjem gena p53 i HPV16 E6 metodom PCR te Western blot metodom detekcije proteina p53. Kao kontrola u svim pokusima, korištene su stanice HPV16-pozitivnog raka vrata maternice CaSki te stanice HPV-negativnog raka vrata maternice C33A. Kako bi se istražile potencijalne razlike u vezivanju onkoproteina E6 s proteinima DLG1 i SCRIB ovisno o

anatomskoj regiji, proveden je esej interakcija metodom GST *pull-down*. Nadalje, ispitan je i utjecaj onkoproteina E6 na endogenu ekspresiju proteina DLG1 i SCRIB u uspostavljenim staničnim linijama keratinocita. Utjecaj E6 na lokalizaciju istih istražen je upotrebom imunofluorescencije i konfokalne mikroskopije, a potvrđen je metodom frakcioniranja stanica koristeći komercijalno dostupan set kemikalija. Nakon pokusa provedenih na uspostavljenim staničnim linijama keratinocita, utjecaj onkoproteina 16E6 na DLG1 i SCRIB istražen je i u primarnim keratinocitima HTK i HFK. Istražen je utjecaj na transkripcijskoj razini koristeći reverznu transkripciju i kvantitativni PCR (eng. reverse transcription quantitative polymerase chain reaction, RT-qPCR). Kao kontrole, korištene su stanice HPV-negativnog tumora jezika CAL27 i SCC040 te stanice HPV16-pozitivnog tumora jezika SCC104 i SCC147. Iste primarne stanice HTK korištene su za uspostavu organotipskih *3D raft* kultura u kojima je praćen utjecaj 16E6 na promjene DLG1 i SCRIB na proteinskoj razini tijekom produktivnog ciklusa virusa, koristeći metodu imunofluorescencijske histokemije. Za određivanje statističke značajnosti, provedena je analiza varijance (eng. analysis of variance, ANOVA). Nadalje, u ovom je istraživanju provedena i analiza utjecaja E6 na proteine DLG1 i SCRIB u arhivskim uzorcima tumora orofarinksa uklopljenima u parafin (eng. formalin fixed paraffin embedded, FFPE). Svi uzorci bili su podijeljeni u skupine obzirom na prisutnost i dokazanu aktivnost HPV-a nakon provedene genotipizacije metodom PCR koristeći specifične početnice za umnažanje dijelova HPV-genoma. U navedenim uzorcima je imunohistokemijski istražena ekspresija biljega koji se trenutno najviše koristi, proteina p16, a zatim i ekspresija proteina DLG1 i SCRIB. Kruskal–Wallis test, a zatim i Dunn podtest za višestruko uspoređivanje korišteni su za evaluaciju mogućih značajnih razlika između testiranih grupa uzoraka tumora orofarinksa.

Rezultati i rasprava:

Stanične linije imortaliziranih keratinocita koje stabilno eksprimiraju onkoproteine E6/E7 HPV tipa 16 uspostavljene su radi usporedbe utjecaja onkoproteina E6 na proteine DLG1 i SCRIB u staničnim modelima pojedinih anatomskih područja. Obzirom da onkoproteini E6 razgrađuju tumorski supresor p53, uspješnost ekspresije virusnih onkoproteina potvrđena je metodom Western blot koja je pokazala smanjenje razine proteina p53 u prisustvu onkoproteina E6. Nadalje, provjereno je i postoje li razlike u vezivanju DLG1 i SCRIB s onkoproteinom E6 ovisno o anatomskom području i tipu HPV-a. Prema dobivenim rezultatima, HPV16 E6 veže SCRIB s većim afinitetom dok HPV18 E6 jače veže DLG1, što je u skladu s rezultatima brojnih prethodnih

istraživanja, no, zanimljivo je da je afinitet vezivanja ostao nepromijenjen u imortaliziranim stanicama izoliranim s različitih anatomskim područja. Obzirom da je preferencija stanične mete ostala nepromijenjena, a da je HPV16 prevladavajući tip virusa u tumorima glave i vrata, dalje je istraživan utjecaj onkoproteina E6 HPV tipa 16 na ekspresiju i lokalizaciju proteina DLG1 i SCRIB. Prema dobivenim rezultatima, čini se da nije bilo značajne razlike u ekspresiji DLG1 proteina u prisustvu 16E6 što je kontradiktorno studijama koje su pokazale da E6 potiče razgradnju proteina DLG1. Međutim, većina tih studija provedena je u uvjetima prekomjerne ekspresije ili u prisustvu HPV18 E6. Nadalje, dobiveni rezultati ovog doktorskog rada su u skladu sa studijom provedenom u sličnim uvjetima odnosno kada je praćen utjecaj E6 na razinu endogeno eksprimiranog DLG1. Međutim, male promjene u prisustvu E6 uočene su na transkripcijskoj razini DLG1 - u stanicama genitalnog podrijetla HFK, u kojima je došlo do povećanja razine transkripcije DLG1 u većoj mjeri nego u stanicama HTK podrijetla iz orofarinksa. Nadalje, ovo je istraživanje pokazalo da prisustvo HPV16 E6 potiče promjenu lokalizacije DLG1 neovisno o anatomskom podrijetlu stanica. Ovakvi su rezultati u skladu sa studijom koja pokazuje smanjeni membranski DLG1 sa značajno povišenim citoplazmatskim razinama u cervikalnim neoplazijama visokog stupnja. Zanimljivo je da veće promjene distribucije nisu zabilježene u pokusima frakcioniranja. Razlog tome može biti nemogućnost razdvajanja staničnih i jezgrinih membrana pokusima frakcioniranja kao i mogućnost nespecifičnog bojanja u pokusima imunofluorescencije koje može doprinijeti lažno pozitivnom signalu. Suprotno, povećanje razine proteina SCRIB zabilježeno je u prisustvu HPV16 E6 neovisno o anatomskoj regiji, što je uočeno i na transkripcijskoj razini. Rezultati su u suprotnosti sa studijom koja je pokazala da HPV16 E6 potiče obilježavanje proteina SCRIB ubikvitinom te razgradnju posredovanu proteasomom. Međutim, prethodne su studije uglavnom provedene u uvjetima prekomjerne ekspresije proteina SCRIB i E6. Kako je SCRIB membranski protein koji stupa u interakcije s brojnim staničnim proteinima poput vimentina, moguće je da takva interkacija ima zaštitničko djelovanje i npr. mijenja konformaciju proteina SCRIB koja više ne odgovara vezivanju onkoproteina E6. Nadalje, pokazano je da je prisutnost SCRIB potrebna za povećanje stabilnosti E6, pa ovakav učinak stabilizacije može pridonijeti u provođenju određenih funkcija onkoproteinu E6 koje su bitne za rane faze infekcije. Zanimljivo je da postoje studije koje protein SCRIB karakteriziraju i kao onkogen što bi objasnilo povećanje zabilježeno u prisustvu onkoproteina E6. Shodno tome, ovdje su istraživane i potencijalne promjene u DLG1 i SCRIB vezane uz produktivni ciklus virusa s ciljem povezivanja uočenih

razlika s procesom razvoja zloćudnih promjena. Produktivni ciklus virusa strogo je vezan uz diferencijaciju keratinocita, stoga su promjene praćene u organotipskim *3D raft* kulturama keratinocita tonzila koji se koristi kao model za ovakav tip istraživanja. Uočena je promjena lokalizacije proteina DLG1 i SCRIB u bazalnim i parabazalnim slojevima *3D raft* kultura iz membrana u citoplazmu. Razlog tome može biti jača ekspresija onkoproteina E6 u donjim slojevima epitela koji potiče njihovu translokaciju radi potencijale razgradnje, sporijeg zacjeljivanja mikrooštećenja, bržeg širenja lezija ili, ponovno, radi osiguravanja stabilnosti samog E6. Dosadašnji rezultati istraživanja u staničnim kulturama i *3D* organotipskim *raft* kulturama mogu poslužiti kao indikatori promjena u stadijima koje prethode zloćudnoj promjeni no ne daju konkretne informacije o potencijalnim promjenama u stvarnim tumorima. Prema tome, potencijalne razlike istražene su i u prikupljenim arhivskim uzorcima tumora orofarinksa. Zanimljivo, čini se da do promjene lokalizacije DLG1 dolazi s progresijom HPV-negativnih tumora orofarinksa. Međutim, promjena je veća u prisustvu onkoproteina 16E6 što implicira da ovakav fenotip doprinosi razvoju zloćudnih promjena neovisno o HPV-u. Nadalje, značajno je smanjenje razine proteina SCRIB uočeno s progresijom HPV-negativnih tumora orofarinksa dok je isto bilo još uočljivije u prisutnosti HPV16. Iz svih korištenih sustava može se zaključiti da onkoprotein 16E6 ima veći utjecaj na svoju preferencijalnu staničnu metu SCRIB. Dobiveni rezultati sugeriraju da određene oscilacije ekspresije i/ili lokalizacije dovode do poremećaja normalnih funkcija regulatora stanične polarnosti i tumorskih supresora DLG1 i SCRIB, što vjerojatno doprinosi razvoju bolesti u području glave i vrata, posebice u prisustvu HPV-a.

Zaključci:

Iz eksperimenata provedenih na imortaliziranim keratinocitima izoliranim s različitih anatomskih mjesta, primarnim keratinocitima, organotipskim *3D raft* kulturama i uzorcima tumora orofarinksa izvedeni su sljedeći zaključci:

- Preferencija vezivanja onkoproteina E6 za DLG1 i SCRIB ostaje nepromijenjena u imortaliziranim keratinocitima bez obzira na anatomsko podrijetlo.
- HPV16 E6 nema utjecaja na endogenu ekspresiju DLG1 proteina, ali utječe na promjenu njegove stanične lokalizacije u imortaliziranim keratinocitima. Ovi učinci su najočitiji u stanicama iHFK.

- HPV16 E6 uzrokuje povećanje razine endogenog proteina SCRIB, ali i male promjene u lokalizaciji što nije ovisno o anatomskom mjestu.
- HPV16 E6 inducira povećanje ukupne razine DLG1 mRNA u primarnim stanicama HFK, dok u primarnim stanicama HTK nije vidljiv takav učinak.
- HPV16 E6 povećava razinu SCRIB mRNA u primarnim stanicama HTK i HFK
- HPV16 uzrokuje promjene u staničnoj lokalizaciji proteina DLG1 i SCRIB s membrana u citoplazmu u bazalnom i parabazalnom sloju organotipskih *3D raft* kultura. Taj je pomak bio još očitiji s produljenjem vremena kultiviranja stanica HPV16-HTK od kojih su *3D raft* kulture napravljene.
- Promjena lokalizacije DLG1 iz membrane u citoplazmu stanica povećava se s napredovanjem HPV-negativnih tumora orofarinksa, ali je učinak veći u prisutnosti HPV16.
- Tijekom progresije HPV-negativnih tumora orofarinksa dolazi do malih promjena u lokalizaciji proteina SCRIB s membrana u citoplazmu.
- Razine proteina SCRIB smanjuju se s napredovanjem HPV-negativnih tumora orofarinksa, a ovo je smanjenje značajnije u prisutnosti HPV16.

(142 stranice, 40 slika, 14 tablica, 322 literaturna navoda, jezik izvornika engleski)

Ključne riječi: HPV, OPSCC, E6, DLG1, SCRIB, cell polarity

Mentor: Vjekoslav Tomaić, doc. dr. sc.

Ocjenjivači: Ivana Ivančić Baće, izv. prof. dr. sc.

Joanna Parish, prof. dr. sc.

Dijana Škorić, prof. dr. sc.

CONTENTS

1 INTRODUCTION

1.1 Head and neck cancer (HNC)

Head and neck squamous cell carcinomas (HNSCCs) are the most common type of head and neck cancers (HNCs), making up more than 90% of cases and those include malignancies of the upper aerodigestive tract that occur from the mucosal epithelium (Johnson et al., 2020). Years ago, HNSCCs were considered a single disease, which evolves from the same cell type origin. However, after extensive research, divergence in epidemiological trends as well as phenotypical patterns i.e., different tumor behavior, severity, and survival, clarified that HNSCCs in fact represent a heterogenous group of malignancies (Olshan, 2010; Pai and Westra, 2009). These include cancers of the lip and oral cavity, nasopharynx, oropharynx, larynx, and hypopharynx (Cramer et al., 2019), as presented in **Figure 1.**

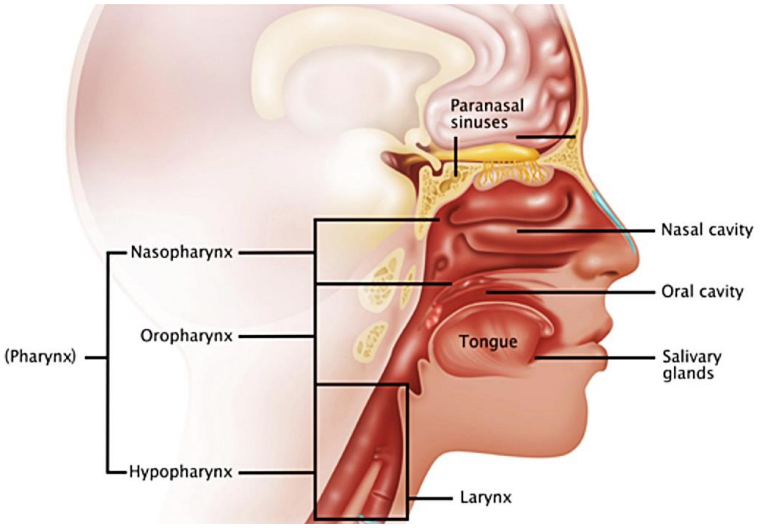

Figure 1. Common anatomical sites of head and neck malignancies. Most frequent cancers occur at paranasal sinuses, nasal cavity, oral cavity, tongue, salivary glands, larynx, and pharynx (including the nasopharynx, oropharynx, and hypopharynx). Adopted from *https://news.cancerconnect.com/head-neck-cancer/overview-of-head-neck-cancer* (accessed 03.02.2022.)

1.1.1 Epidemiology and etiology of HNCs

With a total of 878 348 new cases and 444 347 deaths in 2020, HNCs remain a substantial disease, accounting for approximately 5% of all human cancers. Tracking the epidemiology of HNCs over extended periods of time has shown that these tumors are rising both in incidence and mortality. By 2040, both aspects are estimated to increase by roughly 1.5 times, which will account for approximately 1 288 168 new cases and result in 669 770 deaths (**Figure 2.**).

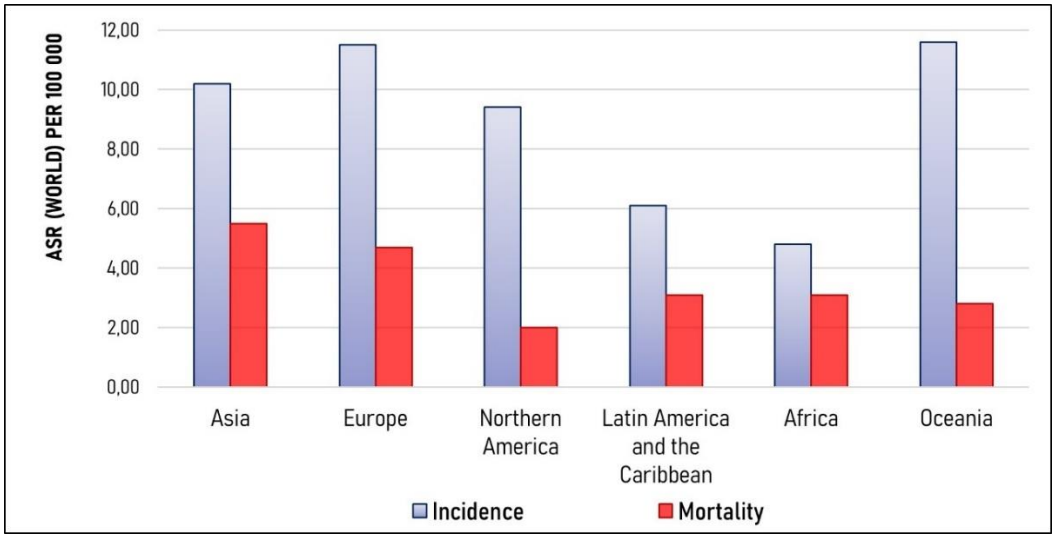

Figure 2. Global incidence and mortality of HNCs. The estimated age-standardized rate of HNCs incidence (blue) and mortality (red) worldwide show combined data for both, male and female. The data represents lip and oral cavity, nasopharyngeal, oropharyngeal, hypopharyngeal and laryngeal cancers from GLOBOCAN, 2020. *https://gco.iarc.fr/today/home*, (accessed 25.02.2022.)

Interestingly, males are affected significantly more than females, with a range from 3:1 to 4:1. Epidemiological studies have unveiled a wide range of HNSCC risk factors including tobacco and alcohol abuse, exposure to carcinogens, diet, poor oral hygiene, family and/or medical history and infection agents (IARC, 2007; Johnson et al., 2020; Pai and Westra, 2009). Of those, tobacco smoking represents the major risk factor and correlates with the intensity and duration of smoking. However, some studies have found a strong association between HNCs and smokeless use of tobacco products like chewing a betel quid (Chen et al., 2008). Interestingly, more recent studies analyzed the impact of e-cigarettes and found that lesions of the oral mucosa were more frequent in e-cigarette users than in former smokers. Nevertheless, epidemiological studies on e-cigarettes and HNC are yet to be conducted (Aupérin, 2020). Alcohol abuse was recognized as a risk factor for oropharyngeal and hypopharyngeal cancers. However, heavy alcohol consumption is strongly synergistic with tobacco use since alcohol, as a chemical solvent, enhances and extends effects of carcinogens in tobacco smoke (Olshan, 2010; Pai and Westra, 2009). Along with those, novel risk factors for a subset of HNCs were shown to be infections with oncogenic viruses, including human papillomaviruses (HPVs), which have been mostly associated with oropharyngeal squamous cell carcinoma (OPSCC) and the Epstein-Barr virus (EBV), which was shown to be linked with nasopharyngeal carcinoma (Brockstein and Masters, 2003). Additionally, Herpes simplex virus-1

is proposed to act as a potential risk factor, but together with tobacco and alcohol abuse or in a co-infection with other oncogenic viruses (Wołącewicz et al., 2019).

1.1.2 Clinical presentation and TNM staging of HNCs

Although HNC subtypes are clinically, histologically, and molecularly distinct, they are all represented with similar symptoms. Typical symptoms usually include swelling or a sore that does not heal, a red or white patch in the mouth, a painful or even painless mass in the HN area, and hoarseness. The diagnosis usually starts with a physical exam that relies on the type of cancer suspected, signs and symptoms, patient's age, general health, and the prior medical exams. It involves endoscopy, biopsy, biomarker testing and imaging (Argiris et al., 2008). Cancer staging and grading are then used to predict the clinical behavior, potential outcome of malignancies and to establish appropriate treatment plan. Cancer grade represents the degree of cancer cells' abnormality compared to healthy cells or a measure of differentiation and is usually graded 1-3. Grade 1 (G1) denotes well-differentiated cancers, meaning that cancer cells are morphologically similar to healthy cells and tissue. Grade 2 (G2) stands for moderately differentiated cancers where cancer cells are somewhat abnormal, while grade 3 (G3) represents poorly differentiated or undifferentiated cancer, in which cancer cells look completely abnormal and have the highest proliferation rate (**Figure 3.**). These cancers typically grow and spread faster than the lower grade cancers (Espina, 2017).

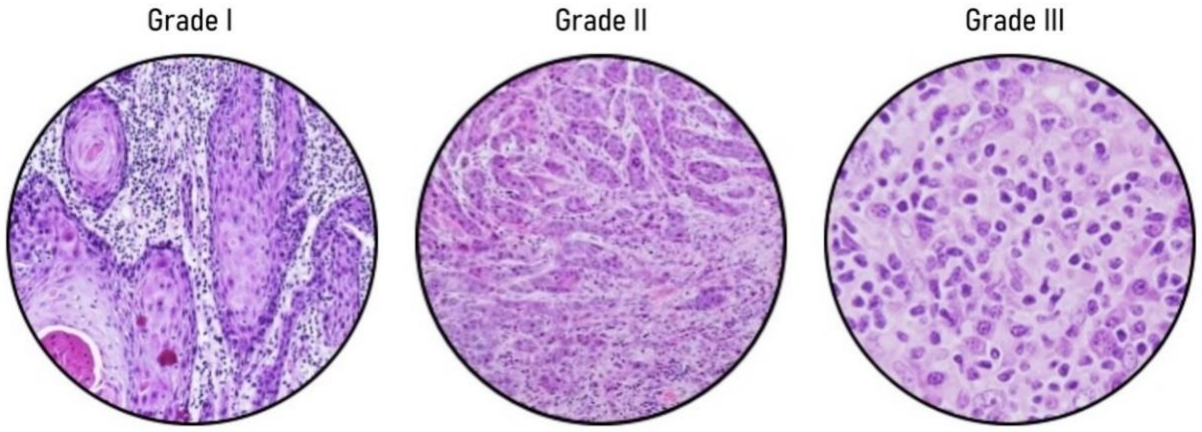

Figure 3. Histopathological view of oral cancer grades 1-3. In Grade 1 or well-differentiated cancers, cancerous cells are similar to healthy cells. However, in Grade 2 or moderately differentiated cancers, malignant cells start to lose their normal morphology and become somewhat abnormal. The highest grade is grade 3 which represents poorly differentiated or undifferentiated cancers in which cancer cells look completely abnormal.

While different cancer grades represent various abnormalities of cancer cells, cancer stages define cancer size and how far it has spread from the primary site. There are several different staging systems, yet the TNM staging system is widely used. It is a three-category system that involves: T, the characteristics of the tumor at the primary site, which can be based on a size and/or location; N, the degree of regional lymph node involvement; and M, the absence or presence of distant metastases. The specific TNM status of each patient is then tabulated to give a numerical status of Stage I, II, III, or IV with stage IV being the most severe stage (Espina, 2017; Zanoni et al., 2019).

1.1.3 Treatment of HNCs

The HNC treatment is fundamentally complex since it requires a multidisciplinary approach for optimal decision making, treatment planning, posttreatment care, support, and overall outcome. Therefore, medical and radiation oncologists, maxillofacial surgeons, radiologists, speech therapists, social workers, psychologists, plastic and/or reconstructive surgeons, and dentists, all need to be involved. Moreover, the role of each is being redefined as new improvements in treatment are being discovered and implemented (Lo Nigro et al., 2017). HNCs are usually treated with surgical dissection, followed by adjuvant radiation therapy (RdT) or chemotherapy (CT) plus radiation (known as chemoradiotherapy or CRdT). This depends on the disease stage, location of the lesion and the functional deficit that may occur. Lately, a targeted therapy is becoming a part of the HNC treatment plan (Johnson et al., 2020). Nowadays, Cetuximab, an immunoglobulin-G1 chimeric monoclonal antibody directed against EGFR, is the only targeted therapy known to contribute to a better locoregional control, progression-free survival, and overall survival. This was shown to be the case both in the localized advanced stage cancer (Bonner et al., 2006) and in the platinum-resistant recurrent and/or metastatic cancer in combination with CT rather than RdT alone (Vermorken et al., 2008). Cetuximab is usually used in the combination with RdT in HPV-negative HNSCCs where comorbidities prevent the use of cytotoxic chemotherapy. Clinical studies in HNC treatment are now more focused on incorporation of other agents like immune checkpoint inhibitors including Nivolumab and Pembrolizumab, which were approved by the Food and Drug Administration (FDA) for treatment of recurrent or metastatic HNSCCs, and Pembrolizumab as the primary treatment for unresectable cancers (Johnson et al., 2020).

1.1.4 Diagnostic markers for HNCs

In recent years, with the continuous advancement of diagnosis and treatment, the mortality of HNC patients seems to gradually decrease, yet its absolute number should not be underestimated. According to the reports from 2010-2016, 5-year survival of HNC patients varied depending on cancer localization. The highest survival rate of 92% was related to lip cancer patients, while the lowest rate of only 32% falls on hypopharyngeal cancer patients (https://www.cancer.org, accessed 12.11.2021.) due to their late diagnosis. Importantly, the overall survival benefits from the appropriate treatment accompanied with smoking and alcohol consumption cessation (Wang et al., 2021). Nevertheless, finding proper biomarkers for early diagnosis of each subtype of HNCs could improve both the prognosis and survival rates. Therefore, several biomarkers with different approaches have been investigated so far (Konings et al., 2020). Promoter hypermethylation is correlated with gene silencing in cancer and is suggested to be an early event in carcinogenesis. This phenotype was observed in HNC patients too, making it a great potential biomarker. Notably, viral infections can induce aberrant DNA methylation, leading to carcinogenesis, and HPV-associated HNSCCs tend to harbor a higher amount of hypermethylated DNA than HPV-negative ones. In addition, DNA methylation could serve as a marker to classify subgroups based on outcome (Nakagawa et al., 2021). More precisely, HPV-positive cancers are suggested to be driven by the promoter hypermethylation in tumor suppressor genes. Especially *CADM1* and *TIMP3*, which seem to be significantly more frequently hypermethylated in HPV-positive and *CHFR* in HPV-negative OPSCCs (Kempen et al., 2014). Though, despite a high specificity of promoter hypermethylation as a biomarker, sensitivity is quite low, so additional research should be conducted to provide more suitable diagnostic tools (Guerrero-Preston et al., 2011; Konings et al., 2020). Additionally, EBV-positive nasopharyngeal and HPV-positive oropharyngeal cancers are usually easily diagnosed due to a combination of high-specificity DNA-load detection together with EBV (Leung et al., 2004) and HPV (Kreimer et al., 2018) seropositivity, respectively. The analysis of DNA-ploidy has also been investigated as a potential biomarker since it allows carcinoma detection months before it can be validated by immunohistochemistry (Hemmer and Kreidler, 1990). Previous analyses revealed that HPV-positive HNSCCs had a significantly smaller nuclei than HPV-negative ones. Therefore, they proposed that the core classification can provide information on the ploidy of HNSCCs and that HPV-positive tumors represent a distinct morphological and genetic carcinoma subtype (Kotb et al., 2010). However, all these studies were

conducted on a rather small number of cases. Also, conventional swabs are quite hard to be used for out-of-reach sites like oropharynx (Konings et al., 2020). Only a few studies so far have investigated metabolites in tissues or body fluids as potential biomarkers and have found that plasma and salivary cortisol levels were significantly higher in HPV-negative oral squamous cell carcinoma (OSCC) than in the controls (Bernabé et al., 2012). Two contradictory studies were published in 2019 and 2021; one proposed that there were significant differences in glycolytic metabolites between HPV-negative and HPV-positive HNSCCs (Fleming et al., 2019), while the other suggested that plasma metabolites related to glycolysis and mitochondrial oxidative phosphorylation may be biomarkers of HNSCC patient prognosis independent of HPV presence or smoking (Eldridge et al., 2021). Thus, future investigations should be conducted to provide more concrete results. Nevertheless, the biggest problems with metabolomics studies underlie in the fact that diet, age, lifestyle, sex, and environment all affect metabolite levels (Konings et al., 2020). Interestingly, microbiome changes were detected between healthy volunteers, patients with oral precursor lesions and oral cancer patients meaning that those differences could be potentially used for monitoring oral cancer progression (Lee et al., 2017). Despite all of this, numerous proteins were investigated as potential biomarkers since examining proteins remains the easiest and the cheapest technique. Moreover, the transformation from normal to abnormal cells carries along significant changes in cellular protein expression not only of cancerous cells, but also of surrounding healthy cells, connective tissue and infiltrating inflammatory cells. These include p50 and IκB proteins reported to be constitutively expressed in HNCs resulting in aberrant cell proliferation, survival and even metastasis. According to the reported results, the level of p50 was high at early stages of the disease and it has slightly decreased posttreatment (Gupta et al., 2016). Protein p50 is a functional subunit of NF-κB, whose activation seems to be regulated conversely by HPV16 oncoproteins - 16E7 inhibits its activation by blocking the upstream signaling (Spitkovsky et al., 2002), whilst 16E6 activates it through the PDZ-binding motif (James et al., 2006). Furthermore, differential gene expression profile analysis revealed that STAT3 and NF-κB target gene signatures could effectively distinguish HPV-positive from HPV-negative HNSCCs (Gaykalova et al., 2015). Similarly, RACK1 protein overexpression was shown to be correlated with the severity of the epithelial dysplasia and with the clinical stage of OSCC. Thus, RACK1 can be proposed as an important predictor of OSCC outcome (Wang et al., 2009). Despite numerous attempts, conventional diagnosis of HNCs nowadays is based on histopathological evaluation of

tissue sections including both biopsies and dissections. So far, p16 protein has been widely used. It is involved in cell cycle regulation and is considered as a tumor suppressor (Serrano, 1997) due to its modulations in multiple cancer types (**Figure 4.**). It has been studied intensively in several cancers, yet its expression varied from complete loss in gastrointestinal stromal tumor (Schneider-Stock et al., 2005), downregulation in bronchial lesions (Brambilla et al., 1999a) and non-small lung carcinoma (Brambilla et al., 1999b), to an obvious overexpression in colorectal adenoma carcinoma (Zhao, 2006), breast cancer (Milde-Langosch et al., 2001), and oral cancer (Buajeeb et al., 2008). Additionally, its overexpression is strongly associated with HPV infections since E7 oncoprotein binds and inactivates pRb and this inactivation releases p16 from its negative feedback control. Consequently, p16 is overexpressed in HPV-induced cancers such as cervical cancers and HNCs. Previous reports suggested that immunostaining of p16 overexpression allows precise identification of even small cervical intraepithelial neoplasia (CIN) or cervical cancer lesions in biopsies (Klaes et al., 2001; Lesnikova et al., 2009). The prognostic value of overexpressed p16 in cervical cancer has been evaluated for several years now. Interestingly, it was suggested that HPV16 and p16 overexpression together were associated with better survival since patients with p16-negative HPV-associated cervical cancer were older, presented with advanced disease and had worse prognosis (da Mata et al., 2021). Although p16 status is of great significance for cervical cancer screening, when used by itself it may not be sufficient for actual diagnosis. Ki-67 is a nuclear antigen that is present only in proliferating cells. It was shown that Ki-67 and p16 were positively correlated with the degree of cervical lesions and when combined for diagnosis, sensitivity and specificity were both at a high level (Shi et al., 2019). Additionally, p16 expression was examined in OPSCCs in the presence and absence of HPV showing minor divergences – about 13% of HPV-positive OPSCCs were p16-negative and *vice versa* (Dok and Nuyts, 2016; Golusiński et al., 2017). Taking all this into account, p16 overexpression should only be used as a surrogate marker to PCR or *in situ* hybridization (Mooren et al., 2014).

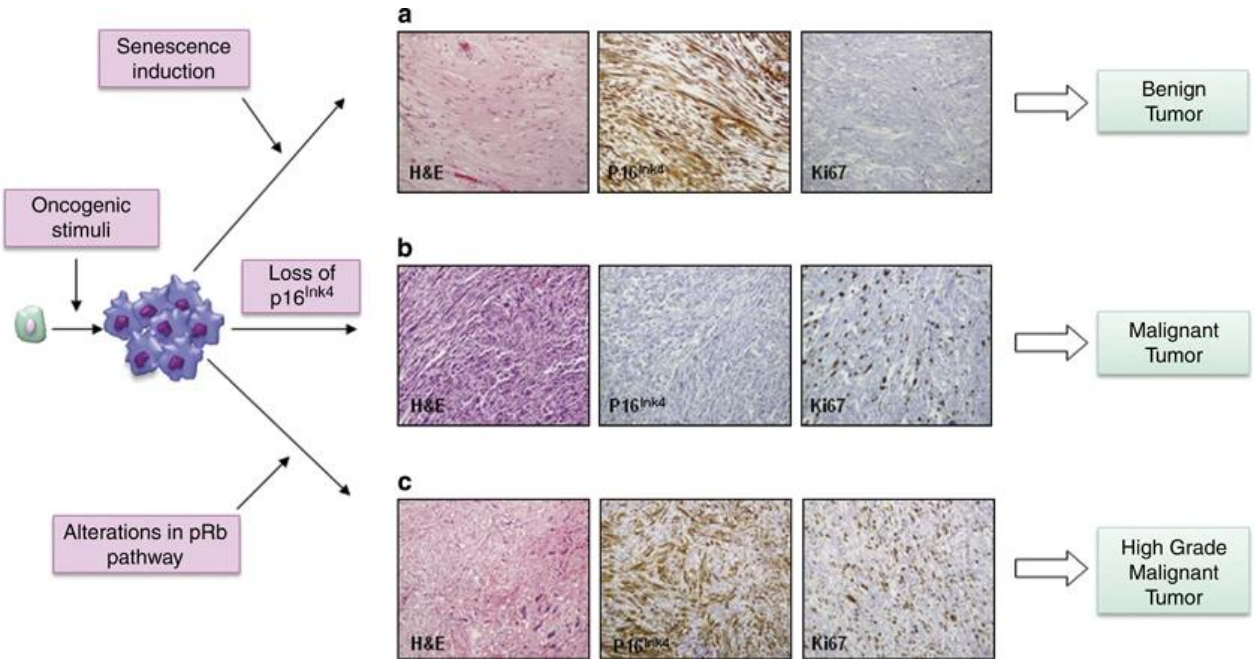

Figure 4. Schematic overview of p16 expression possibilities in human cancers. (a) p16 overexpression in Schwannoma benign lesions is associated with senescence induction in response to oncogenic stimuli. In this case very low Ki67 was observed. (b) Loss of p16 in malignant peripheral nerve sheath tumor showing high Ki67 staining. (c) p16 is overexpressed in high-grade undifferentiated sarcoma associated with pRb alterations. H&E: Hematoxylin/eosin staining. Adopted from (Romagosa et al., 2011).

1.2 Human papillomaviruses

1.2.1 History of human papillomaviruses

Knowing that most sexually active women and men will be infected with HPVs at least once in their lifetime, HPV infection is reasonably considered the most commonly sexually transmitted disease worldwide. However, other non-sexual modes of virus transmission have been reported including saliva exchange, skin-to-skin contact, perinatal fluid, and shared contaminated objects (Petca et al., 2020).

Papillomaviruses (PVs) are small DNA viruses named by the Latin word *papilla* meaning a wart or a nipple, which those infected cells form, and the Greek word *oma* meaning a tumor. They were first discovered back in 1907 by an Italian scientist Giuseppe Ciuffo who injected himself with the cell-free extract of warts just to prove that the growths were caused by an infectious agent. Even though warts were not considered as tumors at the time, his discovery of PVs as transmissible agents causing cytopathogenic changes was supported by numerous groups worldwide (IARC, 2007). Almost 70 years have passed since Ciuffo's discovery until HPV was shown to be associated with human malignancies based on the detection of HPV DNA in genital warts (Zur Hausen, 1976). At first, HPVs were considered as causative agents of anogenital cancers exclusively and of those,

HPV-induced cervical cancers are the most characterized. Cervical cancer development includes well-defined premalignant phases known as cervical intraepithelial neoplasia (CIN) and this is represented by a variety of histological abnormalities graded 1 to 3. CIN1 represents mild dysplasia limited to the basal layer of the epithelium, CIN2 refers to moderate dysplasia, whilst CIN3 features severe dysplasia and is considered as carcinoma *in situ*/precancer stage (Woodman et al., 2007). However, in 1983 HPV was detected in focal epithelial hyperplasia (FEH), and condyloma acuminatum (CA), oral squamous cell lesions, which led to the first hypothesis suggesting of a possible role of HPV infections in certain special types of OSCCs (Syrjänen et al., 1983). Only two years later, the first reports of the specific HPV types in tongue and other oral carcinomas were reported (Löning et al., 1985). All those studies indicated that some members of the PV family were important human carcinogens (**Figure 5.**), which demanded an increase in studies to elucidate HPV roles in human malignancies (Pešut et al., 2021).

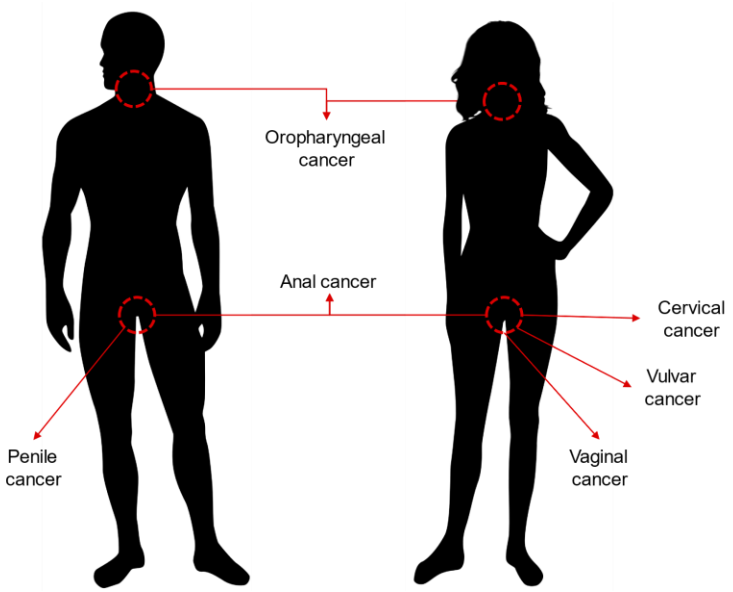

Figure 5. HPV-related cancer sites. HPV was reported to be responsible for more than 90% of anal and cervical cancers, about 70% of vaginal and vulvar cancers, 60% of penile cancers, as well as 50-70% of oropharyngeal cancers (including the tongue, the soft palate, the side and back walls of the throat, and the tonsils), 60% of anus, penis, vagina, and vulva.

1.2.2 Prevention of HPV infection: screening and vaccination

Current methodologies and strategies of HPV screening can be divided into non-molecular and molecular methods. Non-molecular techniques for detection of HPV infection do not in fact detect the presence of HPV, but the appearance of clinical and/or histological changes. Those methods include colposcopy, cytology, and histology. Colposcopy usually relies on color changes of cervical cells after being washed with 3–5% acetic acid or with Lugol's iodin solution (IARC,

2007). Cytology based testing like Papanicolaou (Pap) test rely on the interpretation of morphological changes of cells collected from the cervix. It is a low-cost, painless and quick method, however, it is not completely reliable (Bedell et al., 2020). Because of the low sensitivity of non-molecular methods, HPV testing as a molecular method has been proposed. It is used for primary screening, triage of unclear Pap smears as well as for the follow-up of patients after the treatment of higher grade cervical lesions (Grce et al., 2007). Although HPV detection methods for cervical cancer have improved a lot in the last decades, screening methods for most HPV-caused cancers are still missing. Therefore, the most efficient tools against HPV infections remain to be constant education, large scale screening programs and vaccination.

Three HPV vaccines are currently approved for use by the United States FDA - Gardasil, Cervarix, and Gardasil 9. All these approved vaccines contain L1 virus-like particles (VLPs) derived from the corresponding HPV types. L1 proteins can assemble into highly immunogenic VLPs almost indistinguishable from mature virions (Kirnbauer et al., 1992) and are thus great foundation for HPV vaccine designs. Gardasil by Merck & Co. was the first commercially available HPV vaccine approved by the United States FDA, in 2006. It is a quadrivalent HPV vaccine that protects from two most common high-risk (HR) HPV types - HPV16 and 18, and two most common low-risk (LR) types - HPV6 and 11. Cervarix by GlaxoSmithKline was approved by the European Medicines Agency (EMA) in 2007 and by the FDA in 2009. It is the bivalent HPV vaccine which protects against the most common oncogenic HPV types - HPV16 and 18. A few years later, in 2014, the FDA approved the nine-valent vaccine, Gardasil 9 by Merck & Co. In addition to already covered LR HPV6 and 11 as well as HR HPV16 and 18, Gardasil 9 offers protection against five additional HR types - HPV31, 33, 45, 53, and 58. The collected evidence for all currently available HPV vaccines shows their effectiveness against vaccine-type HPV infection (Villa et al., 2020).

1.2.3 Classification of papillomaviruses

Papillomaviruses belong to the *Papillomaviridae* family, which is divided into 39 genera (**Figure 6.**) that are named using the Greek alphabet (*Alpha-, Beta-, Gamma-, Deltapapillomavirus, etc., and derivatives thereof, e.g., Dyodeltapapillomavirus*). All PVs share an identical structure of a naked, icosahedral capsid of approximately 55 nm in diameter, composed of 72 capsomeres. The classification of PV types is based on the DNA sequence of the L1 gene, the most conserved region within the genome and thus has been used for identification of new types. As agreed at the

International Papillomavirus Workshop in Quebec in 1995, a new type is defined if L1 sequence differs by more than 10% to the closest known type, whereas 2-10% difference in sequence define a subtype and less than 2% difference a new variant (de Villiers et al., 2004; IARC, 2007). HPVs are classified into one of the five genera; *alpha* (α), *beta* (β), *gamma* (γ), *mu* (μ) and *nu* (ν), based on the viral genome sequence, host-species specificity, and biological properties, including the associated diseases. Most HPVs belong to the α and β genera, and all α members have been associated with several malignant or benign conditions. However, a few members of the β and γ genera can also cause diseases in humans, but under specific circumstances i.e. immunodeficiencies or DNA damage where these HPV types act as co-factors in disease development (Doorbar et al., 2015).

In total of 66 HPVs from the *Alphapapillomavirus* genus preferentially infect oral or anogenital mucosa in humans and primates. These were later classified by the International Agency for Cancer Research (IARC) as LR and HR depending on their ability to initiate malignant transformation (IARC, 2007). LR HPVs are commonly associated with oral and genital warts along with benign skin lesions and recurrent respiratory papillomas that tend to be difficult to treat clinically (de Villiers et al., 2004). Although they are rarely found in squamous intraepithelial lesions – most likely as part of multiple infections with HR types (Boda et al., 2018; Bouvard et al., 2009), LR types carry a small (1-3%) risk of cancer progression (Egawa and Doorbar, 2017). Up to date, HPV16, 18, 31, 33, 35, 39, 45, 51, 52, 56, 58 and 59 have been classified by the World Health Organization (WHO) as *carcinogenic to humans* (Group 1). The available studies have shown the unique carcinogenic potential of HPV16 and, to somewhat lesser extent, of HPV18, and those two types are associated with about 70% of HPV-related cervical cancers. HPV63 is defined as *probably carcinogenic* (Group 2A) due to limited evidence so far, whereas types 26, 53, 66, 67, 70, 73 and 82 were defined as *possibly carcinogenic to humans* (Group 2B), as evidence of carcinogenicity is inadequate in humans and limited even in experimental animals (IARC, 2007).

The *Betapapillomavirus* genus contains 64 types associated mostly with the development of cutaneous benign lesions, but have also been identified in normal, precancerous, and cancerous epithelial cells. Although β-HPVs are primarily latent and are considered to be LR in the general population, they may pose a higher risk in certain hypersensitive groups - e.g., patients with severe combined immunodeficiency or with *epidermodysplasia verruciformis* (Egawa and Doorbar, 2017). Some β-HPVs have also been identified as a causative agent of non-melanoma skin cancer

(NMSC), when combined with ultraviolet (UV) radiation or other DNA damage instigators (Tommasino, 2017). *Gamma* (γ), *Mu* (μ) and *Nu* (ν) HPV types all target the cutaneous epithelia and are associated with the development of papillomas and warts with no oncogenic potential (Egawa and Doorbar, 2017).

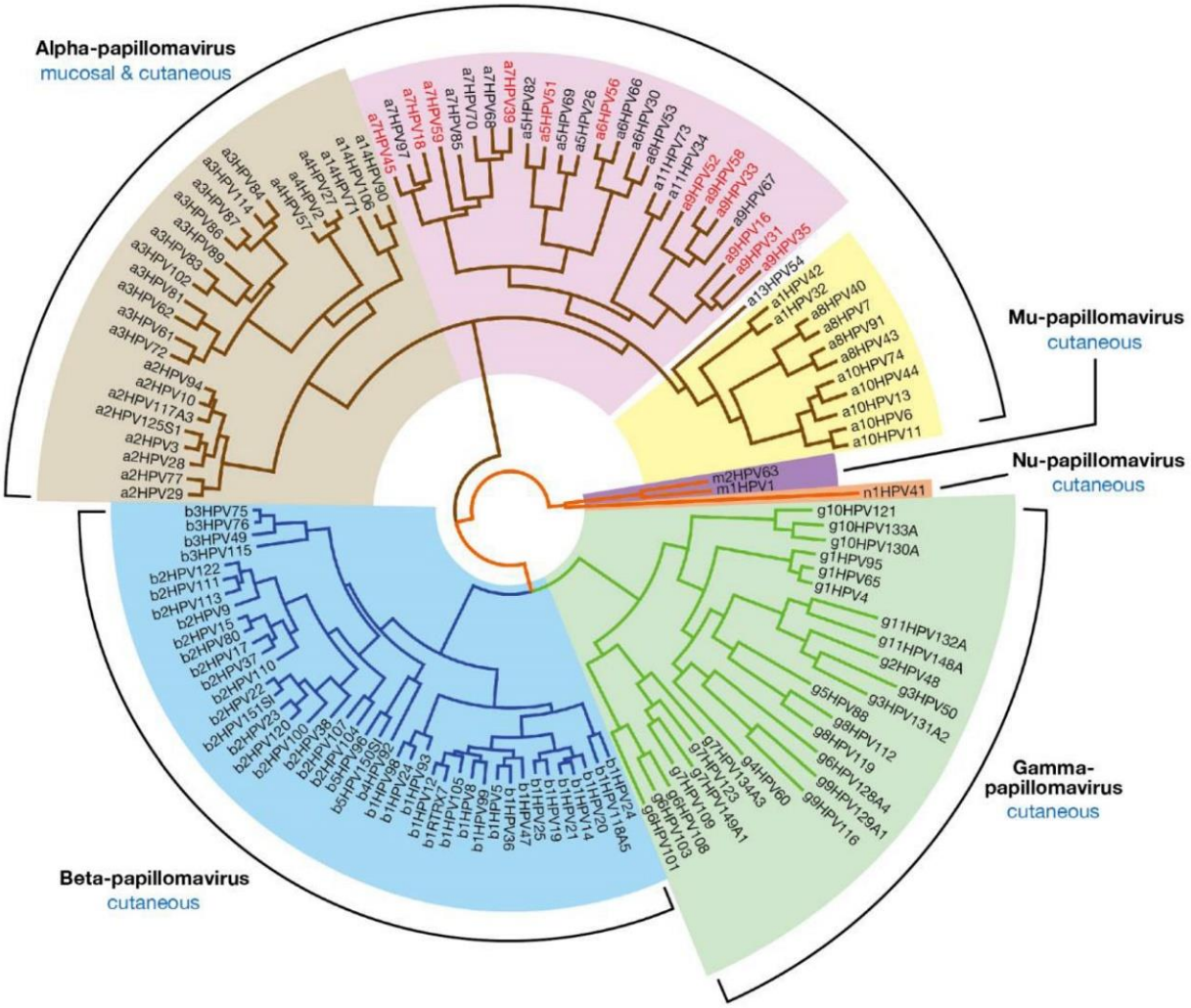

Figure 6. HPV phylogenetic tree. HPVs are classified into five genera (α, β, γ, μ and ν) where α and β represent the majority of HPV types. Within the α genus, HPVs are classified as LR cutaneous viruses (brown), LR mucosal viruses (yellow) or HR mucosal viruses (pink). α types, highlighted in red, are defined as *carcinogenic* virus types (Group 1), while the others of the same group are either *probably* (Group 2A) or *possibly carcinogenic* (Group 2B), categorized by the IARC. Adopted from (Doorbar et al., 2012).

1.2.4 HPV genome organization and protein functions

The HPV genome is a circular double-stranded DNA molecule which varies in size from 5748 to 8607 bp and contains three functional regions - (i) an upstream regulatory region (URR) that regulates the expression and replication of viral genes; (ii) the early region and (iii) the late region (**Figure 7.**). The URR controls gene expression in PVs at various post-transcriptional levels by

cellular and viral transcription factors and different promoters. This region contains four E2 binding sites (E2BS), and two of them separate the URR into three functionally distinct segments: the 5′, the central and the 3′. The 5′-URR segment contains the polyadenylation site that serves as a transcription termination signal while the central part represents the majority of transcription factor binding sites as it contains the epithelial specific enhancer. These motifs include binding sites to AP1, NF1, TEF1, OCT1, YY1, BRN-3a, NF-IL6, KRF-1, NF-kB, FOXA1, and GATA3, and several others (Ribeiro et al., 2018). Finally, the 3′ segment of the URR contains a single E1 binding site, an Sp1 transcription factor binding site, two E2 binding sites and a TATA box. Together, these sites represent the origin of replication and the E6/E7 promoter activity (IARC, 2007).

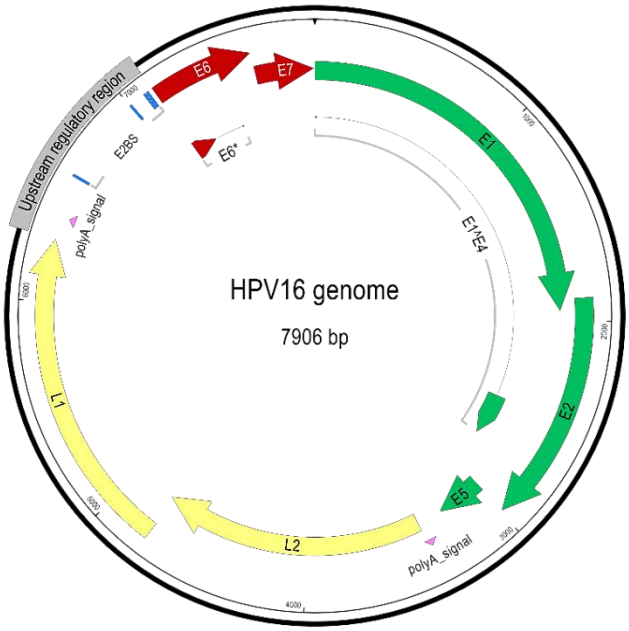

Figure 7. HPV16 genome organization. HPV genome is divided into the URR (grey box), the early and late regions. The URR contains a DNA replication origin and functions as the replication regulator. This region contains four binding sites for viral E2 protein indicated in blue boxes (E2BS). The early region encodes E6 and E7 indicated in red and E1, E2, E4 and E5 shown in green, while the late region encodes structural proteins L1 and L2 displayed in yellow. The early and late polyadenylation sites are shown as pink triangles between the E5 and L2 ORF and L1 and the URR, respectively. Figure was created using SeqBuilder Pro 17.

The early region encodes six proteins (E1, E2, E4, E5, E6, E7, and E8) which are expressed under the early promoter, p97 or p105, in HPV16 or HPV18, respectively, at different stages during epithelial cell differentiation. The early proteins play various roles in viral transcription, viral genome replication and maintaining continuous host cell proliferation. E1 protein is the only HPV protein with an enzymatic activity. It is an adenosine triphosphatase (ATPase) and DNA helicase that recognizes and binds to the viral origin of DNA replication in 3'-URR segment, which makes this protein pivotal in the initiation of transcription (Hughes and Romanos, 1993). E2 is a highly

multifunctional protein playing roles in different viral processes. It is the main transcriptional regulator, which functions by forming a homodimer that can bind to the E2BSs within the URR resulting in either activation or repression of viral transcription, depending on the context of these binding sites and nature of the associated cellular factors (McBride, 2013). E2 enhances E1 DNA binding activity and also plays an important role in the partitioning of newly replicated viral DNA into daughter cells (Dixon et al., 2000; Sedman et al., 1997). Likewise, E2 interacts with the minor viral structural protein L2, as well as with numerous cellular proteins in cultured cells. E4 is a heterogeneous protein made of a 5-amino acid sequence from the N-terminus of E1 spliced to the E4 ORF (E1^E4). Despite its genomic location and its 'early' name, E4 is predominantly expressed at later stages of viral productive cycle and is the most abundant viral protein expressed during this process. It is detected both in the proliferative and highly differentiated cells that express late genes, however, it is not present in new viral particles. Therefore, E4 is reported to have important roles in supporting the viral genome amplification, regulation of late genes expression, and likely, the control of the viral maturation and release (Doorbar, 2013). The E5 oncoprotein is a small viral protein of 8 to 9.5 kDa, expressed by a subset of HPV types. Its primary function was proposed to be the inhibition of death receptor-mediated apoptosis in human keratinocytes (Kabsch and Alonso, 2002). E5 oncoprotein was also suggested to have a role in the productive stage of viral cycle (DiMaio and Petti, 2013). Regardless of the mentioned mechanisms, E5 oncoprotein is most likely not vital for HPV-induced oncogenesis since it is expressed in only few HPV-positive cancers and its silencing would not lead to cessation of cancer cell growth or apoptosis (Müller et al., 2015). Conversely, E6 and E7 were demonstrated to play multiple roles in cell transformation, since E6 enables apoptosis avoidance, whereas E7 promotes continuous cell proliferation. Although these two functions are considered as some of the most important, others essential for the process of carcinogenesis are described in Chapters 1.2.6-8.

The late region encodes virion-forming L1 and L2 capsid proteins (Bravo and Félez-Sánchez, 2015; García-Vallvé et al., 2005). L1 is the major structural protein of about ~55 kDa which can self-assemble into pentamers, while a total of 72 pentamers set up virus-like particles or VLPs (Buck et al., 2013). As described, the discovery that L1 protein can assemble into highly immunogenic VLPs almost indistinguishable from mature virions, except they lack encapsulated viral DNA (Kirnbauer et al., 1992), has provided a platform for modern HPV vaccine designs. Moreover, this also established a basis for creating pseudovirions by which the process of infection, entry and

internalization is studied. L1 almost completely covers the outer surface of the mature virion and is required for initial attachment to host tissues or cells. L2 is a protein of 64-78 kDa (Doorbar and Gallimore, 1987) which plays major roles in both papillomavirus assembly and the infectious process but lacks the capacity to form VLPs (Wang and Roden, 2013). Nevertheless, L2 is highly conserved among HPV types and has now been used as an alternative target antigen to develop a broadly protective HPV vaccine since immunizations with isolated L2 proteins induce low-titer cross-neutralizing antibodies to a diverse range of genotypes (Yadav et al., 2019).

1.2.5 Productive HPV cycle

The coevolution of papillomaviruses with their target host cells has contributed to the development of their tropism for squamous epithelial cells. The ability of HPV to have a productive cycle depends both on the site of infection and on the microenvironment (**Figure 8.**). It is assumed that the existence of microtraumas is necessary for HPV infection to occur at all. Through them virus reaches cells of the basal lamina of the stratified epithelium which is believed to be vital for two reasons: first, because the virus enters in cells that have a high proliferative capacity, which allows the formation of permanent lesions (Doorbar et al., 2012; Schiller et al., 2010), and secondly because active cell division, which occurs as a response to the damage, allows the expansion of infection and the production of new virions (Ledwaba et al., 2004; Schiller et al., 2010). Likewise, it was reported that HPV infection can occur in a setting where virus enters cells at the squamocolumnar junctions (Herfs et al., 2012). Further studies have shown that cell cycle progression through the early stages of mitosis is critical for successful HPV infection. Cellular events in the early prophase include nuclear envelope breakdown and changes in chromatin structure which are necessary for the HPV DNA to enter the nucleus (Pyeon et al., 2009).

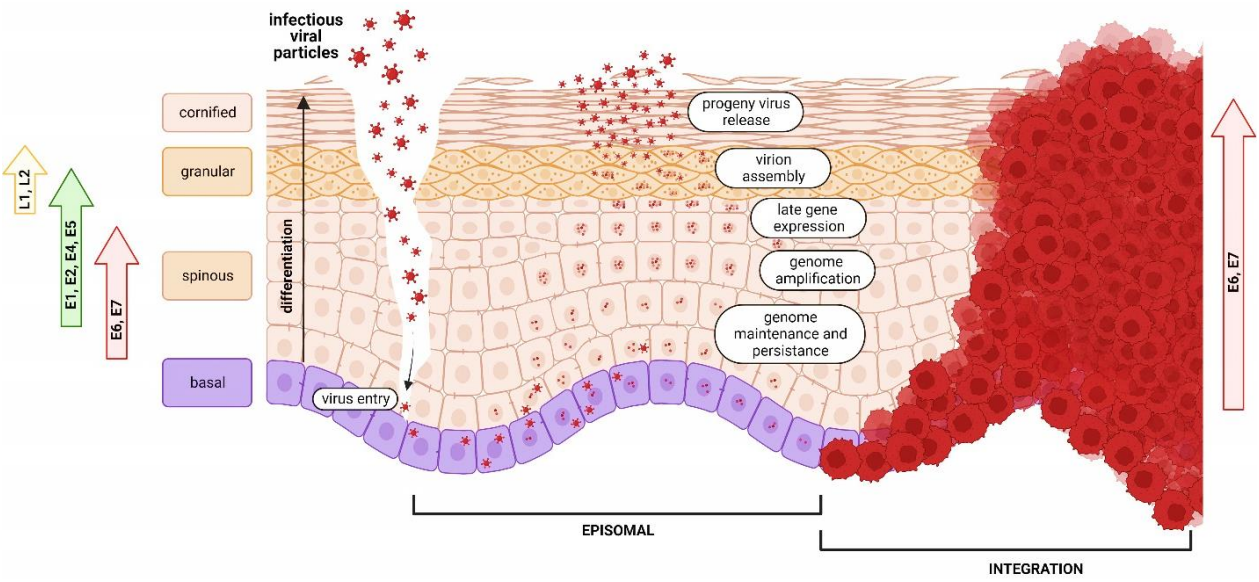

Figure 8. From HPV infection to malignancy. HPV infects cells of the basal lamina through microtraumas. In these cells, early genes E1, E2, E5, E6 and E7 are expressed, and the viral DNA is maintained in episomal form within the nuclei of the cells. In the suprabasal layer of epithelia, the viral episomes are maintained at a low copy number. As cells divide, they move towards the upper layers and the late stage of the productive cycle occurs. During the late phase, late genes L1 and L2, and E4 are expressed. Virions are then assembled, and newly synthesized virions are released from keratinocytes in cornified epithelium. The host immune system usually resolves viral infection within a few months of the initial infection. However, if the infection becomes persistent, cells in the parabasal layers become dysplastic leading to the formation of precancerous lesions. If HPV genome integration occurs, the viral cycle becomes abortive. This leads to E6 and E7 DNA integration to the host genome and they become expressed uncontrollably, which can finally result in cancer development. Red arrows indicate viral oncoproteins E6 and E7 during the productive cycle and malignancy on the left and right sides of the figure, respectively. The green arrow represents the E1, E2, E4, E5 expression, while yellow arrow represents the expression of late genes, L1 and L2. Figure was made using BioRender.

HPV infection is initiated upon virus arrival at the basal cells. The virus binds to heparan sulfate proteoglycan chains (HSPGs) on the cell membrane or on the extracellular matrix via the L1 capsid protein, leading to the structural changes and exposure to the L2 capsid protein (Gheit, 2019). Although the exact mechanism of the virus internalization is not completely understood, it appears to vary between different HPV types. It was reported that L2 exposure is followed by endocytosis via clathrin-, caveolin-, cholesterol-, lipid raft- and dynamin-independent mechanisms (Schelhaas et al., 2012). After internalization, the viral capsid is disassembled in the late endosomes to L1 and L2-viral DNA complexes. L2 then mediates relocation of the viral DNA via the trans-Golgi network to the nucleus, where the initial phase of genome amplification begins. Presumably both E1 and E2 are required to support the amplification of viral DNA (McBride, 2017). In this phase, the genome is thought to be rapidly amplified as an episome in a low copy number, around 50–100 copies per cell (Graham, 2017a; Pyeon et al., 2009). The relatively small HPV genome does not encode proteins with enzymatic functions, apart from E1, so viral replication depends on cellular replicative machinery. Likewise, the virus must use and manipulate the replicative machinery in a

coordinated and regulated manner so productive HPV cycle is closely tied to the biology of keratinocytes and epithelial differentiation (McKinney et al., 2016; Scarth et al., 2021). Following nuclear entry, viral DNA replication begins by binding of E2 proteins to specific sites in the URR, allowing E1 helicase to bind to *ori* (Sanders and Stenlund, 1998). As a small number of copies are amplified, such limited replication can be achieved by the interaction of NCOR/SMRT repressor complexes with E8^E2C proteins, which inhibits viral replication (Dreer et al., 2016). Likewise, viral genome expression is negligible due to E2-mediated repression of the early promoter, which happens as a result of the immune response avoidance (Scarth et al., 2021). After this step, the so-called maintenance phase occurs.

During the maintenance phase a constant number of viral episomes in the nuclei of undifferentiated basal cells is maintained allowing the formation of a long-lasting infection. In addition to E1 and E2 proteins, the action of E6 and E7 oncoproteins is necessary for the stable maintenance of viral episomes (Park and Androphy, 2002; Thomas et al., 1999). Vegetative or productive viral replication begins in the stratified squamous epithelium where new virions are produced (Maglennon et al., 2011; Moody and Laimins, 2010). In uninfected basal keratinocytes, cells undergo asymmetrical division to produce two daughter cells; one remaining in the basal cell layer with a mitotic potential and the other daughter cell entering the process of differentiation in the upper layers of epithelium (Koster and Roop, 2007). As cells migrate away from the basal layer, they exit the cell cycle, and the DNA replication is halted. This signifies a problem for HPV cycle as it depends upon host's replication machinery. To overcome this, HPVs have developed strategies to prevent cell cycle arrest and apoptosis. This happens through the abundant expression of E6 and E7 oncoproteins that associate with cell cycle and apoptosis regulators (Doorbar et al., 2012).

The late stage of the productive cycle occurs in the superficial layers of the stratified epithelium consisting of terminally differentiated cells. It involves the amplification of the viral genome, the expression of E1^E4 and late genes L1 and L2, the encapsidation of synthesized DNA, and the release of the progenitor virions (Doorbar et al., 2012; IARC, 2007; Tomaić, 2016). It was reported that both, E1^E4 and E5 proteins contribute to this phase of the viral cycle (Peh et al., 2004; Wilson et al., 2007). Although the exact E1^E4 functions in the upper layers of the epithelia have not been fully elucidated yet, studies have shown that E1^E4 is able to cause cell cycle arrest between G2 to M phase, to inhibit entry into S phase as well as inhibit cellular DNA replication (Knight et al., 2011; Peh et al., 2004; Wilson et al., 2007). Altogether, the functions of E1^E4 are to provide a

suitable environment required for DNA amplification and the expression of capsid proteins (Doorbar, 2013; Knight et al., 2011). Later, the assembly of viral capsids occurs in the nucleus where 360 molecules of L1 and a variable number of L2 molecules assemble into pentameric units. Those units form an icosahedral structure which is stabilized by the intermolecular disulphide bonds between L1 proteins (Buck et al., 2013; Finnen et al., 2003). Finally, virions are released during the natural sloughing of keratinocytes through a yet undefined process. However, it is speculated that this may be due to E1^E4-mediated disruption of the keratin cytoskeleton (Roberts et al., 1997).

1.2.6 Molecular mechanisms of HPV induced oncogenesis

HPV infections are usually cleared by the immune system within 2 years from the initial viral entry and do not result in the development of any pathologies (zur Hausen, 2002). As described above (**Figure 8.**), during the productive viral cycle, E2 protein is expressed. Aside from its essential role in viral replication, E2 also functions as a transcriptional repressor of the viral oncogenes, E6 and E7. However, if the infection persists for longer periods of time, there may be a collapse of the productive cycle under hitherto unexplained circumstances. Persistence can induce HPV genome integration into the host cell genome leading to the disruption of E2 and finally the upregulation of E6 and E7 (Doorbar et al., 2020; Harden and Munger, 2017). In HNSCCs, however, E2 is more commonly inhibited by DNA methylation of E2BS, leading again to continuous and uncontrolled expression of E6 and E7 (Nakagawa et al., 2021). There are several molecular mechanisms by which HPV oncogenes cause malignancies including regulation of cell proliferation and differentiation, DNA damage response (DDR) and base excision repair (BER). Additionally, HPV can modulate epigenetics again contributing to malignant transformation of infected cells.

As described, non-infected cells in the suprabasal layers of stratified epithelium exit cell cycle and terminally differentiate. Interestingly, E7 oncogene was characterized as both necessary and sufficient for cellular transformation since inactivation of pRb alone caused inducement of the host DNA replication machinery and prolonged cell proliferation (Halbert et al., 1991). This was also confirmed in transgenic mice showing that HPV16 E7 can alter epithelial cell growth to potentiate tumorigenesis (Herber et al., 1996). Additionally, in a study in transgenic mouse HNSCC model, E7 was shown to act as the major transforming oncogene, whereas E6 more likely plays a secondary role in contributing to later stages of carcinogenesis (Strati and Lambert, 2007). E7 also induced

progression to microinvasive cervical cancers in transgenic mouse model of cervical cancer, while E6 elevated centrosome copy number and eliminated detectable p53 protein, but did not provoke neoplasia or cancer (Riley et al., 2003). All these suggest that E6 alone is not sufficient for cellular transformation, but the presence of E7 is required. E6 also contributes to this phenotype by binding to various PDZ domain-containing proteins (Accardi et al., 2011; Nguyen et al., 2003). In addition, HPV16 E5 was described to contribute to cell cycle progression to the S-phase and synthesis of DNA, since it was linked to the downregulation of the cellular tumor suppressors p21 and p27, on the transcriptional level or through the reduction of their half-lives (Pedroza-Saavedra et al., 2010; Tsao et al., 1996). However, p53 degradation by E6 results in modulation of apoptosis, again leading to cellular immortalization. E6 also contributes to this process through the induction of telomerase expression (Klingelhutz et al., 1996) as well as through provoking degradation of the transcriptional repressor, NFX1-91 (Gewin et al., 2004). HPV E5 oncoprotein can enhance cellular immortalization regulated by E6/E7 probably because it inhibits the normal downregulation of the EGFR. Therefore, this mitogenic stimulus caused by E5 may produce actively growing cells which are more efficiently transformed than quiescent cells suggesting E5 could play a role in the pathogenesis of early HPV infections (Maufort et al., 2010; Stöppler et al., 1996).

Intriguingly, cells have developed a DDR pathway to repair the newly induced DNA damage in the DNA. This response plays a crucial role in cell division because after the repairment of DNA, the cell cycle checkpoints are diminished, and cells continue to divide. Apart from the well-known interactions described above, HPVs were shown to have an impact on DDR. Precisely, in HPV positive cervical cancers, the host DDR, including the ataxia telangiectasia mutated-dependent (ATM) pathway and the ataxia telangiectasia mutated-dependent DNA-related (ATR) pathway, have been shown to be constitutively activated. Those DDR alterations were considered to be required for the completion of the productive viral cycle in the cervical epithelium (Moody and Laimins, 2010). Indeed, increased activation of DDR factors, particularly members of the ATR pathway and FANCD2 were reported in HPV-positive as compared to HPV-negative HNCs and the control tissue (Kono et al., 2020; Kono and Laimins, 2021). Likewise, HPV16 E7 was reported to lessen the DDR and promote cell division by accelerating claspin degradation (Spardy et al., 2009). So far, this was shown only for this specific type. Additionally, p53 was reported to have a role in the BER (Zhou, 2001). Because of E6-mediated degradation of p53, the damage response

fails to pose apoptotic threats to cells and allows replication to produce rearranged host genome with multiple breakpoints.

In addition to stimulating cell growth and preventing any type of cell death, methylation aberration is often considered as one of the hallmarks of cancer (Mesri et al., 2014). HPV-mediated cancers are unique because viral oncoproteins also contribute to these methylation changes. Precisely, methyltransferase is regulated by both, E6 and E7. E6-mediated degradation of p53 leads to decreased inactivation of Sp1 transcriptional factor. Hence, the remaining active Sp1 increases DNMT1 transcription. On the contrary, E7-mediated interactions with pRb causes the release of E2F that further promotes DNMT1 expression. E7 then binds to DNMT1, promotes its activity, and leads to significant increase in methylation levels (Durzynska et al., 2017). However, change in methylation patterns was reported in both the host's and HPV DNAs.

1.2.7 HPV E7 oncoprotein

E7 is a small acidic protein which consists of approximately one hundred amino acid residues. It does not share significant structural similarities with cellular proteins other than the LxCxE motif. However, its structural integrity is critical for E7 activities (Patrick et al., 1994; Tomaić, 2016). The N-terminus contains two E1A adenovirus protein-like regions; a small portion of the conserved region 1 (CR1), and almost the entire CR2 that are conserved between different HPV types. CR1 and CR2 are separated by non-conserved sequences of different lengths and amino acid composition (Phelps et al., 1992). E7 oncoprotein also contains a conserved zinc-binding finger CR3, at the C-terminus, containing two CxxC domains similar to those in E6 oncoproteins, meaning that the carboxyl terminal domain of HPV E7 can be functionally replaced by the homologous E6 protein sequences without apparent loss of function (Münger et al., 2001). The CR1 domain plays a role in cellular transformation since CR1 has been shown to bind and deactivate UBR4/p600 whose loss of activity induces anchorage independency (DeMasi et al., 2005; Huh et al., 2005). Moreover, ubiquitin ligase UBR4/p600 is required for E7 proteasome-mediated degradation of PTPN14, which correlates with the pRb-independent transforming activity of HR HPV E7 (Szalmás et al., 2017; White et al., 2016). Likewise, CR1 interacts with P/CAF and reduces its acetyltransferase ability. Since pRb acetylation was shown to be necessary for exiting the cell cycle, deactivation of P/CAR causes the reduced acetylation of pRb (Avvakumov et al., 2003). Furthermore, many ubiquitin ligases were reported to interact with E7 via the CR1 domain.

The main one is Cullin-2 ubiquitin ligase complex, which E7 utilizes to drive cell cycle progression by the degradation of pRb and consequent upregulation of cyclin dependent kinase 2 (CDK2) and cyclins A and E (Đukić et al., 2020; Huh et al., 2007). Overall, various cellular pathways were described to be interfered by E7 (**Figure 9.**). Nevertheless, it is believed that the main function of E7 is to keep proliferative cells in competent state for DNA replication by interacting with pRb tumor suppressor.

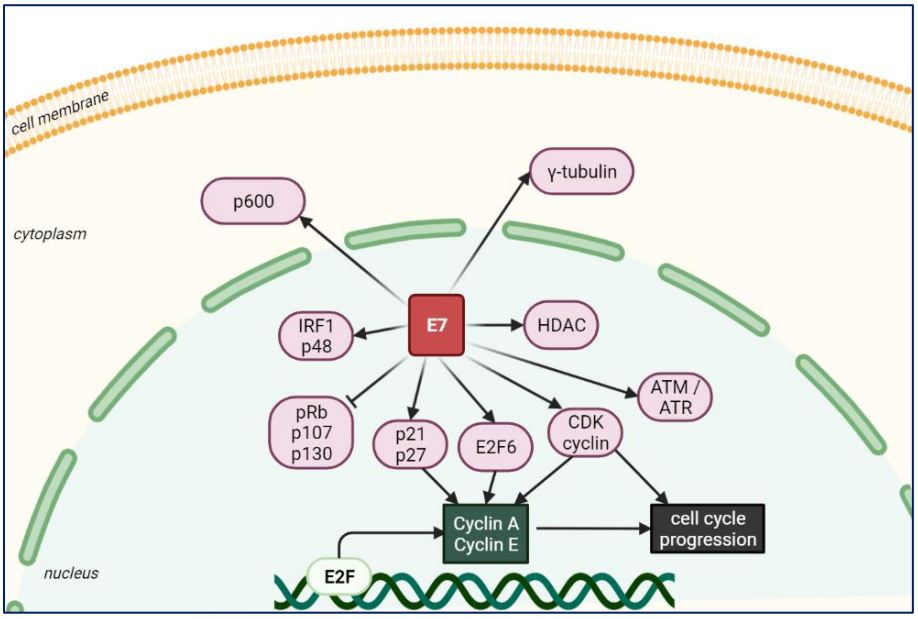

Figure 9. HPV E7 interferes with multiple host's signaling pathways. E7 oncoproteins disrupt cell cycle and induce hyperproliferation through the inhibition of retinoblastoma (pRb) protein family members, which results in subsequent activation of E2F-responsive genes. Cell cycle control is also deregulated through E7 inhibition of CDK inhibitors (such as p21 and p27), stimulation of cyclins and through direct activation of CDK2. Cellular gene expression is affected through interaction with histone deacetylases (HDACs) and E2F6. E7 induces DNA damage and activates the ATM–ATR pathway (ataxia telangiectasia-mutated ATM and RAD3-related DNA damage response), which may contribute to the accumulation of chromosomal alterations. E7 interacts with the components of the interferon (IFN) response (IFN regulatory factor 1 (IRF1) and p48, contributing in this way to escape from the immune surveillance and the establishment of a persistent infection. Adapted from (Moody and Laimins, 2010).

One of the main properties of E7 is that, through its LxCxE motif located in CR2, it binds and inactivates the retinoblastoma protein family members including pRb, p107 and p130. A plethora of published papers characterized pRb as a master regulator of biological pathways as it influences cell growth, cell cycle checkpoints, differentiation, senescence, self-renewal, replication, genomic stability and apoptosis (reviewed by Engel et al., 2014). In normal, non-cancerous cells, pRb is phosphorylated during G1 by active cyclin/CDK complexes - cyclin D1/CDK4, cyclin D1/CDK6 and cyclin 2/CDKE. The phosphorylation of pRb causes its conformational changes leading to the dislocation of transcription factor E2F and ultimately to the initiation of transcription of E2F-responsive genes responsible for the cell cycle progression (Giacinti and Giordano, 2006). In the

presence of antiproliferative signal such as DNA damage, pRb protein is activated by inhibition of CDK complexes. Therefore, active and hypophosphorylated pRb is in a conformation that promotes its ability to bind to E2F. Eventually, pRb/E2F complex prevents the binding of the E2F leading to the repression of transcription of E2F-responsive genes and cell cycle arrest (Hiebert et al., 1992). By binding to hypophosphorylated form of pRb, E7 mimics pRb phosphorylation and enables the inappropriate release of E2F transcription factor. This leads to the stimulation of E2F binding to DNA, which is followed by transcription of genes required for G1 to S phase transition (Münger et al., 2001). Ultimately, E7/pRb interaction drives suprabasal cells into the cell cycle, which leads to the initiation of host defense pathways including p53-mediated apoptosis (Doorbar et al., 2020). These E7/pRb interactions are sufficient for the abrogation of cell cycle arrest in human epithelial cells. However, E7 interactions with other cellular proteins are required for maintaining viral genomes in proliferating cells and modulating numerous cellular processes including cell migration, immune response, and apoptosis (Reinstein et al., 2000). The pRb-related proteins p107 and p130, also bind members of the E2F family. More precisely they bind and inhibit E2F4 and E2F5, respectively, in a manner similar to pRb and these interactions also contribute to the regulation of the cell cycle (Tomaić, 2016). Adjacent to LxCxE motif is a consensus phosphorylation site for casein kinase II (CKII), which has been shown to be important for cell transformation (Barbosa et al., 1990). This CKII phosphorylation site has been shown to be important for E7 ability to target and inactivate pRb and related proteins (Genovese et al., 2008). Likewise, HPV16 E7 was suggested to interact with E2F6, a member of the E2F family of transcription factors, directly and independently of pRb since E2F6 lacks the C-terminal binding domain (Durzynska et al., 2017). E7 oncoproteins have also been shown to retain DNA synthesis competent state in differentiated keratinocytes via abrogating CDK inhibitors p21 and p27 to maintain the activity of CDK2/cyclin A complex (Helt et al., 2002; Shin et al., 2009). Since p21 has multiple cellular functions, E7 may thus regulate a variety of processes ranging from viral persistence in stem cells to vegetative replication in terminally differentiated cells. Similarly, E7 upregulates cyclin E transcription to promote cell cycle progression (Mcintyre et al., 1996). Previous studies have revealed that full-length E7 proteins with mutations outside of the LxCxE motif retain the ability to degrade pRb, but they fail to abrogate cell cycle arrest and facilitate immortalization (Helt et al., 2002). This is due to E7 interactions with class I histone deacetylases (HDACs) comprised of HDAC1, 2, 3 and 8. HDACs enzymes are well known for their removal of

acetyl groups from histone lysine tails, in that way making the chromatin more compact and less accessible to transcription factors. This ultimately leads to the local transcriptional repression of many cellular promoters including E2F-dependent ones. However, the importance of E7/HDAC interactions for HPV carcinogenesis are yet to be elucidated. On the other hand, there is some evidence of the importance of E7/HDAC complexes for productive viral cycle as both, HR and LR E7 proteins, were reported to bind to HDACs (Pešut et al., 2021). Those interactions were speculated to have a role in episomal maintenance (Longworth and Laimins, 2004; Wise-Draper, 2008). E7 was also reported to upregulate interleukin-8 (IL-8) to prevent cellular senescence and evade cellular immune response by interfering with IL-18-mediated lymphocyte activation. This seems to be a combined action of both viral oncoproteins, E6 and E7, and thus may contribute to viral pathogenesis (Richards et al., 2014).

1.2.8 HPV E6 oncoprotein

The E6 oncoproteins are small proteins of about 15 kDa which consist of four CxxC motifs that form the N- and C-terminal zinc fingers connected by a 36 amino acids long-linker (Howie et al., 2009). These CxxC motifs are highly conserved in all E6 oncoproteins and have been defined as vital for E6s' functions (Barbosa and Wettstein, 1987; Cole and Danos, 1987). Structural analysis of E6 revealed that two zinc domains and a linker helix form a basic-hydrophobic pocket, the so-called LxxLL motif. This motif participates in several protein-protein interactions associated with various aspects of transcriptional regulation (Zanier et al., 2013). The first one discovered and one of the best studied interactions which occurs through this motif is the association between E6 and E6-associated protein (UBE3A/E6AP). E6AP is a member of the cellular HECT E3 ubiquitin ligase family, which was demonstrated as crucial for normal brain development since maternally inherited deletions, mutations, and copy number variations of the UBE3A gene in brain tissues, were shown to be responsible for Angelman syndrome development, a severe neurological disorder (Khatri and Man, 2019). E6AP was originally isolated as an interacting partner of the E6 protein of oncogenic HPV types (Huibregtse et al., 1991). Complexing with E6 induces conformational change of E6AP, in this way causing an E6AP specificity shift. Thus, E6 is able to target proteins for a proteasome-mediated degradation, which are normally not recognized by E6AP, thereby contributing to HPV-induced carcinogenesis (Scheffner et al., 1993). Interestingly, E6 was reported to be rapidly degraded by the ubiquitin proteasome system (UPS) when E6AP was silenced in HPV-positive cells. Furthermore, its overexpression stabilized ectopically expressed HPV16 and HPV18 E6, so

these results demonstrated that the stability of E6 is critically dependent upon the presence of E6AP (Tomaić et al., 2009). In addition to LxxLL, the C-terminus of E6 oncoproteins of only HR types contain a conserved amino acid sequence named PDZ-domain binding motif (PBM). This motif is responsible for interactions with several PDZ-domain containing proteins including DLG1, Scribble (SCRIB), MUPP1, MAGI-1/2/3, NHERF1, NHERF2 and many others (Ganti et al., 2015; Saidu et al., 2019). Each interaction achieved through any of these three motifs is beneficial to viral replication and also contributes to the migration and proliferation of infected cells, immune response, Warburg effect, modulation of proteasome system function, sumoylation and tumor formation as summarized in **Figure 10.**

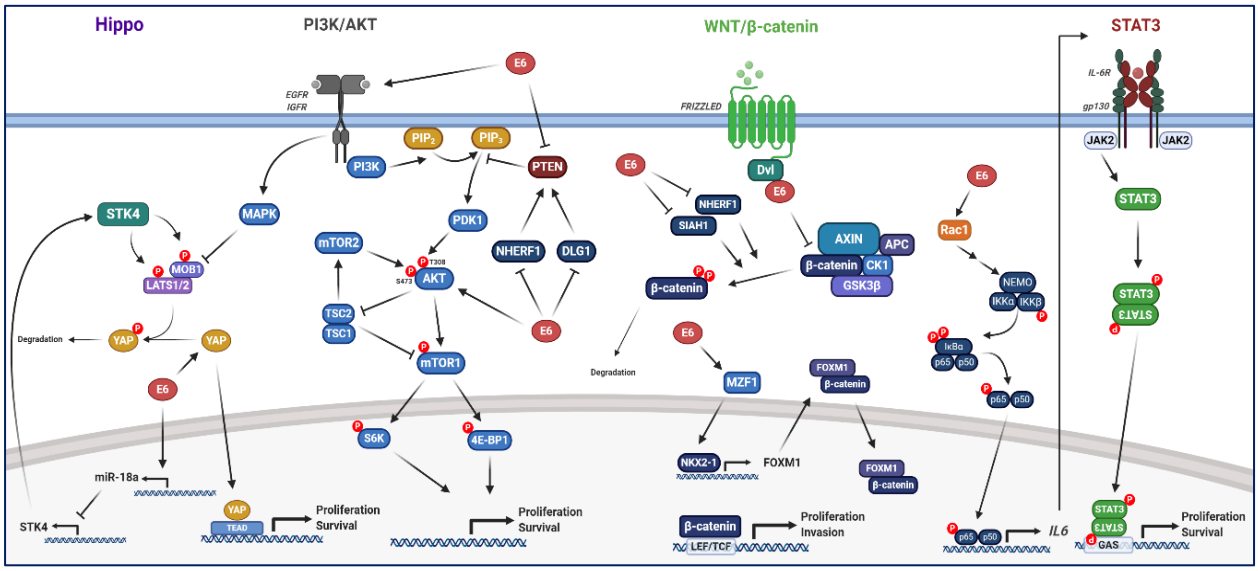

Figure 10. HPV E6 interferes with several host signaling pathways. E6 modulates cellular pathways to avoid apoptosis as well as the host Hippo, PI3K/AKT, Wnt/β-catenin and JAK/STAT signaling pathways by interacting with various cellular proteins. Collectively, these interactions lead to evasion and stimulation of cell proliferation, which typically occur by modulation of the expression of downstream target genes associated with cell growth and survival. Adopted from (Scarth et al., 2021).

1.2.8.1 E6 regulation of apoptosis

The most extensively studied function of E6/E6AP complex is proteasome-mediated degradation of p53, which is considered to be the most important oncogenic function of E6 (Scheffner et al., 1993). Protein p53 is a 53 kDa long nuclear phosphoprotein, which acts as the principal mediator of growth arrest, senescence, and apoptosis in response to a broad range of cellular damages (Levine, 1997). Under normal circumstances, in the absence of HPV or other stressors, p53 is regulated by cellular RING finger domain-containing ubiquitin ligase MDM2. Principally, MDM2 promotes monoubiquitylation and rapid proteasomal degradation of p53 in unstressed cells (Haupt et al., 1997). MDM2 and p53 form an autoregulatory feedback loop since p53 positively regulates

MDM2 through binding to the p53 DNA consensus binding element in the first intron of the *MDM2* gene. The upregulation of p53 can occur because of stresses such as irradiation or active oncogenes. The mechanisms by which p53 regulates MDM2 differs due to the initiator, but can be a result of p53 phosphorylation, which causes the reduced affinity of p53 for MDM2, and thus contributing to increased p53 protein stability and, finally, leading to apoptosis. Additionally, downstream proteins such as ARF or AKT may bind to MDM2, resulting in the segregation of MDM2 from p53, again contributing to p53-induced apoptosis (Hu et al., 2012). Mutations in p53 gene are the most frequent genetic changes reported in many malignancies. However, in HPV-driven malignancies, p53 protein is not mutated, but rather degraded by the proteasome (Brady and Attardi, 2010; Mantovani et al., 2019). Interestingly, while LR E6 oncoproteins are able to bind to E6AP just like HR types, these interactions do not lead to E6-mediated p53 proteasomal degradation (Brimer et al., 2007). This is thought to be due to the different binding of E6 of specific types to different p53 domains. HR E6 oncoproteins were reported to bind to the core region of p53, which appears to be required for E6-mediated degradation (Li and Coffino, 1996). In addition to proteasomal degradation, E6 can also affect p53 function by inhibiting its binding to DNA. This is due to induction of conformational changes in p53 that either prevent p53-DNA binding and/or disruption of already formed p53-DNA complexes (Thomas et al., 1995). One other mechanism by which E6 modulates p53 function distinct from degradation is sequestration, since in E6-expressing cells, a proportion of p53 is retained in the cytoplasm (Pietsch and Murphy, 2008), although, the mechanism behind this is still not fully understood. E6 further disrupts p53 activity by binding to the histone acetyltransferases p300 and CREB binding protein (CBP), inhibiting p53 acetylation, which would otherwise stabilize p53, and increase E6 stability (Patel, 1999; Thomas and Chiang, 2005). Additionally, E6 targets other proteins involved in intrinsic and extrinsic apoptotic pathways, such as Bcl-2 homologous antagonist/killer, BAK (Thomas and Banks, 1998), FADD and caspase-8, leading to their degradation (Filippova et al., 2004) and thus disruption of apoptosis. All this points to the important role of E6 in avoiding apoptosis of infected cells. Along with p53, E6 induces the E6AP-mediated degradation of ΔNp63α protein, a splice variant of p63 and a p53-related protein. Since p63 is important for cell proliferation regulation, this interaction favors cell proliferation (Citro et al., 2020).

1.2.8.2 E6 manipulates DNA ends

E6 also contributes to the extension of the cellular life span through alterations of human telomerase, hTERT (Van Doorslaer and Burk, 2012). hTERT is the host cell enzyme that catalyzes the RNA-dependent extension of 3'-chromosomal termini with the 6-nucleotide telomeric repeat sequences. This elongation of chromosomal ends is important for the immortalization of keratinocytes (Klingelhutz et al., 1996), but is inactive in non-affected somatic cells. Thus, each division and DNA replication causes the slight shortening of telomeres and when they become critically shortened, cells senesce (Katzenellenbogen et al., 2009). Since HPV requires active cell division, it has found a way to overcome cellular senescence due to shortened telomeres - E6 induces activation of the catalytic subunit of hTERT through the degradation of its repressor NFX1-91. This degradation of NFX1-91 then allows c-myc binding to the hTERT-promoter, resulting in induction of hTERT expression (Gewin et al., 2004). Furthermore, E6-mediated activation of the hTERT promoter requires a complex of E6/E6AP to engage the hTERT promoter and this activation is dependent upon c-myc binding sites in the promoter (Liu et al., 2005). E6 also upregulates c-myc expression which enhances hTERT expression even further (McMurray and McCance, 2003). Additionally, regulation of hTERT was observed on a posttranscriptional level in HPV16 E6-expressing human foreskin keratinocytes (HFK) through direct interaction of NFX1-123 to hTERT mRNA, which increases its stability (Katzenellenbogen et al., 2009).

1.2.8.3 E6 modifies host signaling pathways involved in cell proliferation

Signaling pathways are cellular mechanisms involved in determination of cellular fate. Hence, many of them, including JAK/STAT, Hippo, Wnt/β-catenin, and PI3K/AKT have been identified as deregulated in various cancers.

The JAK/STAT pathway plays diverse roles in hematopoiesis, immune regulation, inflammation, cell proliferation and apoptosis. Therefore, aberrant JAK/STAT signaling contributes to cancer progression and metastatic development (Morgan and Macdonald, 2020). STAT3 and STAT5 proteins play an essential role in the development of cervical cancer which is majorly caused by HPVs. STAT3 was identified as critical during productive HPV18 cycle since its inhibition significantly decreased genome maintenance in undifferentiated keratinocytes. The same group also showed that E6 stimulated STAT3 phosphorylation, which led to overexpression of host proteins required for cell cycle progression and survival (Morgan et al., 2018). Additionally,

STAT3 was shown to be overexpressed and constitutively active in cervical cancer, which also seems to increase with the progression, thus indicating its potential role in progression of HPV16 mediated cervical carcinogenesis (Shukla et al., 2010).

The Hippo signaling pathway is an evolutionarily conserved pathway required for various biological processes, including organ size control, cell proliferation, cancer development, and virus-induced diseases. Yes-associated protein (YAP) is the major downstream effector of the Hippo pathway, which was found to be overexpressed in cervical cancer, as it appears that E6 stabilizes YAP and leads to the maintenance of its activity associated with the progression of cervical cancer (He et al., 2015). To obtain this, E6 was shown to decrease the expression of phosphorylated YAP form and preserve the level of YAP by preventing its degradation from proteasome-dependent pathways. Moreover, E6 also regulates the localization of YAP by interacting with cellular PDZ domain-containing proteins, including LRPPRC, RLGAPB, EIF3A, SMC2/3, AMOT, AMOTL1, and ARHGEF1 (Wang et al., 2020).

The Wnt signaling pathway plays a role in development, proliferation, differentiation, adhesion, and cellular polarity. Wnt ligands have been reported to activate at least three signaling pathways - canonical Wnt/β-catenin pathway and two non-canonical pathways: the planar cell polarity pathway (Wnt/PCP) and the Wnt/Ca^{2+} pathway (Bello et al., 2015). Several studies indicated E6 role in the activation of the canonical Wnt/β-catenin pathway. Indeed, HPV16 E6 binds Dishevelled 2 (DVL2) protein, which inhibits formation of the β-catenin degradation complex leading to β-catenin nuclear accumulation. Additionally, E6/E6AP complex was reported to stabilize β-catenin, probably through the interaction and proteasomal degradation of NHERF1, a negative regulator of canonical Wnt signaling (Scarth et al., 2021).

The PI3K/AKT/mTOR signaling pathway affects many fundamental processes including cell survival, growth, proliferation, migration, and energy metabolism. Its aberrant activation can contribute to the malignant phenotype of tumor cells and to therapy resistance (Zhang et al., 2015). NHERF1, a negative regulator of the Wnt pathway, was reported to inhibit PI3K signaling by supporting the binding of PTEN. Thus, HPV16 mediated NHERF-1 degradation correlates with the activation of the PI3K/AKT signaling pathway (Accardi et al., 2011). Another binding partner of PTEN is a known E6 target, DLG1. It was hypothesized that E6 expression was sufficient to increase PI3K and AKT phosphorylation through this DLG1 binding and degradation (Contreras-

Paredes et al., 2009). All things considered, E6 appears to modulate multiple cellular pathways through its interactions with various PDZ domain-containing proteins.

1.3 PDZ-domain containing proteins

1.3.1 Cellular functions of PDZ domain-containing proteins

PDZ domains are abundant protein-protein interaction modules which consist of 80–110 amino acids. They were named as the acronym representing the first three proteins that they were characterized in: postsynaptic density protein of 95 kDa (PSD95), Drosophila disc large tumor suppressor (DlgA), and zonula occludens-1 protein (Zo-1) (Bilder, 2001; Fanning and Anderson, 1999). PDZ domains have a well conserved fold and are usually made of 5 or 6 β-strands and 2 or 3 α-helices, but their secondary structure differs (Lee and Zheng, 2010). These modules typically recognize the extreme C-termini of target proteins containing the PBMs. This was first demonstrated in a study which investigated the interaction between PSD95 and COOH-terminus of the Shaker K^+ (Kim et al., 1995). The study indicated that the binding of PDZ to PBM does not change the PDZ domain structure; PBM rather serves as an extra β-strand and participates in the extensive hydrogen-bonding pattern with the main chain PDZ domain residues (Doyle et al., 1996). Additionally, PDZ domains can also recognize the internal sequence motif of target proteins through a single binding site. The best characterized PDZ-mediated interaction through this internal motif is binding of neuronal NO synthase with either syntrophin or PSD95 (Christopherson et al., 1999). This study suggested that the internal motif-mediated interactions occur only if they are presented within a specific tertiary structure context that conformationally mimics a chain terminus.

Sequence analysis studies have suggested that the human genome encodes from 234 up to 450 PDZ domains (Castro-Cruz et al., 2020), making over 320 PDZ domain-containing proteins (James and Roberts, 2016). These proteins often comprise more than one PDZ domain and/or more than one type of interaction module. According to their modular organization, they are sorted into four main groups (**Figure 11.**).

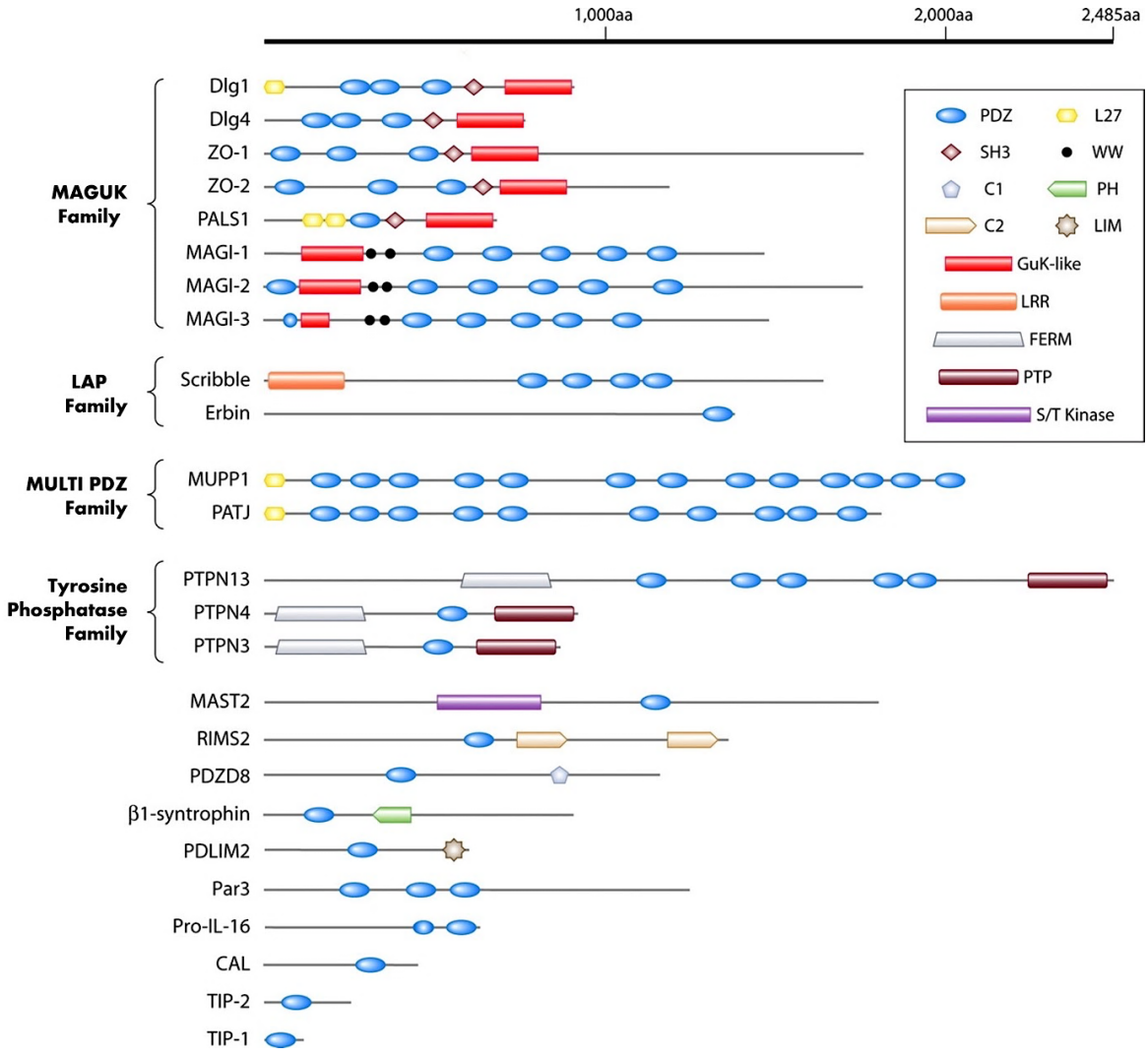

Figure 11. Families of PDZ domain-containing proteins. Proteins are sorted into groups by modular organization. Black lines represent proteins and are scaled to the length of the primary sequence. MAGUK family includes scaffold proteins involved in diverse cellular processes, such as cell–cell communication, cell polarity and signal transduction. LAP family is consisted of proteins that contain both LRR and PDZ domains in the same molecule and are involved in cell polarity and receptor targeting. MULTI PDZ is a diverse family of polypeptides that contains only multiple PDZ domains. Tyrosine Phosphatase family is a superfamily of enzymes that functions in a coordinated manner with protein tyrosine kinases to control signaling pathways of fundamental physiological processes. Indicated domains: PDZ, PSD/DLG/ZO; SH3, Src Homology 3; C1, Protein kinase C conserved region 1; C2, C2 domain; L27, Lin2-7; WW, tryptophan fold; PH, Pleckstrin homology domain; LIM, LIM domain; GuK-like, Guanylate like kinase; LRR, Leucine rich repeat; FERM, 4.1/Ezrin/Radixin/Moesin domain; PTP, Protein tyrosine phosphatase; S/T kinase, serine/threonine-protein kinase. Adopted from (Javier and Rice, 2011).

The membrane associated guanylate kinase (MAGUK) is a superfamily of scaffolding proteins that play roles in signal trafficking, cell polarity, and synaptic polarity (Funke et al., 2005; Zhang et al., 2013). Apart from PDZ domains, MAGUK proteins also comprise domains such as SH3, GuK-like, calcium-calmodulin kinase (CaMK), tryptophan fold (WW) and L27 domains. While the GuK domain is similar to the yeast guanylate kinase, it lacks the main catalytic residues and is catalytically inactive (Harris et al., 2001). The best-known members of MAGUK protein family

are PSD95 and DLG1. The LAP protein family is described by the presence of 16 N-terminal leucine-rich repeats (LRR), two LAP-specific domains, and four PDZ domains. So far, there are only four LAP family proteins identified in mammals: SCRIB, Erbin, Lano, and Densin-180 (Bonello and Peifer, 2019; Santoni et al., 2020). As LAP proteins possess both LRR and PDZ domains in the same molecule, they are involved in cell polarity regulation and receptor targeting (Santoni et al., 2002). Most of the individual PDZ domain-containing proteins are primarily involved in one pathway. However, some of them, such as 26S proteasome non-ATPase regulatory subunit 9 (PSMD9) or PDZ domain-containing protein 11 (PDZD11), are involved in a plethora of different processes (Christensen et al., 2019).

1.3.2 HPV E6 PDZ domain-binding motif (PBM)

Currently, three classes of the PBMs are defined according to the last four amino acid residues making the carboxy-terminal consensus sequences, Class I – III. Class I PBMs bind to the C-terminal motifs with the sequence of [Ser/Thr-x-Φ COOH], Class II bind to the sequence of [Φ-x-Φ-COOH] and Class III prefer the sequence of [Asp/Glu-x-Φ-COOH], where Φ represents any hydrophobic amino acid and x can be any amino acid residue. Sometimes, the recognition of the PBM involves residues placed outside of this consensus sequence. This was first demonstrated for postsynaptic protein CRIPT whose residues at the -1 position and upstream of the last four amino acids determine its specificity for an individual PDZ domain, PDZ3 (Niethammer et al., 1998).

E6 oncoproteins comprise the Class I PBMs at their extreme C-termini. This seems to be a unique feature of HR types since LR E6 oncoproteins do not contain a PBMs (Nicolaides et al., 2011; Thatte et al., 2018). Although all HR E6 oncoproteins comprise the canonical x-Ser/Thr-x-Φ COOH consensus site, they still demonstrate a diversity in their PBMs (Ganti et al., 2015) as shown by the multiple sequence alignment of E6 proteins from different HR HPV types, the MmPV1 E7, and two most frequent LR HPV types (**Figure 12.**).

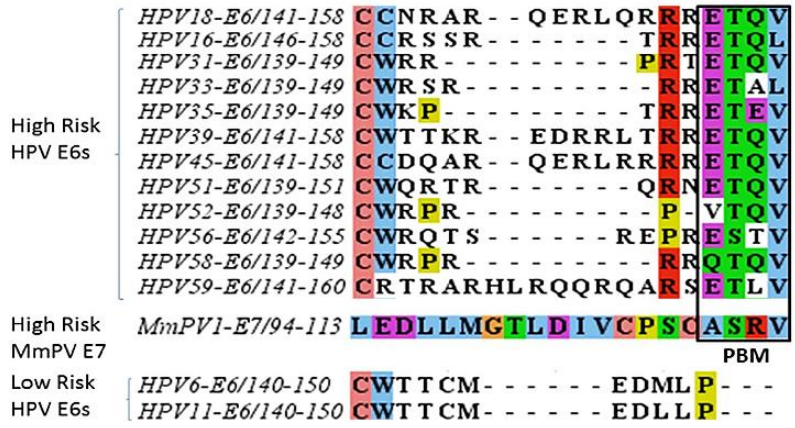

Figure 12. Differences in PBM sequences among E6 oncoproteins of various HR and LR HPV types. C-terminal sequences of most frequent HR and LR HPV E6 oncoproteins were aligned and compared. The bordered amino acids at the extreme C-terminus represent Class I PBM. Adopted from (Ganti et al., 2015).

While the importance of the E6 PBM/PDZ interaction has been primarily studied in the context of HPV-related carcinogenesis, this association seems to also regulate multiple aspects of the productive cycle. Studies in HPV31-transfected HFKs have demonstrated that the depletion or mutations in the E6 PBM lead to reduced growth rates, loss of viral episomes, and increased number of unstable viral genomes (Lee and Laimins, 2004). Furthermore, an exaggerated epithelial to mesenchymal transition (EMT) phenotype and changes in actin cytoskeletal organization were significantly reduced in the cells containing HPV18 E6 PBM mutant (Watson et al., 2003). Furthermore, it was also shown that PBM is required for preserving mitotic stability of HPV18 infected cells, the episomal maintenance and amplification in primary human keratinocytes (Marsh et al., 2017). Additionally, the importance of E6 PBM was studied in transgenic mouse models of HNCs. They showed that in mice expressing E6 with deleted PBM, E6 was still able to induce HNSCCs in co-action with E7 (Jabbar et al., 2010). These results indicate that HNSCC initiation most likely involves a mechanism which is E6 PBM-independent.

Interestingly, some studies have suggested that E6 protein stability is dependent on its intact PBM, since the loss of PBM/PDZ domain-containing proteins interactions resulted in enhanced proteasomal degradation of the HPV16 E6 oncoprotein (Nicolaides et al., 2011). This was further confirmed in a study which showed that SCRIB protein is required for the stability of E6 and this was PBM/PDZ dependent (Kranjec et al., 2016). In addition to their contribution to the optimal completion of the productive viral cycle, PBM/PDZ interactions play important roles in HPV-driven malignancies. This was described both in tissue culture model systems and in transgenic mouse models. In established human tonsillar epithelial cells, HPV16 E6 appears to interact with

protein tyrosine phosphatase (PTPN13) through its PDZ domain leading to its degradation and consequent anchorage-independent growth. However, in those cells which encoded PBM-depleted E6, neither immortalization nor EMT were observed since no PTPN13 degradation has occurred (Spanos et al., 2008). In transgenic mouse models, the integrity of E6 PBM was shown to be required for the induction of hyperplasia. However, the ability of E6 to recognize PDZ domains is not constitutive. These E6 PBM/PDZ domain-containing protein interactions seem to be negatively regulated by the protein-kinase A-mediated phosphorylation of the PBM. A few HR E6 proteins contain canonical cyclic AMP-dependent protein kinase A recognition motifs (R-R/K-x-T/S) within the PBM. Thus, the disruption of this specific event would have profound effects upon keratinocyte growth and on the productive viral cycle. It was described that the loss of PKA recognition site on HPV18 E6 PBM causes the increased cell growth, so changes in PKA signaling pathways could lead to cancer formation and progression (Delury et al., 2013). In addition to regulating E6 PBM-PDZ interactions, PKA phosphorylation allows for E6 interactions with non-PDZ domain-containing proteins such as 14-3-3 family members (Boon et al., 2015; Boon and Banks, 2013).

All these studies indicate the importance of PBMs for various functions of E6 oncoproteins. Intriguingly, a few LR E6 oncoproteins were reported to degrade PDZ-domain containing proteins despite of the lack of PBMs. HPV40 E6 displayed a complete degradation of MAGI-1 protein (James and Roberts, 2016; Van Doorslaer et al., 2015), while HPV11 E6 was reported to degrade NHERF-1 (Drews et al., 2019). Also, LR HPV70 and possibly HR HPV82 E6 oncoproteins were shown to interact and degrade PDZ domain-containing proteins DLG1 and MAGI-1 in the same way as HPV16 and HPV18 E6s do. In contrast, HR HPV66 E6 does not bind to, or degrade DLG1 and MAGI-1 (Muench et al., 2009). All these findings suggest that the ancestor of both HR and LR types acquired the ability to bind PDZ proteins, possibly for a new niche adaptation rather than as an oncogenic trait (Van Doorslaer et al., 2015).

1.3.3 Cell polarity

Cell polarity is the asymmetric organization of the plasma membrane, cytoskeleton, or organelles. It is an evolutionary conserved phenomenon implicated in cell differentiation, proliferation, and morphogenesis of both unicellular and multicellular organisms. There are two types of cell polarity: planar cell polarity (PCP) and apical-basal cell polarity (ABCP). PCP is a coordinated alignment

of cell polarity across the tissue plane important for cell migration and organ morphogenesis through the activation of cytoskeletal pathways (Axelrod, 2020; Etienne-Manneville and Arkowitz, 2020). ABCP is crucial for the formation and function of epithelial cells. It drives the localization of the adhesion molecules and effects the vertical organization of individual cells (Etienne-Manneville and Arkowitz, 2020). Epithelial cells thus contain at least two plasma membrane domains: the apical surface facing the external medium and the basolateral surface turned to connective tissue (Assémat et al., 2008).

1.3.3.1 Apical-basal cell polarity complexes

The proteins that regulate ABCP are grouped into complexes according to their localization (**Figure 13.**). Par and Crumbs complexes have been reported to be localized subapically, while Scribble complex is positioned basolaterally (Assémat et al., 2008). The 'partitioning defective' (Par) complex was first identified in *Caenorhabditis elegans*. This complex includes two Par proteins, Par3 and Par6, the serine/threonine atypical protein kinase C (aPKC) and small GTPases, such as Cdc42 or Rac1 (Joberty et al., 2000). In normal cell types, the Par complex regulates cell polarity and maintains cell homeostasis (Aranda et al., 2008). It is located at the apical region of epithelial cells, together with the Crumbs complex, where it regulates the maintenance of the apical membrane. The Crumbs complex was first identified in *Drosophila melanogaster*. It consists of transmembrane proteins Crumbs and cytoplasmic scaffolding proteins Protein associated with Lin seven 1 (Pals1) and Pals1-associated tight junction (PATJ) (Assémat et al., 2008). It is an evolutionarily conserved complex which acts as a regulator of cell growth and polarity at the apical membranes in polarized epithelia (Médina et al., 2002). Finally, the Scribble complex was also identified in *Drosophila melanogaster.* It consists of Scribble (SCRIB), Discs large (DLG1) and Lethal giant larvae (LGL1) proteins located at the basolateral region. In epithelial cells, the Scribble complex is required for membrane arrangement and maintenance (Bilder and Perrimon, 2000; Elsum et al., 2012).

These three complexes antagonize each other during cell polarity establishment. In the Par complex, Par6 interacts with Crumbs during the establishment of tight junctions (Etienne-Manneville and Arkowitz, 2020). Likewise, aPKC negatively regulates LGL from the Scribble complex by phosphorylation, which prevents its apical localization. In contrast, aPKC stabilizes the Crumbs complex, probably via Par6 binding or directly by phosphorylation of Crumbs proteins.

Furthermore, studies have indicated that Scribble complex restricts the localization of Crumbs and Par complexes to the apical region of epithelial cells, where they may act together to regulate tight junction formation (Assémat et al., 2008; Martin-Belmonte and Perez-Moreno, 2012). Thus, even a slight deregulation of any of the protein members of these polarity complexes can have a negative impact on cellular polarity and therefore, can contribute to cancer progression. Indeed, loss of polarity protein function during tumor progression promotes a dysplastic phenotype that precedes hyper-proliferation to induces neoplastic cell growth (Lin et al., 2015). Some of those PDZ proteins that are known cell polarity regulators have also been reported as targets of HPV E6 oncoprotein and they include SCRIB (Nakagawa and Huibregtse, 2000; Thomas et al., 2005), DLG1 (Gardiol et al., 1999), Par3 (Facciuto et al., 2014), PATJ (Storrs and Silverstein, 2007), and others.

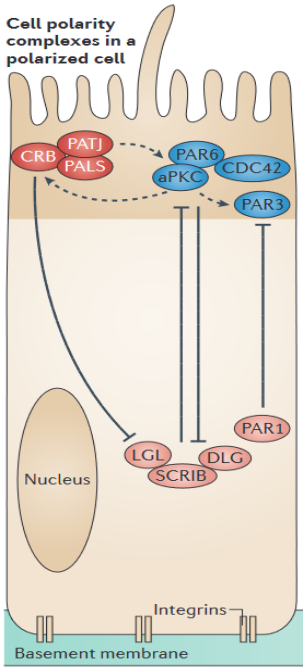

Figure 13. Cell polarity complexes. The CRUMBS complex (blue) is required for establishment of the apical membrane. It comprises the transmembrane protein CRB and the associated cytoplasmic proteins PALS1 and PALS1-associated tight junction protein (PATJ). The PAR complex (red) mediates the establishment of the apical-lateral membrane border and comprises PAR3, PAR6, atypical protein kinase C (aPKC) and cell division control 42 (CDC42). The Scribble complex (pink) comprises lethal (2) giant larvae homologue (LGL), discs large homologue (DLG) and scribble proteins. It defines the basolateral plasma membrane domain. Adapted from (Martin-Belmonte and Perez-Moreno, 2012).

1.3.4 Discs Large Homologue 1 (DLG1)

DLG1 is a member of MAGUK protein family, and, like other members of this family, it is constituted of various domains. Those enable a variety of protein-protein interactions which have an impact of numerous functions. DLG1 is a modular protein which contains a proline-rich N-terminal region, 3 PDZ domains, a SH3 domain, a HOOK (hinge, protein 4.1 binding) domain and

a GUK-like domain. Currently, two DLG1 protein isoforms have been identified which are encoded from *DLG1* gene; DLG1α and DLG1β. These two isoforms differ only by an inclusion of an L27 domain in the N-terminus of DLG1α (**Figure 14.**) and they correlate to *Drosophila* DLGA and DLGS97 proteins, respectively (Maiya et al., 2012; Mendoza et al., 2003). Furthermore, according to the Uniprot data base, there is one validated but 37 described potential isoforms of DLG1 that were computationally mapped and are a result of alternative splicing which mainly occurs in two principal regions: one at the N-terminus, right before the PDZ1 domain and the other in the HOOK region. It is speculated that these isoforms play diverse roles in humans (Roberts et al., 2007; Waites et al., 2009).

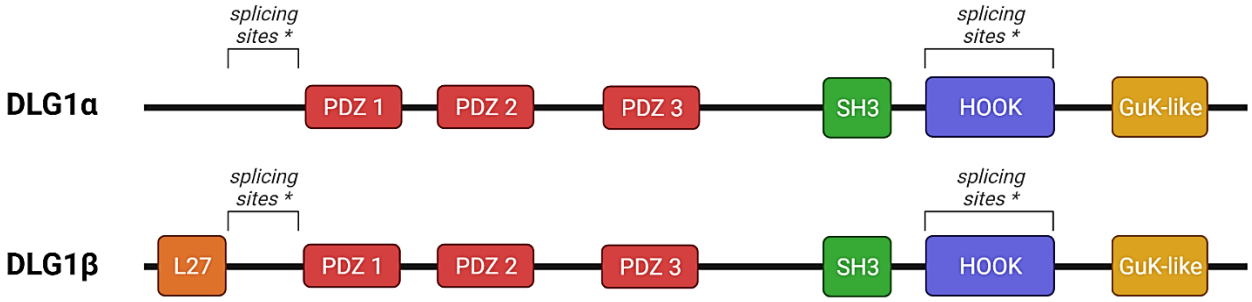

Figure 14. DLG1 isoforms and functional domains. Both DLG1α and DLG1β proteins encode 3 PDZ domains, a SH3 domain, a HOOK domain and a GuK-like domain. The DLG1β also encodes L27 region at N-terminus. Alternative splicing sites at the N-terminus and in the HOOK region are indicated. Adapted from (Roberts et al., 2012).

DLG1 has a modular organization which enables interactions with a plethora of proteins, thus allowing its involvement in various cellular processes. As a component of the conserved Scribble polarity complex, DLG1 is required for cell polarity establishment and maintenance, as well as for asymmetric cell division and cell migration (Marziali et al., 2019; Stephens et al., 2018). Furthermore, DLG1 is expressed in neuronal cells where it contributes to normal nerve cell functions by regulating various signaling pathways. It was reported that DLG1 forms complexes with AMPA and NMDA-type glutamate receptors, both key components of the glutamatergic synapse (Howard et al., 2010). Additionally, DLG1 seems to play a major role in trafficking and anchoring ion channel surface expression via interactions with various potassium channels (Gardoni et al., 2007; Kuras et al., 2012). All things considered, DLG1 is involved in modulation of several important cellular functions and therefore its deregulation can contribute to a number of human disorders and diseases.

1.3.4.1 Involvement of DLG1 modulations in human pathologies

DLG1 interacts with various members of the nervous system pathways so its deregulation can contribute to a wide verity of neurological disorders. Indeed, DLG1 deregulation was noticed in schizophrenia, Alzheimer disease, depression, Parkinson's disease and many others (Dunn et al., 2013; Marcello et al., 2012; Sato et al., 2008). In addition, a growing number of reports have suggested that DLG1 mutations, loss or even overexpression, contributes to various cancer types in humans. DLG1 mutations were reported in breast cancer, whereas a complete loss was detected in lung, larynx, and hepatocellular cancers (Marziali et al., 2019). The reverse pattern, an upregulation of DLG1 in the early stages of the disease, followed by a clear downregulation was observed in colon cancer (Gardiol et al., 2006; Zhu et al., 2017). DLG1 was also described as a target of numerous viral oncoproteins including the adenoviral E4-ORF1 (Kong et al., 2014) and the Tax protein encoded by human T cell leukemia virus type 1 (Hirata et al., 2004; Marziali et al., 2017). Furthermore, DLG1 was the first PDZ-domain containing protein identified as a target of HR E6 oncoproteins (Kiyono et al., 1997). This interaction occurs via one of two PDZ domains in DLG1, PDZ1 and PDZ2, and E6 PBM, which ultimately leads to proteasome-mediated degradation (Gardiol et al., 1999). Surprisingly, recent analyses suggested that this E6 driven process is E6AP-independent (Vats et al., 2019). Interestingly, E6 degrades DLG1, but it does not completely eliminate it due to E6 specific affinity for a subset of nuclear and hyperphosphorylated forms of DLG1 (Massimi et al., 2006, 2004). Likewise, the specificity of various HPV E6 oncoproteins for binding DLG1 depends on their PBMs sequences (Thomas et al., 2002) and HPV18 E6 was shown to be one of the E6s that preferentially targets DLG1 (Thomas et al., 2005). This seems to be due to the threonine residue in 18E6 PBM, which was shown to be essential for this interaction, since substitutions with other residues inhibit the binding and subsequent protein turnover at the proteasome (Gardiol et al., 1999). Interestingly, the specificity appears to be also reliant on cellular localization of DLG1, since it was suggested that 18E6 preferentially targets cytoplasmic and nuclear forms of DLG1 (Massimi et al., 2004; Narayan et al., 2009). All these findings and the fact that HPV induces more than 99% of cervical cancers, have risen a question of DLG1 involvement in cervical cancer. A few studies have indicated DLG1 to be an important factor in the progression of low-grade cervical intraepithelial lesions (LSILs), since it was upregulated in all LSILs that progressed to high-grade squamous intraepithelial lesions (HSIL) (Cavatorta et al., 2004; Lin et al.,

2004). In contrast, a reduction of DLG1 was observed in the invasive cervical carcinoma implying to the diversity of its regulation in premalignant and malignant lesions.

1.3.5 Scribble (SCRIB)

SCRIB protein is an approximately 1700 amino acids long member of the LAP protein family. As the other members of this family, it contains 16 leucine rich repeats (LRRs) and four PDZ domains (**Figure 15.**). LRRs are necessary and sufficient for membranous localization of LAP proteins and this seems to require the engagement of E-cadherin (Navarro et al., 2005). Interestingly, only a few known binding partners, including LGL, associate with SCRIB via LRRs (Kallay et al., 2006; Santoni et al., 2020). Additionally, SCRIB has phosphorylation sites which are responsible for the control of its ligand localization and consequently the signaling pathways they regulate. Ras signaling pathway protein kinase ERK appears to bind and phosphorylate SCRIB, which could prevent ERK translocation to the nucleus and thus regulate ERK signaling. SCRIB also has a PKA protein kinase phosphorylation site which was suggested to play a role in regulating ERK binding to SCRIB (Stephens et al., 2018).

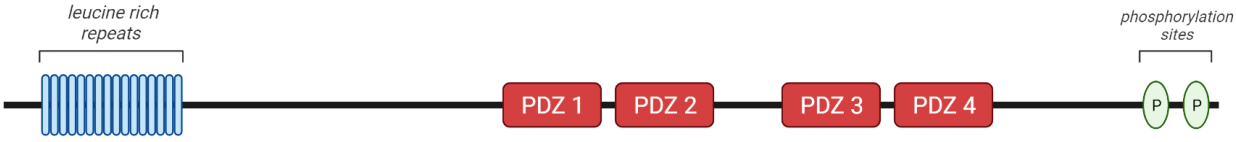

Figure 15. SCRIB structure and functional domains. SCRIB protein comprises 16 LRRs (blue) required for its localization into cell membranes. In addition, it contains four PDZ domains (red), each enabling different interactions with various cellular proteins. SCRIB function seems to depend on the phosphorylation state regulated by ERK and PKA protein kinases at indicated sites.

Due to a variety of domains, SCRIB acts as a scaffold protein and enables key molecular interactions at distinct subcellular localizations. SCRIB has a role in regulation of different aspects of polarized cell differentiation during epithelial and neuronal morphogenesis as well as T-cell polarization. Most of these interactions occur through PDZ domains and interestingly, although similar, each of SCRIB PDZ domains can exhibit unique binding preferences towards specific ligands (Lim et al., 2017). The best-described function of SCRIB is its involvement in establishment and maintenance of cell polarity. Together with DLG1 and LGL, SCRIB is a part of the Scribble complex required for apical-basal polarity (Elsum et al., 2012). Along with the regulation of cell polarity, SCRIB is also involved in cell migration as it was shown to have a strong impact on the function of PAK and Rac, two key molecules implicated in this process (Nola et al., 2008). Due to its role in cell polarity regulation and migration, SCRIB has also been implicated in

EMT, where it was shown to be involved in stabilization of the association of E-cadherin with catenin. This was demonstrated to lead to the regulation of epithelial cell adhesion and migration (Qin et al., 2005). Thus, any deficiency in SCRIB function impairs cell polarity and cell movement, although the exact mechanisms have yet to be elucidated.

Junctional localization of SCRIB seems to be the foundation for its tumor suppressive role (Feigin et al., 2014). Indeed, in the collaboration with c-myc oncogene, the loss of SCRIB leads to the transformation of epithelial cells. In addition, in human epithelial cells which express oncogenic Ras or Raf, loss of SCRIB was shown to promote invasion of cells through the extracellular matrix in an organotypic culture system (Dow et al., 2008). Similarly, mislocalization of SCRIB from cell-cell junctions alone was shown to be adequate to promote cell transformation (Zhan et al., 2008). Surprisingly, analysis of human and mouse tumors have revealed both downregulated and mislocalized SCRIB suggesting its likely evolutionary conserved roles in carcinogenesis among different species.

1.3.5.1 SCRIB modulations leading to human pathologies

SCRIB expression and localization have been investigated in several human pathologies. SCRIB deregulations are not unique in cancers since SCRIB was reported as degraded, mislocalized, or even upregulated in various cancer types. These reports suggested its dual function, both as tumor suppressor and oncogene. The tumor suppressive role of SCRIB was first discovered in *Drosophila* when it was shown that its mutations lead to neoplastic overgrowth (Bilder, 2004). Its tumor suppressive role was later supported in studies showing the disruption of SCRIB protein expression in various human cancers. For example, downregulation of SCRIB was associated with the lack of epithelial cell polarity and disorganized tissue architecture in colon cancer (Gardiol et al., 2006). Additionally, a study investigating breast cancers showed that most lobular tumors did not express SCRIB, again suggesting its role as a tumor suppressor (Navarro et al., 2005). Aside from its downregulation, it was also reported that mislocalized SCRIB functions as a neomorph to promote mammary tumorigenesis by affecting subcellular localization of PTEN and activating an Akt/mTOR/S6kinase signaling pathway (Feigin et al., 2014). Similarly, SCRIB was reported to be mislocalized in breast cancer, in which this deregulation affected polarity, morphogenesis, and apoptosis (Zhan et al., 2008). A tumor suppressive function of SCRIB was further confirmed after it was characterized as a target of HPV E6 oncoproteins. Unlike DLG1, SCRIB is targeted for

ubiquitination and proteasome mediated degradation by the E6/E6AP complex (Nakagawa and Huibregtse, 2000; Vats et al., 2019). Also, on the contrary to DLG1 being preferential target of HPV18 E6, 16E6 was reported to target and degrade SCRIB more efficiently via PBM-PDZ interaction than other E6 oncoproteins (Thomas et al., 2005). Unveiling that SCRIB is a cellular target of E6 initiated a series of studies aimed at investigating its expression in cervical cancer progression. These analyses indicated that E6-mediated degradation of SCRIB increases during the progression from LSIL to HSIL. The same study proposed that downregulation of SCRIB mRNA expression in combination with ubiquitin-mediated degradation of SCRIB led to the complete ablation of SCRIB during the progression from HSIL to invasive cervical cancer (Nakagawa et al., 2004). In contrast to the previous reports, some studies demonstrated SCRIB to be overexpressed in several human cancers (Vaira et al., 2011), suggesting its oncogenic role in certain malignancies. Hence, SCRIB was found to be highly expressed in patients with colorectal cancer, where this upregulation was associated with malignant characteristics, such as increased proliferation, cessation of apoptosis, and promoted EMT (Shen et al., 2021). Furthermore, a recent study in ovarian cancer cell lines described overexpression of SCRIB to stimulate cell proliferation and invasion (Hussein et al., 2021). Moreover, loss of SCRIB was also reported to delay the onset of myc-driven lymphoma, once again suggesting it has oncogenic functions in some human cancers (Hawkins et al., 2016). Given the numerous studies showing the contradictory behavior of the SCRIB protein, its role in oncogenesis is still not fully elucidated. Therefore, SCRIB remains one of the focuses of further research which could provide important novel information about its roles in the process of carcinogenesis.

2 HYPOTHESIS AND AIMS

A total of 15 HPV types are classified as HR due to their ability to cause malignant transformation at various anatomical sites. In the cervix, the process from the initial infection to development of malignancy is well defined - it is dependent on the co-action of E6 and E7 oncoproteins. Along with p53 targeting, E6 from all HR HPVs forms interactions with PDZ-domain containing proteins DLG1 and SCRIB, which have vital roles in cell polarity establishment and maintenance. Variations in both DLG1 and SCRIB expression was observed to be associated with progression of certain cancers, including some that are HPV-positive. Obtained results suggested that E6 may be responsible for those variations. Interestingly, the role of HPV in HN carcinogenesis is still unclear. Moreover, 70% of cervical cancers are caused by HPV16 and HPV18, while HPV16 is the predominant type in HN area, causing 90-95% of HNSCCs. This indicates that the process of HPV-driven cell transformation might be significantly different in this anatomical region. Therefore, we hypothesized that the diversity in preference of 16E6 targeting DLG1 and SCRIB may cause modulations of their normal cellular functions, which could potentially be significant for the onset of HN malignancy.

To validate the hypothesis, this research aimed to:

- Establish previously immortalized keratinocyte isolated from HN (iNOK and iHTK) and genital area (iHFK) cell lines which stably express 16 E6/E7 oncoproteins.
- Investigate the binding capacity of HPV16 E6 and HPV18 E6 with DLG1 and SCRIB and examine the impact of 16E6 on their protein levels in three keratinocyte cell lines.
- Examine 16E6-mediated modulations in the localization and distribution of DLG1 and SCRIB proteins in previously established immortalized keratinocyte cell lines.
- Correlate changes in E6, DLG1 and SCRIB transcription levels in primary keratinocyte cell lines containing HPV16 episomes with HPV-positive and HPV-negative OPSCC-derived cell lines.
- Associate observed fluctuations in transcription levels with changes in the localization of DLG1 and SCRIB proteins during HPV16 productive cycle in HTK derived organotypic 3D raft cultures.
- Elucidate biological impacts of DLG1 and SCRIB deregulation in HPV16-positive and HPV-negative OPSCC tissues.

3 MATERIALS AND METHODS

3.1 Materials

3.1.1 Plasmids

All the plasmids which were used to prepare this doctoral thesis are listed in **Table 1**. Briefly, plasmids pcDNA3 E6 and E7 were used as DNA templates, while donor vectors pAAVS1-BSD-DNR and pUltra-GFP as well as plasmids pCas-Guide and p-Cas Scramble were used to establish keratinocytes stably expressing HPV oncogenes. Additionally, pMD2.G and psPAX2 were used for production of lentiviruses encoding HPV16 E6.

Table 1. Plasmids for cloning experiments and establishment of keratinocytes expressing HPV16 genes.

Plasmid	***Description***	***Manufacturer***	***Cat. number***
pcDNA3 E6	pcDNA3 expressing HA-tagged HPV16 E6	Kind gift from Lawrence Banks	
pcDNA3 E7	pcDNA3 expressing HA-tagged HPV16 E7		
pAAVS1-BSD-DNR	Donor vector with AAVS1 homologous arms, C-terminal Myc-DDK tag, Blasticidin resistance	OriGene, Maryland, USA	GE100035
pCas-Scramble	pCAS-Scramble, pCas-Guide vector with a scrambled sequence as a negative control	OriGene, Maryland, USA	GE100003
pCas-Guide	pCas-Guide vector (with Cas9 expression) for genomic target sequence cloning	OriGene, Maryland, USA	GE100002
pUltra-GFP	3rd generation Lentiviral vector for bi-cistronic expression of EGFP and gene of interest	Addgene, Massachusetts, USA	24129
pMD2.G	VSV-G envelope expressing plasmid	Addgene, Massachusetts, USA	12259
psPAX2	2nd generation lentiviral packaging plasmid.	Addgene, Massachusetts, USA	12260
pT2Zh HPV16	plasmid carrying all HPV16 early genes	Kind gift from John Doorbar	

3.1.2 Nucleotides

The nucleotides which were used for PCR amplifications of genes of interest in experiments of plasmid constructions as well as cloning validation are listed in **Table 2**.

Table 2. Nucleotides for PCR amplifications in cloning and genotyping experiments.

Nucleotides	***Manufacturer***	***Cat. number***
dATP, PCR Grade	Roche Holding AG, Switzerland	11934511001
dTTP, PCR Grade	Roche Holding AG, Switzerland	11934546001
dCTP, PCR Grade	Roche Holding AG, Switzerland	11934520001
dGTP, PCR Grade	Roche Holding AG, Switzerland	11934538001

3.1.3 PCR primers

Specific primer sequences used for verifying DNA isolation, confirming the quality of DNA and HPV genotyping by PCR are listed in **Table 3**.

Table 3. PCR primers for determining gene expression.

Gene	*Primers*		*Length*	*Tm*
Beta actin	6999-7018	5'- CCACACTGTGCCCATCTACG	100 bp	60 °C
	7097-7072	5'- AGGATCTTCATGAGGTAGTCAGTCAG		
PGMY/ beta globin	PGMY11 A	5'-GCACAGGGACATAACAATGG	450 bp / 256 bp	51 °C
	PGMY11 B	5'-GCGCAGGGCCACAATAATGG		
	PGMY11 C	5'-GCACAGGGACATAATAATGG		
	PGMY11 D	5'-GCCCAGGGCCACAACAATGG		
	PGMY11 E	5'-GCTCAGGGTTTAAACAATGG		
	PGMY09 F	5'-CGTCCCAAAGGAAACTGATC		
	PGMY09 G	5'-CGACCTAAAGGAAACTGATC		
	PGMY09 H	5'-CGTCCAAAAGGAAACTGATC		
	PGMY09 Ia	5'-GCCAAGGGGAAACTGATC		
	PGMY09 J	5'-CGTCCCAAAGGATACTGATC		
	PGMY09 K	5'-CGTCCAAGGGGATACTGATC		
	PGMY09 L	5'-CGACCTAAAGGGAATTGATC		
	PGMY09 M	5'-CGACCTAGTGGAAATTGATC		
	PGMY09 N	5'-CGACCAAGGGGATATTGATC		
	PGMY09 Pa	5'-GCCCAACGGAAACTGATC		
	PGMY09 Q	5'-CGACCCAAGGGAAACTGGTC		
	PGMY09 R	5'-CGTCCTAAAGGAAACTGGTC		
	HMB01b	5'-GCGACCCAATGCAAATTGGT		
GP5/6	GP5	5'-TTTGTTACTGTGGTAGATAC	142 bp	40 °C
	GP6	5'-GAAAAATAAACTGTAAATCA		
SPF10	SPF 1A	5'-TAATACGACTCACTATAGGGCICAGGGICACAATAATGG	65 bp	51 °C
	SPF 1B	5'-TAATACGACTCACTATAGGGCICAGGGICATAACAATGG		
	SPF 1CD	5'-TAATACGACTCACTATAGGGCICARGGICATAATAATGG		
	SPF 2BD	5'-ATTTAGGTGACAACTATAGGTIGTATCIACWACAGTAACAAA		
	SPF 1A	5'-TAATACGACTCACTATAGGGCICAGGGICACAATAATGG		
HPV16 E6/E7	16E6/E7_ F	5'- GGTCGGTGGACCGGTCGATG	99 bp	54 °C
	16E6/E7_R	5'- GCAATGTAGGTGTATCTCCA		
p53 full	p53 Full_F	5'- TTCTTGCGGAGATTCTCTTCCT	1386 bp	63 °C
	p53 Full_R	5'-CCATCTACAAGCAGTCACAGCA		
p53 exon 11	p53 eg11_F	5'- TTTGGGTCTTTGAACCCTTG	81 bp	63 °C
	p53 eg11_R	5'-GATTTGAATTCCCGTTGTCC		

3.1.4 qPCR primers

RT-qPCR primer sequences used to determine DLG1 and SCRIB transcription levels in differentiating keratinocytes containing HPV16 episomes are listed in **Table 4**.

Table 4. RT-qPCR primers for defining transcription level rates of mRNA of interest.

Gene	*Primers*		*Length*	*Tm*
HPV16 E6	HPV16_E6_F	5'-CAGGAGCGACCCAGAAAGT	116 bp	60 °C
	HPV16_E6_R	5'-AGTCATATACCTCACGTCGCAG		
DLG1β	DLG1β_F	5'-CGGAAGCAAGATACCCAGAG	113 bp	59 °C
	DLG1β_R	5'-AATTGGTTCAGACGGCTTTG		
DLG1 HOOK	DLG1 HOOK_F	5'-GCCCATTCCTAGCGCATGAACTCC	98 bp	59 °C
	DLG1 HOOK_R	5'-GCCATTCTGGTGGATGGCAGAG		
SCRIB	SCRIB_F	5'-CCTGCCAGCTCCAGCACCAC	147 bp	59 °C
	SCRIB_R	5'-CGGCTGGGGTGGGGCAGTTA		

3.1.5 Enzymes and enzyme-related buffers

Enzymes and their corresponding buffers which were used for cloning experiments including multiplying DNA fragments, DNA restriction and insert ligation are listed in **Table 5.**

Table 5. Enzymes and enzyme-related buffers.

Enzymes and buffers	*Manufacturer*	*Cat. number*
GoTaq G2 DNA Polymerase	Promega, Wisconsin, USA	M7841
GoTaq G2 Hot Start Taq Polymerase	Promega, Wisconsin, USA	M7401
T4 DNA Ligase	Promega, Wisconsin, USA	M1801
AscI	New England biolabs, Massachusetts, USA	R0558S
XbaI	New England biolabs, Massachusetts, USA	R0145S
MluI	New England biolabs, Massachusetts, USA	R0198S
SalI-HF	New England biolabs, Massachusetts, USA	R3138S
BclI-HF	New England biolabs, Massachusetts, USA	R3160S
BamHI-HF	New England biolabs, Massachusetts, USA	R3136S
EcoRI-HF	New England biolabs, Massachusetts, USA	R3101S
5X Green GoTaq® Reaction Buffer	Promega, Wisconsin, USA	M791A
T4 DNA Ligase 10X Buffer	Promega, Wisconsin, USA	C126A
CutSmart® Buffer	New England biolabs, Massachusetts, USA	B7204S

3.1.6 Antibodies

Primary and secondary antibodies used to determine protein expression levels and localization in cells, organotypic 3D raft cultures or tissues, and to verify protein interactions are all listed in **Table 6**.

Table 6. Primary and secondary antibodies for Western blot and immunohistochemistry.

Antibody	*Manufacturer*	*Cat. number*
Anti-SAP 97 Antibody (2D11)	Santa Cruz Biotechnology, Texas, USA	sc-9961
Anti-Scrib Antibody (C-6)	Santa Cruz Biotechnology, Texas, USA	sc-55543
Anti-Scrib Antibody (D-2)	Santa Cruz Biotechnology, Texas, USA	sc-374139
Anti-p53 Antibody (DO-1)	Santa Cruz Biotechnology, Texas, USA	sc-126
Anti- β-Actin HRP (AC-15)	Sigma-Aldrich, Missouri, USA	A3854
Anti-β-Actin (AC-74)	Sigma-Aldrich, Missouri, USA	A2228
Anti-THOC1 Antibody (p84, E-10)	Santa Cruz Biotechnology, Texas, USA	c-514123
Anti-α Tubulin (B-7)	Santa Cruz Biotechnology, Texas, USA	sc-5286
Anti-CD71/ (3B8 2A1)	Santa Cruz Biotechnology, Texas, USA	sc-32272
Anti-Vimentin Antibody (V9)	Santa Cruz Biotechnology, Texas, USA	sc-6260
Rabbit Anti-Mouse HRP	Agilent Technologies, California, USA	P0161
Goat anti-Mouse IgG (H+L) HRP	Thermo Fisher Scientific, Massachusetts, USA	31430
Swine Anti-Rabbit /HRP	Agilent Technologies, California, USA	P0217
Alexa Fluor 488 donkey anti-mouse IgG (H+L)	Invitrogen by Thermo Fisher Scientific, Massachusetts, USA	A21202
Alexa Fluor 488 donkey anti-rabbit IgG (H+L)	Invitrogen by Thermo Fisher Scientific, Massachusetts, USA	A21206
Rhodamine Red-X Goat anti-mouse (H+L)	Invitrogen by Thermo Fisher Scientific, Massachusetts, USA	R6393

3.1.7 DNA ladders and protein markers

In **Table 7**. are depicted all DNA ladders and protein markers used to determine the correct size of amplified PCR products or corresponding-size protein bands in Western blot, respectively.

Table 7. DNA ladders and protein markers.

	Marker	*Manufacturer*	*Cat. number*
DNA ladders	BenchTop 1kb DNA Ladder	Promega, Wisconsin, USA	G754A
	GelPilot 100 bp Ladder	Qiagen, Germany	239035
	GelPilot 50 bp Ladder	Qiagen, Germany	239025
	Quick-load Purple 1 kb Plus DNA Ladder	New England biolabs, Massachusetts, USA	N0550S
	Quick-load Purple 100 bp DNA Ladder	New England biolabs, Massachusetts, USA	N0551S
Protein markers	Precision Plus Protein Standard All Blue	Bio-Rad Laboratories, California, USA	1610373
	PageRuler™ Plus Prestained Protein Ladder	Thermo Fisher Scientific, Massachusetts, USA	26619
	Regular Range Protein Marker	ProteinTech Group, United Kingdom	PL00001

3.1.8 Growth media and supplements

The supplemented media used for growing and maintaining cells depended on the cell type. Bacterial cells used for plasmid production were grown in liquid lysogeny broth (LB) and on agar plates. HeLa, CaSki, C33A, HEK293, HEK293T and 3T3-J2 were grown in Dulbecco's Modified

Eagle Medium (DMEM). Immortalized keratinocytes iNOK, iHFK and iHTK were grown in Keratinocyte supplement free medium (KSFM) supplemented with bovine Pituitary Extract (BPE) and EGF, Human Recombinant to make KGM complete media, while primary keratinocytes iHTK were grown in E-media. All the media and corresponding supplements are listed in **Table 8**.

Table 8. Growth media and corresponding supplements for cultivation of human, bacterial and mice cells.

Media	***Product***	***Manufacturer***	***Cat. number***
LB broth and LB agar plates	Agar	Sigma-Aldrich, Missouri, USA	05040
	LB Broth	Sigma-Aldrich, Missouri, USA	L3022
	Ampicillin sodium salt	Sigma-Aldrich, Missouri, USA	A9518
DMEM complete	Dulbecco's Modified Eagle Medium (DMEM)	Thermo Fisher Scientific, Massachusetts, USA	31600-083
	Gibco Sodium Pyruvate (100 mM)	Thermo Fisher Scientific, Massachusetts, USA	11360039
	L-glutamine, ≥99% TLC	Sigma-Aldrich, Missouri, USA	G-3126
	Gibco Penicillin-Streptomycin (10,000 U/mL)	Thermo Fisher Scientific, Massachusetts, USA	15140122
	Gibco Fetal Bovine Serum (FBS)	Thermo Fisher Scientific, Massachusetts, USA	26140079
KGM complete	Gibco Keratinocyte supplement free medium (KSFM)	Invitrogen by Thermo Fisher Scientific, Massachusetts, USA	17005-059
	Bovine Pituitary Extract (BPE)	Invitrogen by Thermo Fisher Scientific, Massachusetts, USA	supplied with KSFM
	EGF, Human Recombinant	Invitrogen by Thermo Fisher Scientific, Massachusetts, USA	
E-media and 3T3-J2 media	DMEM – high glucose	Thermo Fisher Scientific, Massachusetts, USA	D5796-500ML
	Adenine	Sigma-Aldrich, Missouri, USA	A-2786
	Cholera enterotoxin	ICN Biomedicals, Inc., Ohio, USA	856011
	Gibco F-12 Nut Mix (Ham)	Thermo Fisher Scientific, Massachusetts, USA	21765-029
	Hydrocortisone	Sigma-Aldrich, Missouri, USA	H-0888
	Insulin	Sigma-Aldrich, Missouri, USA	I-6634
	Transferrin	Sigma-Aldrich, Missouri, USA	T-1147
	3,3′,5-Triiodo-L-thyronine	Sigma-Aldrich, Missouri, USA	T-6397
	GIBCO Penicillin-Streptomycin	Invitrogen by Thermo Fisher Scientific, Massachusetts, USA	15140122

3.1.9 Commercially available kits

All commercially available kits which were used for various experiments, from DNA isolation to immunofluorescence are listed in the **Table 9**.

Table 9. Commercial kits for implementation of various experiments.

Product	*Manufacturer*	*Cat. number*
CINtec p16 Histology Kit	Roche Holding AG, Switzerland	9511
Dako EnVision+ Dual Link System-HRP (DAB+)	Agilent Technologies, California, USA	K4065
Glutathione−Agarose	Sigma-Aldrich, Missouri, USA	G4510
Monarch DNA Gel Extraction Kit	New England biolabs, Massachusetts, USA	T1020G
Monarch PCR & DNA Cleanup Kit	New England biolabs, Massachusetts, USA	T1030G
NucleoBond PC 500, Maxi	Macherey-Nagel Gmbh, Germany	740574.50
NucleoSpin DNA FFPE XS	Macherey-Nagel Gmbh, Germany	740980.50
ProteoExtract® Subcellular Proteome Extraction Kit	The Calbiochem by Merck KGa, Germany	539790
Protease Inhibitor Cocktail set I	The Calbiochem by Merck KGa, Germany	539131
Qiagen Plasmid Maxi Kit	Qiagen, Germany	12163
Wizard Plus SV Minipreps DNA Purification System	Promega, Wisconsin, USA	A1460
Wizard SV Gel and PCR Clean-Up System	Promega, Wisconsin, USA	A9282
Direct-zol™ RNA Miniprep	Zymo research, California, United States	R2050
FuGENE® HD Transfection Reagent	Promega, Wisconsin, USA	E2311
Viromer® PLASMID Transfection Reagent	Lipocalyx GmbH, Germany	VpD-01LB-01
VIROMER® RED Transfection Reagent	Lipocalyx GmbH, Germany	VR-01LB-00
Lipofectamine™ 2000 Transfection Reagent	Thermo Fisher Scientific, Massachusetts, USA	11668019
RNeasy Mini Kit	Qiagen, Germany	74104
QuantiTect Reverse Transcription Kit	Qiagen, Germany	205311
RNase-Free DNase Set	Qiagen, Germany	79254
Tetro cDNA Synthesis Kit	Meridian Bioscience Inc., Ohio, USA	BIO-65043
Power SYBR™ Green PCR Master Mix	Thermo Fisher Scientific, Massachusetts, USA	4368577
SensiFAST SYBR No-ROX Kit	Meridian Bioscience Inc., Ohio, USA	BIO-98020
PVDF Western Blotting Membranes	Roche Holding AG, Switzerland	03010040001

3.1.10 Other reagents

Table 10. includes a list of all the chemical solutions which were used for preparation of buffers and for conduction of various experiments in this doctoral research.

Table 10. Other reagents for various experiments and cell treatment.

Product	*Manufacturer*	*Cat. Number*
2-Mercaptoethanol	Sigma-Aldrich, Missouri, USA	60242
5-Bromo-2 -deoxyuridine	Sigma-Aldrich, Missouri, USA	B-9285
Acetic acid	Sigma-Aldrich, Missouri, USA	695092
Acrylamide	Carl Roth Gmbh & Co. Kg, Germany	7871.2
Agarose	Sigma-Aldrich, Missouri, USA	A9539
Amersham ECL Western Blotting Detection Reagent	Cytiva, United Kingdom	RPN2106

Product	*Manufacturer*	*Cat. Number*
Ammonium persulfate	Sigma-Aldrich, Missouri, USA	09913-100
BioClear New	Biognost, Croatia	BCL-1L
Biomount new	Biognost, Croatia	BMN30
Bovine Serum Albumin Fraction V	Roche Holding AG, Switzerland	10735078001
Bovine Serum Albumin Standard Ampules, 2 mg/mL	Thermo Fisher Scientific, Massachusetts, USA	23209
Brilliant Blue R	Sigma-Aldrich, Missouri, USA	B-0149
Bromophenol Blue sodium salt Dye	Sigma-Aldrich, Missouri, USA	114405
Calcium chloride, $CaCl_2$	Kemika d.d., Croatia	1146609
Cintec Wash Buffer 10x	Roche Holding AG, Switzerland	8550
Dako Mayer's Hematoxylin Histological Staining reagent	Agilent Technologies, California, USA	S3309
EDTA	Sigma-Aldrich, Missouri, USA	E-5134
Ethanol absolute pro analysi	Gram mol, Croatia	P147300
Fluoroshield	Sigma-Aldrich, Missouri, USA	F6182
Glycerol	Kemika d.d., Croatia	07119 01
Glycine	Sigma-Aldrich, Missouri, USA	33226
HEPES	Sigma-Aldrich, Missouri, USA	H4034
Histo-Clear	National Diagnostics, Georgia, USA	HS-200
Methanol, pro analysi	Gram mol, Croatia	P140500
MgCl2, 25 mM	Promega, Wisconsin, USA	A3511
N,N,N′,N′-Tetramethylethylenediamine, TEMED	Sigma-Aldrich, Missouri, USA	T9281
N,N′-Methylenebisacrylamid	Sigma-Aldrich, Missouri, USA	M7279
NaCl	Gram mol, Croatia	7647-14-5
$NaHCO_3$	J.T. Baker, New Jersey, USA	3506-01
NaOH	J.T. Baker, New Jersey, USA	3722-01
NP-40	Thermo Fisher Scientific, Massachusetts, USA	28324
Ponceau-s	Sigma-Aldrich, Missouri, USA	P3504
Protein Assay Dye Reagent Concentrate	Bio-Rad Laboratories, California, USA	500-0006
QIAzol Lysis Reagent	Qiagen, Germany	79306
Rat tail collagen type I	Corning Inc., New York, USA	354249
Sodium dodecyl sulfate, SDS	Sigma-Aldrich, Missouri, USA	L3771
SuperSignal™ West Pico PLUS	Thermo Fisher Scientific, Massachusetts, USA	34580
Tris	Merck KGa, Germany	KB313482
Tris-HCl	Sigma-Aldrich, Missouri, USA	1185-53-1
Tween-20	Sigma-Aldrich, Missouri, USA	P2287

3.1.11 Buffers

All buffers and their composition with the exact amounts of each component are listed in **Table 11**. The buffers were used for either washing cells, rafts, tissues, or membranes, for making agarose and acrylamide gels, for cell lysis etc.

Table 11. Buffers composition.

Buffer	*Components*	*Amount*
PBS, pH 7.4	NaCl	137 mM
	KCl	2.7 mM
	Na_2HPO_4	10 mM
	KH_2PO_4	1.8 mM
TBS, pH 7.4	NaCl	1.5 M
	Tris-HCl	0.5 M
2x HBS	HEPES	50 mM
	NaCl	280 mM
	Na_2HPO_4	1.5 mM
Acrylamide stock	Acrylamide	5.3 M
	Bisacryalmide	65 mM
TE	Tris	10 mM
	EDTA	1 mM
E1A buffer	HEPES	250 mM
	NaCl	5 M
	EDTA	0.5 M
	NP-40	10%
Running buffer	Tris-HCl	25 mM
	Glycine	190 mM
	SDS	0,10%
Transfer buffer	Tris-HCl	25 mM
	Glycine	190 mM
	Methanol	20%
Laemmli 2x buffer/loading buffer	SDS	4%
	2-Mercaptoethanol	10%
	glycerol	20%
	bromophenol blue	0,00%
	Tris-HCl	125 mM
Destain buffer	Methanol	40%
	Acetic acid	7%
TAE buffer	Tris	40 mM
	Acetate	20 mM
	EDTA	1 mM
TBST 1x buffer	NaCl	1.5 M
	Tris-HCl	0.5 M
	Tween-20	0,10%
Ponceau-s	Ponceau-s	0,10%
	acetic acid	5%
Coomassie Brilliant Blue	Coomassie Brilliant Blue R250	3 g/L
	Glacial acetic acid	10%
	Methanol	45%

Buffer	*Components*	*Amount*
10x Reconstitution buffer (in NaOH)	$NaHO_3$	2.2%
	HEPES	4.77%
	NaOH	0.05 M
Ab solution	TBS 1X	
	BSA	1%
	FBS	10%
	Triton X-100	0,3%
EDTA buffer (pH 8)	EDTA	1 mM
	Tween-20	0,1%
	NaOH	

3.1.12 Instruments and programs

All the instruments which were used for performing experiments and computer programs used for data analysis and visualization are listed in **Table 12**.

Table 12. Instruments and programs for data analysis and visualization.

Group	*Product*	*Manufacturer*
Cell culture equipment	BB-16 D-63450 Incubator	Heraeus group, Germany
	Laminar flow, fume hood KTV-S	Klimaoprema d.d., Croatia
	OmniPET Pipette Filler	Cleaver Scientific Ltd, UK
	Easypet® 4421 pipetting aid	Eppendorf, Germany
	LABSONIC® M The ultrasonic homogenizer	Montreal Biotech Inc., Montreal, Canada
	Probe 0.5 mm and 1 mm	Montreal Biotech Inc., Montreal, Canada
	NanoPhotometer® N60	Implen GmbH, Germany
	CellDrop FL Fluorescence Cell Counter	DeNovix Inc., Delaware, USA
Thermal Cyclers	Applied Biosystems Veriti™ 96-Well Fast Thermal Cycler	Thermo Fisher Scientific, Massachusetts, USA
	Stratagene MX3005P Real-Time QPCR System	Agilent Technologies, California, USA
Microscopes	Olympus CK30 Culture microscope	Olympus Corporation, Japan
	Olympus BX51 Fluorescence microscope	Olympus Corporation, Japan
	Olympus U-RFL-T power supply	Olympus Corporation, Japan
	Eclipse E600 Fluorescence microscope	Nikon Corporation, Tokyo, Japan
	Nikon HB-10103AF Power Supply	Nikon Corporation, Tokyo, Japan
	Leica TCS SP8 X	Leica Microsystems, Germany
Imaging systems	EVOS FLoid Imaging System	Thermo Fisher Scientific, Massachusetts, USA
	Alliance 4.7 Fluorescence and Chemiluminescence Systems	Uvitec Ltd, UK
	Alliance Q9 Advanced Chemiluminescence Imager	Uvitec Ltd, UK
Centrifuges	Centrifuge 5403	Eppendorf, Germany
	Centrifuge 5415 C	Eppendorf, Germany
	Centrifuge 5415 R	Eppendorf, Germany

Group	*Product*	*Manufacturer*
	Heraeus Multifuge 3S-R	Thermo Scientific, Massachusetts, USA
	Sorvall LYNX 4000 Superspeed Centrifuge	Thermo Scientific, Massachusetts, USA
	Optima XL-100K Ultracentrifuge	Beckman Coulter Inc., California, USA
Rotators	SARMIX® M2000 Rotation mixer	Sarstedt AG & Co. KG, Germany
	Multi Bio RS-24 Programmable rotator	Biosan Laboratories, Inc., Michigan, USA
Electrophoresis and transfer systems	omniPAGE	Cleaver Scientific, UK
	PowerPRO 300 Power Supply	Cleaver Scientific, UK
	Mini-PROTEAN® Electrophoresis System	Bio-Rad Laboratories, California, USA
	PowerPac™ Basic Power Supply	Bio-Rad Laboratories, California, USA
	Trans-Blot® Turbo™ Transfer System	Bio-Rad Laboratories, California, USA
Programs	ImageJ Fiji	National Institutes of Health, USA
	Leica Application Suite X (LAS X)	Leica Microsystems, Germany
	PhotoScape X	MOOII Tech, Korea
	GraphPad Prism	GraphPad Inc., California, USA
	MxPro QPCR Software	Agilent Technologies, California, USA

3.2 Cell culture

All cell culture work was carried out in a HEPA-filtered laminar flow hood. Surfaces were wiped clean with 70% ethanol, while the interior and contents were sterilized using UV lamp for 15 min prior and after work.

3.2.1 Cell lines

All cell lines used for this research are indicated in **Table 13**. All those are adherent cell lines and will grow *in vitro* until complete confluency, or the medium is depleted of nutrients.

HeLa, CaSki, C33A and HEK293 cell lines have been used as control cell lines. Three keratinocyte cell lines isolated from different anatomical sites and immortalized by hTERT: normal oral keratinocytes (iNOK), human tonsillar keratinocytes (iHTK) and human foreskin keratinocytes (iHFK) were kind gifts from Dr Karl Münger and Dr Aloysius Klingelhutz. They were used for immunocytochemical evaluation of antibodies and for studying various aspects of DLG1 and SCRIB proteins.

Primary human tonsillar (HTK) and foreskin (HFK) keratinocyte cells were isolated under ethical approval granted to Professor J Parish (REC #06/Q1702/45) and transfected with HPV16 genomes (HPV16-HTK, HPV16-HFK) in the Parish laboratory. These cells were later used for the establishment of organotypic 3D raft cultures. The γ-irradiated 3T3-J2 cells were used as feeder cells for growing keratinocyte cell lines.

HEK293T cell line was used for lentiviral production and were a kind gift of Filip Rokić.

Table 13. Cell lines.

Cell line	*Properties*
HeLa	HPV18-positive cervical adenocarcinoma cell line
CaSki	HPV16-positive advanced cervical carcinoma cell line
C33A	HPV-negative cervical cancer cell line
HEK293	Adenovirus- immortalized human embryonic kidney cell line
3T3	mouse embryonic fibroblast cells
iNOK	h-TRET immortalized normal oral keratinocyte cell line
iHTK	h-TRET immortalized human tonsillar keratinocyte cell line
iHFK	h-TRET immortalized human foreskin keratinocyte cell line
HTK	primary human tonsillar keratinocyte cell line
HFK	primary human foreskin keratinocyte cell line
HPV16-HTK	primary human tonsillar keratinocytes transfected with HPV16 genomes in the Parish lab
HPV16-HFK	primary human foreskin keratinocytes transfected with HPV16 genomes in the Parish lab
HEK293T	stable clone derivative of HEK293 expressing the large T antigen of Simian virus 40

3.2.2 Cell maintaining

HeLa, CaSki, C33A, HEK293 and HEK293T cells were maintained in DMEM medium supplemented with 10% (v/v) FBS, 2 mM L-glutamine and 1 mM sodium pyruvate with 1% (v/v) penicillin/streptomycin (DMEM complete). Cells were passaged when they were ≥ 80% confluent. Firstly, cell media was aspirated off cells, and afterwards they were washed with PBS. After PBS removal, 1 mL/10 cm dish of Trypsin/EDTA warmed to room temperature was added and dish was returned to incubator for 1-5 min, which was sufficient for cells to detach completely from the dish surface. Trypsin/EDTA was inactivated by addition of 5 mL of fresh DMEM complete media since FBS quenches the trypsin enzymatic activity. Media was pipetted gently up and down to allow breakage of formed cell clusters. The appropriate volume of cells needed for 1:5 - 1:10 dilution was transferred into new dishes. Transferred cells were distributed evenly by shaking the dish back and forth and then placed in the incubator at 37 °C with 5% CO_2.

iNOK, iTONS and iHFK keratinocyte cell lines were grown in Keratinocyte growth medium (KGM) complete media consisting of keratinocyte SFM (KSFM-keratinocyte supplement free medium) supplemented with human recombinant epidermal growth factor (rEGF) and bovine pituitary extract (BPE) provided along with media and 1% (v/v) penicillin/streptomycin (KGM complete). Cells were passaged when they were ≥ 90% confluent. Cell media was aspirated off the cells, and cells were washed with PBS. Cells were then detached by addition of 1 mL

Trypsin/EDTA warmed to room temperature. Trypsin/EDTA was inactivated by addition of 5 mL of 2% FBS-PBS. Cells in suspension were transferred into a 15 mL conical tube and centrifugated at 4 °C for 4 min at 800 x g. Supernatants were aspirated and cell pellets were resuspended in KGM complete media by gentle up-and-down pipetting. The appropriate volume of cells needed for 1:4 dilution was transferred into new dishes and the cells were distributed evenly by shaking dish back and forth. Cells were grown in the incubator at 37 °C with 5% CO_2.

3T3-J2 cells were maintained in DMEM medium supplemented with 10% Gibco adult bovine serum (v/v) and 2,5% (v/v) HEPES. Cells were split at 80-85% confluency. As described previously for other cells, media was removed, and cells were then washed with room temperature PBS. Cells were detached using 2 mL TrypLE trypsin solution per 10 cm dish, followed by incubation at 37 °C. Trypsin was inactivated with complete DMEM media and cells in suspension were transferred to a 15 mL conical tube and centrifugated for 5 min at 250 x g. Cells were then resuspended in complete DMEM media, counted using the FAST READ 102® system and plated at a density of 2×10^4 cells per dish. Cells were grown in the incubator at 37 °C with 5% CO_2.

Primary HTK, HFK, and HPV16-HTK and HPV16-HFK cell lines were grown in E-media supplemented with 10% (v/v) fetal calf serum (complete E-media, CEM) on a layer of γ-irradiated 3T3-J2 feeder cells. For this, 3T3-J2 cells were grown to 80% confluency, harvested by trypsinization, and resuspended at $2x10^6$ cells/ml in CEM before irradiation with 30 Gray using a Caesium-137 radiation source (Biomedical Services Unit, University of Birmingham, UK)

Irradiated 3T3- J2 cells were plated out in the CEM at a concentration of $2x10^6$ per 10 cm tissue culture dish and allowed to settle for at least two hours before the addition of HPV16 genome containing primary keratinocytes. Keratinocytes were split once they reached 80-85% confluency. The media was removed, cells were washed with PBS and detached using 2 mL/10 cm dish of TrypLE trypsin solution with incubation at 37 °C. Trypsin was inactivated with CEM and cell suspension was then transferred to a 15 mL conical tube and centrifugated for 5 min at 250 x g. Cells were then resuspended in CEM, counted using the FAST READ 102® system and plated at a density of 2×10^5 cells per dish on existing layer of irradiated 3T3-J2 cells. Cells were grown in the incubator at 37 °C with 5% CO_2.

3.2.3 Organotypic 3D raft cultures

Organotypic 3D raft cultures of primary HTK were used to study DLG1 and SCRIB protein expression levels and localization in differentiating epithelium and during productive HPV16 cycle.

Firstly, the stainless-steel metal grids were treated with sulfuric acid for 1 h to remove any residues that could interfere with the differentiation process. Grids were then rinsed overnight with tap water and for an additional 3-5 h with double distilled water, dried out and autoclaved. For each raft, one collagen gel was required.

Non-irradiated 3T3-J2 fibroblasts were grown as mentioned before, collected in E-media and $2x10^6$ cells/gel were spun down for 5 min at 250 x g. Cell pellet was placed on ice.

For each collagen gel, 9.6 mg rat-tail collagen type I, 0.3 mL 10x reconstitution buffer and 0.3 mL of 10x DMEM without $NaHCO_3$ were gently added with cold pipettes and mixed in the tube containing 2×10^6 3T3-J2. By adding a couple of drops of filtered, sterilized 1 M NaOH and gently mixing, the gel mixture has changed the color from yellow to reddish indicating the correct pH. Two mL of collagen mix was quickly added to 35 mm dishes using a cold pipette and the collagen mix was set to solidify in the incubator at 37 °C for 30 min. Then, 2 mL of E-media with EGF was added on top of solidified collagen and dishes were returned to the incubator at 37 °C for 1 day. The following day keratinocytes were prepared for differentiation. Keratinocytes were grown in E-media as previously described, trypsinized, collected with E-media and spun down for 5 min at 250 x g. For each raft, 2×10^6 keratinocytes were placed onto the top of the prepared collagen gel and allowed to grow to confluency. E-media was replaced daily, and confluency was confirmed by color change from reddish to yellow the day after the media was changed, which usually takes 2-4 days. When keratinocytes were confluent, an autoclaved metal grid was placed in a 100-mm dish using sterile forceps. The media was removed from the collagen gel and the perimeter of the gel was cut with a sterile spatula to release it from sides of the dish. To remove collagen gel, dish was slightly tilted, and gel was lifted by sliding a spatula underneath. Collagen gel was laid on a metal grid without generating any bubbles between the grid and gel. To create an air-liquid interface, E media without EGF was added to the bottom of the dish so that the medium was touching the metal grid but not the collagen (**Figure 16.**). Rafts were incubated at 37 °C and media was changed every other day and after 13 days, 6 h before fixation, 20 μM of the thymidine analogue 5-bromo-2'-

deoxyuridine was added to media. BrdU was incorporated into the newly synthesized DNA allowing the detection of replicating cells. In preparation for downstream immunofluorescent analysis, rafts were fixed by flooding the raft-containing dish with 3.7% (w/v) paraformaldehyde in DMEM and then were paraffin embedded.

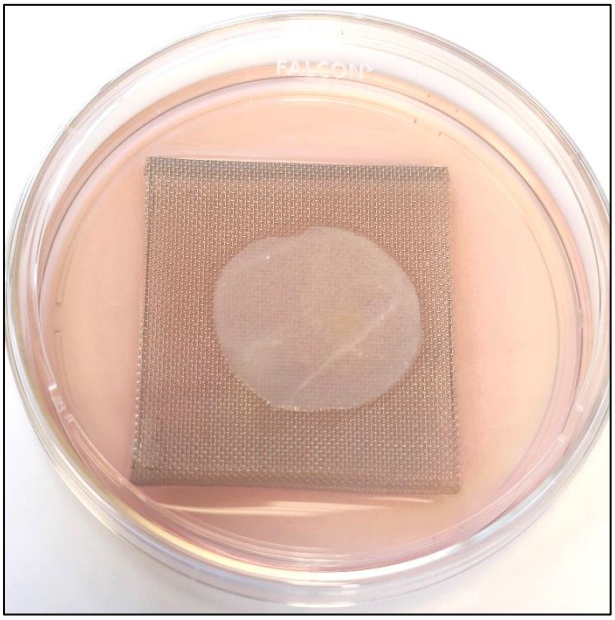

Figure 16. Collagen gel on metal grid. Cells were cultured with E media without EGF, forming an air-liquid interface at the raft grid. This induced cell differentiation, leading to the formation of a stratified epithelium.

3.2.4 Cryopreservation of cells

For maintaining the stock of cells, cells were frozen at -80 °C or in liquid nitrogen at -196 °C. After trypsinization as mentioned above, cells were collected from a dish with 2% FBS-PBS and transferred into a 15 mL conical tube. Cells were pelleted by centrifugation for 4 min at 800 x g, resuspended in 1 mL 10% DMSO-FBS and transferred into cryovials, which were then transferred into -80 °C freezer. The next day, some of the cryovials were relocated and stored at -196 °C in the liquid nitrogen tank.

3T3-J2 cells were processed as above for cell maintenance and after centrifugation, cells were resuspended to $2x10^6$ cells/ml in freezing media; complete DMEM containing 10% (v/v) DMSO. Primary keratinocytes were frozen to $2x10^6$ cells/cryovial in CEM supplemented with 10% (v/v) FCS containing 20% (v/v) glycerol and stored at -80 °C in a Nalgene Mr Frosty system. For long-term storage, cells were relocated and stored at -196 °C in the liquid nitrogen tank.

3.2.5 Thawing cells

All the cells, excluding 3T3-J2 cells and HPV16-HTK and HPV16-HFK, were thawed rapidly after which were added to 5 mL of 2% FBS-PBS in 15 mL conical tubes. To completely remove DMSO, cells were separated by centrifugation at 4 °C at 800 x g for 4 min. Cells were then gently resuspended in either DMEM complete or KGM complete media depending on the cell line and placed in the incubator at 37 °C with 5% CO_2.

3T3-J2 cells and primary HTK and HFK were removed from liquid nitrogen and allowed to thaw briefly in a water bath set to 37 °C. Cells in the solution were transferred to a conical tube containing 10 ml of required media, before centrifugation for 5 min at 1000 x g. Cells were then resuspended in fresh media and plated out at the required density.

3.3 Cell biology

3.3.1 Calcium phosphate transient transfection

A day prior to transfection, 2-4x10^5 cells/6 cm dish were seeded in 2,5 ml DMEM complete media so that, at the time of transfection, cells would be about 20-30% confluent. The following day transfection was carried out in a 1,5 mL tube as follows: 95 µL of TE buffer was mixed with 11 µL of $CaCl_2$ and the specific amount of DNA depending on the experiment and used plasmid size. The mixture was vortexed quickly and then 100 µL of 2X HBS was added dropwise while aerating. The final transfection mix was incubated for 45 min at room temperature and then drop-by-drop added around the dish. Dish was gently mixed back and forth, after which was placed back in the incubator at 37 °C and 5% CO_2. Approximately 16 h post transfection, cell media was aspirated and replaced with fresh DMEM complete media or cells were harvested for further experiments.

3.3.2 Lipofectamine 2000 transfection

A day before transfection, 3x10^5 cells/well were seeded in 6-well plates in 1 mL of KGM complete media so that cell confluency would be 70-90% at the time of transfection. For each sample, transfection complexes were prepared so that DNA:lipofectamine ratio would be 1:3 in this manner: 0.5 µg DNA was diluted in KGM complete media to make 50 µL in total in the first 1.5 mL tube. In the other tube, 1.5 µL of Lipofectamine 2000 were diluted in 50 µL of KGM complete media in the second 1.5 mL tube. Mixtures were incubated separately for 5 min at room temperature and were then combined gently by pipetting. The combined mixtures were then incubated for 20 min at room temperature and added dropwise on cells. The 6-well plate was mixed gently by

shaking back and forth, after which was left in the incubator at 37 °C and 5% CO_2 for 24-48 h prior to testing for transgene expression. The media was changed 4-6 h later when formed complexes already entered cells.

3.3.3 Viromer transfection

A day prior to transfection, $8x10^4$ cells per well were seeded in a 24-well plate in 500 µL of KGM complete media.

Transfection was carried out in two separate tubes in DNA:Viromer ratios 3.3, 5 or 6.7 as follows: calculated amount of DNA was diluted to 11 ng/µL using provided buffer in total volume of 135 µL. Depending on used ratio, specific amount of Viromer reagent was placed onto the wall of a fresh tube and provided buffer was added immediately in a total volume of 15 µL. The solution was vortexed for 3-5 s. DNA-buffer mixture was pipetted from Tube 1 onto the 15 µL of the Viromer solution in Tube 2, mixed and incubated for about 15 min at room temperature. Formed transfection complexes were added to cells and they were returned in the incubator at 37 °C and 5% CO_2 until needed for further experiments.

3.3.4 FuGENE transfection

A day before transfection, $2x10^5$ cells were seeded in 6 cm dishes in 1 mL of KGM complete media so that cells would reach 70-90% confluency at the time of transfection.

For each sample, transfection complexes were prepared in a polystyrene tube so that DNA:FuGENE ratio would be 1:3 as follows: 100 µL of KGM complete media were mixed with 2 µg of DNA and 6 µL of provided Trans reagent. The mixture was then incubated for 15 min at room temperature. During the incubation, the cell media was gently aspirated and replaced with 1 mL of fresh KGM complete media. The transfection mix was added dropwise on cells after which the dishes were returned in the incubator.

For transfections with HPV16 genomes, 1.6 µg of a plasmid containing whole HPV16 genome and 0.4 µg of a plasmid carrying blasticidin resistance were mixed. The transfection protocol was the same as mentioned above yet antibiotic selection was carried out 24 h after transfection. The cell media was aspirated after which dishes were washed with PBS. After removing PBS, 2 ml of fresh KGM complete with 1.75 µL of blasticidin were added to each dish which were placed in the incubator and passaged as needed for further experiments.

3.3.5 Single cell colony in 96-well plate

Limited dilution method was used to obtain single cell colony carrying selection. Cells were plated at very low cell densities (< 1 well per well) in 96-well plates and expanded to form colonies. The whole time, cells were grown in KGM complete media containing 0.7 µg/mL blasticidin in the incubator under previously described conditions.

3.3.6 Immunohistochemical analysis of DLG1 and SCRIB proteins

3.3.6.1 Tissue samples

The study was conducted on FFPE OPSCC samples (n = 66) grouped and named HPV16-positive oropharyngeal cancer (n = 21), HPV-negative oropharyngeal cancer (n = 36) graded 1-3, and healthy tonsillar tissue (n = 8). The tissue samples were obtained from the archives of the Department of Pathology and Cytology, University Hospital Dubrava (ethical permit no. BEP-55 48/2-2016) and the Department of Pathology and Cytology University Hospital Centre, Zagreb, Croatia (ethical permit no. 02/21 AG, Class 8.1-21/15-2). All the tissue samples were previously fixed in 10% buffered formalin and embedded in paraffin.

3.3.6.2 DNA isolation

From each FFPE block, five to seven slices of 10 µm were cut on microtome and used for DNA isolation. DNA was then isolated using a commercial kit NucleoSpin® DNA FFPE XS, according to the manufacturer's instructions. The concentration of the isolated DNA was measured using NanoPhotometer® N60. The efficacy and quality of the isolated DNA were validated by PCR, using primers generating 99 bp long beta-actin fragments. Briefly, 50 ng of DNA sample was used as a template. DNA was amplified in a Veriti™ 96-Well Fast thermal cycler under the following conditions: initial denaturation at 95 °C for 12 min, followed by a total of 40 cycles of 95 °C for 30 s, 60 °C for 1 min, and 72 °C for 1 min. Final elongation was performed at 72 °C for 7 min. PCR products were analyzed on 2% agarose gel using gel electrophoresis.

3.3.6.3 Detection and Genotyping

For HPV DNA detection, PCR was performed using short primers suitable for FFPE tissue samples GP5/6 (~142 bp) and SPF 10 (~65 bp) to avoid false negative results, due to high DNA degradation of FFPE samples. GP5/6 was amplified using nested PCR, a technique that reduces nonspecific amplification of the DNA template. For GP5/6 detection, PGMY/β-globin PCR reaction was performed with primers that cover the L1 sequence. For this, 50 ng of isolated DNA were used as

a template. PCR was performed in Veriti™ 96-Well Fast thermal cycler under the following conditions: initial denaturation at 95 °C for 9 min, followed by a total of 40 cycles of 95 °C for 1 min, 51 °C for 1 min, and 72 °C for 1 min with final elongation at 72 °C for 5 min. After the first PCR, a second reaction for GP5/6 detection was performed using amplificons form the first PCR reaction as a template. This time, 1 µL of PCR products was used as a template and DNA was amplified in a thermal cycler as follows: initial denaturation at 95 °C for 9 min, followed by 45 cycles of 94 °C for 1 min, 40 °C for 2 min, and 72 °C for 90 s with final elongation at 72 °C for 4 min.

SPF10 PCR was performed in a Veriti™ 96-Well Fast thermal cycler using Hot Start Taq polymerase as demonstrated: initial denaturation at 95 °C for 4.5 min, followed by 40 cycles of 95 °C for 30 s, 51 °C for 30 s, and 72 °C for 30 s with final elongation at 72 °C for 7 min. The PCR products (10 µL) were run on 3% agarose gels and sample was considered as HPV-positive if either the GP5/6 or SPF10 PCR was positive.

In addition, for the detection of HPV16 E6/E7, a supplementary primer pair, generating a shorter DNA sequence (98 bp), was used. HPV16 E6/E7 DNA was amplified in Veriti™ 96-Well Fast thermal cycler using following steps: initial denaturation at 95 °C for 10 min; 40 cycles of 95 °C for 1 min, 54 °C for 1 min and 72 °C for 2 min; with a final elongation at 72 °C for 7 min. The PCR efficacy was confirmed by loading 10 µL of PCR products on 3% agarose gels.

3.3.6.4 Antibodies

DLG1 and SCRIB were detected in FFPE tissue sections using mouse monoclonal antibodies anti-SAP97 (DLG1, 2D11) or anti-SCRIB (C-6) at 1:20 dilutions. Biotinylated secondary antibodies were provided in commercial kits CINtec® Histology kit system and EnVision® + Dual Link System-HRP.

3.3.6.5 Immunohistochemistry

Seven µm FFPE tissue sections were mounted on pretreated glass slides, deparaffinized in xylene substitute BioClear, and rehydrated using a graded ethanol series as follows: 100%, 95% and 70%. The expression of p16 was analyzed using the CINtec® Histology kit system in accordance with the manufacturer's instructions and compared with the previously determined HPV status of the corresponding tissue.

Endogenous expression of DLG1 and SCRIB was detected using EnVision® + Dual Link System in line with the manufacturer's instructions. Negative controls for each sample were processed in the same way, except that the primary antibody was replaced with the negative control solution provided in CINtec® Histology kit system for p16 determination or Ab solution. The intensity of DLG1 and SCRIB immunoreactivity was graded and scored by three independent pathologists as follows: 0 (no staining), 1+ (low intensity), 2+ (medium intensity), and 3+ (strong intensity).

3.3.6.6 Statistical Analysis

Descriptive statistics were used to evaluate differences in DLG1 and SCRIB protein expression and localization in HPV-positive and HPV-negative OPSCCs.

A Kruskal–Wallis test was used to evaluate possible significant differences between the designated groups, HPV-negative OPSCCs grades 1–3 and HPV16-positive OPSCCs with Dunn's multiple comparison posttest. The ratio of DLG1- or SCRIB-positive staining in tumor cells was evaluated by three independent pathologists.

Pearson's $\chi 2$ test was used for evaluation of any significant differences in DLG1 or SCRIB localization between designated groups: HPV-negative OPSCCs grades 1–3 and HPV16-positive OPSCCs. All statistical analyses were performed using GraphPad Prism software.

3.3.7 Immunofluorescence (IF)

3.3.7.1 IF staining of cells and analysis by confocal microscopy

One day prior to IF assay, the sterile cover slips were placed in 12 or 24 well plates, rinsed with PBS, followed by a quick rinse with culture media. Cells were plated on cover slips at a density of ~ 10,000/well. The other day, cells were rinsed with PBS and fixed with 3.7% PFA in PBS for 30 min at room temperature. Cells were then washed gently three times with PBS and permeabilized with 0.1% Triton for 5 min at room temperature. After permeabilization, cells were again washed three times with PBS and incubated in PBS containing 2% BSA for 30 min at room temperature and then washed again three times in PBS. Cells were then incubated overnight at + 4°C in primary antibody diluted 1:30 in Ab solution. The next day, cells were gently washed three times with PBS and incubated for 30 min at room temperature in secondary antibody diluted 1:700 in Ab solution. Cells were rinsed again three times with distilled water and cover slips with cells were mounted facing down on the glass slides. Excess liquid was removed with filter paper and cover slips were sealed with nail polish. Confocal fluorescent images were obtained by laser scanning microscope

Leica TCS SP8 X, equipped with a HC PL APO CS2 63×/1.40 oil objective and analyzed by Leica Application Suite X (LAS X) software.

3.3.7.2 IF analysis of organotypic 3D raft cultures

Raft sections were prepared at Human Biomaterials Resource Centre, College of Medical and Dental Sciences, University of Birmingham. Four nm raft sections were deparaffinized in Histo-Clear TMl for 10 min and rehydrated by incubation in 100% ethanol for 5 min. Slides were then rinsed three times in distilled water. A heat-induced epitope retrieval (HIER) technique using an EDTA buffer was applied to paraffin-embedded and formalin-fixed samples. To enhance the staining intensity of antibodies the sections were immersed overnight in EDTA buffer, heated to 65 °C and continually agitated on a stirrer. Retrieved raft sections were then washed with distilled water and blocked in Blocking buffer containing of 20% v/v heat-inactivated goat serum (HINGS) with 0.1% w/v BSA in PBS, for 2 h at room temperature in humidified dark chamber. Primary antibody was diluted in the same blocking buffer according to tested dilutions, applied to raft sections and incubated overnight at 4 °C in humidified dark chamber. Excess antibody was removed by washing sections in PBS for 5 min with continuous agitation, three times. The appropriate secondary fluorophore-conjugated antibody was diluted in the same blocking buffer, applied to each slide, and incubated for 1 h at 37 °C in humidified dark chamber. The sections were then washed in PBS for 5 min with continuous agitation, three times as before. Slides were then immersed in PBS containing 20 µl of 4'.6-diamidino-2-phenylindole (DAPI) for highlighting the cell nuclei. Slides were mounted using Fluoroshield and visualized on a Nikon Eclipse E600 microscope.

3.4 Molecular methods

3.4.1 CRISPR-Cas9 Knock-in

3.4.1.1 PCR amplification of HPV16 E6 or HPV16 E7

Donor plasmids pAAVS1-16E6-DNR and pAAVS1-16E7-DNR were constructed by subcloning of the coding sequence for the HPV oncogenes from original plasmids pcDNA3.1. Multiple PCR reactions were performed using specific primers for more successful purification and better yield.

Both HPV16 E6 and E7 genes were amplified in Veriti™ 96-Well Fast thermal cycler using the same PCR conditions for both in this order: initial denaturation at 94 °C for 3 min; 35 cycles of 94 °C for 40 s, 58 °C for 30 s and 72 °C for 2.5 min; with a final elongation at 72 °C for 7 min.

3.4.1.2 DNA purification

For DNA separation, agarose was dissolved in TAE buffer by heating to make a 2% solution. This was later quickly cooled, and Midori Green detection dye was added before pouring into the mold.

DNA samples were loaded on a gel and were ran in a tank containing TAE buffer at 120 V. DNA marker was used for determination of bands molecular weights. Proper-sized DNA bands were excised from gel, placed in a 1.5 ml microcentrifuge tube and DNA was purified using Wizard® SV Gel and PCR Clean-Up System according to the manufacturer's instructions. Briefly, once gel slice containing DNA has dissolved, an equal volume of Membrane Binding Solution was added to the PCR amplification and the solution was transferred to the Minicolumn assembly. The solution was removed by centrifugation and DNA fragments were washed and eluted using provided nuclease-free water. The concentration of purified DNA was measured by NanoPhotometer® N60.

3.4.1.3 Construction of pAAVS1-16E6-DNR and pAAVS1-16E7-DNR donor plasmids

Before ligation, both vector pAAVS1-BSD-DNR and HPV16 E6/E7 inserts were cut by restriction digestion enzymes *Asc*I and *Mlu*I. The *Asc*I degradation was performed in the appropriate buffer compatible with both enzymes in the total reaction volume of 40 µL or 100 µL for HPV inserts or donor vector, respectively. After 1 hour at 37 °C *Asc*I was inactivated by heating the solution to 80 °C for 20 min. The solution was cooled to 37 °C and *Mlu*I was added for additional 1 h at 37 °C. In the vector ligation solution, calf intestinal alkaline phosphatase (CIP) was added 30 min after *Mlu*I enzyme to prevent religation of linearized plasmid DNA.

The enzymatically treated vector and HPV oncogene inserts were ligated in the ratio 1:10 (vector:insert) using the enzyme T4 DNA ligase in the total volume of 30 µL. Two negative controls were used; one was vector only without insert and T4 ligase while other contained vector and T4 ligase without insert. The ligation was performed overnight at 16 °C.

3.4.2 Generation of HPV16 E6-encoding lentiviruses

3.4.2.1 PCR amplification of HPV oncogenes

HPV16 E6 gene was amplified using the same PCR conditions in Veriti™ 96-Well Fast thermal cycler as described: initial denaturation at 95 °C for 5 min; 40 cycles of 95 °C for 40 s, 62-63 °C for 40 s and 72 °C for 2.5 min; with final elongation at 72 °C for 7 min. PCR amplificons were loaded on a 2% gel and gel-purified as described above.

3.4.2.2 Construction of pUltra-GFP-16E6 vector

As previously described, before ligation, both vector pUltra-GFP and HPV E6 inserts were digested by appropriate specific restriction enzyme pair *Xba*I/*Sal*I-HF. The digestion was performed in the appropriate buffer compatible with both enzymes in the total reaction volume of 50 µL or 100 µL for HPV inserts or donor vector, respectively at 37 °C for 2 h. CIP was added in the vector ligation solution 1 h after digestion started to prevent religation of linearized plasmid DNA.

The vector and the HPV insert were ligated in the ratio 1:10 (vector:insert) using T4 DNA ligase in the total volume of 30 µL overnight at 16 °C.

3.4.2.3 Preparation of lentiviral particles

Properly constructed plasmids containing HPV oncogenes were co-transfected in HEK293T cells with additional two plasmids, pMD2.G and psPAX2, VSV-G envelope expressing plasmid and gag-, pol- packaging expressing plasmid respectively.

A day prior to transfection, $4x10^6$ HEK293T cells were seeded in 10 cm dish in DMEM complete media. Transfection was performed using either Lipofectamine 2000 or calcium phosphate as described above with difference being in equimolar usage of 18 µg of DNA in total. Cells were incubated at 37 ℃ and 5% CO_2 for 18-20 h after which cell media was replaced with 6 mL of fresh DMEM complete media. The supernatant containing lentiviral particles was collected 48 and 72 h after transfection, respectively. Fresh DMEM culture medium was replaced after the collection of supernatant, at 48 h time point. After collecting the virus twice, the transfected HEK293T cells were discarded, and the collected supernatant was filtered with 0.45 µm filter membrane to an ultracentrifuge tube. This was then centrifuged at 164000 x g for 1.5 h at 21 ℃ using ultracentrifuge, the supernatants were discarded, lentiviral deposition was resuspended in 3 mL of fresh medium, aliquoted in 300 µL aliquots and kept at -80 °C.

3.4.2.4 Titration of purified lentiviruses

Lentiviral titer was determined with fluorescent microscopy. One day in advance, $9×10^5$ keratinocytes/well were seeded in a 24-well plate. Various amounts (0-500 µL) of lentiviral particles were added to each well per virus. Two days post infection, fluorescent positive cells were visualized using EVOS FLoid Imaging System for estimating the lentiviral titer.

3.4.3 Transfection of HPV16 genomes

Keratinocytes isolated from various anatomical site origins were transfected with pT2ZH plasmid, a derivative of pUC19 containing the entire HPV16 genome cloned into the unique *Bam*HI site. The cells were transfected using FuGENE reagent as previously explained in detail. Transfected cells were grown and passaged without 3T3-J2 feeder cells for a longer period in KGM complete media at 37 °C and 5% CO_2. This fastened the integration of HPV E6/E7 oncogenes into host cell genome and establishment of stable keratinocyte cell lines expressing HPV16 E6/E7 oncoproteins.

3.4.3.1 DNA isolation

Established cells containing HPV16 E6/E7 oncogenes were grown in KGM complete media. Cells were collected and total DNA was isolated. Cell pellets were resuspended in 700 µL of TEX buffer, 15-25 µL of proteinase K depending on the pellet size were added, and the solution was incubated overnight at 37 °C with agitation. The next day, 1/3 vol. of cold 5 M NaCl was added and incubated for 15 min at 4 °C. The solution was centrifugated for 15 min at 15000-16000 x g at +4 °C and supernatant was divided into two new 1.5 mL tubes. In each, 2 vol. of cold 96% ethanol was added, the content was briefly vortexed and incubated at -20 °C for at least 2 h for DNA to precipitate. Tubes were centrifuged at 2 °C for 30 min at 17000-18000 x g, supernatant was discarded, and remaining DNA pellets were washed with 2 mL of ice-cold 70% ethanol. After the incubation of 15 min at -20 °C, DNA was separated by centrifugation at 2 °C for 15 min at 17000-18000 x g and incubated at 56 °C for 2-3 min to allow the ethanol to completely evaporate. DNA was diluted in miliQ water depending on DNA pellet size at 37 °C for 1-2 h and stored at -20 °C.

3.4.4 RT-qPCR

The gene expression quantification was then given as a ratio of the levels of mRNA transcripts of the gene of interest in an experimental sample (HPV16-containing keratinocytes of various anatomical sites: iHTK, iNOK, iHFK) to a defined control sample (non-transfected iHTK, iNOK, iHFK respectively) as well in CaSki and C33A control cells.

3.4.4.1 RNA isolation

Prior to RT-qPCR reactions, cells were collected, counted, and washed twice in 1.5 mL of PBS. Cell pellets were then resuspended in QIAzol buffer according to cell number (300 µL of QIAzol to $1x10^6$ cells or 100 µL more for each additional $1x10^6$ cells). RNA isolation was then proceeded using Direct-zol™ RNA Miniprep according to manufacturer's instructions. Briefly, an equal

volume of absolute ethanol (95-100%) was added to a lysed sample, mixture was mixed thoroughly, transferred into a Zymo-Spin™ IICR Column in a collection tube and centrifuged. The column was transferred into a new collection tube and the flow-through was discarded. The column was washed using RNA Wash Buffer and DNase I treatment was performed directly on column. For that, DNase I and DNA Digestion Buffer mixture was added to the column matrix followed by incubation at room temperature for 15 min. RNA was washed using Direct-zol™ RNA PreWash and then with RNA Wash Buffer. RNA was eluted into an RNase-free tube by addition of DNase/RNase-Free Water directly to the column matrix. Concentrations of isolated RNAs were measured using NanoPhotometer® N60 and were considered to be pure if $A_{260/280}$ ratio was more than 1.8.

3.4.4.2 Reverse transcription and quantitative PCR

Preceding RT-qPCR, isolated and purified RNA was transcribed into complementary DNA (cDNA) using a QuantiTect Reverse Transcription Kit according to manufacturer's instructions. RNA samples were then used directly in the process of reverse transcription, using a master mix prepared from Quantiscript Reverse Transcriptase, Quantiscript RT Buffer, and RT Primer Mix. The mixture was incubated at 42 °C for 25 min and Quantiscript Reverse Transcriptase was inactivated by sample incubation at 95 °C for 3 min. The reverse-transcription reactions were placed on ice until further usage.

RT-qPCR was used for detection of DLG1β, DLG1 HOOK isoforms and SCRIB transcript levels in primary keratinocytes and OPSCC-derived cell lines. Each reaction contained 40 ng of cDNA template, 10 µl of SYBR SensiFAST mix, 0.25 µl of 10 µM primer mix, made up to a total volume of 20 µl with nuclease-free water. Reactions were set up in triplicates in 96-well reaction plates and analyzed using the Stratagene Mx3005p machine. Samples were initially subjected to a denaturation step at 95 °C for 5 min, followed by 40 cycles of denaturation at 95 °C for 30 s, annealing at 59 °C for 30 s and extension step at 72 °C for 30 s.

As control, HPV16 E6 and β-actin RT-qPCR was performed using the same conditions apart from annealing temperature. Annealing was completed at 50°C for HPV16 E6 and at 60°C for β-actin.

3.5 Bacterial methods

3.5.1 DH5α transformation

DH5-α are chemically competent *Escherichia coli* cells suitable for high efficiency transformation. For a transformation, 50 µL of DH5-α were mixed with 30 µL of ligation mixture and incubated on ice for 2 min. This blend of bacteria and DNA was then placed at 42 °C for 2 min (heat shock) and then put back on ice for additional 10 min. LB medium without antibiotic was added and the transformed cells were incubated at 37 °C for 1 h with agitation for generation of the antibiotic resistance proteins encoded in the plasmid backbone. Entire transformation mix was then plated onto a 10 cm LB agar plate containing the ampicillin and plates were incubated overnight at 37 °C. The next day, a few colonies were picked and grown in liquid LB media with ampicillin overnight at 37 °C with agitation.

3.5.2 XL-1 transformation

For lentiviral plasmid production XL-1 Blue competent *E. coli* cells were used. XL-1 Blue cells are endonuclease (*endA*) and recombination (*recA*) deficient, so using those can greatly improve the quality of DNA prep and insert stability, respectively. The procedure mildly variates from DH5α transformation protocol described above. After combining of 50 µL of XL-1 bacteria with 30 µL of ligation solution, the mixture was incubated on ice for 30 min and then placed at 42 °C for 45 s (heat shock). Cells were then placed back on ice for additional 2 min. Hundred µL of preheated LB media without antibiotics were added and the transformed cells were incubated at 37 °C for 1 h with agitation for generation of the antibiotic resistance proteins encoded in the plasmid backbone. All of the transformation mix was plated onto a 10 cm LB agar plate containing ampicillin and plates were incubated overnight at 37 °C.

3.5.3 DNA plasmid preparation

For large scale plasmid production in DH5α cells, bacterial cells were grown in 400 mL LB overnight at 37 °C with agitation, after which they were pelleted, and plasmid DNA was isolated using Qiagen Maxi-prep kit according to manufacturer's instructions. Briefly, DH5α which produced the desired plasmid were resuspended, lysed, and neutralized using the appropriate buffers. Cell lysate was cleared by centrifugation at 12000 x g and DNA was bound on provided QIAGEN-tip column. The solution was removed by centrifugation and DNA was washed and eluted using provided elution buffer. DNA was then precipitated using isopropanol and the solution

was removed by centrifugation. Precipitated DNA was washed in 70% ethanol, after which ethanol was removed, and ultrapure DNA was diluted in a suitable amount of nuclease-free water or TE buffer depending on the storage length. The concentration of purified DNA was measured on NanoPhotometer® N60.

3.6 Protein biochemistry

3.6.1 Total protein extraction

When fully confluent, cells were collected and resuspended well in a suitable amount of E1A buffer depending on pellet size. The mix of protease inhibitors was added in 1:25 dilution. The solution was incubated on ice for 30 min and centrifugated for 30 min at 16000 x g at 4 °C. Proteins solubilized in supernatant were collected in a new 1.5 mL tube and concentration was measured using Bio-Rad protein assay.

3.6.2 Bio-Rad protein assay

The Bio-Rad protein assay is a dye-binding assay based on the method of Bradford in which the Coomassie Brilliant Blue G-250 color change occurs in response to various concentrations of proteins.

Firstly, the dye reagent was prepared by diluting 1 part of Dye reagent concentrate with 4 parts of distilled water. Then, the BSA protein standard was prepared in dilution from 2-0 mg/mL with PBS in 96-well plate. Samples were prepared and loaded on the same plate in triplicates in 1:3 to 1:5 dilutions with PBS. In total 5 µL of diluted samples were loaded in each well. Three hundred µL of prepared dye reagent were added per well. The plate was incubated in a dark at room temperature for at least 5 min and absorbance at 595 nm was measured. According to obtained data for BSA standard dilutions, a chart of absorbance dependence on concentration was created. Protein concentrations were determined using the graph equation.

3.6.3 Western Blot analysis

3.6.3.1 SDS-PAGE for Western Blot assay

Different separating gel percentages were used depending on the protein size (**Table 14.**). Freshly prepared separating gel mixture was poured between glass plates and covered with isopropanol to prevent polymerization inhibition and straighten the separating gel border. After complete polymerization of separating gel, the isopropanol was removed using filter papers, and the stacking

gel was poured on top of the stacking gel. The comb was placed to form wells during gel polymerization. Equal amounts of protein samples were loaded into wells of the SDS-PAGE gels, along with molecular weight protein marker. Gels were run at 100-120 V.

Table 14. Western Blot gels composition

Separating gel	***7.5%***	***10%***
dH2O	4,7	3,8
1.5 M Tris-HCl pH 8.8	3	3
30% Acrylamide	2,6	3,5
10% SDS	0,1	0,1
10% APS	0,15	0,07
TEMED	0,003	0,003

Stacking gel	***4%***
dH2O	3,7
1 M Tris-HCl pH 6.8	0,65
30% Acrylamide	0,8
10% SDS	0,05
10% APS	0,05
TEMED	0,005

3.6.3.2 Protein transfer to nitrocellulose membrane

Nitrocellulose membrane, Whatmann papers and sponges were soaked in 1x Transfer Buffer prior to assembly of the transfer cassette. After SDS-PAGE, the gel was removed from the tank the transfer cassette was prepared. All air bubbles were gently removed with a roller so the inhibition of protein transfer to the membrane was avoided. Prepared WB cassette was placed into a transfer tank and proteins were transferred to a membrane overnight at a constant voltage of 20 V.

3.6.3.3 Immunoblotting

After protein transfer, membranes were rinsed briefly in 1x TBST and stained with Ponceau S solution for a few minutes to visualize protein bands as a confirmation that the protein transfer was successful. The Ponceau S staining was rinsed with several washes in 1x TBST until membrane became clear. The membrane was blocked in TBST with 10% milk for 1 h at room temperature with constant agitation, followed by incubation in primary antibody which was diluted as 1:500 in 1x TBST with 10% milk, overnight at 4 ˚C with gentle agitation. Membrane was washed with 1x TBST three times for 10 min each with gentle rocking and incubated with the appropriate secondary antibody diluted in 1x TBST with 1% milk or BSA for 1-2 h at room temperature with gentle rocking. Membranes were then again washed in 1x TBST three times, each wash for 10 min, with gentle agitation. To visualize separated proteins, membranes were incubated with ECL or SuperSignal West Pico Substrate for 1-5 min and developed using Uvitec Alliance Q9 Mini system.

3.6.3.4 Statistical Analysis

Descriptive statistics were used to evaluate differences in DLG1 and SCRIB protein expression in iNOK, iHTK and iHFK-expressing HPV16 E6/E7 to their non-transfected matching controls.

An ordinary one-way ANOVA test was used to evaluate possible significant differences between keratinocytes expressing E6/E7 oncogenes and their matched controls. All statistical analyses were performed using GraphPad Prism software.

3.6.4 GST-pull down

3.6.4.1 GST fusion protein production

For production of GST fused proteins, 50-100 µL of bacterial glycerol stock was inoculated in 40 mL LB with ampicillin and grown overnight at 37 °C with constant shaking. The whole overnight culture was transferred to a new 400 mL of LB with ampicillin at a final concentration of 75 µg/ml and incubated at 37 °C with shaking until OD_{600} was 0.5-0.6. To this culture isopropyl β-D-1-thiogalactopyranoside (IPTG) was added to a final concentration of 1 mM, and the suspension was incubated on a shaker at 28 °C for additional 3-5 h. The bacteria were then separated for 15 min at 7000 x g. The supernatant was discarded, the bacterial pellet resuspended in 10 mL of ice-cold PBS + 1% Triton X-100 and transferred to a 30 mL conical tube. Cells were then sonicated 2x 30 s at 40-50% amplitude with at least 30 s pause between pulses and centrifugated for 10-15 min at 12000 x g. The supernatant was stored for next steps. Meanwhile, glutathione-S-transferase agarose beads were rehydrated in cold PBS. The beads were separated by centrifugation at + 4 °C, combined with bacterial supernatant and incubated overnight at +4 °C on a rotating wheel. The beads were centrifuged at +4 °C for 4 min at 825 x g, the supernatant was discarded, and beads were washed at least 3 times in ice-cold PBS with 1% Triton. Twenty µL of GST bound agarose beads were ran on a gel to check the purity and the amount of produced protein. The amounts of produced GST fused proteins for GST-pull down assays were balanced depending on the result of the gel. The rest of the beads were resuspended in sufficient amount of cold PBS with 1% Triton-X-100 and 20% glycerol and stored at -80 °C.

3.6.4.2 GST-pull down assay

Cells were collected, and proteins were extracted in E1A buffer as described previously. From prepared protein extracts, 10% were transferred into a new 1.5 mL tube without beads which served as an input. Meanwhile, the previously determined amount of glutathione-S transferase agarose beads was prepared in 15 mL conical tube and washed three times with standard E1A buffer. Using a Hamilton needle, the whole E1A buffer was removed from the beads, and they were incubated with protein lysates overnight at + 4 °C on a rotating wheel. The other day, beads were separated

by centrifugation for 3 min at 825 x g. The beads were washed at least three times with E1A buffer. Using Hamilton needle, the whole supernatant was removed from the beads, followed by addition of 2x SDS loading buffer. The beads were vortexed well and boiled for 10 min at 95 °C. The bound proteins were analyzed on 7,5 or 10% gel using Western Blot analysis as described above.

3.6.5 Fractionation assays

Cells were fractionated into 4 fractions: cytosolic (F1), membrane/organelle (F2), nucleic (F3) and cytoskeletal (F4) using ProteoExtract® Subcellular Proteome Extraction Kit according to manufacturer's instructions. For the extraction, $2.5x10^5$ cells were collected and washed carefully with cold PBS. They were resuspended in 600 µl Wash buffer, transferred to a tube, and incubated for 5 min on ice. Cell pellets were resuspended in 300 µL of Extraction buffer I with 1.5 µL Protease Inhibitor Cocktail set I and incubated for 10 min on ice. The suspension was centrifuged for 10 min at 500-1000 x g at + 4 °C and the supernatant (F1) was collected in a new tube. The remaining pellet was resuspended in 300 µL Extraction Buffer II with 1.5 µL Protease Inhibitor Cocktail Set I and incubated for 10 min on ice. The suspension was centrifuged for 10 min at 5000-6000 x g at + 4 °C and the supernatant (F2) was collected in a new tube. Cellular pellets were then resuspended in 150 µL of the Extraction Buffer III with 1.5 µL of Protease Inhibitor Cocktail Set I and incubated for 10 min on ice. These were again centrifuged for 10 min at 6800 x g at + 4 °C and the supernatants (F3) were collected in a new tube. The remaining cell pellet was resuspended in 150 µL Extraction Buffer IV with 1.5 µL Protease Inhibitor Cocktail set I and stored as F4. Extracted proteins were validated using Western Blot.

4 RESULTS

4.1 Establishment of HPV16 E6/E7 expressing cell lines

Three hTERT-immortalized keratinocyte cell lines iNOK, iHTK and iHFK were used for establishing cell lines which stably express HPV16 E6/E7 oncoproteins. This was first attempted using the CRISPR-Cas9 Knock-in transfection system which utilizes incorporation of the gene of interest into AAVS1 locus in human cells, and results in its robust and stable expression. Briefly, it is constituted of three plasmids: pCas-Guide-AAVS1, pCas-Guide-Scramble and donor plasmid pAAVS1-BSD-DNR, which is used as a vector for cloning a gene of interest (16E6 or 16E7) into the multiple cloning site and it also provides an antibiotic marker for selection of transfected cells. E6 oncogene insert was successfully amplified from the template pcDNA3.1 HPV16 E6 (**Figure 17.A**). To subclone the insert into the pAAVS1-BSD-DNR donor vector, both purified PCR product and donor vector were digested using *Asc*I/*Mlu*I restriction enzyme pair and ligated by T4 ligase. To validate the effectiveness of cloning, triple validation was carried out. Firstly, after growing selected colonies and isolating the plasmids, they were digested by the same restriction enzyme pair and the products separated on an agarose gel. The lane which contained two bands of the sizes corresponding to the insert and the vector represented the colony transformed with the cloned donor vector (**Figure 17.B**). To further confirm this, HPV16 E6 was PCR amplified from the constructed plasmid (**Figure 17.C**). Finally, to additionally verify the cloning efficiency, the constructed plasmid was sent for sequencing. The obtained data were aligned with HPV16 E6 FASTA downloaded from NCBI and FLAG and HA-tags. Those tags were fused to DNA insert to allow easier detection of E6 protein due to the absence of commercially available specific anti-16E6 antibodies. According to the aligned results (**Figure 17.D**), E6 oncogene was successfully cloned into the pAAVS1-BSD-DNR donor vector and could have been used for further experiments.

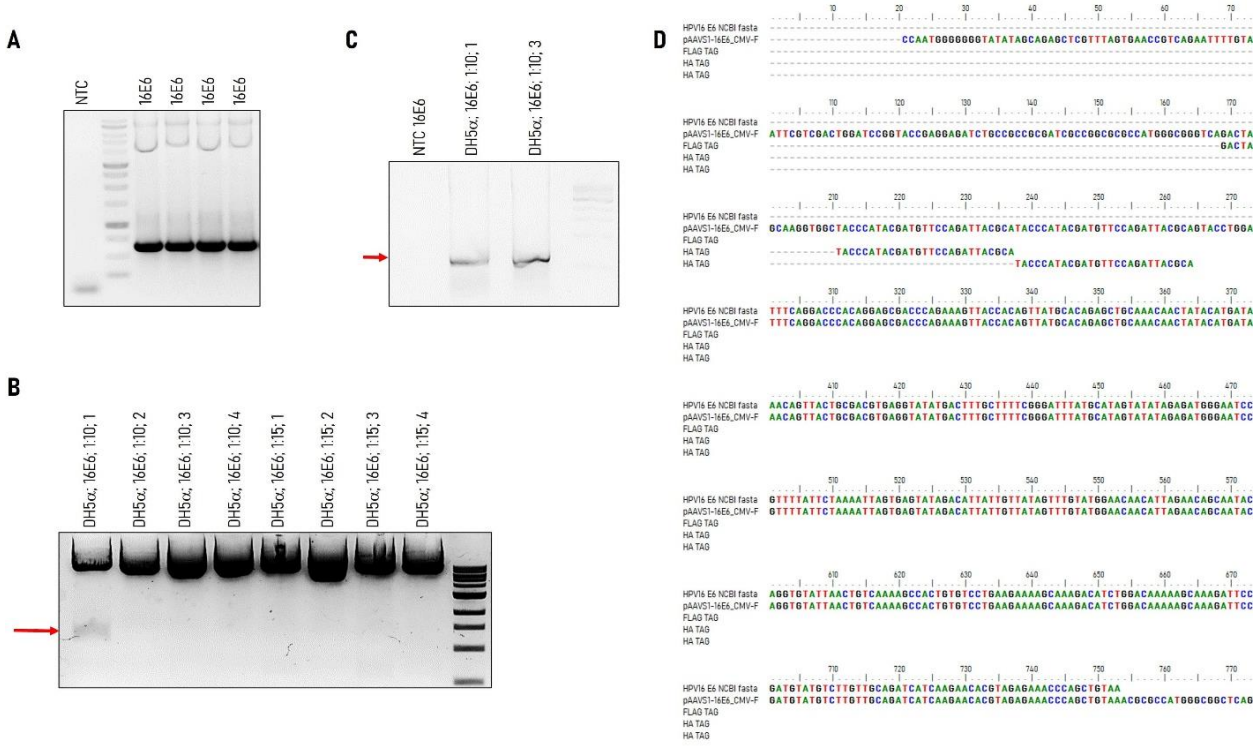

Figure 17. Cloning of HPV16 E6 sequence into the pAAVS1-BSD-DNR donor vector. (A) 16E6 PCR amplification from pcDNA3.1 16E6 template, (B) Ligation validation by *Mlu*I/*Asc*I digestion, (C) Ligation validation by PCR amplification, (D) Cloning verification by DNA sequencing.

Using the same principle as for cloning and constructing plasmid containing 16E6, donor plasmid pAAVS1-BSD-DNR-16E7 was also created. The oncogene 16E7 was cloned from pcDNA3.1 HPV16 E7 template and subcloned into the pAAVS1-BSD-DNR vector previously digested with *Asc*I/*Mlu*I enzyme pair (**Figure 18.A**). Once again, to confirm the efficacy of cloning, the triple validation was performed as above described for HPV16 E6 oncogene (**Figure 18.B-D**).

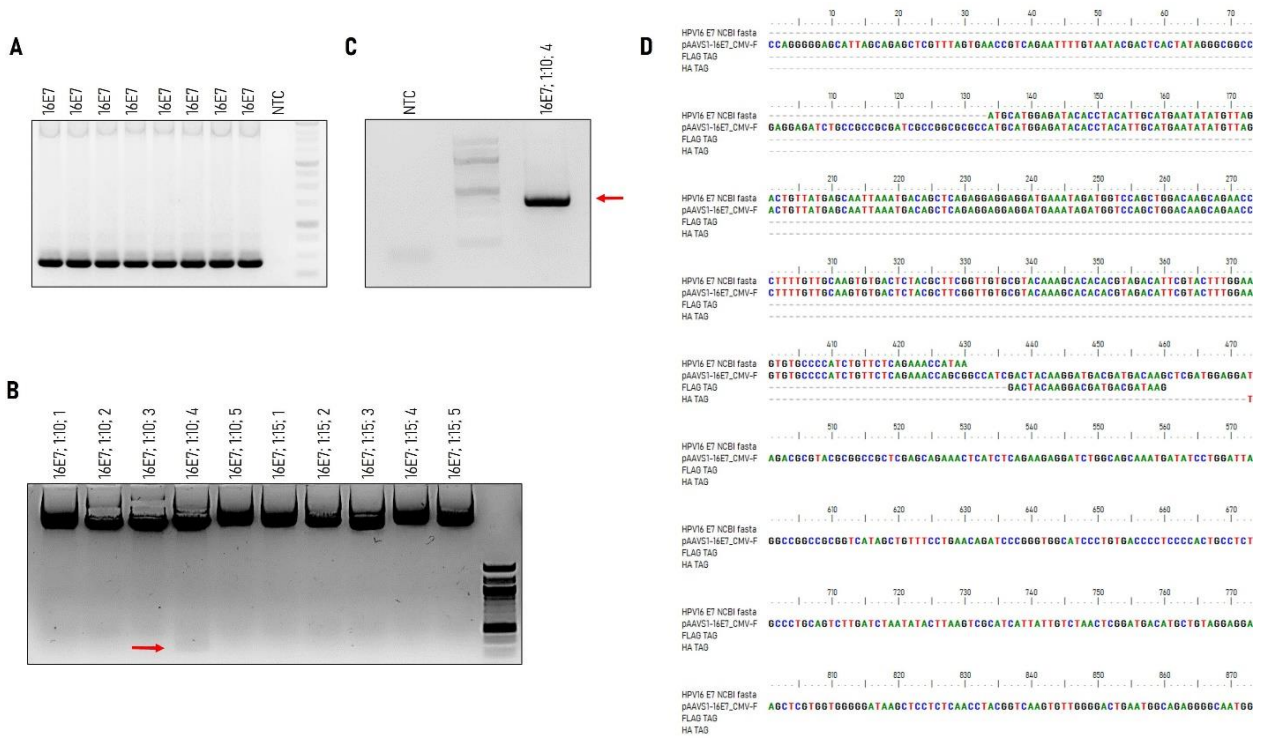

Figure 18. Cloning of HPV16 E7 sequence into the pAAVS1-BSD-DNR donor vector. (A) 16E7 insert PCR amplification from pcDNA3.1 16E7 template, (B) Ligation validation by Mlu/AscI digestion, (C) Ligation validation by PCR amplification, (D) Cloning verification by DNA sequencing.

Once verified, the constructed donor vectors were co-transfected with either pCas-Guide-AAVS1 or pCas-Scramble plasmids into three keratinocyte cell lines (**Figure 19.A-B**). The optimization of transfection conditions including transfection reagents, incubation time and temperatures was conducted to obtain the optimal transfection conditions of keratinocytes. To do that, the constructed plasmids together with pGFP plasmid for easier microscopic detection of transfected cells were co-transfected into iNOK. A small proportion of the GFP positive cells was obtained when FuGene in DNA: reagent ratio 1:3 respectively, was used (**Figure 19.C-D)**.

Among all the used transfection reagents, FuGene in DNA:reagent ratio 1:3, respectively, resulted in the maximal number of transfected cells. The same transfection conditions were then used for transfecting iNOK, iHFK and iHTK cell lines. Blasticidin selection was carried out 24 h post-transfection since blasticidin resistance gene was the antibiotic selection marker included in the used plasmid. Cells that survived the antibiotic selection were then used for obtaining a single-cell colony in 96-well plates. They were grown until confluent, and the efficacy of transfection was validated using Western Blot analysis. However, even though a proportion of the transfected cells survived the selection, E6 and E7 were not detected (data not shown).

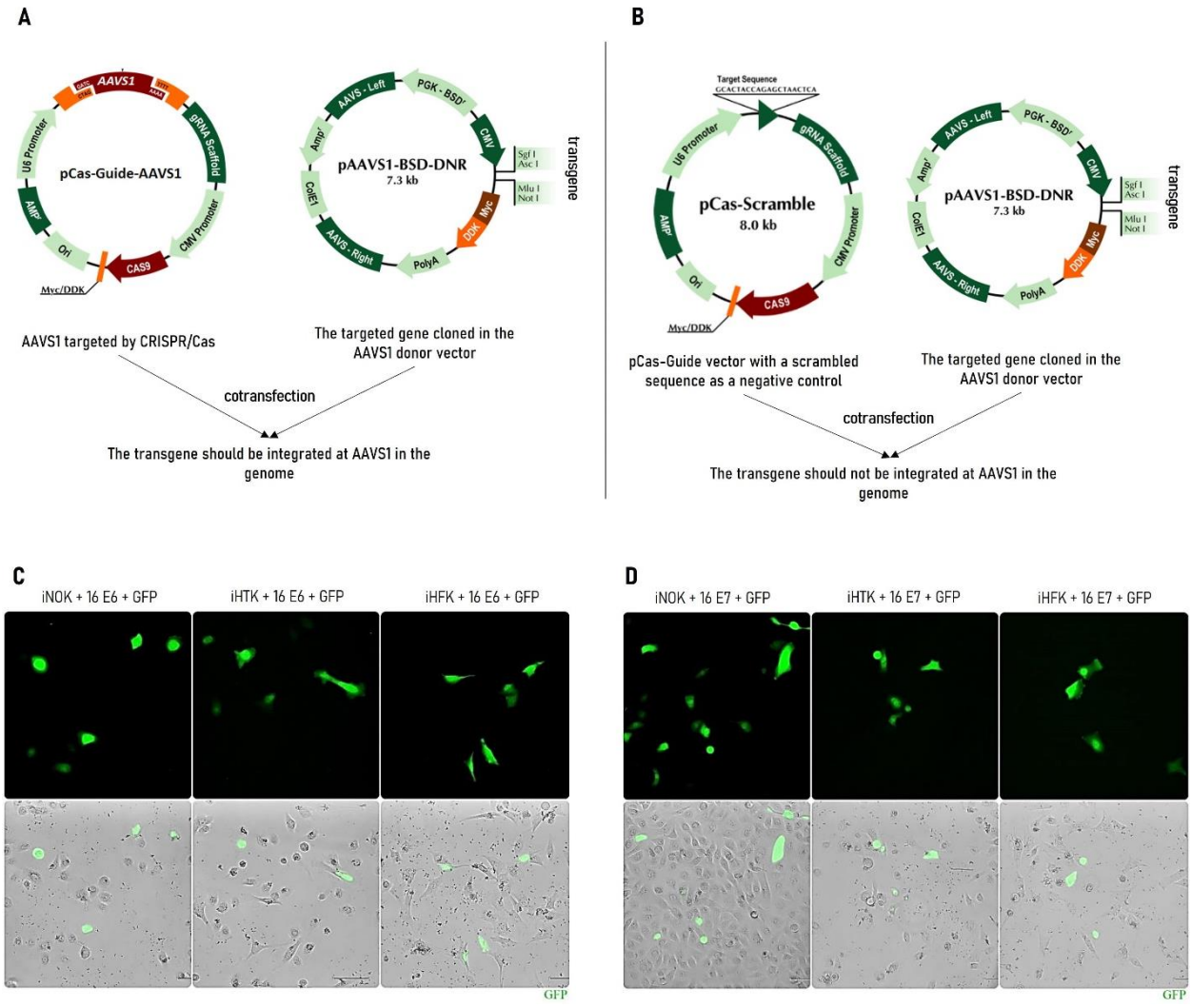

Figure 19. CRISPR Cas9 Knock-in transfection. (A) pCas-Guide-AAVS1 and HPV16 E6 or HPV16 E7 constructed vectors used in co-transfection experiments. pCas-Guide-AAVS1 contains Cas9 and guide RNA allowing the introduction of a double-strand break in the AAVS1 site in host cells. The donor pAAVS1-BSD-DNR vector contains transgene in the MCS and the left and right homologous arms of AAVS1 for homologous repair, allowing the integration of the transgene cassette into the AAVS1 locus. (B) Negative scramble control. pCas-Scramble was used as a negative control that contains a nonspecific gRNA sequence in the pCas-Guide vector. iNOKs transfected with pAAVS1-16E6 (C) or pAAVS1-16E7 (D) knock-in vector using FuGene in DNA:reagent = 1:3 ratio are shown.

Since transfecting the CRISPR knock-in construct did not result in established keratinocyte cell lines stably expressing the oncoproteins, a different approach was used. Lentiviral transduction was reported to be an efficient method for transgene delivery to mammalian cells, since it enables a robust and stable expression of transgenes (Elegheert et al., 2018). To establish lentiviruses encoding HPV16 E6 oncogene three plasmids were used: pUltra-GFP, psPAX2 and pMD2.G. Plasmid pUltra-GFP is the 3rd generation lentiviral vector used for bicistronic expression of GFP and the gene of interest for easier selection of transduced cells. To construct such a plasmid, HPV16

E6 oncogene was amplified from the same pcDNA3.1 16E6 template as described above. It was then subcloned into pUltra-GFP previously digested using *Sal*I/*Xba*I restriction enzyme pair (**Figure 20.A-B**), after which the double validation was conducted to confirm the efficacy of cloning. Firstly, HPV16 E6 was amplified from the constructed pUltra-GFP-16E6 (**Figure 20.C**) and secondly, the constructed plasmid was sequenced, and the results were aligned with HPV16 E6 FASTA. As the construction was successful (**Figure 20.D**), it was proceeded with the lentiviral production in HEK293T cells. As previously reported, HEK293T cells produce superior viral titers compared to HEK293 cells (Merten et al., 2016). To determine the exact titer of produced lentiviruses needed for keratinocyte transduction, various amounts of the lentiviruses were tested. Since pUltra-GFP-16E6 encodes GFP-16E6 fused protein, cells containing the constructed plasmid were expected to emit the green signal. However, although the amount of used lentiviral titer varied, none of the concentration was good enough to obtain cells emitting GFP signal (data not shown). These results suggested a potential problem with the lentiviral production.

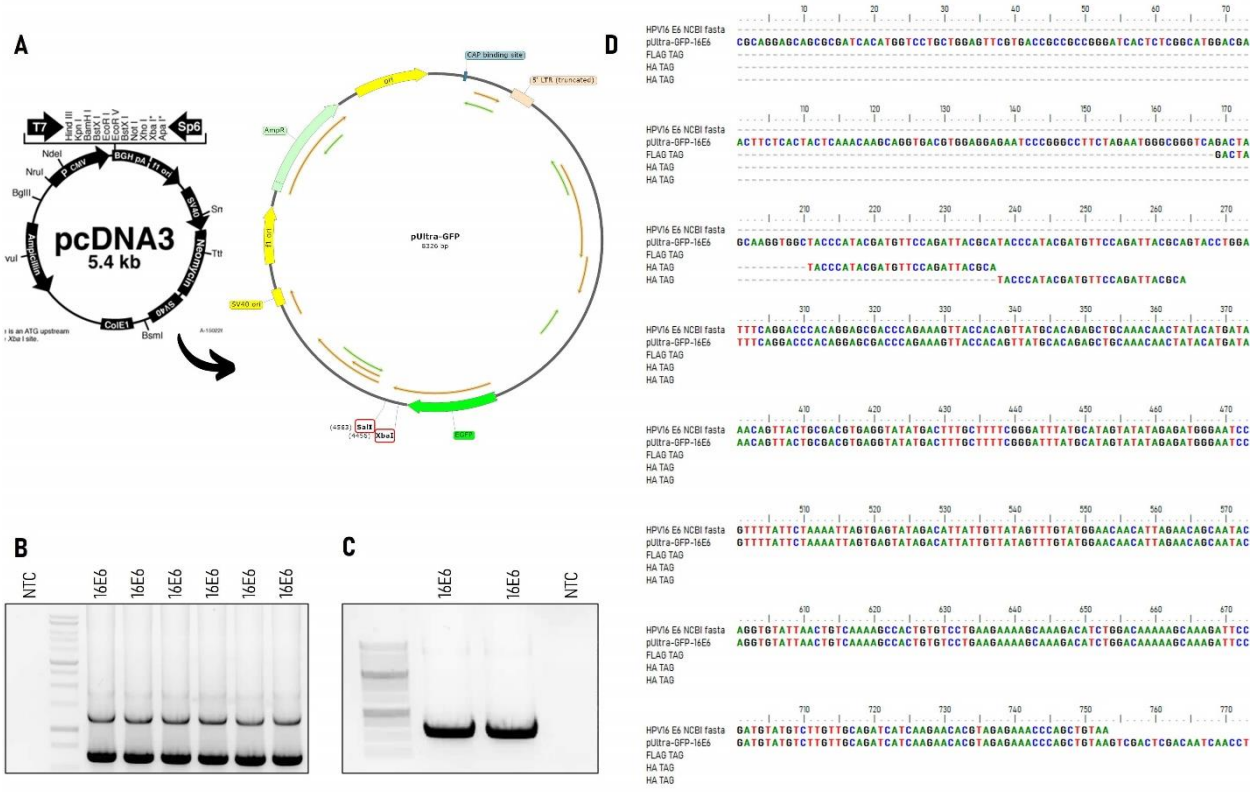

Figure 20. Cloning of HPV16 E6 into the pUltra-GFP-DNR donor vector. (A) HPV16 E6 was cloned from pcDNA3.1 16E6 DNA template and inserted into pUltra-GFP vector previously digested by restriction enzymes *Sal*I and *Xba*I, (B) 16E6 PCR amplification from pcDNA3.1 16E6 template, (C) Ligation was verified by PCR amplification, (D) Cloning verification by DNA sequencing.

Therefore, a third approach to engineer E6/E7 expressing keratinocytes was applied, in which transfection of HPV16 genomes in iNOK, iHTK and iHFK was used for creation of these cell lines which would stably express HPV16 E6/E7 oncoproteins. To do so, cells were co-transfected with HPV16 genomes and a plasmid carrying the blasticidin resistance gene to enable the selection of transfected cells. Transfected keratinocytes were grown and passaged for at least 15 passages without irradiated 3T3-J2 feeder cells. To validate whether keratinocytes were successfully transfected, DNA was isolated from the matched iNOK, iHTK and iHFK cell lines as well as HPV16 E6/E7 expressing CaSki cells, which served as a positive control. HPV16 E6 was successfully amplified using the specific primers (**Figure 21.A**). Since E6 was shown to mediate p53-degradation on the protein level (Scheffner et al., 1993), firstly, p53 gene presence was confirmed in all used cell lines (**Figure 21.B**). After this was validated, HPV presence was corroborated by showing p53 degradation in transfected iNOK, iHTK and iHFK as well as in CaSki control cells. A clear degradation of p53 was detected in all transfected cell lines compared to non-transfected matched control (**Figure 21.C**). Taken together, these results confirmed a successful establishment of iNOK, iHTK and iHFK stably expressing HPV16 E6/E7.

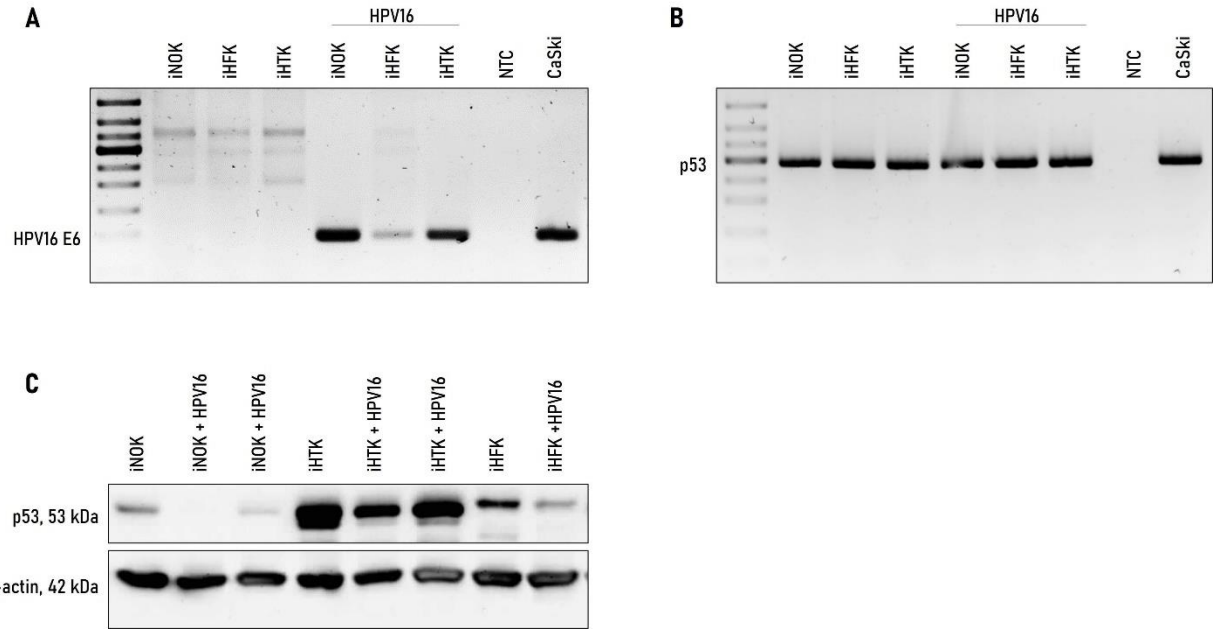

Figure 21. Characterization of HPV16 E6/E7-expressing keratinocytes isolated from various anatomical sites. Immortalized keratinocyte cell lines were transfected with HPV16 genomes. Transfection efficiency was verified using PCR. (A) HPV16 E6 amplification showed presence of 16E6 in all transfected cell lines and CaSki cells, which served as a positive control. (B) p53 amplification was performed to confirm the existence of p53 gene in tested cell lines (C) The presence of E6 was once again confirmed by Western blot analysis showing p53 downregulation in the presence of E6. β-actin was used as the control for equal protein loading.

4.2 HPV16 and 18 E6 bind DLG1 and SCRIB with different affinities

Non-transfected iNOK, iHTK and iHFK cell lines were also used to examine the interacting capacity of E6 with DLG1 and SCRIB, which were previously characterized as preferential targets of HPV18 E6 and HPV16 E6, respectively, in series of GST-pull down assays of *in vitro* translated PDZ domain-containing proteins (Thomas et al., 2005). To investigate if E6's binding capacity with DLG1 and SCRIB was altered in any way depending on the anatomical site, GST-pull down assays were conducted. The obtained data (**Figure 22.A**) demonstrate an interaction between HPV16 E6 and DLG1, but the interaction was evidently stronger between 18E6 and DLG1 in all three cell lines used for comparison. In contrast, a strong interaction was visible between HPV16 E6 and SCRIB in iNOK and iHFK, whilst a somewhat weaker, but still evident interaction was detected between HPV18 E6 and SCRIB. However, although SCRIB was visible in the input of iHTK cells, it was not detected with either GST-16E6 or GST-18E6 possibly due to lower amounts of bound protein. Taken together, these results corroborate those previously published, showing that while E6 oncoproteins from distinct HPV types can bind to DLG1 and SCRIB, DLG1 was preferentially targeted by HPV18 E6, whereas HPV16 E6 preferentially targeted SCRIB (Thomas et al., 2005) in iNOK and iHFK. GST beads alone were used as negative control (**Figure 22.B**).

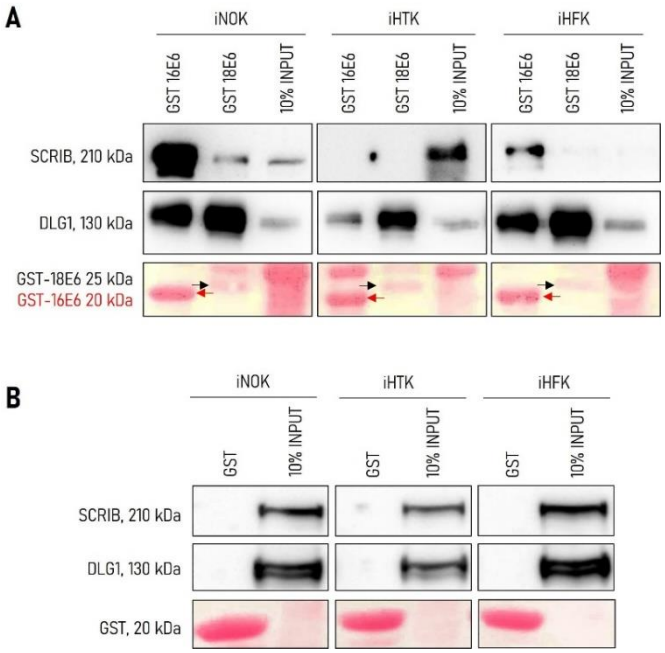

Figure 22. HPV16 and HPV18 E6 bind DLG1 and SCRIB with different affinities. (A) Immortalized keratinocytes were harvested, and cell lysates were incubated with GST-16E6, and GST-18E6 fusion proteins. After washing, bound DLG1 and SCRIB were separated on SDS-page and proteins were detected by Western blotting using corresponding anti-SAP97 (DLG1, 2D11) or anti-SCRIB (C-6) antibodies, respectively. They were compared to the amounts of DLG1 or SCRIB present in 10% input. (B) GST alone was used as a control. The lower gel shows the positions of purified GST proteins used in the pull-down assays visualized by Ponceau-S staining.

4.3 HPV16 E6 exhibits effects on DLG1 and SCRIB endogenous expression

Considering that HPV16 is the predominant cancer causing HPV type in HNSCCs (Simoens et al., 2021), it was further analyzed how E6 oncoprotein of this specific type influences DLG1 and SCRIB expression levels in these cell lines. This would then allow determination of possible differences which could be anatomical site dependent. Three HPV16 E6-expressing keratinocytes, their matching non-transfected controls, as well as CaSki and HPV-negative cervical cancer cells C33A were grown until fully confluent. Cells were then collected, and proteins extracted. Protein concentrations were determined, and equal amounts were used for further Western blot analyses. Protein levels of p53 were once again validated as a confirmation of HPV16 E6 presence, while expression of housekeeping gene β-actin was used as a loading control. A representative result of the Western blot analysis is shown (**Figure 23.A**).

Interestingly, from three independent experimental repeats used for statistical analysis, E6 was shown to have only marginal effects on DLG1 protein levels (**Figure 23.B**). It was shown to be slightly upregulated in HPV16 E6/E7-expressing iHFK cells, whilst in contrast, it seems that DLG1 protein levels remained unaffected regardless of HPV16 E6 presence in iNOK and iHTK, both isolated from HN area. From the densitometry analysis of multiple experiments (**Figure 23.C**)**,** it is evident that SCRIB was upregulated in the presence of HPV16 E6 and this was not dependent on the anatomical origin of the cells. Interestingly, the expression of SCRIB was decreased in CaSki, HPV16-positive cervical cancer cell line, when compared to iNOK, iHTK or iHFK expressing 16E6/E7. On the other hand, DLG1 levels appeared to be higher in CaSki cells and in iHFK in the presence of HPV16 E6/E7, while in iNOK and iHTK DLG1 protein levels remain unchanged. These results suggested that HPV16 E6 has different effects on SCRIB and DLG1 protein expression levels, which may be important for the process of HPV-induced oncogenesis at various anatomical sites.

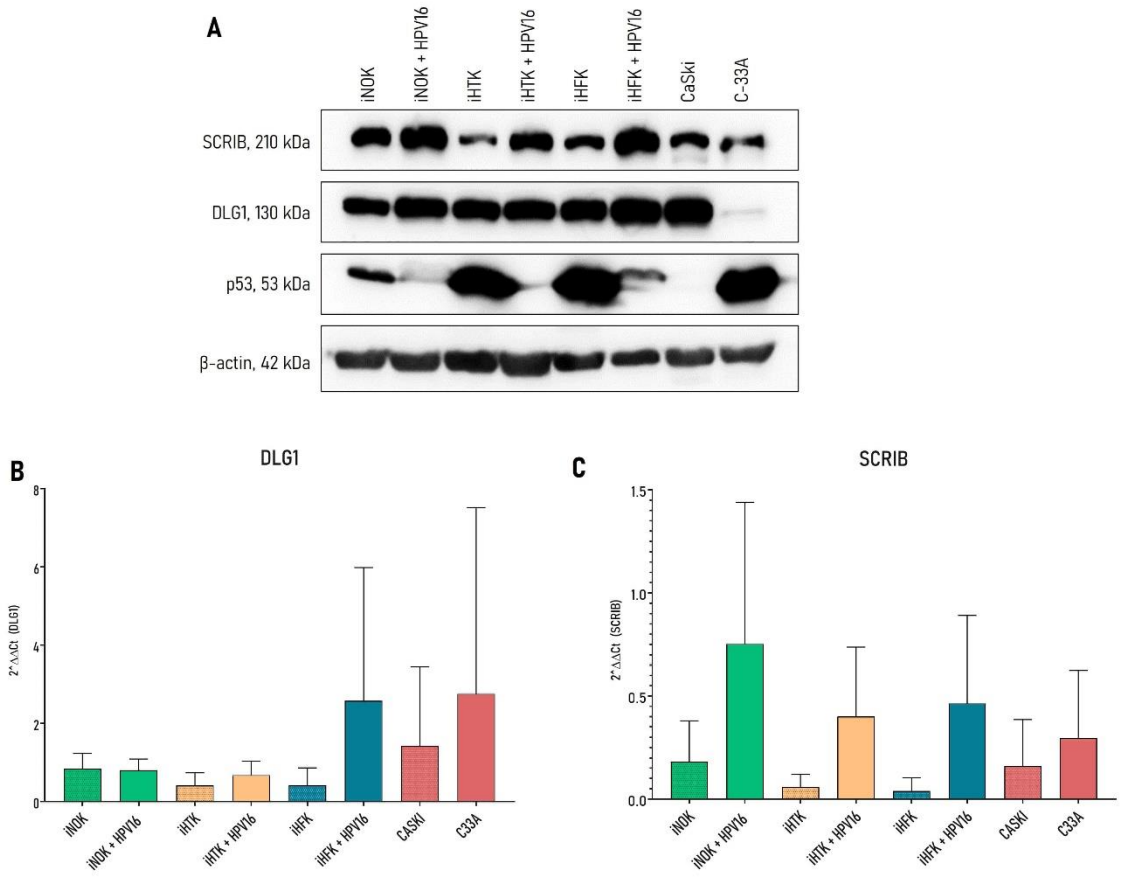

Figure 23. The effect of HPV16 E6 on DLG1 and SCRIB protein expression levels in immortalized keratinocytes from various anatomical sites. (A) Cells were grown until fully confluent and harvested. Isolated proteins from complete cell lysates were separated on SDS-page, detected by anti-SAP97 (DLG1, 2D11) or anti-SCRIB (C-6) antibodies and visualized by chemiluminescence. β-actin was used as the control for equal protein loading. Densitometric analysis of three independent experiments for DLG1 (B) or SCRIB (C) was performed using ImageJ software. The band densities were first normalized with background for each sample after which relative expression was calculated by dividing normalized density with β-actin normalized density. The intensity fold change was calculated by dividing the relative expression of co-transfected samples with non-transfected matching controls, and the base 2 logarithm of that fold change was depicted on the bar chart, so that the increase in intensity is seen as a positive value and the decrease as a negative value. Graphs were designed using GraphPad Prism software.

4.4 HPV 16 E6 effects on DLG1 and SCRIB cellular localization and distribution

Normal protein functions can be disrupted by degradation, but also by changes in its common cellular localization. This mislocalization can block proteins from performing their regular cellular functions and together with fluctuations in expression levels, it can be a prerequisite for cancer development and metastasis (Wang and Li, 2014). Hence, the cellular localization of DLG1 and SCRIB proteins was investigated using immunofluorescence (IF). To do so, cells were grown on coverslips until 70-80% confluent and were then fixed with paraformaldehyde. Cover slips were stained with the corresponding antibodies, and DLG1 and SCRIB cellular localization was then monitored by confocal microscopy. DLG1 was predominantly localized in the cytoplasm and, to a lesser extent, in the nucleus of iNOK cells (**Figure 24.A**). Conversely, in iHTK, DLG1 was

detected on its previously reported cellular sites, at cellular junctions, while some DLG1 was also detected in the nucleus and cytoplasm. In iHFK cells, DLG1 was localized in the cytoplasm, cellular membranes and vaguely in the nuclei. Next, the effects of 16E6 on the localization of DLG1 protein were investigated in established keratinocytes stably expressing HPV16 E6/E7 oncoproteins. In those (**Figure 24. B**), DLG1 localization appeared to be slightly affected in iNOK and iHTK cells in the presence of HPV16 E6. In iNOK-16E6/E7, DLG1 was detected in the cytoplasm and nucleus with more intense staining visible in the perinuclear space. DLG1 was additionally visible in the cellular junctions of iHTK-HPV16/E7 cells. In contrast, DLG1 was not detected in the membranes of iHFK-16E6/E7 cells like it was in their matching non-transfected controls. However, in these cells DLG1 appeared to be accumulated in the perinuclear space. Taken together, these results imply that 16E6 had a less intense effect on DLG1 in cells isolated from HN area compared to those derived from genital area, which supports the results of E6 impact on protein expression obtained through Western blot analysis.

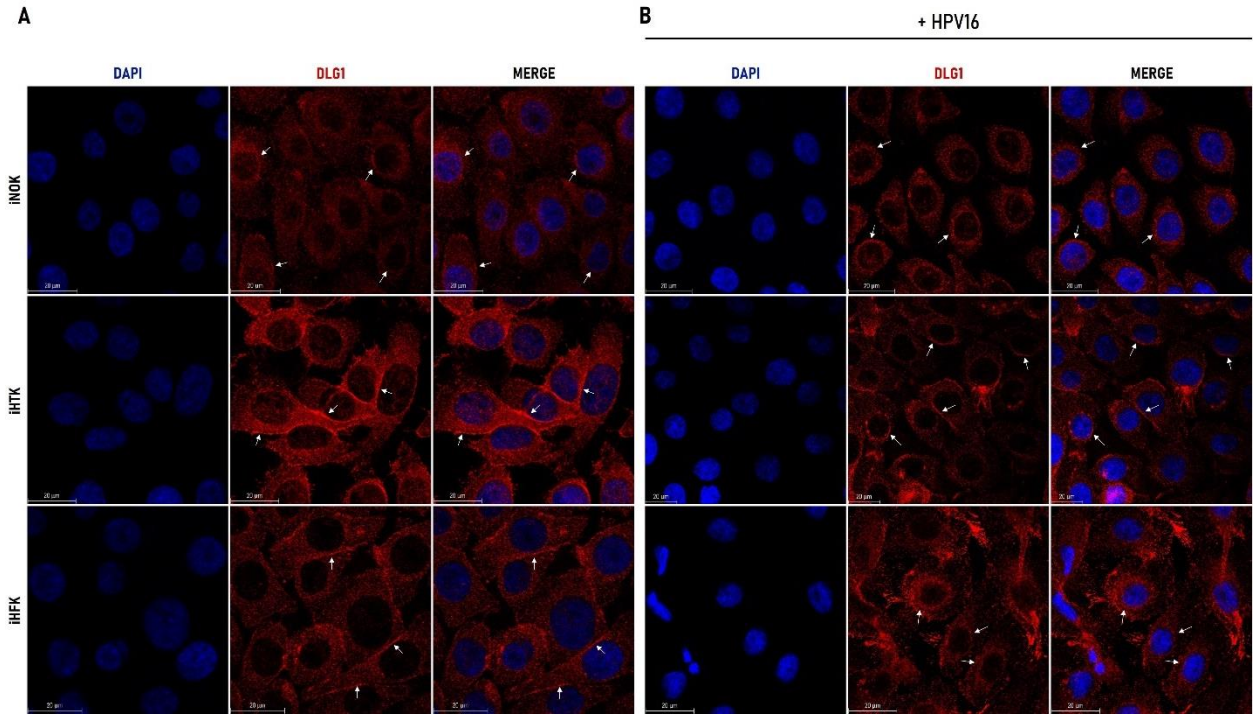

Figure 24. DLG1 localization in immortalized keratinocytes derived from various anatomical sites. Immunofluorescent 2D confocal images of DLG1 localization in (A) non-transfected iNOK, iHTK and iHFK and (B) HPV16 E6/E7-expressing iNOK, iHTK and iHFK. DLG1 antigen was targeted using anti-SAP97 (DLG1, 2D11) and rhodamine red-X goat anti-mouse secondary antibodies. The nuclei were identified by DAPI staining. White arrows indicate DLG1 localization. Scale bars = 20 μm.

SCRIB cellular localization was then analyzed in the same cell lines in the presence and absence of HPV16 E6. The results (**Figure 25.A**) demonstrate a positive SCRIB signal at the plasma membrane of iNOK cells, with a small amount of SCRIB staining visible in the nuclei. Furthermore, SCRIB was also accumulated in the cytoplasm and the perinuclear space in iNOK. In iHTK, SCRIB was barely visible at the plasma membranes, whilst the majority was concentrated around the nuclei with some nuclear staining. On the other hand, SCRIB was abundantly associated with the plasma membranes of iHFK cells, with some cytoplasmic and nuclear staining also visible.

Next, SCRIB cellular localization was investigated in the keratinocyte 16E6/E7-expressing cell lines. As can be seen, the presence of 16E6 had an effect of SCRIB localization (**Figure 25.B**). Precisely, in iNOK-16E6/E7 and iHFK-16E6/E7 cells, SCRIB was seen predominantly accumulated in the cytoplasm, whereas membranous staining was barely visible. On the contrary, it appeared that 16E6 caused an accumulation of SCRIB at the plasma membranes in iHTK cells, which was not observed in the absence of 16E6 in these cells. Taken together these results suggest that 16E6 causes changes in the localization of SCRIB proteins to a greater extent than of DLG1.

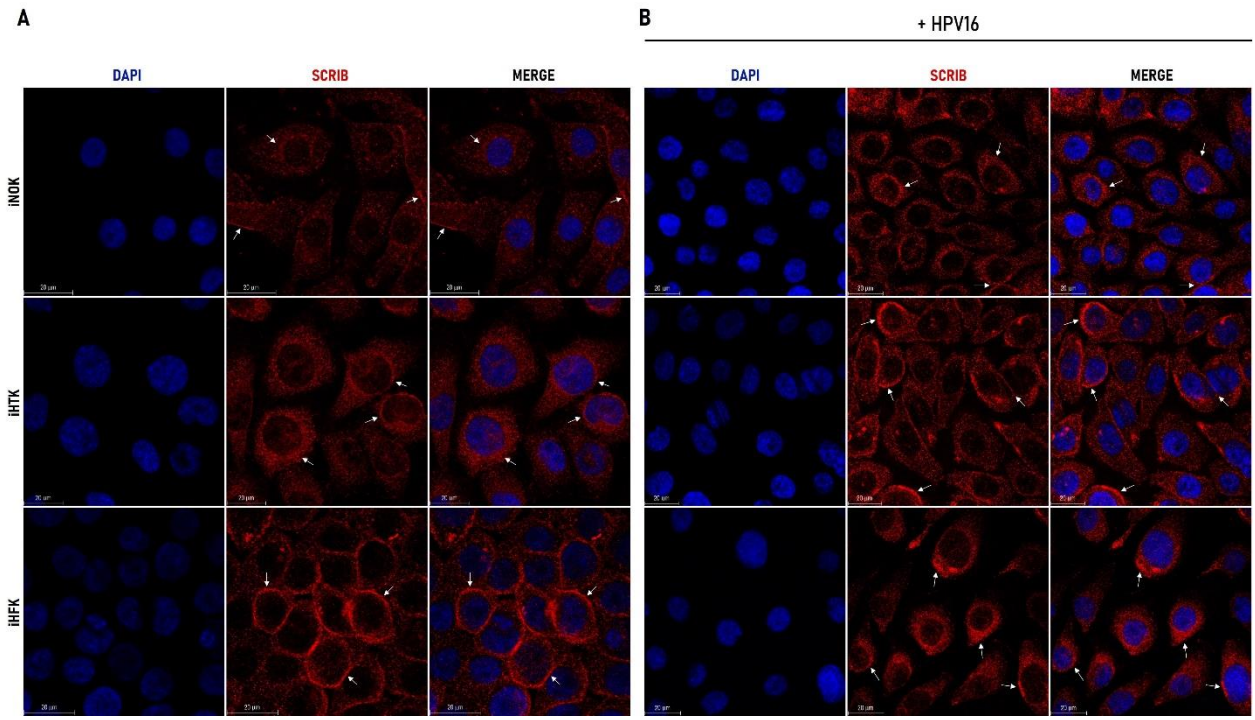

Figure 25. SCRIB localization in immortalized keratinocytes derived from various anatomical sites. Immunofluorescent 2D confocal images of SCRIB localization in (A) non-transfected iNOK, iHTK and iHFK and (B) iNOK, iHTK and iHFK stably expressing 16E6/E7. SCRIB antigen was targeted using anti-SCRIB (C-6) and rhodamine red-X goat anti-mouse secondary antibodies. The nuclei were visualized by DAPI staining. White arrows indicate SCRIB localization. Scale bars = 20 μm.

Since the established cell lines were not cancer-derived cell lines, DLG1 and SCRIB protein distribution was further examined and compared with CaSki and C33A cells, which were originally isolated from cervical cancer patients. DLG1 was demonstrated to localize at adherent junctions in C33A, an HPV-negative cancer cell line (**Figure 26.A**). Interestingly, of somewhat lower intensity, but still very evident DLG1 signal was also observed in the cytoplasm and nuclei. In contrast, in HPV16-positive cancer line CaSki, DLG1 was shown to be almost completely mislocalized from cell-cell contacts to the cytoplasm and only a small amount visible in the nuclei. These results imply that 16E6 promotes delocalization of DLG1 and this change was even more apparent in comparison with iHFK-16E6 cells which were also isolated from anogenital region. Accordingly, DLG1 localization changes might serve as an indicator of highly HPV-transformed cells.

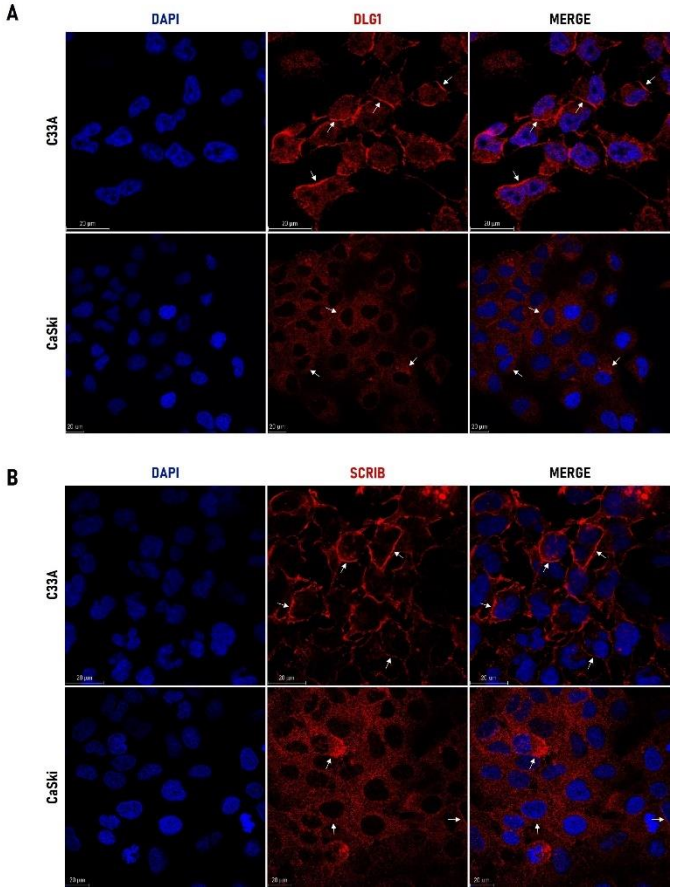

Figure 26. DLG1 and SCRIB localization in CaSki and C33A cells. (A) Immunofluorescent 2D confocal images of DLG1 localization in CaSki and C33A cancer cell lines. DLG1 antigen was targeted using anti-SAP97 (DLG1, 2D11) and rhodamine red-X goat anti-mouse secondary antibodies. (B) Immunofluorescent 2D confocal images of SCRIB localization in CaSki and C33A cancer cell lines. SCRIB antigen was targeted using anti-SCRIB (C-6) and rhodamine red-X goat anti-mouse secondary antibodies. In both cases, the nuclei were visualized by DAPI staining. White arrows indicate the protein localization. Scale bars = 20 μm.

Analyses of SCRIB localization, revealed that the majority of SCRIB protein was detected at cellular junctions in C33A cells, whilst cytoplasmic SCRIB was barely visible. On the other hand, SCRIB appeared to be predominantly located into the cytoplasm and nuclei in CaSki cells (**Figure 26.B**). Put together, these results show that 16E6 causes the alteration of SCRIB subcellular localization in all cell lines regardless of their anatomical origin. However, the change was more evident in CaSki then in iHFK-16E6/E7 cells, which were both isolated from the genital region, but the ratio of HPV-integration in those possibly varies. Taken together, HPV16 E6 possibly affects the localization of DLG1 and SCRIB proteins, which most likely contributes to the disruption of their normal cellular polarity maintenance function, and this is more evident with SCRIB. Additionally, this effect seems to be more pronounced in the cell line derived from an HPV-positive cervical cancer patient.

To further expand these analyses, DLG1 and SCRIB distribution changes were investigated in the presence of HPV16 E6 in the same three keratinocyte cell lines. To do that, fractionation assays were performed. Subcellular fractionation was carried out on immortalized keratinocytes harvested at 90% confluency. The results demonstrate that DLG1 was mostly detected in the membranes and nuclei of iNOK cells, whilst the bands of lower intensity were also observed in the cytoplasmic

and cytoskeletal fractions (

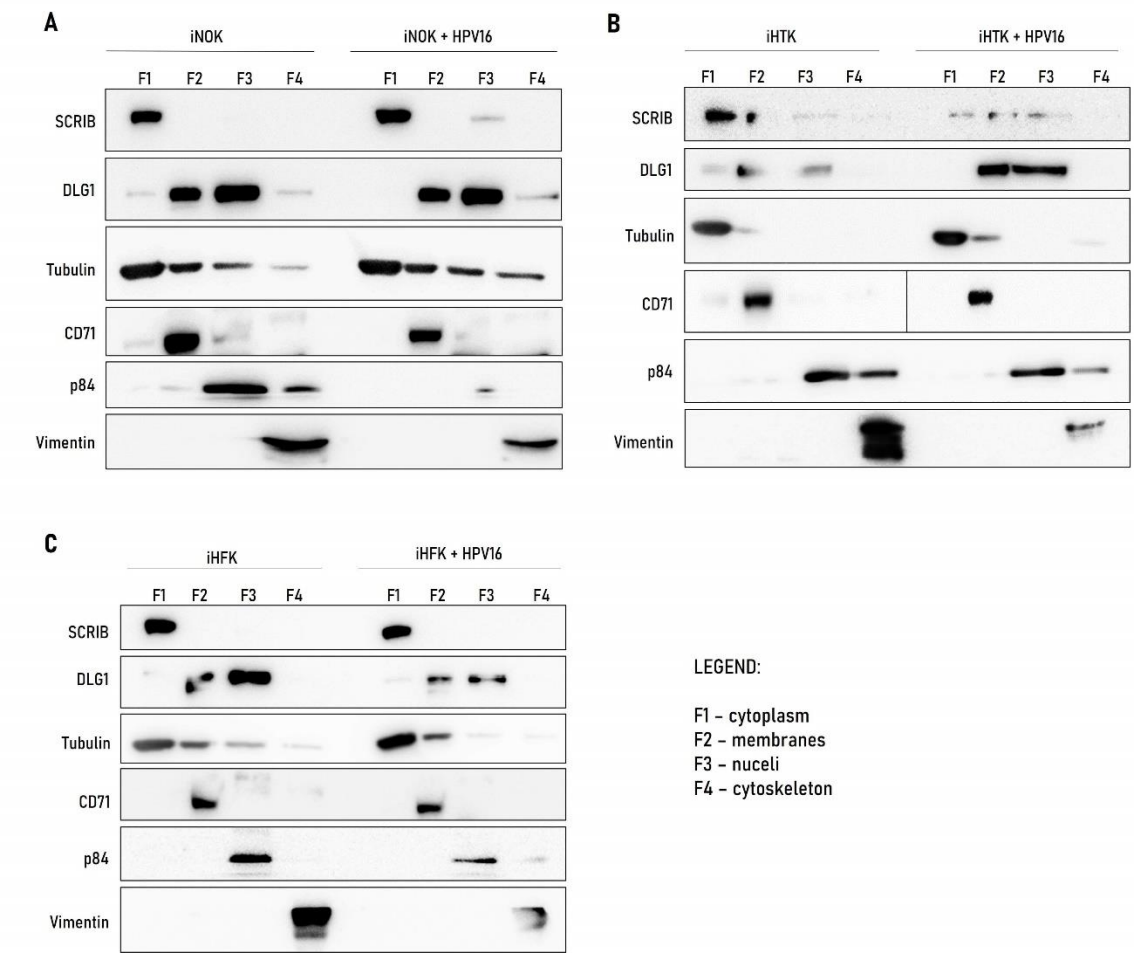

Figure 27.A). In the presence of HPV16 E6, the cytoplasmatic DLG1 was depleted, but in the other cellular compartments DLG1 remained unchanged. In iHTK (**Figure 27.B**), DLG1 was predominantly detected in the membranes and nuclei. Still, somewhat weaker, but distinct DLG1 staining was observed in the cytoplasm as well. However, in the presence of 16E6, DLG1 was detected only in the membranes and nuclei, while the cytoplasmic proportion was not observed. Interestingly, no change to DLG1 subcellular localization was observed in iHFK regardless of 16E6 presence (**Figure 27.C**). In both cell lines, DLG1 was detected only in the membranes and nuclei. Since distinct changes were observed in iNOK and iHTK cells isolated from HN area, but not in iHFK derived from genital area, this once again supports the notion that 16E6 differently affects DLG1 distribution in cells of various anatomical origin.

In non-transfected iNOK cells, SCRIB was detected solely in the cytoplasm (**Figure 27.A**). Nevertheless, in the presence of HPV16 E6, a small portion of SCRIB was visible in the nuclei as

well. Similarly, SCRIB was mostly detected in the cytoplasm of non-transfected, control iHTK cells, with a smaller proportion being visible in the membranes and nuclei as well (**Figure 27.B**). As presented, it appears that SCRIB distribution remains unchanged in the presence of HPV16 E6. Interestingly, SCRIB localization remained unaffected in the presence of HPV16 E6 in iHFK cells (**Figure 27.C**). Interestingly, both DLG1 and SCRIB distributions were impacted by 16E6 in cells isolated from HN area, suggesting a possible variation in the influence of E6 on these PDZ-domain containing targets, which could be dependent on the anatomical area.

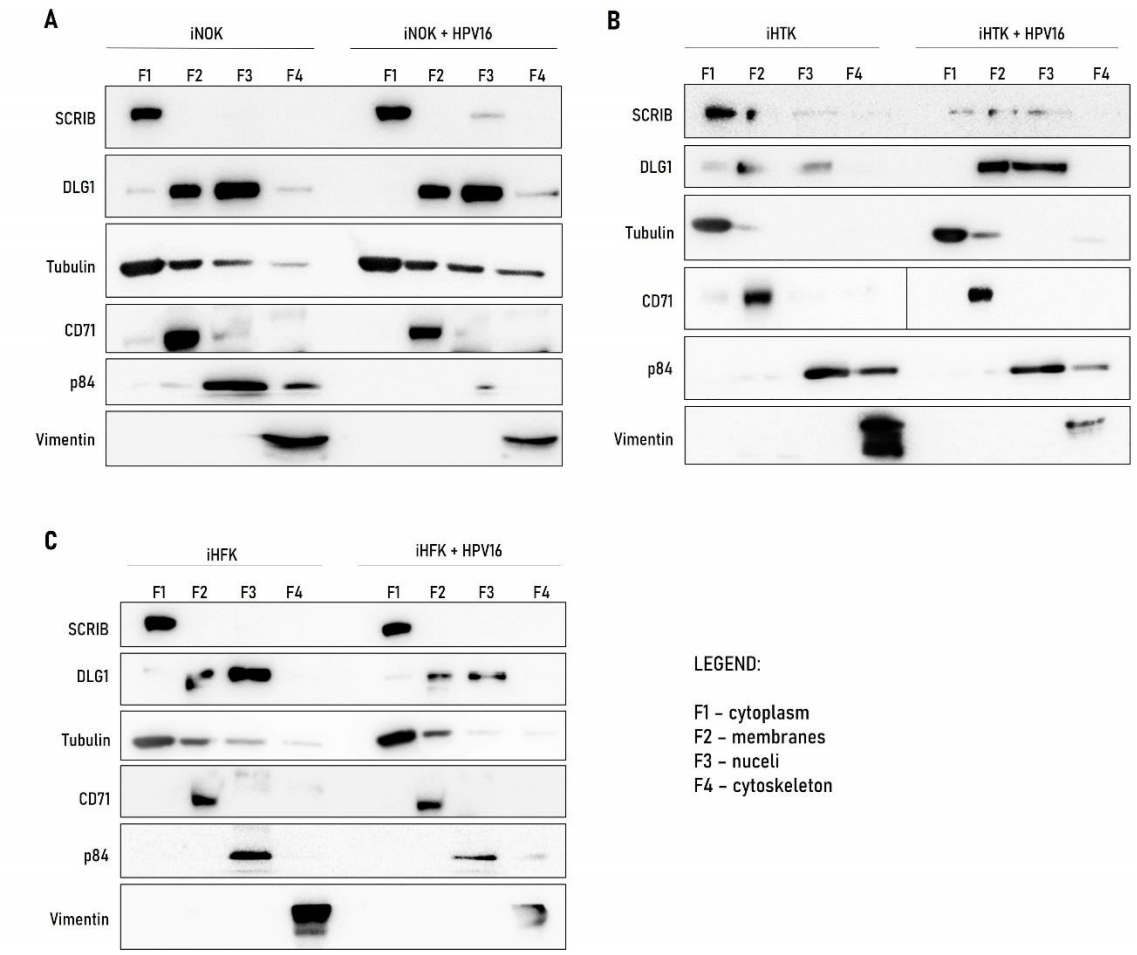

Figure 27. DLG1 and SCRIB distribution in immortalized keratinocytes in presence and absence of 16E6. To investigate DLG1 and SCRIB protein distribution, cells were grown until fully confluent, harvested, and fractionated. Proteins were separated on SDS-page, detected by anti-SAP97 (DLG1, 2D11) or anti-SCRIB (C6) antibodies and visualized by chemiluminescence. Tubulin, CD71, p84 and vimentin were used as the confirmation of F1, F2, F3 and F4 fractions, respectively. DLG1 and SCRIB distribution was investigated in iNOK (A), iHTK (B) and iHFK (C) cell lines.

4.5 DLG1 and SCRIB transcription is HPV16 E6-dependent

Although many studies have described alterations in DLG1 and SCRIB protein levels in the presence of HPV16 E6, only a few of them have investigated and reported changes on the

transcriptional levels of PDZ domain-containing proteins (Dizanzo et al., 2020; Lazić et al., 2012). Therefore, RT-qPCR was conducted to evaluate if the transcription of E6 increases with the maintenance time or number of passages, and how these changes affect DLG1 and SCRIB transcription levels. Moreover, discrepancies were also examined in the primary cell lines isolated from genital and HN anatomical sites, HFK and HTK, respectively, which contained HPV16 episomes. To strengthen the significance of the obtained data, analysis was performed in two independent keratinocyte donor backgrounds and in 3 biological replicas of each non-transfected, low-passage (p5-p8) and high-passage (p19-p22) HPV16 episome-containing HTK cells. Likewise, to investigate differences in transcription depending on the anatomical site, two independent donors of HFK cells were also used. Those HFK cells were harvested at passage p5. Changes in the transcript levels were calculated relative to non-transfected cells of the same donor. As expected, the presence of HPV16 E6 transcripts exclusively in the transfected cells regardless of the donor background (**Figure 28.A**). Observably, E6 levels were higher in HTK harvested at higher passages then in low-passaged ones. More interestingly, although harvested at p5, HFK containing HPV16 episomes have shown extremely high transcription levels when compared to low-passage HTK. Potential differences in DLG1 and SCRIB transcript levels were further investigated in the same cell lines. From the obtained results (**Figure 28.B**), 16E6 causes the upregulation of SCRIB transcription and this is not anatomical site dependent. Furthermore, this change was significant for high-passage HTK in comparison to their non-transfected controls. The levels of DLG1 were examined by using two different primer pairs, one detecting only DLG1β isoform, and other specific for the HOOK region of DLG1. According to the results, DLG1β isoform levels were slightly lower in HPV16 episome-containing HTK cells and continued to decline with the length of the maintenance time or number of passages. On the contrary, the presence of HPV16 contributed to higher transcript levels of DLG1β isoform in HFK cell line (**Figure 28.C**). As for DLG1 HOOK (**Figure 28.D**), results were incoherent for HTK since the downregulation was observed in low-passage HPV16-HTK cells, but the upregulation in high-passage, when compared to non-transfected matching control. However, significant upregulation of DLG1 HOOK was detected in the presence of HPV16 in HFK cells. These results again suggest that HPV16 E6 has more pronounced impact on SCRIB then on DLG1. All things considered, in performed experimental analyses, E6 was observed to cause the upregulation of SCRIB on the

transcriptional level, which is likely to be required for early stages of infection and optimal completion of productive HPV cycle.

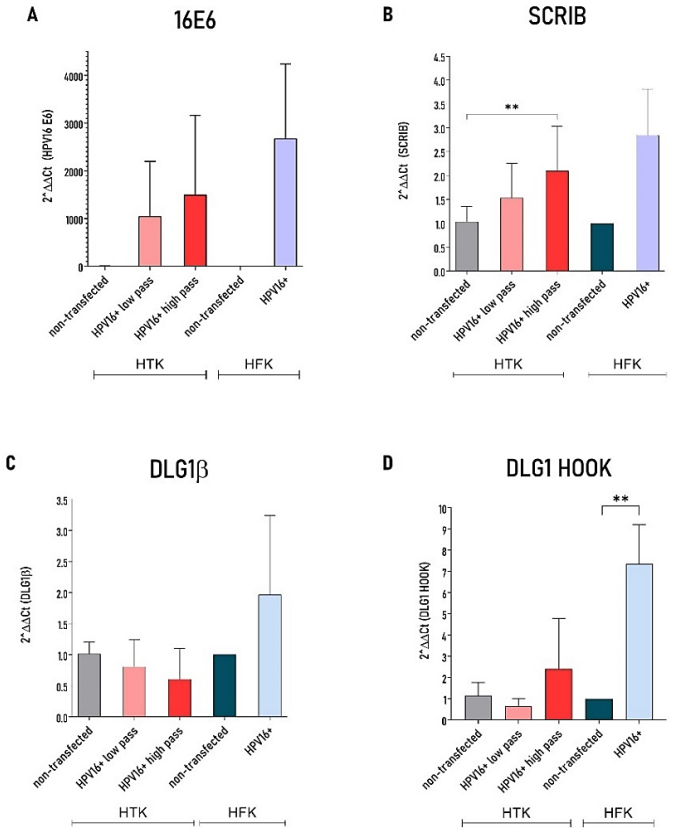

Figure 28. Relative transcript levels of HPV16 E6, SCRIB, DLG1β and DLG1 HOOK isoforms in primary HTK and HFK cells containing HPV16 episomes. RNA was extracted from primary keratinocytes containing HPV16 episomes grown to either low-passages (p5-p7) or high-passages (p18-p22), alongside non-transfected HTK (red bars) or HFK (blue bars) from two independent donors. Transcript levels were normalized to an internal β-actin control and then to the transcript levels in non-transfected cells of the same donor background. Transcript levels of (A) HPV16 E6, (B) SCRIB, (C) DLG1β and (D) DLG1 HOOK are shown after combining donors by anatomical regions. N = 18 (3 biological replicates in 3 technical replicas for 2 donors) for HTK and 6 (1 biological replicate in 3 technical replicas for 2 donors) for HFK. SD error bars quantify the scatter among the values. Significance was determined in GraphPad using one-way ANOVA test with P<0,01 taken as significant and marked with **.

To investigate any potential changes in DLG1 and SCRIB mRNA transcripts that occur during actual malignant transformation in HN area, the analysis was expanded to HPV-positive, and HPV-negative OPSCC-derived cell lines. Four cell lines were examined: two HPV16-positive (SCC104 and SCC147) and two HPV-negative (SCC040 and CAL27). The transcript levels in OPSCC-derived cell lines were normalized to an internal β-actin control and then to the transcript levels in HTK non-transfected cells. For the confirmation of HPV16 positivity, E6 transcript levels were also determined and as expected, E6 was detected exclusively in HPV16-positive OPSCC cell lines (**Figure 29.A**). The results (**Figure 29.B**) demonstrate that SCRIB levels remained unchanged in HPV-negative OPSCC-derived cells when compared to non-transfected HTK cells. However, a

more abundant transcription of SCRIB was observed in HPV16-positive OPSCC cell lines. With respect to DLG1, DLG1β transcripts were shown to be higher in both OPSCC cell lines compared to the non-transfected HTK regardless of HPV16 presence (**Figure 29.C**). Conversely, DLG1 HOOK domain containing transcripts were decreased in both HPV-negative and HPV16-positive OPSCC cell lines (**Figure 29.D**). All things considered, these results suggest that in HNC, HPV16 E6 exhibits a stimulatory effect on SCRIB transcription levels, and this was not the case with DLG1. However, interestingly, there is an evident change in DLG1 transcription levels in HN tumors regardless of HPV presence, which may be a consequence of DLG1 perturbations in the process of carcinogenesis in general.

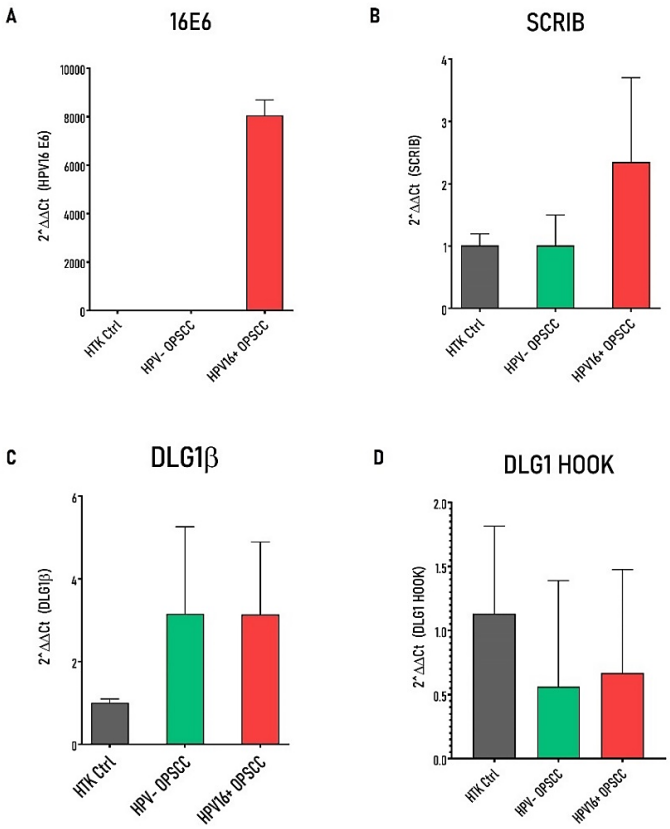

Figure 29. Comparison of HPV16 E6, SCRIB, DLG1β and DLG1 HOOK transcript levels in OPSCCs derived cell lines. Transcript rates of (A) HPV16 E6, (B) SCRIB, (C) DLG1β and (D) DLG1 HOOK are shown after combining donors by HPV positivity. N=12 (2 biological replicates in 3 technical replicas for each OPSCC cell line). SD error bars quantify the scatter among the values**.** Graphs were designed using GraphPad Prism software.

4.6 DLG1 and SCRIB localization is altered during HPV16 cycle in HN area

The effects of observed fluctuations at the transcriptional level of DLG1 and SCRIB were then correlated with changes in their protein localization during the HPV16 productive cycle in cells derived from the HN area. Since the HPV productive cycle is intimately linked to keratinocyte

differentiation (Graham, 2017b), the alterations in DLG1 and SCRIB localization were examined in HTK and HPV16-HTK keratinocytes grown in organotypic 3D raft culture. This experimental model mimics cellular differentiation and is sufficient for studying protein modifications which are likely to occur during the productive viral cycle. The rafts were grown for previous studies from the Roberts and Parish laboratories. As seen, established raft cultures showed the typical pattern of keratinocyte differentiation **Figure 30**so the basal epithelial layer, the lower suprabasal and the upper suprabasal layers were clearly distinguishable (**Figure 30.**). In the control raft derived from non-transfected primary HTKs, the upper suprabasal layer was shown to be accompanied with nucleus-free cells making the granular layer. In rafts derived from HTKs containing HPV16 episomes, a similar morphological growth was visible. However, there was an obvious expansion of the suprabasal layer and preservation of the nuclei was visible throughout all the layers. The longer the culturing time of these cells (i.e., the greater the number of passages), the higher levels of viral gene transcripts, including E6/E7. Since E7 stimulates cell proliferation, as the cell division numbers were increasing, this was reflected on the expansion of the rafts thickness.

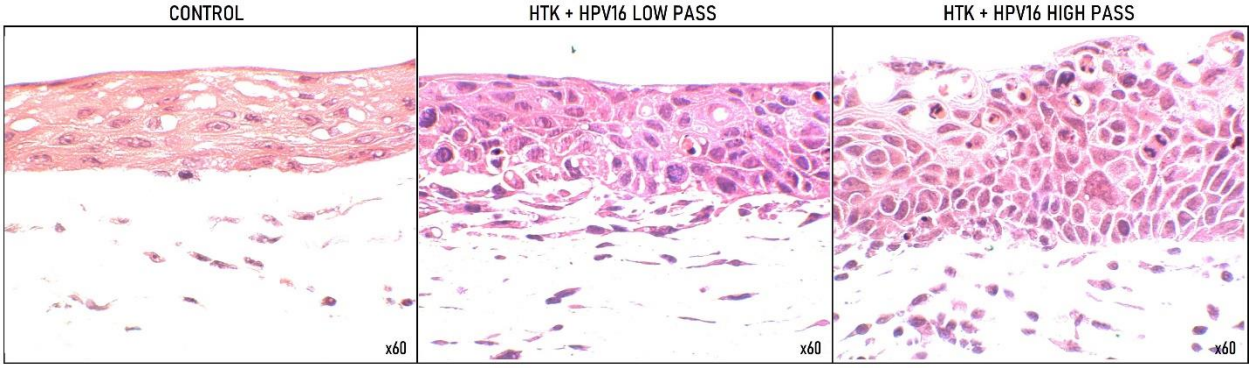

Figure 30. Morphological analysis of organotypic 3D raft cultures derived from low and high-passage HPV16 episome containing HTK cells compared to primary HTK. Hematoxylin and eosin staining show pattern typical for keratinocytes differentiation. Layers are clearly distinguishable. In the presence of HPV16 episomes, rafts were thicker and contained more suprabasal layers. They were visualized by a light microscope with a magnification x60. Property of S. Roberts and J.L. Parish (University of Birmingham).

After confirming the typical pattern of keratinocyte differentiation in the raft cultures, DLG1 and SCRIB protein expression changes were explored during the productive phase of HPV16 cycle in HTK derived raft cultures. Cells with or without HPV16 episomes were subjected to cellular differentiation by growth in organotypic raft cultures for 13 days, after which they were formalin-fixed, embedded in paraffin and cut in sections. As shown (**Figure 31.**), DLG1 was localized in the membranes of cells in the upper layers of non-transfected HTK control rafts (top panel). Some

cytoplasmatic staining was detected in both basal and upper layers, however, no cytoplasmic DLG1 was visible in the middle suprabasal layers. In the rafts derived from low-passaged HTK containing HPV16 episomes (middle panel), DLG1 was detected in the cytoplasm and membranes, but some nuclear staining was detected as well. In the high-passaged HPV16-HTK-derived rafts (lower panel), membranous DLG1 was noticeable in the upper layers. Though, a shift from the membranes to the cytoplasm was apparent in the lower layers. These results indicate that 16E6 impacts DLG1 localization during the productive viral cycle and this was more pronounced in high-passage HPV16-HTK-derived raft cultures.

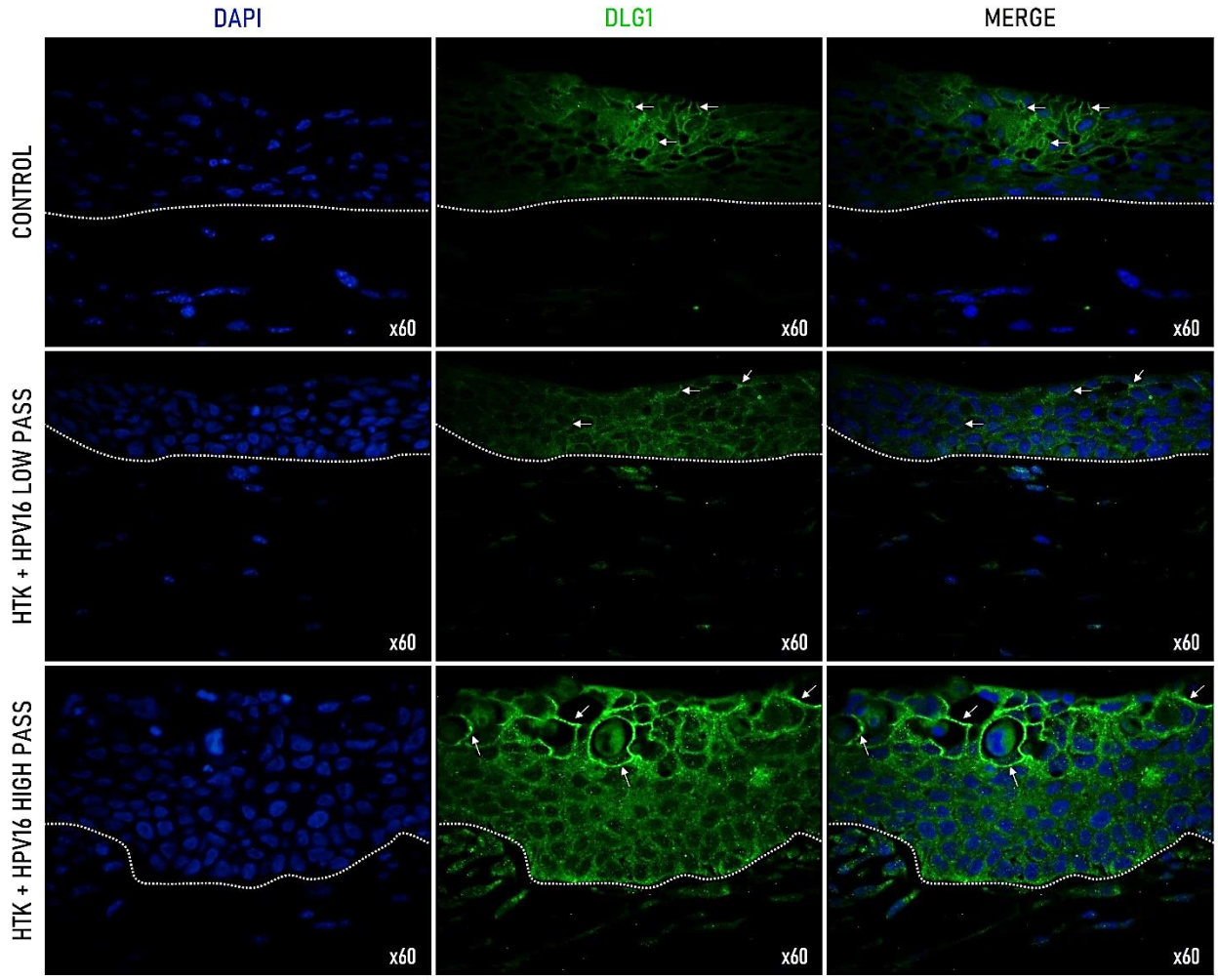

Figure 31. DLG1 is delocalized in HPV16 positive HTK 3D organotypic raft cultures. Raft cultures were grown on a gel made of collagen and mouse fibroblasts for 13 days, harvested and fixed with 3.7% paraformaldehyde. Individual sections were cut and stained for DLG1 using 2D11 mouse monoclonal antibody and Alexa Fluor 488 donkey anti-mouse antibody (green). The nuclei were stained with DAPI (blue). White dots represent the basal membrane. White arrows indicate DLG1 localization. Images were taken under x60 magnification.

Next, modifications in the subcellular localization of SCRIB were investigated under the same experimental conditions. Sections from the same rafts were immunostained for SCRIB to investigate potential differences in SCRIB localization during the keratinocyte differentiation in the presence or absence of HPV16 episomes. The representative images are visible in **Figure 32**.

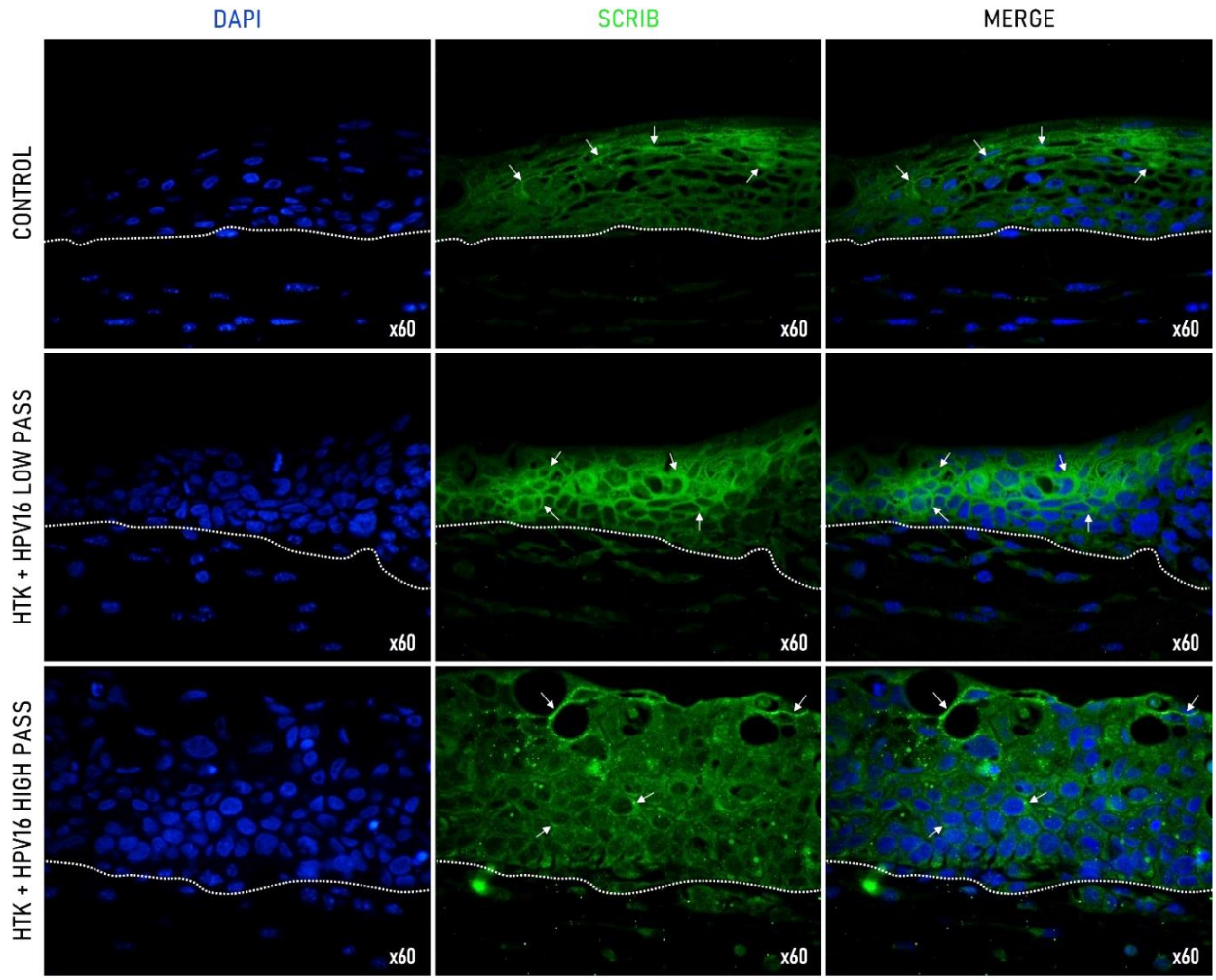

Figure 32. SCRIB is delocalized in HPV16-positive HTK organotypic 3D raft cultures. Raft cultures were grown on a gel made of collagen and mouse fibroblasts for 13 days, harvested and fixed with 3.7% paraformaldehyde. Individual sections were cut and stained for SCRIB using D-2 (green) mouse monoclonal antibody and Alexa Fluor 488 donkey anti-mouse antibody. The nuclei were stained with DAPI (blue). White dots represent basal membrane. White arrows indicate SCRIB protein. Images were taken under x60 magnification.

In non-transfected HTK control raft (top panel), SCRIB was localized in the membranes of cells throughout all the layers and a weak staining appeared in the lower layers closer to the basal membrane. In the rafts grown from the low-passaged HTK cells containing HPV16 episomes (middle panel), SCRIB was detected with higher intensity through the middle layers. In high-passaged HPV16-HTK- derived rafts (lower panel), membranous SCRIB was detected in some

cells of the upper layer. However, most of SCRIB was evidently mislocalized from the membranes into the cytoplasm throughout the layers implying that E6 manipulates SCRIB localization for achieving conditions required for optimal HPV replication. However, such changes during the long-term infection accompanied with HPV E6/E7 integration may be a significant feature required for the development of malignancy in HN area.

4.7 DLG1 and SCRIB are distinctly regulated during the progression of OPSCC

After demonstrating in several assays that HPV16 E6 has a greater impact on both transcriptional and protein levels of SCRIB, in comparison to DLG1, this research was further expanded to investigate how these findings reflect on the specific situation in HPV-negative and HPV16-positive OPSCCs. A total of 66 OPSCC and 8 healthy, non-cancerous and non-infected tonsillar tissue samples as controls were collected. DNA was isolated and sample quality was validated by PCR amplification of β-actin used as an internal control (**Figure 33.**).

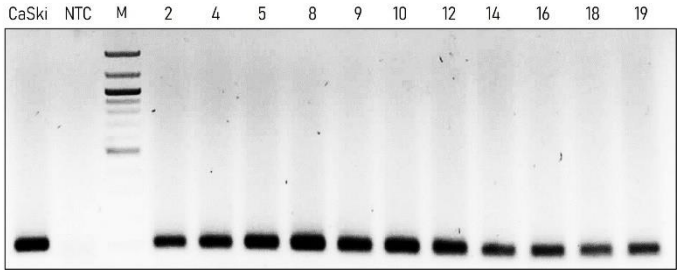

Figure 33. DNA quality validation. DNA was isolated using NucleoSpin® DNA FFPE XS kit according to manufacturer's instructions. PCR amplification of β-actin was performed as an internal control of quality. Representative image shows positive reactions for all samples except for non-template control, NTC. Lane numbers correspond to the sample number. M = Quick-Load Purple 100 bp ladder

4.7.1 HPV genotyping

After confirming that the DNA was of adequate quality for further experiments, two consensus PCR amplification protocols using GP5/6 and SPF10 primers were conducted, and representative images are shown (**Figure 34.A-B**). The applied protocols are the most widely used PCR methods for the detection of mucosal HPV types since these primer pairs are designed to cover the conserved region of the L1 open reading frame. It is generally agreed that if either GP5/6 or SPF10 PCR results in a positive reaction, a sample is considered as HPV-positive. After all GP5/6 or SPF10 positive samples were detected, an additional PCR reaction using primers for specific region containing the end of the 16E6 and the beginning of the 16E7 gene was performed (**Figure 34.C**). Based on the genotyping results, 21 out of 66 OPSCC samples, were classified as HPV16-positive

and 36 as HPV-negative OPSCC. The remaining nine samples were excluded, as they were inconclusive due to the insufficient DNA amount. Interestingly, some of the samples were detected as either GP5/6 or SPF10 positive, but HPV16 E6 negative suggesting that this small proportion of collected OPSCCs could have been caused by other HPV types.

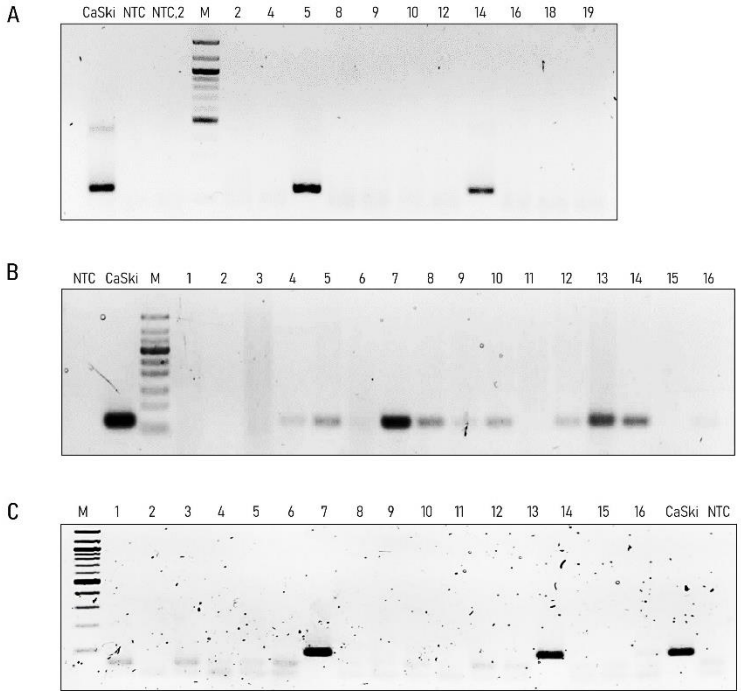

Figure 34. HPV genotyping of FFPE OPSCCs samples. To distinguish HPV positive samples, conserved region of L1 was amplified using two different primer sets: (A) GP5/6 amplifying a product of ~142 bp and (B) SPF10 amplifying a product of ~65 bp. Samples that resulted with a band for either of them, were used to isolate HPV16 positive samples. (C) 16E6 amplification using primers which generate a product of 99 bp. Representative images are shown. Markers that were used GelPilot 50 bp Ladder, Qiagen (A) and are Quick-Load Purple 100 bp ladder, NEB (B, C).

4.7.2 The p16 expression

Although, as discussed in the introduction, there isn't a 100% correlation between p16 protein expression and HPV positivity in OPSCCs, its expression was investigated in all samples, including healthy tonsillar tissue. A specific staining of the reticulated cryptal epithelium was observed in healthy tonsillar tissue (**Figure 35.I**). This staining was different than described in various malignancies, but it corresponded to that previously shown in healthy tissues (Klingenberg et al., 2010). The expression of p16 was then examined in HPV16-positive and HPV-negative OPSCCs. According to the obtained results, the vast majority of HPV16-positive OPSCCs (18/21 or 85.71%) were also p16-positive. Interestingly, a noticeable proportion of HPV-negative OPSCCs (3/36 or 8.33%) also showed p16 positivity. Although a rather small sample size was investigated, these results correlated well with the results of the previous studies (Dok and Nuyts, 2016; Golusiński et

al., 2017). Representative images of every combination of p16 and HPV positivity are depicted (**Figure 35.II**). Taking all this into account, p16 positivity was shown again as an unreliable biomarker of HPV16 positivity.

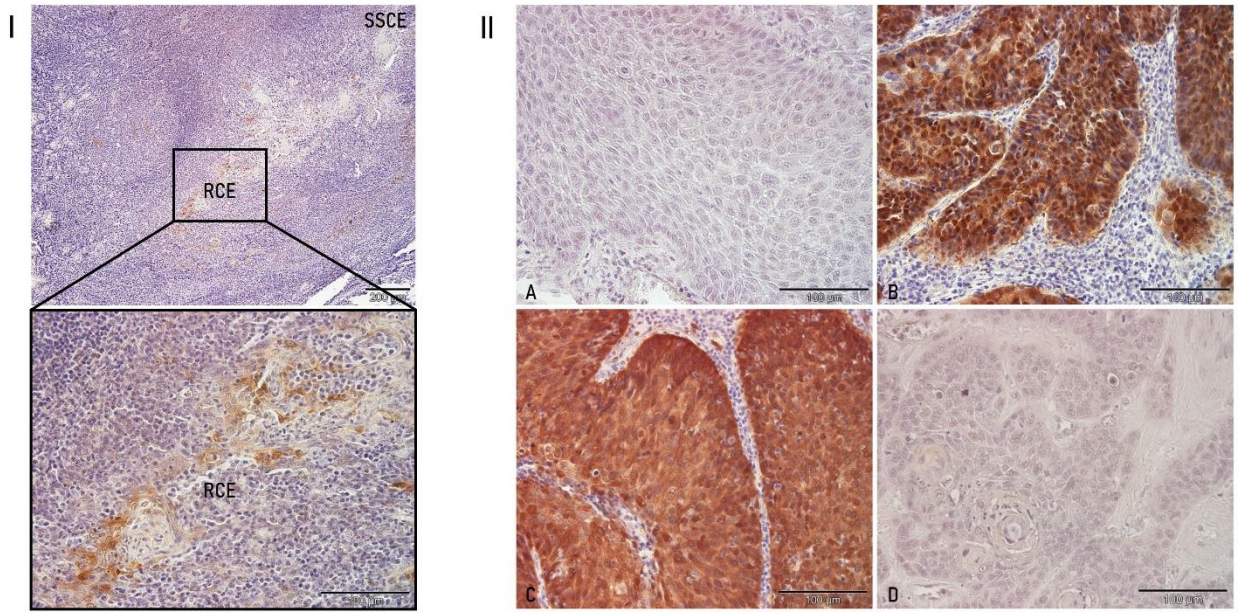

Figure 35. Immunohistochemical analysis of p16 expression. Paraffin-embedded tissue sections were immunostained for p16, counterstained with hematoxylin, and visualized by a light microscope. Representative images: (I) Positive p16 immunoreactivity was detected in the reticulated crypt epithelium (RCE), but not in the superficial squamous cell epithelium (SSCE). (II) A. No p16 immunoreactivity was detected in the majority of HPV-negative OPSCCs. B. p16 immunoreactivity was observed in a few HPV-negative OPSCCs. C. p16 immunoreactivity was detected in the majority of HPV16-positive OPSCCs. D. No p16 immunoreactivity was observed in a few HPV16-positive OPSCCs. Scale bars = 200 μm and 100 μm (I); 100 μm (IIA–D).

4.7.3 DLG1 and SCRIB protein expression in healthy tonsillar tissue samples

The patterns of DLG1 and SCRIB distribution were examined in healthy control tissue prior to investigating any potential differences that may contribute to malignant progression in the oropharynx. DLG1 and SCRIB protein expression was observed in all 8 samples of the healthy tonsillar tissue samples. As seen, both DLG1 and SCRIB were expressed mostly in the intermediate layer of stratified squamous epithelia (**Figure 36.**). Intriguingly, they were almost completely absent in the basal and superficial layers. When considering localization, both DLG1 and SCRIB were predominantly expressed in the cytoplasm of cells in the upper parts of the intermediate layer. These protein expression patterns were similar in all the healthy control tissue samples.

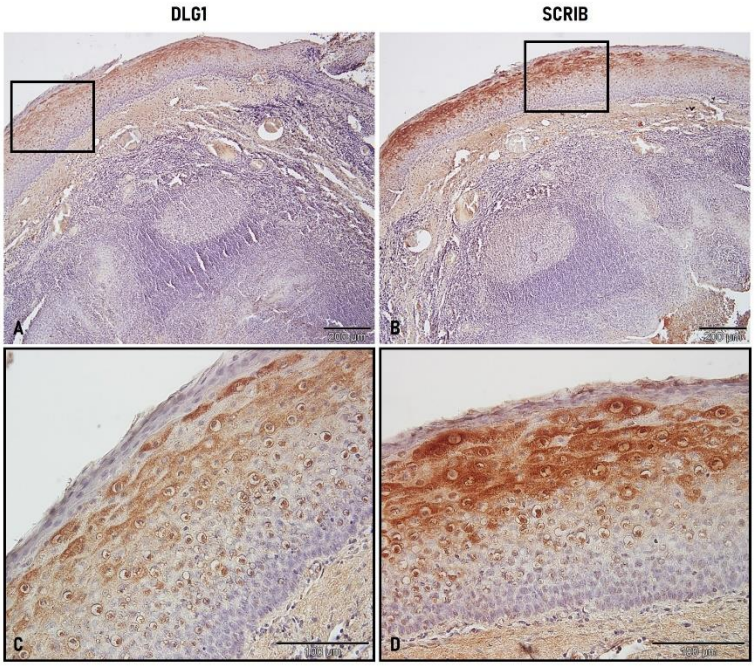

Figure 36. DLG1 and SCRIB expression patterns in cancer-free healthy tonsillar tissues. Paraffin-embedded biopsies were immunostained with anti-SAP97 (DLG1, 2D11) and anti-SCRIB (C-6) antibodies, counter stained with hematoxylin, and visualized by a light microscope. Representative images: (A) Positive cytoplasmic and membranous DLG1 immunoreactivity in squamous cell epithelium. (B) Positive cytoplasmic and membranous SCRIB immunoreactivity in squamous cell epithelium. (C, D) Enlargements of (A) and (B), respectively. Scale bars = 200 µm (A, B); 100 µm (C, D).

4.7.4 DLG1 and SCRIB expression patterns in HPV-negative OPSCCs

Initially, DLG1 and SCRIB protein patterns were studied in HPV-negative OPSCCs to investigate whether their localization and expression change during the malignant progression. From the collected samples, three groups were defined by pathologists; G1 represented well differentiated (7/36), G2 moderately differentiated (10/36), and G3 poorly differentiated or undifferentiated (19/36) HPV-negative OPSCCs. Representative images of each group are shown (**Figure 37.**). As indicated, DLG1 protein was detected with mostly low to middle intensity. Moreover, DLG1 was equally localized in the cytoplasm and at cell–cell contacts of well differentiated OPSCCs. This pattern was observed in all analyzed samples. In moderately differentiated HPV–negative OPSCCs, DLG1 was absent in 2/10 or 20% of the OPSCCs and was expressed at a low intensity in one sample. The remaining samples demonstrated mostly a medium intensity (5/10) of DLG1-positive staining. However high intensity staining, as observed in healthy tonsils, was detected in only 2/10 samples. Similarly, DLG1 protein was evenly localized in the cytoplasm and at cell–cell contacts. Most of the HPV-negative OPSCCs were classified as poorly differentiated. In only one G3 sample DLG1 was completely absent, while the vast majority showed either a low or medium

DLG1 expression signal. In most of these samples, DLG1 was localized mainly in the cytoplasm, but was also detected at cell–cell contacts. Taken together, only marginal changes in the levels of DLG1 expression were seen in all three groups of HPV-negative OPSCCs when compared to cancer-free healthy tonsillar tissues. Still, the observed increase in relocation of DLG1 could potentially lead to the disruption of its function. Although, DLG1 was observed in most of the samples, its localization was changed, so it is speculated that this could potentially be caused by modifications of DLG1 at the post-transcriptional and/or post-translational levels, rather than being caused by genomic mutations in this set of tumors. Next, SCRIB protein expression changes were monitored during the progression of HPV-negative OPSCCs. In well differentiated OPSCCs, most samples showed low to middle intensity of SCRIB staining, similar to what was observed in the healthy tonsillar tissue. In those, SCRIB was predominantly localized in the cytoplasm of cancer cells. However, both cytoplasmic and membranous staining was observed in only one sample. Interestingly, in moderately-differentiated OPSCCs, SCRIB was completely absent from 9/19, while an additional 9/19 samples showed low intensity SCRIB staining. But, in one sample a medium intensity SCRIB staining in a small proportion of cancerous cells was detected. In samples in which positive SCRIB staining was observed, SCRIB was predominantly localized in the cytoplasm, although membranous staining was noticeable in two samples. In the highest-grade tumors, the poorly differentiated samples, SCRIB was not detected in 2/10 samples. A further 4/10 samples showed only a low intensity SCRIB staining and 3/10 showed a medium intensity staining. Interestingly, in only one sample SCRIB staining was comparable to that noted in healthy tissue. As before, when detected, SCRIB protein was mostly localized in the cytoplasm, apart from one sample where both cytoplasmic and membranous staining were detected. These results suggest that loss of SCRIB protein increases with the progression of HPV-negative OPSCCs.

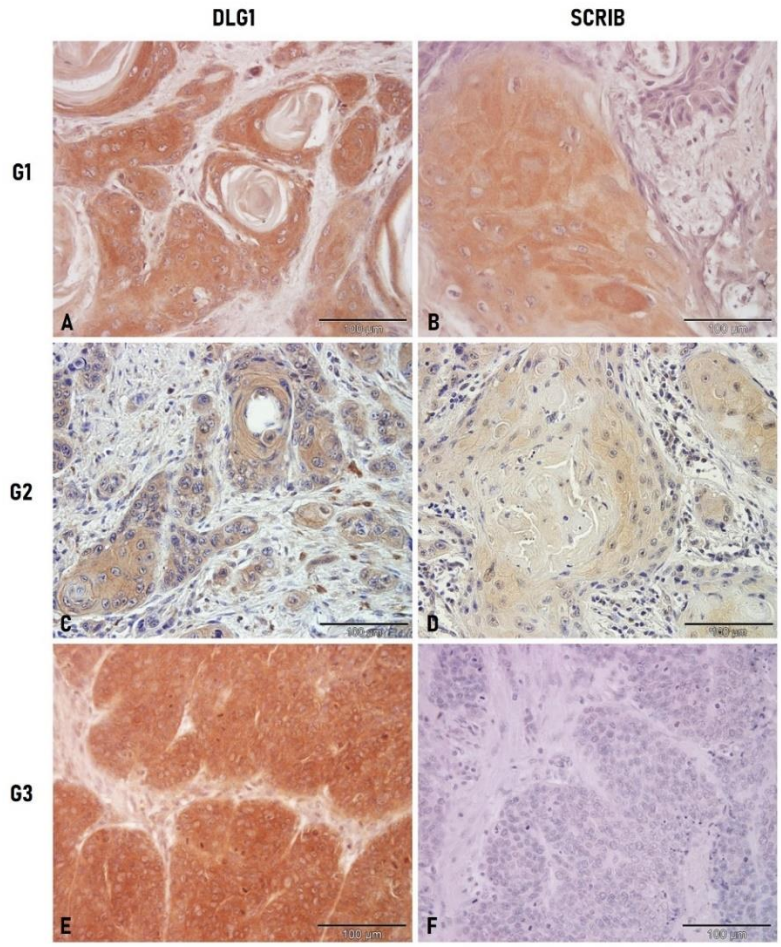

Figure 37. DLG1 and SCRIB expression levels in HPV-negative OPSCCs of various grades. Prior to investigating DLG1 and SCRIB patterns, HPV-negative OPSCCs were graded and classified into three groups by pathologist; G1, well differentiated; G2, moderately differentiated; G3, poorly differentiated or undifferentiated. Paraffin-embedded biopsies were immunostained with anti-SAP97 (DLG1, 2D11) and anti-SCRIB (C-6) antibodies, counterstained with hematoxylin, and visualized by a light microscope. Representative images are shown: G1. (A) Positive cytoplasmic and membrane DLG1 immunoreactivity. (B) Positive cytoplasmic SCRIB immunoreactivity. G2. (C) Positive cytoplasmic and membrane DLG1 immunoreactivity. (D) Positive cytoplasmic SCRIB immunoreactivity. G3. (E) Positive DLG1 immunoreactivity. (F) Negative SCRIB immunoreactivity. Scale bars = 100 μm.

4.7.5 DLG1 and SCRIB expression patterns in HPV16-positive OPSCCs

Potential changes in the protein expression patterns and cellular localization of DLG1 and SCRIB were analyzed in HPV16-positive OPSCCs to investigate 16E6 impact on these two substrates in actual cancer cases. Representative images of the analyses are shown (**Figure 38**.). According to the obtained results, DLG1 was absent in only 3/21 samples, which is consistent with the previously reported preference of HPV16 E6 targeting of SCRIB over DLG1 (Thomas et al., 2005). Of the remaining 18/21 samples that stained positive for DLG1, 8/21 showed low-intensity cytoplasmic staining. Interestingly, in total 9/21 samples showed medium intensity staining, similar to that observed in healthy tonsillar tissue, while only 1/21 sample showed high intensity staining in the

majority of cancer cells. In these HPV16-positive OPSCCs, DLG1 was predominantly localized in the cytoplasm (13/21), while 5/21 showed both cytoplasmic and membrane DLG1 positivity, similar to the pattern observed in the healthy tonsillar tissue. These results suggest that the presence of HPV16 did not have an impact on DLG1 protein turnover. Next, the pattern of SCRIB protein expression and localization was evaluated in the same samples. According to the observations, SCRIB was completely absent in the majority of samples (17/21). This did not come as a surprise since HPV16 E6 mediates proteasomal degradation of SCRIB, which is increased in more malignant stages of the disease (Nakagawa and Huibregtse, 2000). Of the remaining four samples, in 3/21, a low-intensity SCRIB staining was detected, and only 1/21 showed a higher intensity staining in a small proportion of all cancer cells. More interestingly, in those samples where SCRIB was still detectable, it was localized entirely in the cytoplasm of cancer cells, suggesting that relocation of SCRIB from cell–cell contacts may contribute to cell transformation in these cancers.

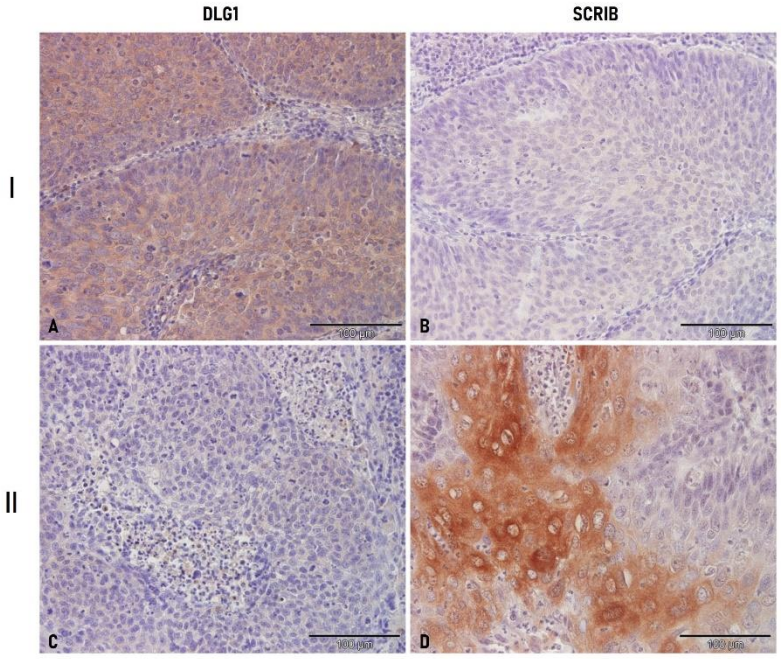

Figure 38. DLG1 and SCRIB expression levels in HPV16-positive OPSCC. Paraffin-embedded biopsies were immunostained with anti-SAP97 (DLG1, 2D11) and anti-SCRIB (C-6) antibodies, counterstained with hematoxylin, and visualized by a light microscope. Representative images: I. Pattern observed in most samples: (A) positive cytoplasmic DLG1 immunoreactivity; (B) negative SCRIB immunoreactivity. II. Conflicting pattern observed in several samples: (C) negative DLG1 immunoreactivity; (D) positive SCRIB immunoreactivity. Scale bars = 100 μm.

The statistical analysis showed a reduction in SCRIB levels, which was concurrent with the progression of HPV-negative malignancies (**Figure 39.**). More interestingly, this was much more evident in the presence of HPV16 E6. Although, a relatively small sample size was studied, the

change in SCRIB expression levels in HPV16-positive OPSCCs compared to either well-differentiated (G1) or moderately differentiated (G2) HPV-negative OPSCCs was significant (p = 0.0003). However, this was not observed with DLG1; DLG1 expression levels in HPV16-positive OPSCCs seemed to change significantly (p = 0.0214) only when compared to poorly differentiated (G3) HPV-negative group. Taken together, these results suggests that fluctuations in DLG1 protein levels are not likely to contribute to disease progression in the same way as SCRIB.

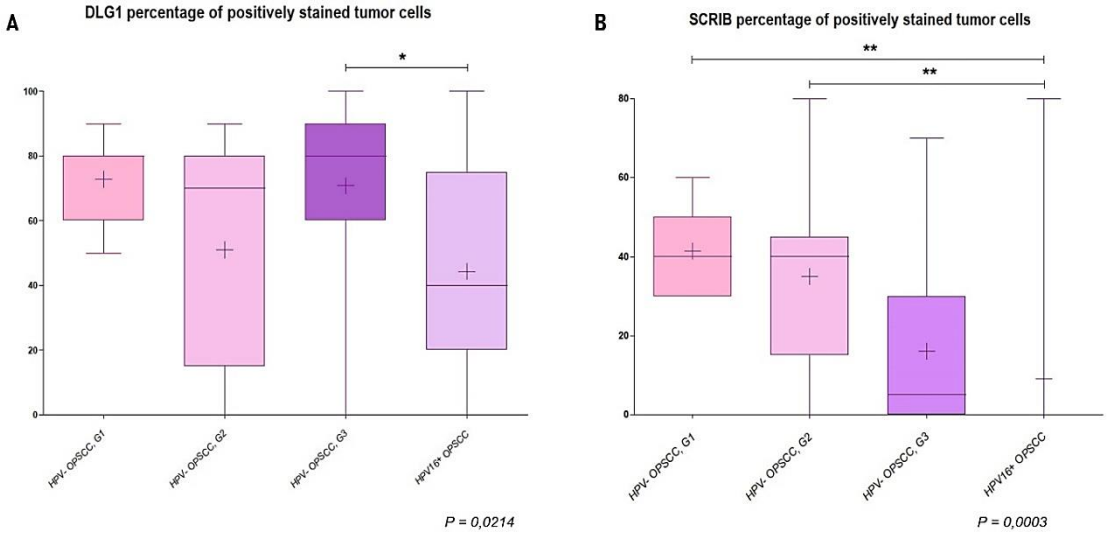

Figure 39. The ratio of DLG1 and SCRIB-positive staining in HPV-negative OPSCCs of various grades and in HPV16-positive OPSCCs. The score of DLG1 (I)- and SCRIB (II)-positive staining observed by pathologists was evaluated between HPV16-positive and HPV-negative OPSCCs grades 1–3. Significance was determined using the Kruskal–Wallis test with Dunn's multiple comparison posttest with: I. p-value (*) 0.0214, II. p-value (**) 0.0003.

Changes in protein localization for DLG1 and SCRIB were then compared between the different groups. According to the data presented (**Figure 40.**), DLG1 localization changed with the progression of HPV-negative OPSCCs. Interestingly, this was even more noticeable in the presence of HPV16 E6. In contrast, the change in localization was not apparent in the case of SCRIB protein. All things considered, these results suggest differences in the modulation of these two proteins during malignant progression, regardless of HPV16 presence.

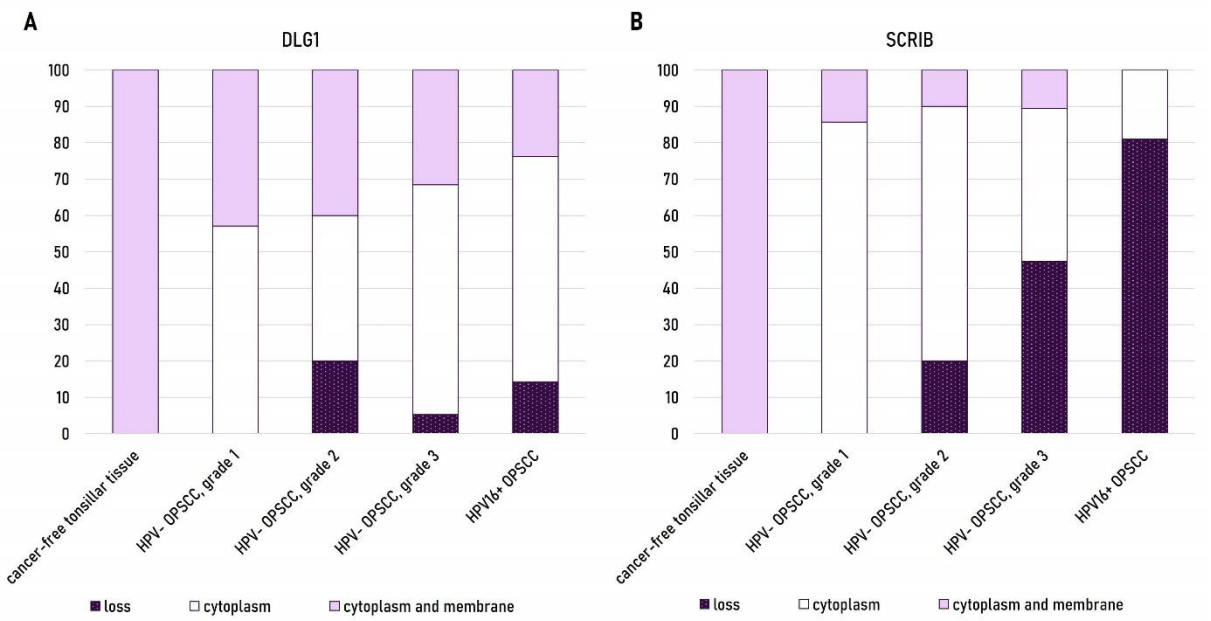

Figure 40. Changes in expression and localization of DLG1 and SCRIB proteins in HPV16-positive OPSCCs and in HPV-negative OPSCCs of various grades. Dark purple doted bars show the percentage of FFPE samples with a complete loss of antigen. White bars represent the percentage of samples with only cytoplasmic localization of antigen. Light violet bars represent the percentage of samples with both cytoplasmic and membranous localization of antigen.

5 DISCUSSION

Almost 50 years have passed since the first attempt of finding HPV DNA in cervical cancer began (Hausen et al., 1974; Zur Hausen, 1976). Shortly afterwards, this was confirmed by the isolation of HPV16 DNA, the first cervical-cancer-linked HPV type (Dürst et al., 1983). All of this has created a basis for decades of research on genital HPVs, which led to the discovery of multiple viral types. To date, nearly 200 HPV genomes have been sequenced and sorted into 5 genera, one third of which are referred to as *Alphapapillomavirus* species that preferentially infect anogenital and oral mucosal epithelia (Bernard et al., 2010). After IARC classification, it has become widely accepted that a total of 15 HR HPV types (HPV 16, 18, 31, 33, 35, 39, 45, 51, 52, 53, 56, 58, 59, 66 and 68) are causative agents of practically all cervical cancer cases (IARC, 2007). Interestingly, almost simultaneously, HPV-caused lesions were also detected beyond the typical HPV infection site (Gissmann et al., 1982; Syrjänen et al., 1983) by numerous follow up studies, which showed that anal, vulvar, and penile cancers can all be caused by HPVs. In addition, more recent studies have also recognized HPV infection as a causative agent of HNC at several different locations at this anatomical site (Elrefaey et al., 2014; IARC, 2007). The vast majority of HNCs arise from squamous epithelial cells lining the oral cavity, pharynx, larynx, or, more rarely, the nasal cavity and are referred to as HNSCCs (Cramer et al., 2019). Risk factors such as alcohol consumption, smoking, and/or chewing of tobacco increase the risk for HNSCC, but HPVs also significantly contribute to these cancers accounting for 30-65% of all HNCs and 50-80% of OPSCCs (Blitzer et al., 2014). The HPV prevalence to infect the oropharynx compared to other HN sites is yet unresolved, but may be linked to the presence of transitional mucosa in the tonsillar tissue which shows histological similarities to the cervical mucosa (Elrefaey et al., 2014). Over the past 30 years, numerous studies have characterized HPV-induced OPSCCs to be epidemiologically, clinically, anatomically, and biologically distinct disease from HPV-negative OPSCCs. Although rising in prevalence when compared to HPV-negative OPSCCs, HPV-positive OPSCCs have a favorable prognosis when treated with chemotherapy, radiation, surgery, or chemoradiotherapy possibly due to their remarkable treatment sensitivity (Sabatini and Chiocca, 2020). Additionally, the incidence of distant metastases seems to be lower in patients with HPV-related OPSCC compared to HPV-negative OPSCC cancers, again contributing to better overall prognosis (Rahimi, 2020). However, prediction of the disease development, early detection of primary cancers, and prevention of the disease progression are still needed for survival rates to improve. Nowadays, approximately 4.5%

cancers worldwide are attributable to HPVs, with HPV16 being consistently the most frequent type (de Martel et al., 2017; McBride, 2022). Although being the most common sexually transmitted viral infection, in most cases, T cells from the cell-mediated immune response infiltrate lesions and clear them rapidly and spontaneously, leaving no long-term effects. Otherwise, HPV infections become chronic, and infected individuals are at an increased risk for cancer development (zur Hausen, 2002). This process from the primary infection to cancer development is well defined in the cervix. The oncogenic capacity of HR HPVs relies on synergy of both viral oncoproteins, E6 and E7, which inactivate multiple cellular targets and pathways including tumor suppressors, p53 and pRb, respectively. E7 binds to pRb and disrupts its attachment to the E2F transcription factors causing E2F release (Huh et al., 2007). Ultimately, free and active E2F promotes the transcription of a group of genes that encode proteins essential for cell cycle progression (Müller et al., 2001). Additionally, E6 disrupts p53 signaling, which is required for cell growth inhibition, senescence, and apoptosis (Huibregtse et al., 1991; Lechner et al., 1992). Inactivation of these two tumor suppressor by the viral oncoproteins leads to a genomic instability and malignant progression (Doorbar et al., 2012; Klingelhutz and Roman, 2012). In addition to provoking p53 degradation, numerous studies have indicated that E6 has many other cellular targets including proteins which contain PDZ domains, ubiquitous protein interaction modules involved in organizing and maintaining scaffolding complexes (Mittal and Banks, 2017). Some of the best characterized E6 interactors which contain PDZ domains are proteins from the Scribble polarity complex: SCRIB and DLG1, and E6 has been proven to promote degradation of these proteins by the UPS (Nakagawa and Huibregtse, 2000; Pim et al., 2000). Since SCRIB and DLG1 play roles in establishing and maintaining cell polarity, cells which express E6 form weaker cellular contacts and grow in a more disorganized manner (Pim et al., 2000). Consequently, by inactivating them, E6 contributes to the development of later stages of HPV-induced malignancies in anogenital area (Cavatorta et al., 2017; Lin et al., 2004). Interestingly, the same process from the initial infection to cancer development in HN area is still poorly understood. However, it seems to be much brisker than in cervix where it generally takes 12–15 years for a persistent infection to result in the development of carcinoma (Snijders et al., 2006). Besides the process being shorter in HN, the prevalence of HPV type specificity somewhat varies. It is reported that approximately 70% of cervical cancers and precancerous cervical lesions are caused by two types, HPV16 and HPV18 (Thomas et al., 2008). Intriguingly, HPV16 seems to be the predominant viral type associated with

OPSCC development, accounting for 90-95% of all cases (Elrefaey et al., 2014; Kreimer, 2005). These variations in HPV prevalence and high mortality rates of OPSCCs patients in general, point to the need for other more specific prognostic biomarkers that could be more accurate in predicting the development of the disease in early stages at atypical infection sites. So far, p16 overexpression is used as a surrogate marker for HPV infection in HNSCCs. However, it is not exclusive, since approximately 10% of HPV-negative HNCs show p16 overexpression and *vice versa* (Seiwert, 2021). Therefore, the aims of this research were to better understand the process of HPV-driven oncogenesis in HN area, to detect potential similarities and/or differences in 16E6 impact on DLG1 and SCRIB, which perturbations are likely to be important for the onset of malignancy at this anatomical region.

5.1 Establishment of HPV16 E6/E7-expressing immortalized keratinocytes

In this research, DLG1 and SCRIB localization and expression patterns in the presence and absence of 16E6 were investigated in monolayer cultures of keratinocytes isolated from various anatomical sites, in organotypic 3D raft cultures and finally in FFPE OPSCC samples. To do this, firstly, cell lines that stably express HPV16 E6/E7 oncoproteins were established. Three previously immortalized keratinocyte cell lines were used: iNOK, iHTK and iHFK. The initial attempt in achieving stable expression of individual E6 and E7 oncoproteins was performed by CRISPR Cas9 Knock-in method. In particular, the AAVS1 transgene knock-in transfection system which generates double strand DNA brakes at AAVS1 locus was applied. This locus allows stable, long-term transgene expression in many cell types. Moreover, its disruption is not associated with any known disease, so it is often considered as a safe-harbor for transgene targeting (Oceguera-Yanez et al., 2016). After successful construction of the donor plasmid pAAVS1-BSD-DNR containing E6 or E7 oncogenes, the transfection conditions were optimized by applying various kinds of transfection reagents. This step was performed since keratinocytes are generally quite hard to transfect. To further obtain homogenous E6 or E7-expressing cell lines, single-cell colony isolation in 96-well plates was conducted. To verify that the transfected lines were expressing HPV oncoproteins, cellular proteins were isolated, separated on SDS-PAGE and analyzed by Western blotting. FLAG or HA antibodies were used to detect tags fused to E6 or E7 oncoproteins, however, there was no positive signal detected. Given that all the previous steps have been confirmed to be successful and that the cells survived the antibiotic selection, it is likely that the problem with the integration of transgenes may have occurred. It is estimated that only about 10% of adeno-

associated viral (AAV) vectors integrate into the host cell genome, while the majority of vector plasmids persist in an episomal and non-integrated forms (Smith, 2008). Thus, the transfected cells could have survived the antibiotic selection even if the transgenes were not integrated. On the other hand, even if the integration of the HPV oncogenes was an effective one, it is likely that a very small number of the insert DNA became integrated. However, theoretically, only one integrant should be sufficient for expressing high levels of E6/E7 thus this effect was more likely to be due to epigenetic changes under the challenge for cell survival (Van Tine et al., 2004). Apparently, CpG methylation modifications may affect HPV productive cycle, but this is not yet mechanistically understood. It has been observed that episomal form of HPV DNA in premalignant biopsies is unmethylated indicating that methylation may occur after HPV integration into the host DNA leading to reduction of viral transcription (Burley et al., 2020). Also, there was a possibility that the viral DNAs became transcriptionally inactive due to a type of integration. There are two types of HPV integration processes which occur in natural HPV infections. In type 1, a single genome is integrated into cellular DNA while in type 2, multiple tandem head-to-tail repeats have been found at a single locus (Jeon et al., 1995). In those, it is reported that usually only the 3'-junctional copy of the viral genome is transcriptionally active (McBride, 2017). Hence, if type 2 integration has occurred due to targeting of the specific AAVS1 locus, most of the integrated viral DNA copies would be transcriptionally inactive. Moreover, high-throughput viral integration detection (HIVID) method identified so-called hotspots for HPV integration in specific human genes of which many encode proteins in cancer-associated pathways. This suggested that HPV is integrated within the genome initially at random and that the integration occurs at some loci which provides a selective advantage to host cells. However, there is no evidence of showing the AAVS1 locus being one of the hot spots (Hu et al., 2015). After trying several times and obtaining unsuccessful results, the approach was changed. Knowing that close to 100% infection efficiency of keratinocytes can be achieved by retroviral vectors (Garlick et al., 1991), lentiviruses encoding HPV16 E6 oncogene were produced. Construction of the donor vector containing HPV16 oncogene begun with E6 amplification from pcDNA3.1 16E6 template, followed by the insert ligation into pUltra-GFP vector. To validate the cloning efficiency, a double validation was performed, including PCR amplification and sequencing. After the confirmation, lentiviruses encoding 16E6 oncogene were produced in HEK293T cells. Prior to transduction of iNOK, iHFK and iHTK cells, it was necessary to determine the viral titer by using various amounts of lentiviral

particles on iNOK cells. Surprisingly, none of the lentiviral particle concentrations which was used resulted in cells emitting green 16E6-GFP signal. Although the sequencing confirmed the successful cloning it is possible that transcription or translation did not occur. Therefore, to verify this, HEK293 cells were transfected with only pUltra-GFP-16E6, and positive fluorescent signal was observed meaning that the transcription and translation processes were functional. Although the plasmid construction was successful, it seemed that the production of viral particles was ineffective. This might have occurred because HEK293T cells used for lentiviral production were grown in DMEM supplemented with 10% FBS, since the presence of heat-labile complement proteins and immunoglobulin G apparently inhibits viral production (Powers and Trobridge, 2013). Moreover, for some transgenes, transfection optimization simply is not enough to get a sufficient titer due to inefficient packaging of larger inserts (Kumar et al., 2001). Finally, keratinocyte cell lines expressing E6/E7 were established by transfections with HPV16 genomes, which was shown to be a reliable method. Since the plasmid containing HPV16 genome does not contain any selective markers, to easily select transfected cells, cells were co-transfected with HPV16 genomes and a plasmid carrying blasticidin resistance gene. Cells were passaged for at least 15 passages for viral DNA integration to occur. This approach yielded cell lines which were then used for further investigation of 16E6 effects on DLG1 and SCRIB at various anatomical sites.

5.2 HPV16 E6 exhibits distinct effects on DLG1 and SCRIB endogenous expression

Several proteomic analyses have demonstrated that E6 oncoproteins of different HPV types have distinct binding affinities for PDZ domain-containing proteins, including DLG1 and SCRIB (Vats et al., 2021; Vincentelli et al., 2015). Indeed, HPV16 E6 more efficiently interacts with SCRIB protein, while DLG1 is strongly bound by HPV18 E6 (Gardiol et al., 1999; Pim et al., 2000; Thomas et al., 2005). As demonstrated, binding affinities depend upon the precise amino acid sequence of the E6 PBMs. HPV16 is the only oncogenic HPV type having E6 PBM Leucine at the first amino acid position, rather than Valine, which was demonstrated to increase the preference for binding SCRIB (Thomas et al., 2005). Moreover, the preference of 16E6 for SCRIB may be also due to the fact that E6 is able to bind to any or even all of the PDZ domains of SCRIB protein (Nakagawa and Huibregtse, 2000). However, no studies have yet indicated whether the binding preference changes depending on the anatomical area. To assess this, GST-pull down assays were performed, and they displayed that E6 binding preferences did not change towards DLG1 and SCRIB depending on the anatomical area. Although, iNOK and iHTK are cell lines both derived

from HN area, SCRIB interaction with 16E6 was not detected in iHTK possibly due to low SCRIB expression levels or lower intensity interaction between these two proteins at this specific anatomical site. This has further risen a question whether 16E6 potentially exhibits different effects on DLG1 and SCRIB endogenous protein expression levels and this was examined in three established keratinocyte cell lines stably expressing HPV16 E6/E7 using Western Blot analysis. According to the obtained data, 16E6 presence had only marginal effects on DLG1 protein levels, since it was vaguely upregulated in iHFK-16E6/E7 cells, whilst it remained unaffected regardless of 16E6 presence in iNOK and iHTK. This was surprising since numerous studies have shown E6-mediated DLG1 degradation and thus its downregulation. However, those studies were conducted on *in vitro* translated E6 and/or DLG1 or even under the conditions of overexpression. Also, in those analyses, HPV18 E6 effects on DLG1 were examined (Gardiol et al., 1999; Kühne et al., 2000; Pim et al., 2000). Here, effects of 16E6 on endogenous DLG1 protein levels were investigated and, so far, there are hardly any reports which investigated 16E6 impact on DLG1 in this experimental setting. However, in a study set under similar conditions, comparable observations were made - in primary immortalized HFK infected with retroviruses containing HPV16 E6/E7 did not result in reduced levels of endogenous DLG1 (Choi et al., 2013). If considering the established iHFK-16E6/E7 cell line as a model of genital higher-grade premalignant lesions in which integration has occurred, our study suggests that DLG1 is upregulated as a cellular defense mechanism, while a reduction is observed in CaSki, HPV16-positive cervical cancer cell line. This is in a correlation with a study showing that DLG1 was overexpressed in intraepithelial cervical, vulvar, and laryngeal HPV-associated lesions, while a marked level of reduction was observed in HPV-positive invasive cervical carcinomas (Cavatorta et al., 2004; Watson, 2002).

In contrast to DLG1, results of this doctoral thesis showed upregulation of SCRIB in all three keratinocyte cell lines at the protein level in the presence of HPV16 E6. This conflicts with previous studies showing that 16E6 binds and targets SCRIB for a proteasome-mediated degradation (Nakagawa and Huibregtse, 2000; Thomas et al., 2005). However, studies showing clear SCRIB degradation were conducted under the conditions of ectopic expression. Since endogenously expressed SCRIB is a membranous protein which interacts with various cellular proteins, those interactions may have a protective role, i.e., change in its confirmation which could potentially inhibit E6-mediated degradation. Also, there might be an insufficient amount of endogenously

expressed E6 in these cell lines, which is inadequate to degrade SCRIB, its primary PDZ-domain containing substrate, but not the general target. This lower cellular quantity of E6 most likely targets primarily p53 rather than SCRIB or other cellular interactors. Likewise, with both being overexpressed, SCRIB could potentially be expressed in a different cellular compartment, in the cytoplasm, where protein turnover at proteasomes occurs, and thus be more accessible to be targeted by E6 for a proteasome-mediated degradation. Also, endogenously and exogenously expressed SCRIB proteins may undergo different posttranslational and posttranscriptional modifications that affect their solubility and therefore this might make some of these SCRIB forms more accessible to E6, which is also likely to lead to its degradation. Indeed, in a study on cancer-derived cells, different cellular pools of SCRIB were investigated showing that the majority of soluble SCRIB protein was degraded by the proteasome (Massimi et al., 2004). Up to date, a very few studies reported an upregulation of endogenous SCRIB protein. One study was conducted to determine whether SCRIB protein levels were altered due to increased E6/E7 expression. They used clonal cells from a human CINs harboring the HPV16 genome either in episomal (W12E) or integrated form (W12I), CaSki and C33A cells. As reported, Western blot analyses indicated that SCRIB was somewhat decreased in W12I and CaSki when compared to W12E. Since this decrease was not observed in C33A cells, they suggested that diminished SCRIB could be dependent on E6 expression. They performed additional Western blots to compare the level of SCRIB in the soluble and insoluble fractions of NIKS and NIKS harboring the HPV16 genome and showed that SCRIB levels might be upregulated in the presence of HPV16 (Simonson et al., 2005). Therefore, HPV16 is also likely to be causing upregulation of endogenous SCRIB to stabilize itself. Interestingly, the presence of SCRIB was previously reported to be required for maintaining high levels of E6 protein (Kranjec et al., 2016). However, this was shown only in HeLa, HPV18-driven cancer cells, whilst the same has not been investigated for HPV16 type. The observed SCRIB upregulation is also in a correlation with a study showing that SCRIB was overexpressed in atypical dysplastic glands of the polyp and its levels decrease with the disease progression (Gardiol et al., 2006). In addition, to possibly stabilizing E6 protein levels in three keratinocyte cell lines, SCRIB might also play a role as an oncogene. This was previously shown in a transgenic mouse model for mammary carcinoma, where loss of SCRIB in conjunction with oncogenic activation of c-myc significantly enhanced the size of tumors compared with activating c-myc alone (Zhan et al., 2008). All things considered, the difference in the binding fondness between 16E6 and DLG1 as well as 16E6 and SCRIB reflected

on the patterns of their expression. A stronger effect of 16E6 was observed on SCRIB than on DLG1 expression regardless of the anatomical sites, which all points to the importance of E6/SCRIB interaction in the process of HPV16-mediated oncogenesis.

5.3 DLG1 and SCRIB are delocalized in the presence of HPV16 E6

Both DLG1 and SCRIB were previously characterized as tumor suppressors and cell polarity regulators; DLG1 is essential for the regulation of polarity and cellular growth in response to cell–cell contact (Pim et al., 2012), whilst SCRIB is required for maintenance of an epithelial phenotype at low cell densities (Nakagawa and Huibregtse, 2000). Consequently, even a minor shifts in localization of these proteins can impact the loss of cell polarity and therefore contribute to cancer progression and consequent cell invasiveness, which is observed during metastasis (Snijders et al., 2006). Moreover, mislocalization of cell polarity regulators is considered as a hallmark of cancer, since it can drive cancer development and metastasis (Wang and Li, 2014). Hence, we sought to investigate DLG1 and SCRIB localization in the presence and absence of HPV16 E6 in iNOK, iHTK and iHFK cell lines using IF confocal microscopy and fractionation assays. According to the IF results, the presence of 16E6 had a negligible impact on DLG localization in iNOK cells, while slight deregulation of cytoplasmic DLG1 was observed in iHTK-16E6/E7 cells. Intriguingly, 16E6 instigated complete delocalization of membranous DLG1 into the cytoplasm in iHFK cells. These results further confirmed observations from the experiments in which endogenous DLG1 protein expression was monitored and proposed that 16E6 has a greater effect on DLG1 protein levels in cells isolated from genital than from HN area. Furthermore, iHFK-16E6/E7 cells are likely to mimic some of the events which occur in premalignant lesions of the anogenital area. Although viral DNA integration is present, the degree of cell transformation is not the same as in cells isolated from late stages of HPV cancers. Still, these results are in agreement with the study showing diminished membranous DLG1, while the cytoplasmic levels have significantly increased in high-grade cervical neoplasia (Watson, 2002). Interestingly, fractionation assays did not show any differences in DLG1 distribution in iHFK in the presence of 16E6. However, it should be taken into consideration that the fractionation kit does not have the ability to separate the nuclear and cytoplasmic membrane into individual fractions. Likewise, this divergence of IF and fractionation results may also be due to partly non-specific IF staining which might have occurred.

Next, strong binding affinity of 16E6 towards SCRIB was correlated with changes in its cellular localization and distribution in the same cell lines. Firstly, SCRIB localization was investigated in iNOK cells, in which SCRIB was detected in the membranes and cytoplasm, whilst the minority was visible in the nuclei as well. As observed, 16E6 caused the shift of SCRIB protein with the majority being detected in the cytoplasm and this was corroborated with the fractionation assays. SCRIB delocalization was observed in iHTK-16E6/E7 in comparison to the control iHTK cells as well. Surprisingly, although in this specific anatomical cell origin background, the change in localization seems to be reversed, SCRIB was delocalized from the perinuclear space to the cellular membranes and, interestingly this was in collaboration with results of the fractionation assays. Finally, SCRIB was nicely detected in or just under the membranes of iHFK cells, yet some cytoplasmic and nuclear staining were visible as well. However, exclusively cytoplasmic staining was detected only in the presence of HPV16 E6. This contrasts with fractionation assays, which showed a preserved cytoplasmic localization independent of 16E6 presence, suggesting that some IF signal might have been produced due to the non-specific staining. Additionally, no markers could have been used in this study for co-localization assays with either SCRIB or DLG1 due to the cross-reactivity and origin limitation, so potentially visible membranous staining may represent the accumulation right beneath the cell membrane. Regardless of what was mentioned above, importantly, HPV16 E6 impacted SCRIB localization in all immortalized cell lines, which are likely to resemble some of the phenotype characteristic for HPV-caused neoplasias as well as in CaSki cells derived from a cervical cancer patient. These observations are in agreement with a study showing that modulated SCRIB was associated with the clinical stage, histopathological differentiation, and lymph node metastasis in the development of endometrial cancer (Ouyang et al., 2009). All this once again alludes on a stronger effect of 16E6 on SCRIB, causing changes in its cellular localization and distribution, which likely impacts its normal functions, and in this way contributes to malignant cellular transformation.

5.4 DLG1 and SCRIB transcript levels correlate with E6 transcript abundance

Most studies which investigated E6 impact on DLG1 and SCRIB were conducted at the protein level and reported their altered expression and localization. However, only a few of them have investigated and reported changes in the levels of transcription of PDZ-domain containing proteins (Dizanzo et al., 2020; Lazić et al., 2012). Therefore, a series of studies were conducted in primary HFK and HTK cells which contained HPV16 episomes to evaluate if the transcription level of E6

increases with the number of passages, and how this might affect the transcription levels of DLG1 and SCRIB. Interestingly, E6 mRNA levels increased proportionally with the higher number of passages in HTK. This might be because the number of viral genomes increases with the cultivation time, so longer-passaged cells contained higher amounts of viral genomes, which over all consequently resulted in increased mRNA levels. Likewise, although these cells were grown on irradiated 3T3-J2 feeder cells, to keep HPV16 in the episomal form as long as possible, a small proportion of them might have still integrated, consequently leading to uncontrolled and increased transcription of E6/E7 oncogenes. Remarkably, although harvested at p5, HFK cells containing HPV16 episomes have shown higher transcription levels, when compared to HTK implying that the viral genome is more transcriptionally active in HFK than in HTK. This is in a correlation with the results showing that greater percentage of the total HPV16 virions grown in tonsillar epithelium become fully mature and stable faster than in foreskin tissue (Israr et al., 2016). Thus, since new virions mature slower in HFK, E6 activities are likely to be more pronounced in these cells. It was further investigated whether in this setting E6 has any effects on DLG1 on the transcriptional level. DLG1 transcript levels were examined using two different primer pairs, one detecting only DLG1β isoform, and the other specific for the HOOK region in DLG1. The two primer sets were used because it was suggested that HPV can manipulate with serine-arginine-rich (SR) proteins involved in multiple stages of mRNA maturation, including the constitutive and alternative splicing (Prescott et al., 2014). According to obtained data, DLG1β isoform levels were slightly lower in HTK cells containing HPV16 episomes and continued to decline with the cultivation time. Conversely, the presence of HPV16 episomes induced higher transcript levels of both DLG1β and DLG1 HOOK in HFK cell line. Since the HOOK region is present in all DLG1 isoforms, these results suggest that 16E6 initiates upregulation of overall DLG1 mRNA levels in cells regardless of the anatomical area. Furthermore, potential changes in SCRIB transcription levels were also assessed due to the 16E6 increased transcription over time. Interestingly, SCRIB transcription levels correlated with E6 mRNA levels regardless of the donor background, which is in the line with the results of the endogenous protein expression analysis. Apart of using SCRIB as a protein stabilizer, E6 may also upregulate SCRIB transcription to prolong the infectivity period and make the environment suitable for optimal completion of productive viral cycle.

The cell lines investigated in this doctoral thesis were artificially established HPV-positive cell lines. They contained episomal forms of HPV16 and in this way were used to mimic early stages

of HPV infections. Therefore, this analysis was expanded to cell lines derived from HPV16-positive, and HPV-negative OPSCCs for comparison of how much the presence of different forms of HPV16 E6 contributes to these differences. In those cells, DLG1β transcripts were higher in both types of OPSCCs compared to the non-transfected HTK, so this effect on DLG1β levels appeared to be HPV16-independent. In contrast, DLG1 HOOK domain transcripts were decreased both in HPV-negative and HPV16-positive OPSCCs. This observation was in correlation with a study demonstrating a downregulation of DLG1 mRNA levels in CaSki and HeLa cells in comparison to C33A and HaCaT, spontaneously immortalized and transformed skin keratinocytes, in which the highest DLG1 mRNA expression rates were demonstrated (Mantovani et al., 2001). Although DLG1 transcription was not downregulated in C33A, HPV-negative cervical cancer cell line in previously mentioned study, downregulation of DLG1 mRNA was observed in other cancers such as non-small cell lung cancer tissue in comparison to normal tissue (Szymanowska-Narloch et al., 2013). Interestingly, SCRIB levels remained unchanged in HPV-negative OPSCC cells when compared to non-transfected HTK control cells, but were increased in HPV16-positive OPSCC, suggesting that E6 modulation of SCRIB mRNA levels is an important aspect of HPV16-driven oncogenesis. However, additional studies are required to elucidate the link between the transcriptional levels of E6 and SCRIB in greater detail.

5.5 DLG1 and SCRIB are differently regulated during HPV16 cycle

It was further investigated if the variations in DLG1 and SCRIB transcript levels in the presence of 16E6 somehow reflect on their protein localization during the productive viral cycle. It is a well-established fact that HPV replication cycle is closely linked to epithelial differentiation (Graham, 2017a). Hence, potential differences in DLG1 and SCRIB distribution during the productive viral cycle, were investigated in HTK organotypic 3D raft culture, an *in vitro* system that faithfully recapitulates epithelial differentiation, so it can be used for studying HPV cycle. In control raft cultures grown without HPV16 episomes, DLG1 was localized preferentially in the cytoplasm of the basal cells, but in the suprabasal layers it was predominantly present in the membranes. However, no cytoplasmic DLG1 was visible in the middle suprabasal layers. This is in correlation with the study showing that both DLG1 and SCRIB expression gradually increased towards the upper colonic crypt areas. As cells divide, they move towards the upper layers of the epithelium, differentiate, and lose their proliferative capacity. Thus, this increase in DLG1 and SCRIB expression levels may suggest their role in epithelial differentiation and in the negative control of

cell proliferation (Gardiol et al., 2006). In rafts grown from low-passage HTK cells containing HPV16 episomes, DLG1 was detected in the cytoplasm and membranes, but it appeared that membranous DLG1 was partially shifted to the cytoplasm in the lower and suprabasal layers where E6/E7 expression was reported to be the highest (Doorbar et al., 2020). In the upper layers of those rafts, membranous DLG1 was preserved likely because in these layers new virions were produced and E6/E7 expression was minimal. This was even more evident in rafts grown from high-passage HTK cells containing HPV16 episomes, again implying that E6-mediated DLG1 manipulation is required for successful viral replication and these changes in DLG1 may be important for the malignant development. These observations support a study which investigated DLG1 expression in HFK organotypic 3D cultures containing HPV18 episomes. The authors showed that DLG1 was localized preferentially in the cytoplasm of the basal cells, but in the suprabasal areas it was predominantly present at cell contacts (Valdano et al., 2016). In control HPV-negative rafts, SCRIB expression was comparable to DLG1 - it was localized in the membranes of cells throughout all the layers with higher intensity observed in the upper layers closer to the cornified epithelium, as previously described in colon (Gardiol et al., 2006). In rafts grown from low-passaged HTK cells containing HPV16 episomes, SCRIB showed higher intensity through the middle layers, which builds well on the results of SCRIB upregulation observed on the protein level in immortalized iHTK-16E6/E7, as well as on the transcript levels increase in the same cells used for growing these rafts. Additionally, in rafts derived from high-passaged HTK cells containing HPV16 episomes, membranous SCRIB was detected in some cells of the upper layer. However, most of SCRIB was evidently mislocalized from the membranes into the cytoplasm. Based on the observed results, HPV16 presence could potentially stimulate the delocalization of SCRIB and DLG1 to expand the infection through the tissue. Likewise, this regulation might also contribute to slowing down the healing of micro ruptures in the epithelium, which is likely to alleviate new viral infection and consequently production of new virions.

5.6 DLG1 and SCRIB are distinctly regulated in OPSCCs independently of 16E6

The previously presented results obtained from the experiments in monolayer cell cultures and organotypic 3D raft cultures can serve as indicators of changes that are likely to precede the onset of cancer development. Therefore, we further sought to verify whether similar changes occur in FFPE OPSCC samples and, if so, whether changes in the expression levels and/or localization of DLG1 and SCRIB are dependent upon HPV status. If so, they could then be used as a potential

marker since, currently, the guidelines for HPV detection in OPSCCs and prediction of the disease development in early stages have not met the golden standard. Even though IHC staining of p16 is widely used as a surrogate marker for diagnosis of HPV positivity in OPSCC, approximately 10% of HPV-negative HNCs show p16 overexpression and *vice versa* (Seiwert, 2021). In combined analysis of PCR genotyping and p16 IHC staining, 14.3% of the total of HPV16-positive samples analyzed were p16-negative. Comparably, 8.3% of HPV-negative samples were, at the same time, p16-positive. Thus, these results corroborated reports showing p16-positivity both in HPV-negative and HPV-positive OPSCCs (Dediol et al., 2016; Inoue and A. Fry, 2018). To have a basis for comparison, DLG1 distribution and expression were first examined in control tonsillar tissue. In those, DLG1 was localized both in the cytoplasm and to the adherent junctions, mostly in the intermediate layer of the stratified squamous epithelium but was absent from the basal and superficial layers. This distribution pattern corroborated with one observed in 3D raft cultures and was also similar to that found in tonsillar tissues in The Human Protein Atlas. Next, to examine potential changes that occur during disease progression, DLG1 was examined in a series of HPV-negative OPSCCs, which were graded by pathologists depending on the level of differentiation from well- to poorly-differentiated, G1 to G3, respectively. In G1 samples (7/36), DLG1 expression levels varied, but the localization remained similar to that in control tonsillar tissue. In G2 OPSCCs (10/36), DLG1 expression was not detected in two samples, but in the remaining, it was of a medium or high intensity. In those, DLG1 localization was unaffected. Finally, in poorly-differentiated OPSCC samples (19/36), DLG1 was diminished in only one sample, while the vast majority showed either low or medium intensity expression, with cytoplasmic and membranous localization. These results are in agreement with a study showing exclusive membranous DLG1 staining in normal mammary epithelial ducts with intensely cytoplasmic staining in ductal in situ carcinoma cases (Fuja et al., 2004). Similarly, a downregulation of the membranous DLG1 was observed in semi-differentiated colon adenocarcinomas with DLG1 protein being almost undetectable in poorly differentiated stages (Cavatorta et al., 2004; Gardiol et al., 2006). Taking all this together, perturbations in DLG1 localization seem to increase with the cancer progression implying that deregulation of DLG1 normal function is likely to be linked with the disease development. These alterations could have occurred because of other processes during cancer progression. It was speculated that acquisition of certain mutations in DLG1 gene can promote malignant transformation. So far, missense mutations G338R, I348V, Y349S, K352R, K352E,

G356A, H360Q, and H360N in the DLG1 PDZ-2 domain have been observed in breast cancer (Fuja et al., 2004) and were later suggested to disable DLG1 interaction with the tumor suppressors APC and PTEN (Marziali et al., 2019; Sotelo et al., 2012). These results emphasized the importance of DLG1 functions and suggest that any alterations in DLG1 function may contribute to the process of oncogenesis, which is in correlation with the hypothesis of DLG1 acting both as a tumor suppressor and cell polarity regulator (Elsum et al., 2012; Marziali et al., 2019). DLG1 expression and localization patterns were further examined in HPV16-positive OPSCCs to investigate whether E6 has any effects in this background. In those, DLG1 expression was reduced significantly when compared to G3 HPV-negative cancers only, but localization was almost unaffected suggesting that HPV16 E6 does not evidently affect localization of DLG1.

The changes in SCRIB distribution patterns were next investigated in control tonsillar tissues. In those, SCRIB was expressed both in the cytoplasm and membranes of cells from the parabasal layer of the stratified squamous epithelium but was absent from the basal and superficial layers. This observation is contradictory to the one from The Human Protein Atlas, where SCRIB was demonstrated to be detected in the basal and intermediate layers of squamous epithelia, but not in the superficial layers. However, similar SCRIB pattern was observed in the organotypic raft cultures as mentioned above. In the HPV-negative OPSCCs, SCRIB expression remained unaffected in almost all G1 and G2 samples, but one sample showed SCRIB levels that were similar to those seen in control tonsillar tissues. SCRIB was predominantly delocalized from the membranes to the cytoplasm of cancerous cells. However, in G2 OPSCCs, SCRIB was completely absent in 2/10 samples and the loss was more obvious in G3 samples, implying that SCRIB mislocalization could be a risk factor for malignant transformation. Indeed, these results were consistent with studies on breast cancer cells and on mutant transgenic mice, showing that cytoplasmic SCRIB promotes cancer development by affecting subcellular localization of PTEN and activation of the Akt/mTOR/S6 kinase signaling pathway (Feigin et al., 2014; Stephens et al., 2018). HPV16-positive OPSCCs samples are classified as poorly differentiated, and thus share morphological similarities with G3 HPV-negative ones. Therefore, no significant change was observed in SCRIB expression and localization pattern between G3 HPV-negative and HPV16-positive OPSCCs. More precisely, SCRIB was diminished in almost all samples, but in those where it was detected, it was expressed at low levels and solely in the cytoplasm. However, significant changes in both SCRIB mislocalization and expression were detected between lower graded HPV-

negative cancers (G1 and G2) and HPV16-positive ones, suggesting that the relocation of SCRIB is likely to be an important event in promoting malignant transformation. Since SCRIB is a membrane protein which interacts with various cellular proteins, its delocalization could disrupt those interactions causing modulations in functions of the interacting partners. Likewise, it is likely that SCRIB has a dual function under certain conditions, so any mutations or presence of E6 could cause the shift to growth promotion rather than inhibition. Even though the complete delocalization or loss of SCRIB protein was not an exclusive result of HPV16 infection in the HN area, the overall SCRIB expression was significantly lower in HPV16-positive OPSCCs than in HPV-negative ones. This is in line with a cervical cancer study showing that E6-mediated degradation was one of the causal roles for the progressive decrease of SCRIB expression during the disease progression from LSIL to HSIL. This then led to the complete decrease of SCRIB expression during the process of carcinogenesis from HSIL to invasive cervical cancer (Nakagawa et al., 2004). Most importantly, a marked, progression-dependent SCRIB downregulation was detected in the HPV-negative OPSCCs, especially in G3 HPV-negative samples. Similarly, decreased expression and changed localization of SCRIB were associated with clinical stage, histopathological differentiation, and lymph node metastasis suggesting that SCRIB is involved in the development of endometrial cancer (Ouyang et al., 2019, 2009). Therefore, results of this doctoral study suggest that certain fluctuations in SCRIB expression and localization patterns are likely to correlate with higher grades of OPSCCs. Moreover, these oscillations are even more evident in the presence of HPV16 implying that the loss of SCRIB could serve as a potential late-stage marker in oropharyngeal carcinogenesis.

.

6 CONCLUSIONS

HPV16 is the predominant type in HPV-induced OPSCCs, thus this research aimed to get a better understanding of the process of HPV-mediated oncogenesis at this anatomical site by investigating potential similarities and differences in 16E6 effects on DLG1 and SCRIB. The results were obtained from experiments on immortalized keratinocytes isolated from anogenital and HN area, primary keratinocytes, organotypic 3D raft cultures and on OPSCCs samples. From those, it was concluded that:

- The preference of HPV E6 oncoproteins' binding to DLG1 and SCRIB remains unaltered in immortalized keratinocytes regardless of the anatomical origin.
- HPV16 E6 has no effect on endogenous expression of DLG1 protein but impacts its cellular localization in immortalized keratinocytes. These effects are the most evident in iHFK-16E6/E7.
- HPV16 E6 causes an increase in endogenous SCRIB protein expression levels, but it exhibits minor changes in cellular localization, and this is not anatomical site-dependent.
- HPV16 E6 induces upregulation of overall DLG1 mRNA levels in primary HFK cells, while there is no evident effect on DLG1 mRNA levels in primary HTK cells.
- HPV16 E6 upregulates SCRIB mRNA levels in primary HTK and HFK.
- HPV16 causes a shift in cellular localization from the membranes to the cytosol of both DLG1 and SCRIB proteins in the basal and parabasal layers of organotypic 3D raft cultures. This was more evident in rafts grown from high passaged HPV16-expressing HTKs.
- DLG1 delocalization from the membranes to the cytoplasm increases with the progression of HPV-negative OPSCC and this is even more evident in the presence of HPV16 E6.
- SCRIB is insignificantly mislocalized from the membranes to the cytoplasm during the progression of HPV-negative OPSCCs.
- SCRIB proteins levels decrease with the progression of HPV-negative OPSCCs and this loss of SCRIB is significant in the presence of HPV16 E6.

Put together, this research provides novel insights about the roles of HPV16 E6 in HN carcinogenesis, through effects on DLG1 and SCRIB proteins, and shed a light on DLG1 and SCRIB similarities and differences in their behavior during the process of carcinogenesis in oropharynx, in the presence and absence of HPV16 E6.

7 BIBLIOGRAPHY

Accardi, R., Rubino, R., Scalise, M., Gheit, T., Shahzad, N., Thomas, M., Banks, L., Indiveri, C., Sylla, B.S., Cardone, R.A., Reshkin, S.J., Tommasino, M., 2011. E6 and E7 from Human Papillomavirus Type 16 Cooperate To Target the PDZ Protein Na/H Exchange Regulatory Factor 1. J Virol 85, 8208–8216. https://doi.org/10.1128/JVI.00114-11

Aranda, V., Nolan, M.E., Muthuswamy, S.K., 2008. Par complex in cancer: a regulator of normal cell polarity joins the dark side. Oncogene 27, 6878–6887. https://doi.org/10.1038/onc.2008.340

Argiris, A., Karamouzis, M.V., Raben, D., Ferris, R.L., 2008. Head and neck cancer. The Lancet 371, 1695–1709. https://doi.org/10.1016/S0140-6736(08)60728-X

Assémat, E., Bazellières, E., Pallesi-Pocachard, E., Le Bivic, A., Massey-Harroche, D., 2008. Polarity complex proteins. Biochimica et Biophysica Acta (BBA) - Biomembranes 1778, 614–630. https://doi.org/10.1016/j.bbamem.2007.08.029

Aupérin, A., 2020. Epidemiology of head and neck cancers: an update. Current Opinion in Oncology 32, 178–186. https://doi.org/10.1097/CCO.0000000000000629

Avvakumov, N., Torchia, J., Mymryk, J.S., 2003. Interaction of the HPV E7 proteins with the pCAF acetyltransferase. Oncogene 22, 3833–3841. https://doi.org/10.1038/sj.onc.1206562

Axelrod, J.D., 2020. Planar cell polarity signaling in the development of left–right asymmetry. Current Opinion in Cell Biology 62, 61–69. https://doi.org/10.1016/j.ceb.2019.09.002

Barbosa, M.S., Edmonds, C., Fisher, C., Schiller, J.T., Lowy, D.R., Vousden, K.H., 1990. The region of the HPV E7 oncoprotein homologous to adenovirus E1a and Sv40 large T antigen contains separate domains for Rb binding and casein kinase II phosphorylation. The EMBO Journal 9, 153–160. https://doi.org/10.1002/j.1460-2075.1990.tb08091.x

Barbosa, M.S., Wettstein, F.O., 1987. Transcription of the cottontail rabbit papillomavirus early region and identification of two E6 polypeptides in COS-7 cells. J Virol 61, 2938–2942. https://doi.org/10.1128/jvi.61.9.2938-2942.1987

Bedell, S.L., Goldstein, L.S., Goldstein, A.R., Goldstein, A.T., 2020. Cervical Cancer Screening: Past, Present, and Future. Sexual Medicine Reviews 8, 28–37. https://doi.org/10.1016/j.sxmr.2019.09.005

Bello, J., Nieva, L., Paredes, A., Gonzalez, A., Zavaleta, L., Lizano, M., 2015. Regulation of the Wnt/β-Catenin Signaling Pathway by Human Papillomavirus E6 and E7 Oncoproteins. Viruses 7, 4734–4755. https://doi.org/10.3390/v7082842

Bernabé, D.G., Tamae, A.C., Miyahara, G.I., Sundefeld, M.L.M., Oliveira, S.P., Biasoli, É.R., 2012. Increased plasma and salivary cortisol levels in patients with oral cancer and their association with clinical stage. J Clin Pathol 65, 934–939. https://doi.org/10.1136/jclinpath-2012-200695

Bernard, H.-U., Burk, R.D., Chen, Z., van Doorslaer, K., Hausen, H. zur, de Villiers, E.-M., 2010. Classification of papillomaviruses (PVs) based on 189 PV types and proposal of taxonomic amendments. Virology 401, 70–79. https://doi.org/10.1016/j.virol.2010.02.002

Bilder, D., 2004. Epithelial polarity and proliferation control: links from the *Drosophila* neoplastic tumor suppressors. Genes Dev. 18, 1909–1925. https://doi.org/10.1101/gad.1211604

Bilder, D., 2001. PDZ proteins and polarity: functions from the fly. Trends in Genetics 17, 511–519. https://doi.org/10.1016/S0168-9525(01)02407-6

Bilder, D., Perrimon, N., 2000. Localization of apical epithelial determinants by the basolateral PDZ protein Scribble. Nature 403, 676–680. https://doi.org/10.1038/35001108

Blitzer, G.C., Smith, M.A., Harris, S.L., Kimple, R.J., 2014. Review of the Clinical and Biologic Aspects of Human Papillomavirus-Positive Squamous Cell Carcinomas of the Head and Neck. International Journal of Radiation Oncology*Biology*Physics 88, 761–770. https://doi.org/10.1016/j.ijrobp.2013.08.029

Boda, D., Docea, A., Calina, D., Ilie, M., Caruntu, C., Zurac, S., Neagu, M., Constantin, C., Branisteanu, D., Voiculescu, V., Mamoulakis, C., Tzanakakis, G., Spandidos, D., Drakoulis, N., Tsatsakis, A., 2018. Human papilloma virus: Apprehending the link with carcinogenesis and unveiling new research avenues (Review). Int J Oncol. https://doi.org/10.3892/ijo.2018.4256

Bonello, T.T., Peifer, M., 2019. Scribble: A master scaffold in polarity, adhesion, synaptogenesis, and proliferation. Journal of Cell Biology 218, 742–756. https://doi.org/10.1083/jcb.201810103

Bonner, J.A., Azarnia, N., Jones, C.U., Jassem, J., Baselga, J., Rowinsky, E.K., 2006. Radiotherapy plus Cetuximab for Squamous-Cell Carcinoma of the Head and Neck. The New England Journal of Medicine 12.

Boon, S.S., Banks, L., 2013. High-Risk Human Papillomavirus E6 Oncoproteins Interact with 14-3-3ζ in a PDZ Binding Motif-Dependent Manner. J Virol 87, 1586–1595. https://doi.org/10.1128/JVI.02074-12

Boon, S.S., Tomaić, V., Thomas, M., Roberts, S., Banks, L., 2015. Cancer-Causing Human Papillomavirus E6 Proteins Display Major Differences in the Phospho-Regulation of Their PDZ Interactions. J Virol 89, 1579–1586. https://doi.org/10.1128/JVI.01961-14

Bouvard, V., Baan, R., Straif, K., Grosse, Y., Secretan, B., Ghissassi, F.E., Benbrahim-Tallaa, L., Guha, N., Freeman, C., Galichet, L., Cogliano, V., 2009. A review of human carcinogens—Part B: biological agents. The Lancet Oncology 10, 321–322. https://doi.org/10.1016/S1470-2045(09)70096-8

Brady, C.A., Attardi, L.D., 2010. p53 at a glance. Journal of Cell Science 123, 2527–2532. https://doi.org/10.1242/jcs.064501

Brambilla, E., Gazzeri, S., Moro, D., Lantuejoul, S., Veyrenc, S., Brambilla, C., 1999a. Alterations of Rb Pathway (Rb-p16INK4-Cyclin D1) in Preinvasive Bronchial Lesions 9.

Brambilla, E., Moro, D., Gazzeri, S., Brambilla, C., 1999b. Alterations of expression of Rb, p16INK4A and cyclin D1 in non-small cell lung carcinoma and their clinical significance. J. Pathol. 188, 351–360. https://doi.org/10.1002/(SICI)1096-9896(199908)188:4<351::AID-PATH385>3.0.CO;2-W

Bravo, I.G., Félez-Sánchez, M., 2015. Papillomaviruses. Evolution, Medicine, and Public Health 2015, 32–51. https://doi.org/10.1093/emph/eov003

Brimer, N., Lyons, C., Vande Pol, S.B., 2007. Association of E6AP (UBE3A) with human papillomavirus type 11 E6 protein. Virology 358, 303–310. https://doi.org/10.1016/j.virol.2006.08.038

Brockstein, B., Masters, G. (Eds.), 2003. Head and Neck Cancer.

Buajeeb, W., Poomsawat, S., Punyasingh, J., Sanguansin, S., 2008. Expression of p16 in oral cancer and premalignant lesions: p16 in oral cancer and premalignant lesions. Journal of Oral Pathology & Medicine 38, 104–108. https://doi.org/10.1111/j.1600-0714.2008.00710.x

Buck, C.B., Day, P.M., Trus, B.L., 2013. The papillomavirus major capsid protein L1. Virology 445, 169–174. https://doi.org/10.1016/j.virol.2013.05.038

Burley, M., Roberts, S., Parish, J.L., 2020. Epigenetic regulation of human papillomavirus transcription in the productive virus life cycle. Semin Immunopathol 42, 159–171. https://doi.org/10.1007/s00281-019-00773-0

Castro-Cruz, M., Lembo, F., Borg, J.-P., Trave, G., Vincentelli, R., Zimmermann, P., 2020. The human PDZome 2.0: characterization of a new resource to test for PDZ interactions by Yeast Two-Hybrid (preprint). Molecular Biology. https://doi.org/10.1101/2020.08.06.239343

Cavatorta, A.L., Di Gregorio, A., Bugnon Valdano, M., Marziali, F., Cabral, M., Bottai, H., Cittadini, J., Nocito, A.L., Gardiol, D., 2017. DLG1 polarity protein expression associates with the disease progress of low-grade cervical intraepithelial lesions. Experimental and Molecular Pathology 102, 65–69. https://doi.org/10.1016/j.yexmp.2016.12.008

Cavatorta, A.L., Fumero, G., Chouhy, D., Aguirre, R., Nocito, A.L., Giri, A.A., Banks, L., Gardiol, D., 2004. Differential expression of the human homologue ofdrosophila discs large oncosuppressor in histologic samples from human papillomavirus-associated lesions as a marker for progression to malignancy. Int. J. Cancer 111, 373–380. https://doi.org/10.1002/ijc.20275

Chen, Y.-J., Chang, J.T.-C., Liao, C.-T., Wang, H.-M., Yen, T.-C., Chiu, C.-C., Lu, Y.-C., Li, H.-F., Cheng, A.-J., 2008. Head and neck cancer in the betel quid chewing area: recent advances in molecular carcinogenesis. Cancer Science 99, 1507–1514. https://doi.org/10.1111/j.1349-7006.2008.00863.x

Choi, M., Lee, S., Choi, T., Lee, C., 2013. Roles of the PDZ domain-binding motif of the human papillomavirus type 16 E6 on the immortalization and differentiation of primary human foreskin keratinocytes. Virus Genes 9.

Christensen, N.R., Čalyševa, J., Fernandes, E.F.A., Lüchow, S., Clemmensen, L.S., Haugaard-Kedström, L.M., Strømgaard, K., 2019. PDZ Domains as Drug Targets. Adv. Therap. 1800143. https://doi.org/10.1002/adtp.201800143

Christopherson, K.S., Hillier, B.J., Lim, W.A., Bredt, D.S., 1999. PSD-95 Assembles a Ternary Complex with theN-Methyl-d-aspartic Acid Receptor and a Bivalent Neuronal NO Synthase PDZ Domain. Journal of Biological Chemistry 274, 27467–27473. https://doi.org/10.1074/jbc.274.39.27467

Citro, S., Bellini, A., Medda, A., Sabatini, M.E., Tagliabue, M., Chu, F., Chiocca, S., 2020. Human Papilloma Virus Increases ΔNp63α Expression in Head and Neck Squamous Cell Carcinoma. Front. Cell. Infect. Microbiol. 10, 143. https://doi.org/10.3389/fcimb.2020.00143

Cole, S.T., Danos, O., 1987. Nucleotide sequence and comparative analysis of the human papillomavirus type 18 genome. Journal of Molecular Biology 193, 599–608. https://doi.org/10.1016/0022-2836(87)90343-3

Contreras-Paredes, A., De la Cruz-Hernández, E., Martínez-Ramírez, I., Dueñas-González, A., Lizano, M., 2009. E6 variants of human papillomavirus 18 differentially modulate the protein kinase B/phosphatidylinositol 3-kinase (akt/PI3K) signaling pathway. Virology 383, 78–85. https://doi.org/10.1016/j.virol.2008.09.040

Cramer, J.D., Burtness, B., Le, Q.T., Ferris, R.L., 2019. The changing therapeutic landscape of head and neck cancer. Nat Rev Clin Oncol 16, 669–683. https://doi.org/10.1038/s41571-019-0227-z

da Mata, S., Ferreira, J., Nicolás, I., Esteves, S., Esteves, G., Lérias, S., Silva, F., Saco, A., Cochicho, D., Cunha, M., del Pino, M., Ordi, J., Félix, A., 2021. P16 and HPV Genotype

Significance in HPV-Associated Cervical Cancer—A Large Cohort of Two Tertiary Referral Centers. IJMS 22, 2294. https://doi.org/10.3390/ijms22052294
de Martel, C., Plummer, M., Vignat, J., Franceschi, S., 2017. Worldwide burden of cancer attributable to HPV by site, country and HPV type: Worldwide burden of cancer attributable to HPV. Int. J. Cancer 141, 664–670. https://doi.org/10.1002/ijc.30716
de Villiers, E.-M., Fauquet, C., Broker, T.R., Bernard, H.-U., zur Hausen, H., 2004. Classification of papillomaviruses. Virology 324, 17–27. https://doi.org/10.1016/j.virol.2004.03.033
Dediol, E., Sabol, I., Virag, M., Grce, M., Muller, D., Manojlović, S., 2016. HPV prevalence and p16INKa overexpression in non-smoking non-drinking oral cavity cancer patients. Oral Dis 22, 517–522. https://doi.org/10.1111/odi.12476
Delury, C.P., Marsh, E.K., James, C.D., Boon, S.S., Banks, L., Knight, G.L., Roberts, S., 2013. The Role of Protein Kinase A Regulation of the E6 PDZ-Binding Domain during the Differentiation-Dependent Life Cycle of Human Papillomavirus Type 18. J Virol 87, 9463–9472. https://doi.org/10.1128/JVI.01234-13
DeMasi, J., Huh, K.-W., Nakatani, Y., Münger, K., Howley, P.M., 2005. Bovine papillomavirus E7 transformation function correlates with cellular p600 protein binding. Proc. Natl. Acad. Sci. U.S.A. 102, 11486–11491. https://doi.org/10.1073/pnas.0505322102
DiMaio, D., Petti, L.M., 2013. The E5 proteins. Virology 445, 99–114. https://doi.org/10.1016/j.virol.2013.05.006
Dixon, E.P., Pahel, G.L., Rocque, W.J., Barnes, J.A., Lobe, D.C., Hanlon, M.H., Alexander, K.A., Chao, S.-F., Lindley, K., Phelps, W.C., 2000. The E1 Helicase of Human Papillomavirus Type 11 Binds to the Origin of Replication with Low Sequence Specificity. Virology 270, 345–357. https://doi.org/10.1006/viro.2000.0204
Dizanzo, M.P., Marziali, F., Brunet Avalos, C., Bugnon Valdano, M., Leiva, S., Cavatorta, A.L., Gardiol, D., 2020. HPV E6 and E7 oncoproteins cooperatively alter the expression of Disc Large 1 polarity protein in epithelial cells. BMC Cancer 20, 293. https://doi.org/10.1186/s12885-020-06778-5
Dok, R., Nuyts, S., 2016. HPV Positive Head and Neck Cancers: Molecular Pathogenesis and Evolving Treatment Strategies. Cancers 8, 41. https://doi.org/10.3390/cancers8040041
Doorbar, J., 2013. The E4 protein; structure, function and patterns of expression. Virology 445, 80–98. https://doi.org/10.1016/j.virol.2013.07.008
Doorbar, J., Egawa, N., Griffin, H., Kranjec, C., Murakami, I., 2015. Human papillomavirus molecular biology and disease association. Rev. Med. Virol. 25, 2–23. https://doi.org/10.1002/rmv.1822
Doorbar, J., Gallimore, P.H., 1987. Identification of Proteins Encoded by the Li and L2 Open Reading Frames of Human Papillomavirus la. J. VIROL. 61, 7.
Doorbar, J., Jenkins, D., Stoler, M.H., Bergeron, C., 2020. Biology of the Human Papillomavirus Life Cycle: The Basis for Understanding the Pathology of PreCancer and Cancer, in: Human Papillomavirus. Elsevier, pp. 67–83. https://doi.org/10.1016/B978-0-12-814457-2.00005-2
Doorbar, J., Quint, W., Banks, L., Bravo, I.G., Stoler, M., Broker, T.R., Stanley, M.A., 2012. The Biology and Life-Cycle of Human Papillomaviruses. Vaccine 30, F55–F70. https://doi.org/10.1016/j.vaccine.2012.06.083
Dow, L.E., Elsum, I.A., King, C.L., Kinross, K.M., Richardson, H.E., Humbert, P.O., 2008. Loss of human Scribble cooperates with H-Ras to promote cell invasion through deregulation of MAPK signalling. Oncogene 27, 5988–6001. https://doi.org/10.1038/onc.2008.219

Doyle, D.A., Lee, A., Lewis, J., Kim, E., Sheng, M., MacKinnon, R., 1996. Crystal Structures of a Complexed and Peptide-Free Membrane Protein–Binding Domain: Molecular Basis of Peptide Recognition by PDZ. Cell 85, 1067–1076. https://doi.org/10.1016/S0092-8674(00)81307-0

Dreer, M., Fertey, J., van de Poel, S., Straub, E., Madlung, J., Macek, B., Iftner, T., Stubenrauch, F., 2016. Interaction of NCOR/SMRT Repressor Complexes with Papillomavirus E8^E2C Proteins Inhibits Viral Replication. PLoS Pathog 12, e1005556. https://doi.org/10.1371/journal.ppat.1005556

Drews, C.M., Case, S., Vande Pol, S.B., 2019. E6 proteins from high-risk HPV, low-risk HPV, and animal papillomaviruses activate the Wnt/β-catenin pathway through E6AP-dependent degradation of NHERF1. PLoS Pathog 15, e1007575. https://doi.org/10.1371/journal.ppat.1007575

Đukić, A., Lulić, L., Thomas, M., Skelin, J., Bennett Saidu, N.E., Grce, M., Banks, L., Tomaić, V., 2020. HPV Oncoproteins and the Ubiquitin Proteasome System: A Signature of Malignancy? Pathogens 9, 133. https://doi.org/10.3390/pathogens9020133

Dunn, H.A., Walther, C., Godin, C.M., Hall, R.A., Ferguson, S.S.G., 2013. Role of SAP97 Protein in the Regulation of Corticotropin-releasing Factor Receptor 1 Endocytosis and Extracellular Signal-regulated Kinase 1/2 Signaling. Journal of Biological Chemistry 288, 15023–15034. https://doi.org/10.1074/jbc.M113.473660

Dürst, M., Gissmann, L., Ikenberg, H., zur Hausen, H., 1983. A papillomavirus DNA from a cervical carcinoma and its prevalence in cancer biopsy samples from different geographic regions. Proc. Natl. Acad. Sci. U.S.A. 80, 3812–3815. https://doi.org/10.1073/pnas.80.12.3812

Durzynska, J., Lesniewicz, K., Poreba, E., 2017. Human papillomaviruses in epigenetic regulations. Mutation Research/Reviews in Mutation Research 772, 36–50. https://doi.org/10.1016/j.mrrev.2016.09.006

Egawa, N., Doorbar, J., 2017. The low-risk papillomaviruses. Virus Research 231, 119–127. https://doi.org/10.1016/j.virusres.2016.12.017

Eldridge, R.C., Uppal, K., Hayes, D.N., Smith, M.R., Hu, X., Qin, Z.S., Beitler, J.J., Miller, A.H., Wommack, E.C., Higgins, K.A., Shin, D.M., Ulrich, B., Qian, D.C., Saba, N.F., Bruner, D.W., Jones, D.P., Xiao, C., 2021. Plasma Metabolic Phenotypes of HPV-Associated versus Smoking-Associated Head and Neck Cancer and Patient Survival. Cancer Epidemiology, Biomarkers & Prevention 30, 1858–1866. https://doi.org/10.1158/1055-9965.EPI-21-0576

Elegheert, J., Behiels, E., Bishop, B., Scott, S., Woolley, R.E., Griffiths, S.C., Byrne, E.F.X., Chang, V.T., Stuart, D.I., Jones, E.Y., Siebold, C., Aricescu, A.R., 2018. Lentiviral transduction of mammalian cells for fast, scalable and high-level production of soluble and membrane proteins. Nat Protoc 13, 2991–3017. https://doi.org/10.1038/s41596-018-0075-9

Elrefaey, S., Massaro, M.A., Chiocca, S., Chiesa, F., Ansarin, M., 2014. HPV in oropharyngeal cancer: the basics to know in clinical practice. ACTA otorhinolaryngologica italica 299–309.

Elsum, I., Yates, L., Humbert, P.O., Richardson, H.E., 2012. The Scribble–Dlg–Lgl polarity module in development and cancer: from flies to man. Essays in Biochemistry 53, 141–168. https://doi.org/10.1042/bse0530141

Engel, B., Cress, D., Santiago-Cardona, P., 2014. The retinoblastoma protein: a master tumor suppressor acts as a link between cell cycle and cell adhesion. CHC 1. https://doi.org/10.2147/CHC.S28079

Espina, V. (Ed.), 2017. Molecular Profiling: Methods and Protocols, Methods in Molecular Biology. Springer New York, New York, NY. https://doi.org/10.1007/978-1-4939-6990-6

Etienne-Manneville, S., Arkowitz, R., 2020. Cell polarity inside-out. Current Opinion in Cell Biology 62, iii–iv. https://doi.org/10.1016/j.ceb.2020.01.008

Facciuto, F., Bugnon Valdano, M., Marziali, F., Massimi, P., Banks, L., Cavatorta, A.L., Gardiol, D., 2014. Human papillomavirus (HPV)-18 E6 oncoprotein interferes with the epithelial cell polarity Par3 protein. Molecular Oncology 8, 533–543. https://doi.org/10.1016/j.molonc.2014.01.002

Fanning, A.S., Anderson, J.M., 1999. PDZ domains: fundamental building blocks in the organization of protein complexes at the plasma membrane. J. Clin. Invest. 103, 767–772. https://doi.org/10.1172/JCI6509

Feigin, M.E., Akshinthala, S.D., Araki, K., Rosenberg, A.Z., Muthuswamy, L.B., Martin, B., Lehmann, B.D., Berman, H.K., Pietenpol, J.A., Cardiff, R.D., Muthuswamy, S.K., 2014. Mislocalization of the Cell Polarity Protein Scribble Promotes Mammary Tumorigenesis and Is Associated with Basal Breast Cancer. Cancer Res 74, 3180–3194. https://doi.org/10.1158/0008-5472.CAN-13-3415

Filippova, M., Parkhurst, L., Duerksen-Hughes, P.J., 2004. The Human Papillomavirus 16 E6 Protein Binds to Fas-associated Death Domain and Protects Cells from Fas-triggered Apoptosis. Journal of Biological Chemistry 279, 25729–25744. https://doi.org/10.1074/jbc.M401172200

Finnen, R.L., Erickson, K.D., Chen, X.S., Garcea, R.L., 2003. Interactions between Papillomavirus L1 and L2 Capsid Proteins. J Virol 77, 4818–4826. https://doi.org/10.1128/JVI.77.8.4818-4826.2003

Fleming, J.C., Woo, J., Moutasim, K., Mellone, M., Frampton, S.J., Mead, A., Ahmed, W., Wood, O., Robinson, H., Ward, M., Woelk, C.H., Ottensmeier, C.H., King, E., Kim, D., Blaydes, J.P., Thomas, G.J., 2019. HPV, tumour metabolism and novel target identification in head and neck squamous cell carcinoma. Br J Cancer 120, 356–367. https://doi.org/10.1038/s41416-018-0364-7

Fuja, T.J., Lin, F., Osann, K.E., Bryant, P.J., 2004. Somatic Mutations and Altered Expression of the Candidate Tumor Suppressors CSNK1□, DLG1, and EDD/hHYD in Mammary Ductal Carcinoma 10.

Funke, L., Dakoji, S., Bredt, D.S., 2005. MEMBRANE-ASSOCIATED GUANYLATE KINASES REGULATE ADHESION AND PLASTICITY AT CELL JUNCTIONS. Annu. Rev. Biochem. 74, 219–245. https://doi.org/10.1146/annurev.biochem.74.082803.133339

Ganti, K., Broniarczyk, J., Manoubi, W., Massimi, P., Mittal, S., Pim, D., Szalmas, A., Thatte, J., Thomas, M., Tomaić, V., Banks, L., 2015. The Human Papillomavirus E6 PDZ Binding Motif: From Life Cycle to Malignancy. Viruses 7, 3530–3551. https://doi.org/10.3390/v7072785

García-Vallvé, S., Alonso, Á., Bravo, I.G., 2005. Papillomaviruses: different genes have different histories. Trends in Microbiology 13, 514–521. https://doi.org/10.1016/j.tim.2005.09.003

Gardiol, D., Kühne, C., Glaunsinger, B., Lee, S.S., Javier, R., Banks, L., 1999. Oncogenic human papillomavirus E6 proteins target the discs large tumour suppressor for proteasome-mediated degradation. Oncogene 18, 5487–5496. https://doi.org/10.1038/sj.onc.1202920

Gardiol, D., Zacchi, A., Petrera, F., Stanta, G., Banks, L., 2006. Human discs large and scrib are localized at the same regions in colon mucosa and changes in their expression patterns are correlated with loss of tissue architecture during malignant progression. Int. J. Cancer 119, 1285–1290. https://doi.org/10.1002/ijc.21982

Gardoni, F., Mauceri, D., Marcello, E., Sala, C., Di Luca, M., Jeromin, A., 2007. SAP97 Directs the Localization of Kv4.2 to Spines in Hippocampal Neurons. Journal of Biological Chemistry 282, 28691–28699. https://doi.org/10.1074/jbc.M701899200

Garlick, J.A., Katz, A.B., Fenjves, E.S., Taichman, L.B., 1991. Retrovirus-Mediated Transduction of Cultured Epidermal Keratinocytes. Journal of Investigative Dermatology 97, 824–829. https://doi.org/10.1111/1523-1747.ep12489019

Gaykalova, D.A., Manola, J.B., Ozawa, H., Zizkova, V., Morton, K., Bishop, J.A., Sharma, R., Zhang, C., Michailidi, C., Considine, M., Tan, M., Fertig, E.J., Hennessey, P.T., Ahn, J., Koch, W.M., Westra, W.H., Khan, Z., Chung, C.H., Ochs, M.F., Califano, J.A., 2015. NF-κB and stat3 transcription factor signatures differentiate HPV-positive and HPV-negative head and neck squamous cell carcinoma: NF-κB and STATs pathway dysregulation in HNSCC. Int. J. Cancer 137, 1879–1889. https://doi.org/10.1002/ijc.29558

Genovese, N.J., Banerjee, N.S., Broker, T.R., Chow, L.T., 2008. Casein Kinase II Motif-Dependent Phosphorylation of Human Papillomavirus E7 Protein Promotes p130 Degradation and S-Phase Induction in Differentiated Human Keratinocytes. J Virol 82, 4862–4873. https://doi.org/10.1128/JVI.01202-07

Gewin, L., Myers, H., Kiyono, T., Galloway, D.A., 2004. Identification of a novel telomerase repressor that interacts with the human papillomavirus type-16 E6/E6-AP complex. Genes Dev. 18, 2269–2282. https://doi.org/10.1101/gad.1214704

Gheit, T., 2019. Mucosal and Cutaneous Human Papillomavirus Infections and Cancer Biology. Front. Oncol. 9, 355. https://doi.org/10.3389/fonc.2019.00355

Giacinti, C., Giordano, A., 2006. RB and cell cycle progression. Oncogene 25, 5220–5227. https://doi.org/10.1038/sj.onc.1209615

Gissmann, L., Diehl, V., Schultz-Coulon, H.J., zur Hausen, H., 1982. Molecular cloning and characterization of human papilloma virus DNA derived from a laryngeal papilloma. J Virol 44, 393–400. https://doi.org/10.1128/jvi.44.1.393-400.1982

Golusiński, P., Pazdrowski, J., Szewczyk, M., Misiołek, M., Pietruszewska, W., Klatka, J., Okła, S., Kaźmierczak, H., Marszałek, A., Filas, V., Schneider, A., Masternak, M.M., Stęplewska, K., Miśkiewicz-Orczyk, K., Golusiński, W., 2017. Is immunohistochemical evaluation of p16 in oropharyngeal cancer enough to predict the HPV positivity? Reports of Practical Oncology & Radiotherapy 22, 237–242. https://doi.org/10.1016/j.rpor.2017.01.003

Graham, S.V., 2017a. The human papillomavirus replication cycle, and its links to cancer progression: a comprehensive review. Clinical Science 131, 2201–2221. https://doi.org/10.1042/CS20160786

Graham, S.V., 2017b. Keratinocyte Differentiation-Dependent Human Papillomavirus Gene Regulation. Viruses 9, 245. https://doi.org/10.3390/v9090245

Grce, M., Grahovac, B., Rukavina, T., Vrdoljak-Mozeti, D., Glava, L., Kaliterna, V., 2007. HPV Testing for Cervical Cancer Screening in Croatia. Coll. Antropol. 5.

Guerrero-Preston, R., Soudry, E., Acero, J., Orera, M., Moreno-López, L., Macía-Colón, G., Jaffe, A., Berdasco, M., Ili-Gangas, C., Brebi-Mieville, P., Fu, Y., Engstrom, C., Irizarry, R.A., Esteller, M., Westra, W., Koch, W., Califano, J., Sidransky, D., 2011. NID2 and HOXA9 Promoter Hypermethylation as Biomarkers for Prevention and Early Detection in Oral

Cavity Squamous Cell Carcinoma Tissues and Saliva. Cancer Prev Res 4, 1061–1072. https://doi.org/10.1158/1940-6207.CAPR-11-0006

Gupta, B., Johnson, N.W., Kumar, N., 2016. Global Epidemiology of Head and Neck Cancers: A Continuing Challenge. Oncology 91, 13–23. https://doi.org/10.1159/000446117

Halbert, C.L., Demers, G.W., Galloway, D.A., 1991. The E7 gene of human papillomavirus type 16 is sufficient for immortalization of human epithelial cells. J Virol 65, 473–478. https://doi.org/10.1128/jvi.65.1.473-478.1991

Harden, M.E., Munger, K., 2017. Human papillomavirus molecular biology. Mutation Research/Reviews in Mutation Research 772, 3–12. https://doi.org/10.1016/j.mrrev.2016.07.002

Harris, B.Z., Lim, W.A., Harris, B.Z., Lim, W.A., 2001. Mechanism and role of PDZ domains in signaling complex assembly. Journal of Cell Science 3219–3231, 13.

Haupt, Y., Maya, R., Kazaz, A., Oren, M., 1997. Mdm2 promotes the rapid degradation of p53. Nature 387, 296–299. https://doi.org/10.1038/387296a0

Hausen, H.Z., Meinhof, W., Scheiber, W., Bornkamm, G.W., 1974. Attempts to detect virus-specific DNA in human tumors. I. Nucleic acid hybridizations with complementary RNA of human wart virus. Int. J. Cancer 13, 650–656. https://doi.org/10.1002/ijc.2910130509

Hawkins, E.D., Oliaro, J., Ramsbottom, K.M., Newbold, A., Humbert, P.O., Johnstone, R.W., Russell, S.M., 2016. Scribble acts as an oncogene in Eμ-myc-driven lymphoma. Oncogene 35, 1193–1197. https://doi.org/10.1038/onc.2015.167

He, C., Mao, D., Hua, G., Lv, X., Chen, X., Angeletti, P.C., Dong, J., Remmenga, S.W., Rodabaugh, K.J., Zhou, J., Lambert, P.F., Yang, P., Davis, J.S., Wang, C., 2015. The Hippo/YAP pathway interacts with EGFR signaling and HPV oncoproteins to regulate cervical cancer progression. EMBO Mol Med 7, 1426–1449. https://doi.org/10.15252/emmm.201404976

Helt, A.-M., Funk, J.O., Galloway, D.A., 2002. Inactivation of both the Retinoblastoma Tumor Suppressor and p21 by the Human Papillomavirus Type 16 E7 Oncoprotein Is Necessary To Inhibit Cell Cycle Arrest in Human Epithelial Cells. J Virol 76, 10559–10568. https://doi.org/10.1128/JVI.76.20.10559-10568.2002

Hemmer, J., Kreidler, J., 1990. Flow cytometric DNA ploidy analysis of squamous cell carcinoma of the oral cavity: Comparison with clinical staging and histologic grading. Cancer 66, 317–320. https://doi.org/10.1002/1097-0142(19900715)66:2<317::AID-CNCR2820660220>3.0.CO;2-X

Herber, R., Liem, A., Pitot, H., Lambert, P.F., 1996. Squamous epithelial hyperplasia and carcinoma in mice transgenic for the human papillomavirus type 16 E7 oncogene. J Virol 70, 1873–1881. https://doi.org/10.1128/jvi.70.3.1873-1881.1996

Herfs, M., Yamamoto, Y., Laury, A., Wang, X., Nucci, M.R., McLaughlin-Drubin, M.E., Münger, K., Feldman, S., McKeon, F.D., Xian, W., Crum, C.P., 2012. A discrete population of squamocolumnar junction cells implicated in the pathogenesis of cervical cancer. Proc. Natl. Acad. Sci. U.S.A. 109, 10516–10521. https://doi.org/10.1073/pnas.1202684109

Hirata, A., Higuchi, M., Niinuma, A., Ohashi, M., Fukushi, M., Oie, M., Akiyama, T., Tanaka, Y., Gejyo, F., Fujii, M., 2004. PDZ domain-binding motif of human T-cell leukemia virus type 1 Tax oncoprotein augments the transforming activity in a rat fibroblast cell line. Virology 318, 327–336. https://doi.org/10.1016/j.virol.2003.10.006

Howard, M.A., Elias, G.M., Elias, L.A.B., Swat, W., Nicoll, R.A., 2010. The role of SAP97 in synaptic glutamate receptor dynamics. Proc. Natl. Acad. Sci. U.S.A. 107, 3805–3810. https://doi.org/10.1073/pnas.0914422107

Howie, H.L., Katzenellenbogen, R.A., Galloway, D.A., 2009. Papillomavirus E6 proteins. Virology 384, 324–334. https://doi.org/10.1016/j.virol.2008.11.017

Hu, W., Feng, Z., Levine, A.J., 2012. The Regulation of Multiple p53 Stress Responses is Mediated through MDM2. Genes & Cancer 3, 199–208. https://doi.org/10.1177/1947601912454734

Hu, Z., Zhu, D., Wang, W., Li, W., Jia, W., Zeng, X., Ding, W., Yu, L., Wang, X., Wang, L., Shen, H., Zhang, C., Liu, H., Liu, X., Zhao, Y., Fang, X., Li, Shuaicheng, Chen, W., Tang, T., Fu, A., Wang, Z., Chen, G., Gao, Q., Li, Shuang, Xi, L., Wang, C., Liao, S., Ma, X., Wu, P., Li, K., Wang, S., Zhou, J., Wang, J., Xu, X., Wang, H., Ma, D., 2015. Genome-wide profiling of HPV integration in cervical cancer identifies clustered genomic hot spots and a potential microhomology-mediated integration mechanism. Nat Genet 47, 158–163. https://doi.org/10.1038/ng.3178

Hughes, F.J., Romanos, M.A., 1993. E1 protein of human papillomavirus is a DNA helicase/ATPase. Nucl Acids Res 21, 5817–5823. https://doi.org/10.1093/nar/21.25.5817

Huh, K., Zhou, X., Hayakawa, H., Cho, J.-Y., Libermann, T.A., Jin, J., Wade Harper, J., Munger, K., 2007. Human Papillomavirus Type 16 E7 Oncoprotein Associates with the Cullin 2 Ubiquitin Ligase Complex, Which Contributes to Degradation of the Retinoblastoma Tumor Suppressor. J Virol 81, 9737–9747. https://doi.org/10.1128/JVI.00881-07

Huh, K.-W., DeMasi, J., Ogawa, H., Nakatani, Y., Howley, P.M., Münger, K., 2005. Association of the human papillomavirus type 16 E7 oncoprotein with the 600-kDa retinoblastoma protein-associated factor, p600. Proc. Natl. Acad. Sci. U.S.A. 102, 11492–11497. https://doi.org/10.1073/pnas.0505337102

Huibregtse, J.M., Scheffner, M., Howley, P.M., 1991. A cellular protein mediates association of p53 with the E6 oncoprotein of human papillomavirus types 16 or 18. The EMBO Journal 10, 4129–4135. https://doi.org/10.1002/j.1460-2075.1991.tb04990.x

Hussein, U.K., Ahmed, A.G., Choi, W.K., Kim, K.M., Park, S.-H., Park, H.S., Noh, S.J., Lee, H., Chung, M.J., Moon, W.S., Kang, M.J., Cho, D.H., Jang, K.Y., 2021. SCRIB Is Involved in the Progression of Ovarian Carcinomas in Association with the Factors Linked to Epithelial-to-Mesenchymal Transition and Predicts Shorter Survival of Diagnosed Patients. Biomolecules 11, 405. https://doi.org/10.3390/biom11030405

IARC (Ed.), 2007. IARC Monographs on the Evaluation of Carcinogenic Risks to Humans Volume 90 Human Papillomaviruses, IARC monographs on the evaluation of carcinogenic risks to humans. IARC, Lyon.

Inoue, K., A. Fry, E., 2018. Aberrant expression of p16INK4a in human cancers – a new biomarker? Cancer Rep Rev 2. https://doi.org/10.15761/CRR.1000145

Israr, M., Biryukov, J., Ryndock, E.J., Alam, S., Meyers, C., 2016. Comparison of human papillomavirus type 16 replication in tonsil and foreskin epithelia. Virology 499, 82–90. https://doi.org/10.1016/j.virol.2016.09.004

Jabbar, S., Strati, K., Shin, M.K., Pitot, H.C., Lambert, P.F., 2010. Human papillomavirus type 16 E6 and E7 oncoproteins act synergistically to cause head and neck cancer in mice. Virology 407, 60–67. https://doi.org/10.1016/j.virol.2010.08.003

James, C., Roberts, S., 2016. Viral Interactions with PDZ Domain-Containing Proteins—An Oncogenic Trait? Pathogens 5, 8. https://doi.org/10.3390/pathogens5010008

James, M.A., Lee, J.H., Klingelhutz, A.J., 2006. Human Papillomavirus Type 16 E6 Activates NF-κB, Induces cIAP-2 Expression, and Protects against Apoptosis in a PDZ Binding Motif-Dependent Manner. J Virol 80, 5301–5307. https://doi.org/10.1128/JVI.01942-05

Javier, R.T., Rice, A.P., 2011. Emerging Theme: Cellular PDZ Proteins as Common Targets of Pathogenic Viruses. J Virol 85, 11544–11556. https://doi.org/10.1128/JVI.05410-11

Jeon, S., Allen-Hoffmann, B.L., Lambert, P.F., 1995. Integration of human papillomavirus type 16 into the human genome correlates with a selective growth advantage of cells. J Virol 69, 2989–2997. https://doi.org/10.1128/jvi.69.5.2989-2997.1995

Joberty, G., Petersen, C., Gao, L., Macara, I.G., 2000. The cell-polarity protein Par6 links Par3 and atypical protein kinase C to Cdc42. Nat Cell Biol 2, 531–539. https://doi.org/10.1038/35019573

Johnson, D.E., Burtness, B., Leemans, C.R., Lui, V.W.Y., Bauman, J.E., Grandis, J.R., 2020. Head and neck squamous cell carcinoma. Nat Rev Dis Primers 6, 92. https://doi.org/10.1038/s41572-020-00224-3

Kabsch, K., Alonso, A., 2002. The Human Papillomavirus Type 16 E5 Protein Impairs TRAIL- and FasL-Mediated Apoptosis in HaCaT Cells by Different Mechanisms. J Virol 76, 12162–12172. https://doi.org/10.1128/JVI.76.23.12162-12172.2002

Kallay, L.M., McNickle, A., Brennwald, P.J., Hubbard, A.L., Braiterman, L.T., 2006. Scribble associates with two polarity proteins, lgl2 and vangl2, via distinct molecular domains. J. Cell. Biochem. 99, 647–664. https://doi.org/10.1002/jcb.20992

Katzenellenbogen, R.A., Vliet-Gregg, P., Xu, M., Galloway, D.A., 2009. NFX1-123 Increases hTERT Expression and Telomerase Activity Posttranscriptionally in Human Papillomavirus Type 16 E6 Keratinocytes. J Virol 83, 6446–6456. https://doi.org/10.1128/JVI.02556-08

Kempen, P.M.W., Bockel, L., Braunius, W.W., Moelans, C.B., Olst, M., Jong, R., Stegeman, I., Diest, P.J., Grolman, W., Willems, S.M., 2014. HPV-positive oropharyngeal squamous cell carcinoma is associated with TIMP3 and CADM1 promoter hypermethylation. Cancer Med 3, 1185–1196. https://doi.org/10.1002/cam4.313

Khatri, N., Man, H.-Y., 2019. The Autism and Angelman Syndrome Protein Ube3A/E6AP: The Gene, E3 Ligase Ubiquitination Targets and Neurobiological Functions. Front. Mol. Neurosci. 12, 109. https://doi.org/10.3389/fnmol.2019.00109

Kim, E., Niethammer, M., Rothschild, A., Nung Jan, Y., Sheng, M., 1995. Clustering of Shaker-type K+ channels by interaction with a family of membrane-associated guanylate kinases. Nature 378, 85–88. https://doi.org/10.1038/378085a0

Kirnbauer, R., Booyt, F., CHENGt, N., LowY, D.R., Schiller, J.T., 1992. Papillomavirus Li major capsid protein self-assembles into virus-like particles that are highly immunogenic. Medical Sciences 5.

Kiyono, T., Hiraiwa, A., Fujita, M., Hayashi, Y., Akiyama, T., Ishibashi, M., 1997. Binding of high-risk human papillomavirus E6 oncoproteins to the human homologue of the *Drosophila* discs large tumor suppressor protein. Proc. Natl. Acad. Sci. U.S.A. 94, 11612–11616. https://doi.org/10.1073/pnas.94.21.11612

Klaes, R., Friedrich, T., Spitkovsky, D., Ridder, R., Rudy, W., Petry, U., Dallenbach-Hellweg, G., Schmidt, D., von Knebel Doeberitz, M., 2001. Overexpression of p16INK4A as a specific marker for dysplastic and neoplastic epithelial cells of the cervix uteri. Int. J. Cancer 92, 276–284. https://doi.org/10.1002/ijc.1174

Klingelhutz, A.J., Foster, S.A., McDougall, J.K., 1996. Telomerase activation by the E6 gene product of human papillomavirus type 16.

Klingelhutz, A.J., Roman, A., 2012. Cellular transformation by human papillomaviruses: Lessons learned by comparing high- and low-risk viruses. Virology 424, 77–98. https://doi.org/10.1016/j.virol.2011.12.018

Klingenberg, B., Hafkamp, H.C., Haesevoets, A., Manni, J.J., Slootweg, P.J., Weissenborn, S.J., Klussmann, J.P., Speel, E.-J.M., 2010. p16INK4A overexpression is frequently detected in

tumour-free tonsil tissue without association with HPV: Tumour-free tonsils, p16INK4A and HPV. Histopathology 56, 957–967. https://doi.org/10.1111/j.1365-2559.2010.03576.x

Knight, G.L., Pugh, A.G., Yates, E., Bell, I., Wilson, R., Moody, C.A., Laimins, L.A., Roberts, S., 2011. A cyclin-binding motif in human papillomavirus type 18 (HPV18) E1^E4 is necessary for association with CDK–cyclin complexes and G2/M cell cycle arrest of keratinocytes, but is not required for differentiation-dependent viral genome amplification or L1 capsid protein expression. Virology 412, 196–210. https://doi.org/10.1016/j.virol.2011.01.007

Kong, K., Kumar, M., Taruishi, M., Javier, R.T., 2014. The Human Adenovirus E4-ORF1 Protein Subverts Discs Large 1 to Mediate Membrane Recruitment and Dysregulation of Phosphatidylinositol 3-Kinase. PLoS Pathog 10, e1004102. https://doi.org/10.1371/journal.ppat.1004102

Konings, H., Stappers, S., Geens, M., De Winter, B.Y., Lamote, K., van Meerbeeck, J.P., Specenier, P., Vanderveken, O.M., Ledeganck, K.J., 2020. A Literature Review of the Potential Diagnostic Biomarkers of Head and Neck Neoplasms. Front. Oncol. 10, 1020. https://doi.org/10.3389/fonc.2020.01020

Kono, T., Hoover, P., Poropatich, K., Paunesku, T., Mittal, B.B., Samant, S., Laimins, L.A., 2020. Activation of DNA damage repair factors in HPV positive oropharyngeal cancers. Virology 547, 27–34. https://doi.org/10.1016/j.virol.2020.05.003

Kono, T., Laimins, L., 2021. Genomic Instability and DNA Damage Repair Pathways Induced by Human Papillomaviruses. Viruses 13, 1821. https://doi.org/10.3390/v13091821

Koster, M.I., Roop, D.R., 2007. Mechanisms Regulating Epithelial Stratification. Annu. Rev. Cell Dev. Biol. 23, 93–113. https://doi.org/10.1146/annurev.cellbio.23.090506.123357

Kotb, W.F.M.A., Blind, C., Friedrich, K.-H., Schewe, C., Zhang, Z.G., Zheng, J.M., Deutschman, N., Pacyna-Gengelbach, M., Dietel, M., Petersen, I., 2010. Core classification of head and neck squamous cell carcinomas: Correlations between morphology, DNA ploidy and HPV infection. Pathology - Research and Practice 206, 768–771. https://doi.org/10.1016/j.prp.2010.07.011

Kranjec, C., Tomaić, V., Massimi, P., Nicolaides, L., Doorbar, J., Banks, L., 2016. The high-risk HPV E6 target scribble (hScrib) is required for HPV E6 expression in cervical tumour-derived cell lines. Papillomavirus Research 2, 70–77. https://doi.org/10.1016/j.pvr.2016.04.001

Kreimer, A.R., 2005. Human Papillomavirus Types in Head and Neck Squamous Cell Carcinomas Worldwide: A Systematic Review. Cancer Epidemiology Biomarkers & Prevention 14, 467–475. https://doi.org/10.1158/1055-9965.EPI-04-0551

Kreimer, A.R., Shiels, M.S., Fakhry, C., Johansson, M., Pawlita, M., Brennan, P., Hildesheim, A., Waterboer, T., 2018. Screening for human papillomavirus-driven oropharyngeal cancer: Considerations for feasibility and strategies for research: HPV-Driven OPC Screening Considerations. Cancer 124, 1859–1866. https://doi.org/10.1002/cncr.31256

Kühne, C., Gardiol, D., Guarnaccia, C., Amenitsch, H., Banks, L., 2000. Differential regulation of human papillomavirus E6 by protein kinase A: conditional degradation of human discs large protein by oncogenic E6. Oncogene 19, 5884–5891. https://doi.org/10.1038/sj.onc.1203988

Kumar, M., Keller, B., Makalou, N., Sutton, R.E., 2001. Systematic Determination of the Packaging Limit of Lentiviral Vectors. Human Gene Therapy 12, 1893–1905. https://doi.org/10.1089/104303401753153947

Kuras, Z., Kucher, V., Gordon, S.M., Neumeier, L., Chimote, A.A., Filipovich, A.H., Conforti, L., 2012. Modulation of K $_V$ 1.3 channels by protein kinase A I in T lymphocytes is mediated by the disc large 1-tyrosine kinase Lck complex. American Journal of Physiology-Cell Physiology 302, C1504–C1512. https://doi.org/10.1152/ajpcell.00263.2011

Lazić, D., Hufbauer, M., Zigrino, P., Buchholz, S., Kazem, S., Feltkamp, M.C.W., Mauch, C., Steger, G., Pfister, H., Akgül, B., 2012. Human Papillomavirus Type 8 E6 Oncoprotein Inhibits Transcription of the PDZ Protein Syntenin-2. J Virol 86, 7943–7952. https://doi.org/10.1128/JVI.00132-12

Lechner, M.S., Mack, D.H., Finicle, A.B., Crook, T., Vousden, K.H., Laimins, L.A., 1992. Human papillomavirus E6 proteins bind p53 in vivo and abrogate p53-mediated repression of transcription. The EMBO Journal 11, 3045–3052. https://doi.org/10.1002/j.1460-2075.1992.tb05375.x

Ledwaba, T., Dlamini, Z., Naicker, S., Bhoola, K., 2004. Molecular genetics of human cervical cancer: role of papillomavirus and the apoptotic cascade. Biological Chemistry 385. https://doi.org/10.1515/BC.2004.083

Lee, C., Laimins, L.A., 2004. Role of the PDZ Domain-Binding Motif of the Oncoprotein E6 in the Pathogenesis of Human Papillomavirus Type 31. J Virol 78, 12366–12377. https://doi.org/10.1128/JVI.78.22.12366-12377.2004

Lee, H.-J., Zheng, J.J., 2010. PDZ domains and their binding partners: structure, specificity, and modification. Cell Commun Signal 8, 8. https://doi.org/10.1186/1478-811X-8-8

Lee, W.-H., Chen, H.-M., Yang, S.-F., Liang, C., Peng, C.-Y., Lin, F.-M., Tsai, L.-L., Wu, B.-C., Hsin, C.-H., Chuang, C.-Y., Yang, T., Yang, T.-L., Ho, S.-Y., Chen, W.-L., Ueng, K.-C., Huang, H.-D., Huang, C.-N., Jong, Y.-J., 2017. Bacterial alterations in salivary microbiota and their association in oral cancer. Sci Rep 7, 16540. https://doi.org/10.1038/s41598-017-16418-x

Lesnikova, I., Lidang, M., Hamilton-Dutoit, S., Koch, J., 2009. p16 as a diagnostic marker of cervical neoplasia: a tissue microarray study of 796 archival specimens. Diagn Pathol 4, 22. https://doi.org/10.1186/1746-1596-4-22

Leung, S., Tam, J.S., Chan, A.T.C., Zee, B., Chan, L.Y.S., Huang, D.P., Van Hasselt, A., Johnson, P.J., Lo, Y.M.D., 2004. Improved Accuracy of Detection of Nasopharyngeal Carcinoma by Combined Application of Circulating Epstein–Barr Virus DNA and Anti-Epstein–Barr Viral Capsid Antigen IgA Antibody. Clinical Chemistry 50, 339–345. https://doi.org/10.1373/clinchem.2003.022426

Levine, A.J., 1997. p53, the Cellular Gatekeeper for Growth and Division. Cell 88, 323–331. https://doi.org/10.1016/S0092-8674(00)81871-1

Li, X., Coffino, P., 1996. High-risk human papillomavirus E6 protein has two distinct binding sites within p53, of which only one determines degradation. J Virol 70, 4509–4516. https://doi.org/10.1128/jvi.70.7.4509-4516.1996

Lim, K.Y.B., Gödde, N.J., Humbert, P.O., Kvansakul, M., 2017. Structural basis for the differential interaction of Scribble PDZ domains with the guanine nucleotide exchange factor β-PIX. Journal of Biological Chemistry 292, 20425–20436. https://doi.org/10.1074/jbc.M117.799452

Lin, H., Steller, M., Aish, L., Hanada, T., Chishti, A., 2004. Differential expression of human Dlg in cervical intraepithelial neoplasias. Gynecologic Oncology 93, 422–428. https://doi.org/10.1016/j.ygyno.2004.01.025

Lin, W.-H., Asmann, Y.W., Anastasiadis, P.Z., 2015. Expression of Polarity Genes in Human Cancer. Cancer Inform 14s3, CIN.S18964. https://doi.org/10.4137/CIN.S18964

Liu, X., Yuan, H., Fu, B., Disbrow, G.L., Apolinario, T., Tomaić, V., Kelley, M.L., Baker, C.C., Huibregtse, J., Schlegel, R., 2005. The E6AP Ubiquitin Ligase Is Required for Transactivation of the hTERT Promoter by the Human Papillomavirus E6 Oncoprotein. Journal of Biological Chemistry 280, 10807–10816. https://doi.org/10.1074/jbc.M410343200

Lo Nigro, C., Denaro, N., Merlotti, A., Merlano, M., 2017. Head and neck cancer: improving outcomes with a multidisciplinary approach. CMAR Volume 9, 363–371. https://doi.org/10.2147/CMAR.S115761

Longworth, M.S., Laimins, L.A., 2004. The Binding of Histone Deacetylases and the Integrity of Zinc Finger-Like Motifs of the E7 Protein Are Essential for the Life Cycle of Human Papillomavirus Type 31. J Virol 78, 3533–3541. https://doi.org/10.1128/JVI.78.7.3533-3541.2004

Löning, T., Ikenberg, H., Becker, J., Gissmann, L., Hoepfer, I., zur Hausen, H., 1985. Analysis of Oral Papillomas, Leukoplakias, and Invasive Carcinomas for Human Papillomavirus Type Related DNA. Journal of Investigative Dermatology 84, 417–420. https://doi.org/10.1111/1523-1747.ep12265517

Maglennon, G.A., McIntosh, P., Doorbar, J., 2011. Persistence of viral DNA in the epithelial basal layer suggests a model for papillomavirus latency following immune regression. Virology 414, 153–163. https://doi.org/10.1016/j.virol.2011.03.019

Maiya, R., Lee, S., Berger, K.H., Kong, E.C., Slawson, J.B., Griffith, L.C., Takamiya, K., Huganir, R.L., Margolis, B., Heberlein, U., 2012. DlgS97/SAP97, a Neuronal Isoform of Discs Large, Regulates Ethanol Tolerance. PLoS ONE 7, e48967. https://doi.org/10.1371/journal.pone.0048967

Mantovani, F., Collavin, L., Del Sal, G., 2019. Mutant p53 as a guardian of the cancer cell. Cell Death Differ 26, 199–212. https://doi.org/10.1038/s41418-018-0246-9

Mantovani, F., Massimi, P., Banks, L., 2001. Proteasome degradation of hDlg tumour suppressor protein 8.

Marcello, E., Epis, R., Saraceno, C., Gardoni, F., Borroni, B., Cattabeni, F., Padovani, A., Di Luca, M., 2012. SAP97-mediated local trafficking is altered in Alzheimer disease patients' hippocampus. Neurobiology of Aging 33, 422.e1-422.e10. https://doi.org/10.1016/j.neurobiolaging.2010.09.015

Marsh, E.K., Delury, C.P., Davies, N.J., Weston, C.J., Miah, M.A.L., Banks, L., Parish, J.L., Higgs, M.R., Roberts, S., 2017. Mitotic control of human papillomavirus genome-containing cells is regulated by the function of the PDZ-binding motif of the E6 oncoprotein. Oncotarget 8, 19491–19506. https://doi.org/10.18632/oncotarget.14469

Martin-Belmonte, F., Perez-Moreno, M., 2012. Epithelial cell polarity, stem cells and cancer. Nat Rev Cancer 12, 23–38. https://doi.org/10.1038/nrc3169

Marziali, F., Dizanzo, M.P., Cavatorta, A.L., Gardiol, D., 2019. Differential expression of DLG1 as a common trait in different human diseases: an encouraging issue in molecular pathology. Biological Chemistry 400, 699–710. https://doi.org/10.1515/hsz-2018-0350

Marziali, F., Marina Bugnon Valdano, Clarisse Brunet Avalos, Moriena, L., Cavatorta, A., Gardiol, D., 2017. Interference of HTLV-1 Tax Protein with Cell Polarity Regulators: Defining the Subcellular Localization of the Tax-DLG1 Interaction. Viruses 9, 355. https://doi.org/10.3390/v9120355

Massimi, P., Gammoh, N., Thomas, M., Banks, L., 2004. HPV E6 specifically targets different cellular pools of its PDZ domain-containing tumour suppressor substrates for proteasome-mediated degradation. Oncogene 23, 8033–8039. https://doi.org/10.1038/sj.onc.1207977

Massimi, P., Narayan, N., Cuenda, A., Banks, L., 2006. Phosphorylation of the discs large tumour suppressor protein controls its membrane localisation and enhances its susceptibility to HPV E6-induced degradation. Oncogene 25, 4276–4285. https://doi.org/10.1038/sj.onc.1209457

Maufort, J.P., Shai, A., Pitot, H.C., Lambert, P.F., 2010. A Role for HPV16 E5 in Cervical Carcinogenesis. Cancer Res 70, 2924–2931. https://doi.org/10.1158/0008-5472.CAN-09-3436

McBride, A.A., 2022. Human papillomaviruses: diversity, infection and host interactions. Nat Rev Microbiol 20, 95–108. https://doi.org/10.1038/s41579-021-00617-5

McBride, A.A., 2017. Mechanisms and strategies of papillomavirus replication. Biological Chemistry 398, 919–927. https://doi.org/10.1515/hsz-2017-0113

McBride, A.A., 2013. The Papillomavirus E2 proteins. Virology 445, 57–79. https://doi.org/10.1016/j.virol.2013.06.006

Mcintyre, M.C., Ruesch, M.N., Laimins, L.A., 1996. Human Papillomavirus E7 Oncoproteins Bind a Single Form of Cyclin E in a Complex with cdk2 and p107. Virology 215, 73–82. https://doi.org/10.1006/viro.1996.0008

McKinney, C.C., Kim, M.J., Chen, D., McBride, A.A., 2016. Brd4 Activates Early Viral Transcription upon Human Papillomavirus 18 Infection of Primary Keratinocytes. mBio 7, e01644-16. https://doi.org/10.1128/mBio.01644-16

McMurray, H.R., McCance, D.J., 2003. Human Papillomavirus Type 16 E6 Activates TERT Gene Transcription through Induction of c-Myc and Release of USF-Mediated Repression. J Virol 77, 9852–9861. https://doi.org/10.1128/JVI.77.18.9852-9861.2003

Médina, E., Williams, J., Klipfell, E., Zarnescu, D., Thomas, G., Le Bivic, A., 2002. Crumbs interacts with moesin and βHeavy-spectrin in the apical membrane skeleton of Drosophila. Journal of Cell Biology 158, 941–951. https://doi.org/10.1083/jcb.200203080

Mendoza, C., Olguín, P., Lafferte, G., Thomas, U., Ebitsch, S., Gundelfinger, E.D., Kukuljan, M., Sierralta, J., 2003. Novel Isoforms of Dlg Are Fundamental for Neuronal Development in *Drosophila*. J. Neurosci. 23, 2093–2101. https://doi.org/10.1523/JNEUROSCI.23-06-02093.2003

Merten, O.-W., Hebben, M., Bovolenta, C., 2016. Production of lentiviral vectors. Molecular Therapy 15.

Mesri, E.A., Feitelson, M.A., Munger, K., 2014. Human Viral Oncogenesis: A Cancer Hallmarks Analysis. Cell Host & Microbe 15, 266–282. https://doi.org/10.1016/j.chom.2014.02.011

Milde-Langosch, K., Bamberger, A.-M., Rieck, G., Kelp, B., Löning, T., 2001. Overexpression of the p16 Cell Cycle Inhibitor in Breast Cancer is Associated with a More Malignant Phenotype. Breast Cancer Res Treat 67, 61–70. https://doi.org/10.1023/A:1010623308275

Mittal, S., Banks, L., 2017. Molecular mechanisms underlying human papillomavirus E6 and E7 oncoprotein-induced cell transformation. Mutation Research/Reviews in Mutation Research 772, 23–35. https://doi.org/10.1016/j.mrrev.2016.08.001

Moody, C.A., Laimins, L.A., 2010. Human papillomavirus oncoproteins: pathways to transformation. Nat Rev Cancer 10, 550–560. https://doi.org/10.1038/nrc2886

Mooren, J.J., Gültekin, S.E., Straetmans, J.M.J.A.A., Haesevoets, A., Peutz-Kootstra, C.J., Huebbers, C.U., Dienes, H.P., Wieland, U., Ramaekers, F.C.S., Kremer, B., Speel, E.-J.M., Klussmann, J.P., 2014. P16 ^{INK4A} immunostaining is a strong indicator for high-risk-HPV-associated oropharyngeal carcinomas and dysplasias, but is unreliable to predict low-risk-HPV-infection in head and neck papillomas and laryngeal dysplasias: P16 ^{INK4A} and HPV in head and neck lesions. Int. J. Cancer 134, 2108–2117. https://doi.org/10.1002/ijc.28534

Morgan, E.L., Macdonald, A., 2020. Manipulation of JAK/STAT Signalling by High-Risk HPVs: Potential Therapeutic Targets for HPV-Associated Malignancies. Viruses 12, 977. https://doi.org/10.3390/v12090977

Morgan, E.L., Wasson, C.W., Hanson, L., Kealy, D., Pentland, I., McGuire, V., Scarpini, C., Coleman, N., Arthur, J.S.C., Parish, J.L., Roberts, S., Macdonald, A., 2018. STAT3 activation by E6 is essential for the differentiation-dependent HPV18 life cycle. PLoS Pathog 14, e1006975. https://doi.org/10.1371/journal.ppat.1006975

Muench, P., Hiller, T., Probst, S., Florea, A.-M., Stubenrauch, F., Iftner, T., 2009. Binding of PDZ proteins to HPV E6 proteins does neither correlate with epidemiological risk classification nor with the immortalization of foreskin keratinocytes. Virology 387, 380–387. https://doi.org/10.1016/j.virol.2009.02.018

Müller, H., Bracken, A.P., Vernell, R., Moroni, M.C., Christians, F., Grassilli, E., Prosperini, E., Vigo, E., Oliner, J.D., Helin, K., 2001. E2Fs regulate the expression of genes involved in differentiation, development, proliferation, and apoptosis. Genes Dev. 15, 267–285. https://doi.org/10.1101/gad.864201

Müller, M., Prescott, E.L., Wasson, C.W., Macdonald, A., 2015. Human papillomavirus E5 oncoprotein: function and potential target for antiviral therapeutics. Future Virology 10, 27–39. https://doi.org/10.2217/fvl.14.99

Münger, K., Basile, J.R., Duensing, S., Eichten, A., Gonzalez, S.L., Grace, M., Zacny, V.L., 2001. Biological activities and molecular targets of the human papillomavirus E7 oncoprotein. Oncogene 20, 7888–7898. https://doi.org/10.1038/sj.onc.1204860

Nakagawa, S., Huibregtse, J.M., 2000. Human Scribble (Vartul) Is Targeted for Ubiquitin-Mediated Degradation by the High-Risk Papillomavirus E6 Proteins and the E6AP Ubiquitin-Protein Ligase. MOL. CELL. BIOL. 20, 10.

Nakagawa, S., Yano, T., Nakagawa, K., Takizawa, S., Suzuki, Y., Yasugi, T., Huibregtse, J.M., Taketani, Y., 2004. Analysis of the expression and localisation of a LAP protein, human scribble, in the normal and neoplastic epithelium of uterine cervix. Br J Cancer 90, 194–199. https://doi.org/10.1038/sj.bjc.6601465

Nakagawa, T., Kurokawa, T., Mima, M., Imamoto, S., Mizokami, H., Kondo, S., Okamoto, Y., Misawa, K., Hanazawa, T., Kaneda, A., 2021. DNA Methylation and HPV-Associated Head and Neck Cancer. Microorganisms 9, 801. https://doi.org/10.3390/microorganisms9040801

Narayan, N., Subbaiah, V.K., Banks, L., 2009. The high-risk HPV E6 oncoprotein preferentially targets phosphorylated nuclear forms of hDlg. Virology 387, 1–4. https://doi.org/10.1016/j.virol.2009.02.030

Navarro, C., Nola, S., Audebert, S., Santoni, M.-J., Arsanto, J.-P., Ginestier, C., Marchetto, S., Jacquemier, J., Isnardon, D., Le Bivic, A., Birnbaum, D., Borg, J.-P., 2005. Junctional recruitment of mammalian Scribble relies on E-cadherin engagement. Oncogene 24, 4330–4339. https://doi.org/10.1038/sj.onc.1208632

Nguyen, M.L., Nguyen, M.M., Lee, D., Griep, A.E., Lambert, P.F., 2003. The PDZ Ligand Domain of the Human Papillomavirus Type 16 E6 Protein Is Required for E6's Induction of Epithelial Hyperplasia In Vivo. J Virol 77, 6957–6964. https://doi.org/10.1128/JVI.77.12.6957-6964.2003

Nicolaides, L., Davy, C., Raj, K., Kranjec, C., Banks, L., Doorbar, J., 2011. Stabilization of HPV16 E6 protein by PDZ proteins, and potential implications for genome maintenance. Virology 414, 137–145. https://doi.org/10.1016/j.virol.2011.03.017

Niethammer, M., Valtschanoff, J.G., Kapoor, T.M., Allison, D.W., Weinberg, R.J., Craig, A.M., Sheng, M., 1998. CRIPT, a Novel Postsynaptic Protein that Binds to the Third PDZ Domain of PSD-95/SAP90. Neuron 20, 693–707. https://doi.org/10.1016/S0896-6273(00)81009-0

Nola, S., Sebbagh, M., Marchetto, S., Osmani, N., Nourry, C., Audebert, S., Navarro, C., Rachel, R., Montcouquiol, M., Sans, N., Etienne-Manneville, S., Borg, J.-P., Santoni, M.-J., 2008. Scrib regulates PAK activity during the cell migration process. Human Molecular Genetics 17, 3552–3565. https://doi.org/10.1093/hmg/ddn248

Oceguera-Yanez, F., Kim, S.-I., Matsumoto, T., Tan, G.W., Xiang, L., Hatani, T., Kondo, T., Ikeya, M., Yoshida, Y., Inoue, H., Woltjen, K., 2016. Engineering the AAVS1 locus for consistent and scalable transgene expression in human iPSCs and their differentiated derivatives. Methods 101, 43–55. https://doi.org/10.1016/j.ymeth.2015.12.012

Olshan, A.F. (Ed.), 2010. Epidemiology, Pathogenesis, and Prevention of Head and Neck Cancer. Springer New York, New York, NY. https://doi.org/10.1007/978-1-4419-1472-9

Ouyang, Z., Chen, M., Sun, J., Zhai, J., 2019. Expression and role of hScrib in endometrium, endometriosis, and endometrial adenocarcinoma. Medicine 98, e14076. https://doi.org/10.1097/MD.0000000000014076

Ouyang, Z., Zhan, W., Dan, L., 2009. hScrib, a Human Homolog of *Drosophila* Neoplastic Tumor Suppressor, Is Involved in the Progress of Endometrial Cancer. oncol res 18, 593–599. https://doi.org/10.3727/096504010X12767359114045

Pai, S.I., Westra, W.H., 2009. Molecular Pathology of Head and Neck Cancer: Implications for Diagnosis, Prognosis, and Treatment. Annu. Rev. Pathol. Mech. Dis. 4, 49–70. https://doi.org/10.1146/annurev.pathol.4.110807.092158

Park, R.B., Androphy, E.J., 2002. Genetic Analysis of High-Risk E6 in Episomal Maintenance of Human Papillomavirus Genomes in Primary Human Keratinocytes. J Virol 76, 11359–11364. https://doi.org/10.1128/JVI.76.22.11359-11364.2002

Patel, D., 1999. The E6 protein of human papillomavirus type 16 binds to and inhibits co-activation by CBP and p300. The EMBO Journal 18, 5061–5072. https://doi.org/10.1093/emboj/18.18.5061

Patrick, D.R., Oliff, A., Heimbrook, D.C., 1994. Identification of a novel retinoblastoma gene product binding site on human papillomavirus type 16 E7 protein. Journal of Biological Chemistry 269, 6842–6850. https://doi.org/10.1016/S0021-9258(17)37452-5

Pedroza-Saavedra, A., Lam, E.W.-F., Esquivel-Guadarrama, F., Gutierrez-Xicotencatl, L., 2010. The human papillomavirus type 16 E5 oncoprotein synergizes with EGF-receptor signaling to enhance cell cycle progression and the down-regulation of p27Kip1. Virology 400, 44–52. https://doi.org/10.1016/j.virol.2010.01.009

Peh, W.L., Brandsma, J.L., Christensen, N.D., Cladel, N.M., Wu, X., Doorbar, J., 2004. The Viral E4 Protein Is Required for the Completion of the Cottontail Rabbit Papillomavirus Productive Cycle In Vivo. J Virol 78, 2142–2151. https://doi.org/10.1128/JVI.78.4.2142-2151.2004

Pešut, E., Đukić, A., Lulić, L., Skelin, J., Šimić, I., Milutin Gašperov, N., Tomaić, V., Sabol, I., Grce, M., 2021. Human Papillomaviruses-Associated Cancers: An Update of Current Knowledge. Viruses 13, 2234. https://doi.org/10.3390/v13112234

Petca, A., Borislavschi, A., Zvanca, M., Petca, R.-C., Sandru, F., Dumitrascu, M., 2020. Non-sexual HPV transmission and role of vaccination for a better future (Review). Exp Ther Med 20, 1–1. https://doi.org/10.3892/etm.2020.9316

Phelps, W.C., Münger, K., Yee, C.L., Barnes, J.A., Howley, P.M., 1992. Structure-function analysis of the human papillomavirus type 16 E7 oncoprotein. J Virol 66, 2418–2427. https://doi.org/10.1128/jvi.66.4.2418-2427.1992

Pietsch, E.C., Murphy, M.E., 2008. Low risk HPV-E6 traps p53 in the cytoplasm and induces p53-dependent apoptosis. Cancer Biology & Therapy 7, 1916–1918. https://doi.org/10.4161/cbt.7.12.7169

Pim, D., Bergant, M., Boon, S.S., Ganti, K., Kranjec, C., Massimi, P., Subbaiah, V.K., Thomas, M., Tomaić, V., Banks, L., 2012. Human papillomaviruses and the specificity of PDZ domain targeting: HPV PDZ interactions. FEBS J 279, 3530–3537. https://doi.org/10.1111/j.1742-4658.2012.08709.x

Pim, D., Thomas, M., Javier, R., Gardiol, D., Banks, L., 2000. HPV E6 targeted degradation of the discs large protein: evidence for the involvement of a novel ubiquitin ligase. Oncogene 19, 719–725. https://doi.org/10.1038/sj.onc.1203374

Powers, J.M., Trobridge, G.D., 2013. Effect of Fetal Bovine Serum on Foamy and Lentiviral Vector Production. Human Gene Therapy Methods 24, 307–309. https://doi.org/10.1089/hgtb.2013.097

Prescott, E.L., Brimacombe, C.L., Hartley, M., Bell, I., Graham, S., Roberts, S., 2014. Human Papillomavirus Type 1 E1^E4 Protein Is a Potent Inhibitor of the Serine-Arginine (SR) Protein Kinase SRPK1 and Inhibits Phosphorylation of Host SR Proteins and of the Viral Transcription and Replication Regulator E2. J Virol 88, 12599–12611. https://doi.org/10.1128/JVI.02029-14

Pyeon, D., Pearce, S.M., Lank, S.M., Ahlquist, P., Lambert, P.F., 2009. Establishment of Human Papillomavirus Infection Requires Cell Cycle Progression. PLoS Pathog 5, e1000318. https://doi.org/10.1371/journal.ppat.1000318

Qin, Y., Capaldo, C., Gumbiner, B.M., Macara, I.G., 2005. The mammalian Scribble polarity protein regulates epithelial cell adhesion and migration through E-cadherin. Journal of Cell Biology 171, 1061–1071. https://doi.org/10.1083/jcb.200506094

Rahimi, S., 2020. HPV-related squamous cell carcinoma of oropharynx: a review. J Clin Pathol 73, 624–629. https://doi.org/10.1136/jclinpath-2020-206686

Reinstein, E., Scheffner, M., Oren, M., Ciechanover, A., Schwartz, A., 2000. Degradation of the E7 human papillomavirus oncoprotein by the ubiquitin-proteasome system: targeting via ubiquitination of the N-terminal residue. Oncogene 19, 5944–5950. https://doi.org/10.1038/sj.onc.1203989

Ribeiro, A., Caodaglio, A., Sichero, L., 2018. Regulation of HPV transcription. Clinics 73. https://doi.org/10.6061/clinics/2018/e486s

Richards, K.H., Doble, R., Wasson, C.W., Haider, M., Blair, G.E., Wittmann, M., Macdonald, A., 2014. Human Papillomavirus E7 Oncoprotein Increases Production of the Anti-Inflammatory Interleukin-18 Binding Protein in Keratinocytes. J Virol 88, 4173–4179. https://doi.org/10.1128/JVI.02546-13

Riley, R.R., Duensing, S., Brake, T., 2003. Dissection of Human Papillomavirus E6 and E7 Function in Transgenic Mouse Models of Cervical Carcinogenesis. Cancer Research 63, 4862–4871.

Roberts, S., Ashmole, I., Rookes, S.M., Gallimore, P.H., 1997. Mutational analysis of the human papillomavirus type 16 E1--E4 protein shows that the C terminus is dispensable for keratin cytoskeleton association but is involved in inducing disruption of the keratin filaments. J Virol 71, 3554–3562. https://doi.org/10.1128/jvi.71.5.3554-3562.1997

Roberts, S., Calautti, E., Vanderweil, S., Nguyen, H.O., Foley, A., Baden, H.P., Viel, A., 2007. Changes in localization of human discs large (hDlg) during keratinocyte differentiation is associated with expression of alternatively spliced hDlg variants. Experimental Cell Research 313, 2521–2530. https://doi.org/10.1016/j.yexcr.2007.05.017

Roberts, S., Delury, C., Marsh, E., 2012. The PDZ protein discs-large (DLG): the 'Jekyll and Hyde' of the epithelial polarity proteins. FEBS J 279, 3549–3558. https://doi.org/10.1111/j.1742-4658.2012.08729.x

Romagosa, C., Simonetti, S., López-Vicente, L., Mazo, A., Lleonart, M.E., Castellvi, J., Ramon y Cajal, S., 2011. p16Ink4a overexpression in cancer: a tumor suppressor gene associated with senescence and high-grade tumors. Oncogene 30, 2087–2097. https://doi.org/10.1038/onc.2010.614

Sabatini, M.E., Chiocca, S., 2020. Human papillomavirus as a driver of head and neck cancers. Br J Cancer 122, 306–314. https://doi.org/10.1038/s41416-019-0602-7

Saidu, N.E.B., Filić, V., Thomas, M., Sarabia-Vega, V., Đukić, A., Miljković, F., Banks, L., Tomaić, V., 2019. PDZ Domain-Containing Protein NHERF-2 Is a Novel Target of Human Papillomavirus 16 (HPV-16) and HPV-18. J Virol 94, e00663-19. https://doi.org/10.1128/JVI.00663-19

Sanders, C.M., Stenlund, A., 1998. Recruitment and loading of the E1 initiator protein: an ATP-dependent process catalysed by a transcription factor. EMBO J 17, 7044–7055. https://doi.org/10.1093/emboj/17.23.7044

Santoni, M.-J., Kashyap, R., Camoin, L., Borg, J.-P., 2020. The Scribble family in cancer: twentieth anniversary. Oncogene 39, 7019–7033. https://doi.org/10.1038/s41388-020-01478-7

Santoni, M.-J., Pontarotti, P., Birnbaum, D., Borg, J.-P., 2002. The LAP family: a phylogenetic point of view. Trends in Genetics 18, 494–497. https://doi.org/10.1016/S0168-9525(02)02738-5

Sato, J., Shimazu, D., Yamamoto, N., Nishikawa, T., 2008. An association analysis of synapse-associated protein 97 (SAP97) gene in schizophrenia. J Neural Transm 115, 1355–1365. https://doi.org/10.1007/s00702-008-0085-9

Scarth, J.A., Patterson, M.R., Morgan, E.L., Macdonald, A., 2021. The human papillomavirus oncoproteins: a review of the host pathways targeted on the road to transformation. Journal of General Virology 102. https://doi.org/10.1099/jgv.0.001540

Scheffner, M., Huibregtse, J.M., Vierstra, P.D., Howley't, P.M., 1993. The HPV-16 E6 and E6-AP Complex Functions as a Ubiquitin-Protein Ligase in the Ubiquitination of 53 11.

Schelhaas, M., Shah, B., Holzer, M., Blattmann, P., Kühling, L., Day, P.M., Schiller, J.T., Helenius, A., 2012. Entry of Human Papillomavirus Type 16 by Actin-Dependent, Clathrin- and Lipid Raft-Independent Endocytosis. PLoS Pathog 8, e1002657. https://doi.org/10.1371/journal.ppat.1002657

Schiller, J.T., Day, P.M., Kines, R.C., 2010. Current understanding of the mechanism of HPV infection. Gynecologic Oncology 118, S12–S17. https://doi.org/10.1016/j.ygyno.2010.04.004

Schneider-Stock, R., Boltze, C., Lasota, J., Peters, B., Corless, C.L., Ruemmele, P., Terracciano, L., Pross, M., Insabato, L., Vizio, D.D., Iesalnieks, I., Dirnhofer, S., Hartmann, A., Heinrich, M., Miettinen, M., Roessner, A., Tornillo, L., 2005. Loss of p16 Protein Defines High-Risk Patients with Gastrointestinal Stromal Tumors: A Tissue Microarray Study 9.

Sedman, T., Sedman, J., Stenlund, A., 1997. Binding of the E1 and E2 proteins to the origin of replication of bovine papillomavirus. J Virol 71, 2887–2896. https://doi.org/10.1128/jvi.71.4.2887-2896.1997

Seiwert, T.Y., 2021. Ties That Bind : p16 As a Prognostic Biomarker and the Need for High-Accuracy Human Papillomavirus Testing 32, 3914–3916.
Serrano, M., 1997. The Tumor Suppressor Protein p16INK4a. Experimental Cell Research 237, 7–13. https://doi.org/10.1006/excr.1997.3824
Shen, H., Huang, C., Wu, J., Li, J., Hu, T., Wang, Z., Zhang, H., Shao, Y., Fu, Z., 2021. SCRIB Promotes Proliferation and Metastasis by Targeting Hippo/YAP Signalling in Colorectal Cancer. Front. Cell Dev. Biol. 9, 656359. https://doi.org/10.3389/fcell.2021.656359
Shi, Q., Xu, L., Yang, R., Meng, Y., Qiu, L., 2019. Ki-67 and P16 proteins in cervical cancer and precancerous lesions of young women and the diagnostic value for cervical cancer and precancerous lesions. Oncol Lett. https://doi.org/10.3892/ol.2019.10430
Shin, M.-K., Balsitis, S., Brake, T., Lambert, P.F., 2009. Human Papillomavirus E7 Oncoprotein Overrides the Tumor Suppressor Activity of p21 ^{Cip1} in Cervical Carcinogenesis. Cancer Res 69, 5656–5663. https://doi.org/10.1158/0008-5472.CAN-08-3711
Shukla, S., Shishodia, G., Mahata, S., Hedau, S., Pandey, A., Bhambhani, S., Batra, S., Basir, S.F., Das, B.C., Bharti, A.C., 2010. Aberrant expression and constitutive activation of STAT3 in cervical carcinogenesis: implications in high-risk human papillomavirus infection. Mol Cancer 9, 282. https://doi.org/10.1186/1476-4598-9-282
Simoens, C., Gorbaslieva, I., Gheit, T., Holzinger, D., Lucas, E., Ridder, R., Rehm, S., Vermeulen, P., Lammens, M., Vanderveken, O.M., Kumar, R.V., Gangane, N., Caniglia, A., Maffini, F., Rubio, M.B.L., Anantharaman, D., Chiocca, S., Brennan, P., Pillai, M.R., Sankaranarayanan, R., Bogers, J., Pawlita, M., Tommasino, M., Arbyn, M., Herold-Mende, C., Dyckhoff, G., Mosialos, G., Chiesa, F., Tagliabue, M., Ansarin, M., Boeing, H., Castellsagué, X., de Sanjosé, S., Mena, M., Bosch, F.X., Alemany, L., Esmy, P.O., Jayshree, R.S., Sabitha, K.S., Shenoy, A.M., Vijayakumar, M., Chiwate, A.S., Thorat, R.V., Hublikar, G.G., Lakshetti, S.S., Nene, B.M., Kataki, A.C., Kumar Das, A., Sankaran, S., Ramadas, K., Carreira, C., McKay-Chopin, S., Somanathan, T., Zito, A., 2021. HPV DNA genotyping, HPV E6*I mRNA detection, and p16INK4a/Ki-67 staining in Belgian head and neck cancer patient specimens, collected within the HPV-AHEAD study. Cancer Epidemiology 72, 101925. https://doi.org/10.1016/j.canep.2021.101925
Simonson, S.J.S., Difilippantonio, M.J., Lambert, P.F., 2005. Two Distinct Activities Contribute to Human Papillomavirus 16 E6's Oncogenic Potential. Cancer Res 65, 8266–8273. https://doi.org/10.1158/0008-5472.CAN-05-1651
Smith, R.H., 2008. Adeno-associated virus integration: virus versus vector. Gene Ther 15, 817–822. https://doi.org/10.1038/gt.2008.55
Snijders, P.J., Steenbergen, R.D., Heideman, D.A., Meijer, C.J., 2006. HPV-mediated cervical carcinogenesis: concepts and clinical implications. J. Pathol. 208, 152–164. https://doi.org/10.1002/path.1866
Sotelo, N.S., Valiente, M., Gil, A., Pulido, R., 2012. A functional network of the tumor suppressors APC, hDlg, and PTEN, that relies on recognition of specific PDZ-domains. Journal of Cellular Biochemistry 113, 2661–2670. https://doi.org/10.1002/jcb.24141
Spanos, W.C., Geiger, J., Anderson, M.E., Harris, G.F., Bossler, A.D., Smith, R.B., Klingelhutz, A.J., Lee, J.H., 2008. Deletion of the PDZ motif of HPV16 E6 preventing immortalization and anchorage-independent growth in human tonsil epithelial cells. Head Neck 30, 139–147. https://doi.org/10.1002/hed.20673
Spardy, N., Covella, K., Cha, E., Hoskins, E.E., Wells, S.I., Duensing, A., Duensing, S., 2009. Human Papillomavirus 16 E7 Oncoprotein Attenuates DNA Damage Checkpoint Control

by Increasing the Proteolytic Turnover of Claspin. Cancer Res 69, 7022–7029. https://doi.org/10.1158/0008-5472.CAN-09-0925

Spitkovsky, D., Hehner, S.P., Hofmann, T.G., Möller, A., Schmitz, L.M., 2002. The Human Papillomavirus Oncoprotein E7 Attenuates NF-kB Activation by Targeting the IkB Kinase Complex. Journal of Biological Chemistry 277, i–ii. https://doi.org/10.1074/jbc.M201884200

Stephens, R., Lim, K., Portela, M., Kvansakul, M., Humbert, P.O., Richardson, H.E., 2018. The Scribble Cell Polarity Module in the Regulation of Cell Signaling in Tissue Development and Tumorigenesis. Journal of Molecular Biology 430, 3585–3612. https://doi.org/10.1016/j.jmb.2018.01.011

Stöppler, M.C., Straight, S.W., Tsao, G., Schlegel, R., Mccance, D.J., 1996. The E5 Gene of HPV-16 Enhances Keratinocyte Immortalization by Full-Length DNA. Virology 223, 251–254. https://doi.org/10.1006/viro.1996.0475

Storrs, C.H., Silverstein, S.J., 2007. PATJ, a Tight Junction-Associated PDZ Protein, Is a Novel Degradation Target of High-Risk Human Papillomavirus E6 and the Alternatively Spliced Isoform 18 E6*. J Virol 81, 4080–4090. https://doi.org/10.1128/JVI.02545-06

Strati, K., Lambert, P.F., 2007. Role of Rb-Dependent and Rb-Independent Functions of Papillomavirus E7 Oncogene in Head and Neck Cancer. Cancer Research 67, 11585–11593. https://doi.org/10.1158/0008-5472.CAN-07-3007

Syrjänen, K., Syrjänen, S., Lamberg, M., Pyrhönen, S., Nuutinen, J., 1983. Morphological and immunohistochemical evidence suggesting human papillomavirus (HPV) involvement in oral squamous cell carcinogenesis. International Journal of Oral Surgery 12, 418–424. https://doi.org/10.1016/S0300-9785(83)80033-7

Szalmás, A., Tomaić, V., Basukala, O., Massimi, P., Mittal, S., Kónya, J., Banks, L., 2017. The PTPN14 Tumor Suppressor Is a Degradation Target of Human Papillomavirus E7. J Virol 91, e00057-17. https://doi.org/10.1128/JVI.00057-17

Szymanowska-Narloch, A., Jassem, E., Skrzypski, M., Muley, T., Meister, M., Dienemann, H., Taron, M., Rosell, R., Rzepko, R., Jarząb, M., Marjański, T., Pawłowski, R., Rzyman, W., Jassem, J., 2013. Molecular profiles of non-small cell lung cancers in cigarette smoking and never-smoking patients. Advances in Medical Sciences 58, 196–206. https://doi.org/10.2478/ams-2013-0025

Thatte, J., Massimi, P., Thomas, M., Boon, S.S., Banks, L., 2018. The Human Papillomavirus E6 PDZ Binding Motif Links DNA Damage Response Signaling to E6 Inhibition of p53 Transcriptional Activity. J Virol 92, e00465-18. https://doi.org/10.1128/JVI.00465-18

Thomas, J.T., Hubert, W.G., Ruesch, M.N., Laimins, L.A., 1999. Human Papillomavirus Type 31 Oncoproteins E6 and E7 Are Required for the Maintenance of Episomes during the Viral Life Cycle in Normal Human Keratinocytes. Proceedings of the National Academy of Sciences of the United States of America 96, 8449–8454.

Thomas, M., Banks, L., 1998. Inhibition of Bak-induced apoptosis by HPV-18 E6. Oncogene 17, 2943–2954. https://doi.org/10.1038/sj.onc.1202223

Thomas, M., Massimi, P., Jenkins, J., Banks, L., 1995. HPV-18 E6 mediated inhibition of p53 DNA binding activity is independent of E6 induced degradation. Oncogene 10, 261—268.

Thomas, M., Massimi, P., Navarro, C., Borg, J.-P., Banks, L., 2005. The hScrib/Dlg apico-basal control complex is differentially targeted by HPV-16 and HPV-18 E6 proteins. Oncogene 24, 6222–6230. https://doi.org/10.1038/sj.onc.1208757

Thomas, M., Narayan, N., Pim, D., Tomaić, V., Massimi, P., Nagasaka, K., Kranjec, C., Gammoh, N., Banks, L., 2008. Human papillomaviruses, cervical cancer and cell polarity. Oncogene 27, 7018–7030. https://doi.org/10.1038/onc.2008.351

Thomas, M., Pim, D., Banks, L., 2002. Human papillomavirus E6 protein interactions, in: Perspectives in Medical Virology. Elsevier, pp. 71–99. https://doi.org/10.1016/S0168-7069(02)08017-5

Thomas, M.C., Chiang, C.-M., 2005. E6 Oncoprotein Represses p53-Dependent Gene Activation via Inhibition of Protein Acetylation Independently of Inducing p53 Degradation. Molecular Cell 17, 251–264. https://doi.org/10.1016/j.molcel.2004.12.016

Tomaić, V., 2016. Functional Roles of E6 and E7 Oncoproteins in HPV-Induced Malignancies at Diverse Anatomical Sites. Cancers 8, 95. https://doi.org/10.3390/cancers8100095

Tomaić, V., Pim, D., Banks, L., 2009. The stability of the human papillomavirus E6 oncoprotein is E6AP dependent. Virology 393, 7–10. https://doi.org/10.1016/j.virol.2009.07.029

Tommasino, M., 2017. The biology of beta human papillomaviruses. Virus Research 231, 128–138. https://doi.org/10.1016/j.virusres.2016.11.013

Tsao, Y.P., Li, L.Y., Tsai, T.C., Chen, S.L., 1996. Human papillomavirus type 11 and 16 E5 represses p21(WafI/SdiI/CipI) gene expression in fibroblasts and keratinocytes. J Virol 70, 7535–7539. https://doi.org/10.1128/jvi.70.11.7535-7539.1996

Vaira, V., Faversani, A., Dohi, T., Maggioni, M., Nosotti, M., Tosi, D., Altieri, D.C., Bosari, S., 2011. Aberrant Overexpression of the Cell Polarity Module Scribble in Human Cancer. The American Journal of Pathology 178, 2478–2483. https://doi.org/10.1016/j.ajpath.2011.02.028

Valdano, M.B., Cavatorta, A.L., Morale, M.G., Marziali, F., de Souza Lino, V., Steenbergen, R.D.M., Boccardo, E., Gardiol, D., 2016. Disc large 1 expression is altered by human papillomavirus E6/E7 proteins in organotypic cultures of human keratinocytes. Journal of General Virology 97, 453–462. https://doi.org/10.1099/jgv.0.000364

Van Doorslaer, K., Burk, R.D., 2012. Association between hTERT activation by HPV E6 proteins and oncogenic risk. Virology 433, 216–219. https://doi.org/10.1016/j.virol.2012.08.006

Van Doorslaer, K., DeSalle, R., Einstein, M.H., Burk, R.D., 2015. Degradation of Human PDZ-Proteins by Human Alphapapillomaviruses Represents an Evolutionary Adaptation to a Novel Cellular Niche. PLoS Pathog 11, e1004980. https://doi.org/10.1371/journal.ppat.1004980

Van Tine, B.A., Kappes, J.C., Banerjee, N.S., Knops, J., Lai, L., Steenbergen, R.D.M., Meijer, C.L.J.M., Snijders, P.J.F., Chatis, P., Broker, T.R., Moen, P.T., Chow, L.T., 2004. Clonal Selection for Transcriptionally Active Viral Oncogenes during Progression to Cancer. J Virol 78, 11172–11186. https://doi.org/10.1128/JVI.78.20.11172-11186.2004

Vats, A., Thatte, J., Banks, L., 2019. Identification of E6AP-independent degradation targets of HPV E6. Journal of General Virology 100, 1674–1679. https://doi.org/10.1099/jgv.0.001331

Vats, A., Trejo-Cerro, O., Thomas, M., Banks, L., 2021. Human papillomavirus E6 and E7: What remains? Tumour Virus Research 11, 200213. https://doi.org/10.1016/j.tvr.2021.200213

Vermorken, J.B., Mesia, R., Rivera, F., Remenar, E., Kawecki, A., Rottey, S., Erfan, J., Zabolotnyy, D., Kienzer, H.-R., Cupissol, D., Peyrade, F., Benasso, M., Vynnychenko, I., De Raucourt, D., Bokemeyer, C., Schueler, A., Amellal, N., Hitt, R., 2008. Platinum-Based Chemotherapy plus Cetuximab in Head and Neck Cancer. N Engl J Med 359, 1116–1127. https://doi.org/10.1056/NEJMoa0802656

Villa, A., Patton, L.L., Giuliano, A.R., Estrich, C.G., Pahlke, S.C., O'Brien, K.K., Lipman, R.D., Araujo, M.W.B., 2020. Summary of the evidence on the safety, efficacy, and effectiveness of human papillomavirus vaccines. The Journal of the American Dental Association 151, 245-254.e24. https://doi.org/10.1016/j.adaj.2019.10.010

Vincentelli, R., Luck, K., Poirson, J., Polanowska, J., Abdat, J., Blémont, M., Turchetto, J., Iv, F., Ricquier, K., Straub, M.-L., Forster, A., Cassonnet, P., Borg, J.-P., Jacob, Y., Masson, M., Nominé, Y., Reboul, J., Wolff, N., Charbonnier, S., Travé, G., 2015. Quantifying domain-ligand affinities and specificities by high-throughput holdup assay. Nat Methods 12, 787–793. https://doi.org/10.1038/nmeth.3438

Waites, C.L., Specht, C.G., Hartel, K., Leal-Ortiz, S., Genoux, D., Li, D., Drisdel, R.C., Jeyifous, O., Cheyne, J.E., Green, W.N., Montgomery, J.M., Garner, C.C., 2009. Synaptic SAP97 Isoforms Regulate AMPA Receptor Dynamics and Access to Presynaptic Glutamate. Journal of Neuroscience 29, 4332–4345. https://doi.org/10.1523/JNEUROSCI.4431-08.2009

Wang, J.W., Roden, R.B.S., 2013. L2, the minor capsid protein of papillomavirus. Virology 445, 175–186. https://doi.org/10.1016/j.virol.2013.04.017

Wang, X., Li, S., 2014. Protein mislocalization: Mechanisms, functions and clinical applications in cancer. Biochimica et Biophysica Acta (BBA) - Reviews on Cancer 1846, 13–25. https://doi.org/10.1016/j.bbcan.2014.03.006

Wang, Y., Wang, M., Tang, Y., Sun, B., Wang, K., Zhu, F., 2021. Perioperative mortality of head and neck cancers. BMC Cancer 21, 256. https://doi.org/10.1186/s12885-021-07998-z

Wang, Z., Lu, W., Zhang, Y., Zou, F., Jin, Z., Zhao, T., 2020. The Hippo Pathway and Viral Infections. Front. Microbiol. 10, 3033. https://doi.org/10.3389/fmicb.2019.03033

Wang, Z., Zhang, B., Jiang, L., Zeng, X., Chen, Y., Feng, X., Guo, Y., Chen, Q., 2009. RACK1, an excellent predictor for poor clinical outcome in oral squamous carcinoma, similar to Ki67. European Journal of Cancer 45, 490–496. https://doi.org/10.1016/j.ejca.2008.11.012

Watson, R.A., 2002. Changes in expression of the human homologue of the Drosophila discs large tumour suppressor protein in high-grade premalignant cervical neoplasias. Carcinogenesis 23, 1791–1796. https://doi.org/10.1093/carcin/23.11.1791

Watson, R.A., Thomas, M., Banks, L., Roberts, S., 2003. Activity of the human papillomavirus E6 PDZ-binding motif correlates with an enhanced morphological transformation of immortalized human keratinocytes. Journal of Cell Science 116, 4925–4934. https://doi.org/10.1242/jcs.00809

White, E.A., Münger, K., Howley, P.M., 2016. High-Risk Human Papillomavirus E7 Proteins Target PTPN14 for Degradation. mBio 7, e01530-16. https://doi.org/10.1128/mBio.01530-16

Wilson, R., Ryan, G.B., Knight, G.L., Laimins, L.A., Roberts, S., 2007. The full-length E1^E4 protein of human papillomavirus type 18 modulates differentiation-dependent viral DNA amplification and late gene expression. Virology 362, 453–460. https://doi.org/10.1016/j.virol.2007.01.005

Wise-Draper, T., M., 2008. Papillomavirus E6 and E7 proteins and their cellular targets. Front Biosci 13, 1003. https://doi.org/10.2741/2739

Wołącewicz, M., Becht, Grywalska, E., Niedźwiedzka-Rystwej, P., 2019. Herpesviruses in Head and Neck Cancers.

Woodman, C.B.J., Collins, S.I., Young, L.S., 2007. The natural history of cervical HPV infection: unresolved issues. Nat Rev Cancer 7, 11–22. https://doi.org/10.1038/nrc2050

Yadav, R., Zhai, L., Tumban, E., 2019. Virus-like Particle-Based L2 Vaccines against HPVs: Where Are We Today? Viruses 12, 18. https://doi.org/10.3390/v12010018
Zanier, K., Charbonnier, S., Sidi, A.O.M.O., McEwen, A.G., Ferrario, M.G., Poussin-Courmontagne, P., Cura, V., Brimer, N., Babah, K.O., Ansari, T., Muller, I., Stote, R.H., Cavarelli, J., Vande Pol, S., Travé, G., 2013. Structural Basis for Hijacking of Cellular LxxLL Motifs by Papillomavirus E6 Oncoproteins. Science 339, 694–698. https://doi.org/10.1126/science.1229934
Zanoni, D.K., Patel, S.G., Shah, J.P., 2019. Changes in the 8th Edition of the American Joint Committee on Cancer (AJCC) Staging of Head and Neck Cancer: Rationale and Implications. Curr Oncol Rep 21, 52. https://doi.org/10.1007/s11912-019-0799-x
Zhan, L., Rosenberg, A., Bergami, K.C., Yu, M., Xuan, Z., Jaffe, A.B., Allred, C., Muthuswamy, S.K., 2008. Deregulation of Scribble Promotes Mammary Tumorigenesis and Reveals a Role for Cell Polarity in Carcinoma. Cell 135, 865–878. https://doi.org/10.1016/j.cell.2008.09.045
Zhang, J., Lewis, S.M., Kuhlman, B., Lee, A.L., 2013. Supertertiary Structure of the MAGUK Core from PSD-95. Structure 21, 402–413. https://doi.org/10.1016/j.str.2012.12.014
Zhang, L., Wu, J., Ling, M.T., Zhao, L., Zhao, K.-N., 2015. The role of the PI3K/Akt/mTOR signalling pathway in human cancers induced by infection with human papillomaviruses. Mol Cancer 14, 87. https://doi.org/10.1186/s12943-015-0361-x
Zhao, P., 2006. Aberrant cytological localization of p16 and CDK4 in colorectal epithelia in the normal adenoma carcinoma sequence. WJG 12, 6391. https://doi.org/10.3748/wjg.v12.i39.6391
Zhou, J., 2001. A role for p53 in base excision repair. The EMBO Journal 20, 914–923. https://doi.org/10.1093/emboj/20.4.914
Zhu, G.-D., OuYang, S., Liu, F., Zhu, Z.-G., Jiang, F.-N., Zhang, B., 2017. Elevated Expression of DLG1 Is Associated with Poor Prognosis in Patients with Colorectal Cancer 47, 6.
zur Hausen, H., 2002. Papillomaviruses and cancer: from basic studies to clinical application. Nat Rev Cancer 2, 342–350. https://doi.org/10.1038/nrc798
Zur Hausen, H., 1976. Condylomata Acuminata and Human Genital Cancer.

LIST OF FIGURES

LIST OF TABLES

ABBREVIATIONS

ABPC – apical-basal cell polarity

ANOVA – analysis of variance

ATM – ataxia telangiectasia mutated-dependent pathway

ATPase – adenosine triphosphatase

ATR – ataxia telangiectasia mutated-dependent DNA-related pathwayž

BAK – Bcl-2 homologous antagonist/killer

BER – base excision repair

BPE – bovine pituitary extract

CA – condyloma acuminatum

CBP – CREB binding protein

CDK – cyclin-dependent kinase

CEM – complete E-medium

CIN – cervical intraepithelial neoplasia

CIP – calf intestinal alkaline phosphatase

CKII – casein kinase II

CRT – chemoradiotherapy

CT – chemotherapy

DDR – DNA damage response

DLG1 – Discs Large Homologue 1

DMEM - Dulbecco's Modified Eagle Medium

E2BS – E2 binding sites

E6AP – E6-associated protein

EBV – Epstein-Barr virus

EMA – European Medicines Agency

EMT – epithelial to mesenchymal transition

FDA - Food and Drug Administration

FEH – focal epithelial hyperplasia

FFPE – formalin fixed paraffin embedded

G1-3 – grade 1-3

GST – Glutathione S transferase

HDAC – histone deacetylase

HINGS – heat-inactivated goat serum

HN – head and neck

HNC – head and neck cancer

HNSCC – head and neck squamous cell carcinoma

HPV – human papillomavirus

HR – high-risk

HSIL – high-grade cervical intraepithelial lesions

HSPGs – heparan sulfate proteoglycan chains

hTERT – human telomerase

IARC – International Agency for Cancer Research

IF – immunofluorescence

iHFK – immortalized human foreskin keratinocytes

iHTK – immortalized human tonsilar keratinocytes

iNOK – immortalized normal oral keratinocytes

KGM –keratinocyte growth medium

LGL1 – lethal giant larvae protein

LR – low-risk

LRR- leucine rich repeats

LSIL – low-grade cervical intraepithelial lesions

MAGUK – membrane associated guanylate kinase

OPSCC – oropharyngeal squamous cell carcinoma

OSCC - oral squamous cell carcinoma

Pals1 – Protein associated with Lin seven 1

PAP test – Papanicolaou test

PAR complex – 'partitioning defective' complex

PATJ – Pals1-associated tight junction

PBM – PDZ binding motif

PCP – planar cell polarity

PCR – polymerase chain reaction

pRb – retinoblastoma protein

RCE – reticulated crypt epithelium

RdT – radiation therapy

rEGF – recombinant epidermal growth factor

RT-qPCR – reverse transcription quantitative polymerase chain reaction

SCRIB – SCRIBBLE

SDS-PAGE – sodium dodecyl sulfate polyacrylamide gel electrophoresis

SFM – serum-free medium

SSCE – superficial squamous cell epithelium

UPS – ubiquitin proteasome system

URR – upstream regulatory region

WHO – World Health Organization

YAP – Yes-associated protein

Biography

Lucija Lulić was born on July 2, 1994, in Zagreb. She finished elementary and high school in Zagreb, after which she enrolled in the undergraduate study of Biotechnology at the Faculty of Food Technology and Biotechnology, University of Zagreb. During the study, Lucija was awarded the Rector's Award for Individual Research entitled *"Introduction of mutations into a SCW4 gene in order to study the way of binding the Scw4p protein in the cell wall of yeast Saccharomyces cerevisiae"* which she conducted in Laboratory for Biochemistry, Faculty of Food Technology and Biotechnology. She also went on a two-month student exchange to the Universidade Estadual de Campinas, Brazil. Upon the arrival, Lucija enrolled in a double degree program studying Molecular Biotechnology at the University of Zagreb and Bioindustrial Techniques at the University of Orléans, France. She prepared her graduate thesis *„Targeting LINGO as an innovative approach for the treatment of Amyotrophic lateral sclerosis"* under the guidance of Severine Morriset-Lopez, PhD at the Center de Biophysique Moléculaire, Orléans. In 2018, she was employed at the Ruđer Bošković Institute as a doctoral student of The Croatian Science Foundation on the project *"Elucidating the HPV E6/E7 Oncogenic Functions at Different Anatomical Sites"* under the mentorship of Vjekoslav Tomaić, PhD. During her doctoral study, she received a grant from the British Scholarship Trust and spent two months at the Institute of Cancer and Genomic Sciences, University of Birmingham learning from Joanna Parish, PhD and Sally Roberts, PhD. She participated in five domestic and international symposia and congresses. She is the first author of one scientific article and the first co-author of two review papers.

1. Pešut E*, Đukić A*, **Lulić L***, Skelin J*, Šimić I*, Milutin Gašperov N*, Tomaić V, Sabol I, Grce M. Human Papillomaviruses-Associated Cancers: An Update of Current Knowledge. Viruses. 2021; 13(11):2234.
2. **Lulić L**, Jakovčević A, Manojlović L, Dediol E, Banks L, Tomaić V. Human DLG1 and SCRIB Are Distinctly Regulated Independently of HPV-16 during the Progression of Oropharyngeal Squamous Cell Carcinomas: A Preliminary Analysis. Cancers. 2021; 13(17):4461.
3. Đukić A*, **Lulić L***, Thomas M, Skelin J, Bennett Saidu NE, Grce M, Banks L, Tomaić V. HPV Oncoproteins and the Ubiquitin Proteasome System: A Signature of Malignancy? Pathogens. 2020 Feb 18;9(2):133.